ANALYSIS AND IMPROVEMENT

OF

AIR-CONDITIONING, ENGINE COOLING AND FUEL CONSUMPTION

OF A HIGH PERFORMANCE MOTOR CAR

by

DAVID PARSONS

A thesis submitted in fulfilment of the

requirements for the degree of Doctor of Philosophy

THE UNIVERSITY OF ASTON IN BIRMINGHAM

NOVEMBER 1977

ANALYSIS AND IMPROVEMENT OF AIR-CONDITIONING ENGINE COOLING AND FUEL CONSUMPTION OF A HIGH PERFORMANCE MOTOR CAR
DAVID PARSONS DOCTOR OF PHILOSOPHY 1977

SUMMARY

Two projects considered during the early stages of this research are discussed briefly. These are concerned with engine cooling and exhaust pollution control by fluidised particles. The advantage of cooling an engine by this means is that the engine may be run at an optimum temperature and radiated noise attenuated. The high thermal conductivity and surface area of fluidised particles would result in improved after reaction in comparison with conventional exhaust thermal reactors and catalysts.

The fuel consumption, engine cooling system and air-conditioning system of a Jaguar XJ6 motor car have been studied experimentally and analytically, and mathematical models used for their analysis. Recommendations are made for improvements to performance, cost, and fuel consumption.

The efficiency required of a steplessly variable transmission to compete with the present system on the bases of acceleration and fuel economy has been calculated.

As a result of a literature survey, fluids suitable for air-conditioning a motor car using an absorption cycle are recommended. The advantage of such a system is the reduction of fuel consumption by the removal of the compressor brake load from the engine. The feasibility and limitations of such a system are studied and providing the condenser air flow rate is increased and a reduced refrigeration load at idle is acceptable, such a system may be developed.

AUTOMOBILE AIR-CONDITIONING RADIATOR ABSORPTION FLUIDISATION

"Seek the truth from facts to serve the people"

anonymous graffiti

ACKNOWLEDGEMENTS

The author wishes to express his gratitude and sincere thanks to the following:

The late Professor D. E. Elliott for his help and enthusiasm.

The members of the supervisory team, Mr. D. C. Hickson, Mr. J. N. Randle, Mr. G. A. Montgommerie and Dr. B. J. Tighe, particularly Mr. Hickson for the many early hours spent reading drafts.

Mr. J. N. Randle and Mr. M. G. Oliver for the benefit of their experience in motor car research and development.

The staff of the department of Mechanical Engineering, particularly Mr. G. Rickers, Mr. N. Moss, Mr. C. Geens and others, without whose ingenuity the standard of experimental work would have been greatly reduced.

Marston Radiators Limited for providing experimental and design data on their ranges of radiators and condensers.

Jaguar Cars (B.L.U.K.) Limited, his employer, and the Science Research Council for financial support.

Rank Xerox Limited for the use of facilities for typing, using a Rank Xerox 800 Word Processor, and photocopying using their 9200 machine.

Last but by no means least his wife Dawn, whose support has done much to maintain the enthusiasm needed for this work, and who must take credit for the presentation of this thesis.

CONTENTS

LIST OF FIGURES

LIST OF PLATES

LIST OF GRAPHS

LIST OF TABLES

NOMENCLATURE

Units

Throughout this thesis the S.I. system is followed with the exception of data presented graphically, where road speed is expressed in miles/hour and engine speed in rev/min.

Latin Letters

A area, a constant

b a constant

B a constant

Bi Biot number = $hL/k = z/2\beta$

c specific heat capacity, a constant

C a constant

d diameter (mean)

f friction factor = $\frac{2 g d h}{4 L U^2}$

F fin pitch

g acceleration due to gravity

g_1 ratio fan pulley pitch/engine pulley pitch

g_2 ratio road speed/engine angular velocity

h specific enthalpy, pressure head, surface heat transfer coefficient

I current

j heat transfer factor = $St\ Pr^{2/3}$

k thermal conductivity

L length,load

m mass flow rate, a constant

M a composite defined by equation 1.38

n frequency, a constant

N a composite defined by equation 1.39

Nu Nusselt number = hd/k

P pressure, power

Pr Prandtl number = $c_p \mu / k$

q heat flow

r radius

R electrical resistance, number of tube rows

Re Reynolds number = $\varrho U d / \mu$

s specific entropy

S Strouhal number = $nd/\bar{U}$, surface area

St Stanton number = $h/c_p m''$

t thickness

T temperature, torque

Tu turbulence = $\dfrac{\overline{(U')^2}^{\frac{1}{2}}}{\bar{U}_\infty}$

U velocity, conductance

W width

x a constant, a non dimensional group = $W_f \sqrt{\dfrac{h}{2tk}}$

X a non dimensional group defined by equation A1.5

z a non dimensional group defined by equation A1.4

Greek Letters

α	temperature coefficient of electrical resistance
β	a non dimensional group defined by equation A1.8
γ	ratio of specific heat capacities = c_p/c_v
η	efficiency, a displacement as a fraction of a semi length
θ	temperature difference
μ	absolute viscosity
ϱ	density
τ	a non dimensional group defined by equation A1.9
ϕ	a non dimensional group defined by equation A1.6
ω	angular velocity

Suffixes

air	air side
apparent	as measured
B	safety valve setting
c	condenser
C	compressor
D	design
E	evaporator
effective	effective
f	fan, fin
Fan	fan air component
m	mean, at mean temperature
o	ambient
OVERALL	overall
P	pressure
r	radiator

Suffixes (Cont'd.)

R	refrigerant
Ram	ram air component
Total	total
v	vehicle, volume
w	wire
water	water side

CHAPTER 1

INTRODUCTION

Three different projects were considered during the early stages of this period of research. Two of these, concerning engine cooling by fluidised particles and exhaust pollution control by fluidised particles, are discussed briefly in chapter 2. The third project entails a study of a motor car air-conditioning system and the effects of the system on the fuel economy and engine cooling systems.

The primary function of a motor car air-conditioning system is that it should reduce, and maintain at a reduced level, the humidity and temperature in the passenger compartment, whilst maintaining adequate ventilation. The most severe conditions, with regard to the temperature of the air and surfaces in the car, exist when the car has been left standing in strong sunlight resulting in temperatures higher than ambient. The effectiveness of the air-conditioning unit may be judged by the time taken for the unit to reduce the temperature inside the car to the design level.

The temperature in the car may be reduced either by refrigerating the air in the car or by ventilating the space with air drawn in from outside and refrigerated. The advantage of the latter system is that ventilation is maintained and the refrigeration load is less, on initial starting when the air in the car is hotter than ambient, than if recirculation were employed.

Data for the calculation of the required refrigeration load for motor car refrigeration is contained in a technical report published by the American Coolaire Organisation.[1] The experience of the manufacturer,[2] however, has been that a cooling load dependent on ambient conditions and sufficient to supply 0.15 kg/s of dry air at a temperature a little above $0^{o}C$ (to prevent the evaporator from freezing) provides a performance both adequate and competitive with other vehicle manufacturers' products.

It is the means of providing this cooling load that is the subject matter of the bulk of this project. The present system used by the manufacturer is a vapour compression unit with refrigerant R12 as the working fluid. The compressor is driven from the engine and delivers vapour to a finned tube heat exchanger positioned in front and upstream of the engine cooling radiator. The position of this, the condenser, links the performance of the engine cooling system and the refrigeration system, and a modification to one system cannot be viewed entirely independently of the other. It is necessary therefore in examining the refrigeration system, to also study the engine cooling system.

Initially the project was aimed as a feasibility study of the use of absorption refrigeration for motor car air-conditioning. The advantage to be gained from such a system would be a reduction in engine brake power consumption, giving a fuel consumption benefit. The technical feasibility of the absorption system rests on four factors:

(i) Whether fluids are available which might be deemed safe for use in such a system.

(ii) Whether the refrigerant thought suitable for use in an absorption refrigeration system may be used at the temperatures expected in the condenser and evaporator.

(iii) Whether sufficient heat energy is available from the engine exhaust gas to drive the system at a level competitive with the present system.

(iv) Whether the motor car heat rejection system might be engineered to operate at the higher loads resulting from the expected lower coefficient of performance of a refrigeration system having a low-grade energy input.

The problem of examining these four factors has been tackled by: a survey of literature relevent to absorption refrigeration, an experimental study of energy and mass transfers to and from the engine, and a mathematical model of the present engine, engine cooling system, and refrigeration systems.

The project is broader than this however and examines the present system to find its limitations, its effect on the cooling system and its effect on the fuel consumption. An attempt to improve the present system is undertaken, having found its limitations. The effects of varying parameters, influencing the cooling systems of both the air-conditioned and non air-conditioned versions of the car, on the engine coolant temperatures are examined. The fuel consumption of the vehicle is apportioned to the brake loads imposed on the engine to highlight possible economies. The optimum transmission gear ratios, for both fuel economy and performance, and the required efficiency of a steplessly variable transmission to compete with the present fixed ratio transmission, are calculated.

Chapter 3 deals with the literature survey and a description of the present Jaguar XJ6 motor car, the vehicle used as a basis for the study.

Chapter 4 deals with the heat rejection system by experimental measurement and mathematical analysis for the purpose of extrapolation.

Chapter 5 deals with the engine and experimental determination of engine cooling requirements, fuel flow, exhaust gas enthalpy, and exhaust gas mass capacity rate. Also examined in this chapter is the road load, the transmission efficiency, and the engine coolant mass flow rate.

Chapter 6 is a study of the fuel economy of the non air-conditioned car and the extent to which this is influenced by the brake loads imposed on the engine. The influence of transmission gear ratio and the required efficiency of a hypothetical steplessly variable transmission, to compete with the present system on the bases of fuel economy and performance, are examined.

Chapter 7 is a study of the engine cooling system based on the results from the mathematical model. Both the non air-conditioned and the air-conditioned versions of the car are considered, the latter with the air-conditioning system switched off. The influence of component sizes of both the engine cooling system and the refrigeration system condenser are studied. Finally in this chapter, the result on coolant temperatures of auxiliary brake loads is calculated.

Chapter 8 is concerned with the present refrigeration system and a comparison of the maximum refrigeration load available from a hypothetical absorption system, and the calculated performance of the present system. The mathematical model of the present system, and its limitations are discussed, and the influence of individual components on the system calculated, with a view to suggesting methods of improving the refrigeration load and/or reducing the fuel consumption penalty of running the air-conditioning. The advantages of a vapour compression system using R22 are discussed, together with the limitations for its use. In chapter 9 the conclusions and recommendations are briefly reviewed.

From this research it is believed that in addition to the conclusions arrived at, the experimental techniques and mathematical models of the systems considered will be of use as design and development aids in the future. To this end the complete model in the form of a computer program is given in appendix A5. The program is written to be run on a Hewlett-Packard 9830 calculator, and as such may easily be modified to be used as an interactive package in the design office.

CHAPTER 2

ENGINE COOLING AND EXHAUST POLLUTION CONTROL USING FLUIDISED PARTICLES

INTRODUCTION

At the initiation of this research several alternative projects were given consideration, involving the use of fluidised bed technology. Two of these topics are discussed briefly in this chapter.

ENGINE COOLING BY FLUIDISED PARTICLES

In the internal combustion engine, less than one third of the chemical energy of the fuel is converted into work, one third is lost in the exhaust gases and one third is rejected by cooling. This is an approximate division, the actual balance depending on engine design, type of fuel, cooling system, ambient conditions etc. Heat carried off by cooling must be considered a definite loss because, apart from the fact that no useful work can be obtained from it, part of the engine performance i.e. the mechanical work produced, is frequently used for its removal.

Cooling of the engine is necessary for the following reasons. The maximum temperature of the cylinder walls is determined by lubricating conditions. Above a certain temperature lubrication of the sliding surfaces deteriorates and rapid wear of pistons, piston rings and cylinders commences and seizure may result. The maximum temperature depends on the lubricating oil used and ranges from 160^{o} to $200^{o}C$. In addition to this, the alloys (aluminium) of which the piston and cylinder head are commonly produced are weakened at elevated temperatures. Any heating of the inlet air by heat transfer from the inlet tract decreases the volumetric efficiency. Higher octane fuel is also required at higher engine temperatures.

Further to this, the formation of oxides of nitrogen increase as combustion temperature increases.

Conversely, if the engine is running cool, other problems become apparent. There is a greater heat transfer from the combustion gases to the cylinder resulting in a lower efficiency and higher fuel consumption. Combustion chamber surface temperature affects the unburned hydrocarbon emissions by changing the thickness of the combustion chamber quench layer and the degree of after-reaction. Wentworth[3], in studying the effect of such changes on hydrocarbon emissions from an engine, found a decrease of 1.04 to 0.63 p.p.m. of hexane per Kelvin rise in combustion chamber surface temperature. In one test an increase of 56K decreased hydrocarbon emissions by one third. In addition to changing quench layer thickness and after reaction, increases in engine temperature increase fuel evaporation, resulting in more complete combustion.

When running at low temperatures, products of combustion condense on the walls of the cylinders and etching of the cylinder walls sets in which, together with poor lubrication at these temperatures, causes excessive wear. The highest rate of wear occurs in the top third of the cylinder which may indicate the significance of this chemical action on the bores as suggested by Mackerle[4]. Rich mixture running, when starting from cold, causes fuel to be condensed on the cylinder walls, diluting the film of lubricating oil and decreasing its effectiveness.

A distinct advantage of running an engine at a higher temperature is the decrease in the cooling heat transfer surface required, no matter what means are used to cool the engine. Atmospheric air is the ultimate sink whatever heat transfer system is used. The ambient air temperature may vary between $-40^{o}C$ and $55^{o}C$. For an engine operating at $100^{o}C$ the temperature difference to produce the required heat transfer in a hot climate is 45K. For an engine operating at $200^{o}C$ the temperature difference is 145K. Hence, assuming a similar overall heat transfer coefficient for the two engines, the heat transfer surface area may be reduced by a maximum of approximately 69% for the hotter engine.

A further factor to consider with regard to engine cooling system design is the time taken from initial starting to reach the operating temperature. This involves two factors. The cooling control system and the thermal capacity of the engine. The engine should be designed to operate at an optimum temperature, found by consideration of each of the above mentioned factors. Hence, until it reaches this optimum temperature the disadvantages of running at a low temperature will be manifested. From this point of view the increased levels of hydrocarbon emissions is probably the most critical. The Californian legislation test procedure for measurement of emissions includes starting the engine from cold. At the end of the test the average emissions (in grammes per mile) of hydrocarbons, oxides of nitrogen and carbon monoxide are measured and compared with the maximum statutory levels. During the period of initial starting and low temperature running a large percentage of the unburned hydrocarbons measured in the test are produced. Hence there is a great deal to be gained by designing the engine such that the engine warms up as quickly as possible.

The two systems of engine cooling used to date in vehicles are direct air cooling and water cooling.

Water cooled engines have the advantage that the components are kept at a constant and even temperature. Cooling of exhaust valve gear, injectors, and spark plugs, which are localised high temperature regions, is easier and more effectively carried out on water cooled engines than with any other system at present.

The water cooling system consists of a water jacket surrounding the engine and connected to a remote 'radiator'. If the radiator is mounted at the front of the vehicle then the pressure build up at the front of the vehicle when it is travelling may be sufficient to produce a flow of air through the radiator matrix.

The pressure drop across the 'radiator' is very small and such that, when stationary, only a small fan is needed to blow sufficient air through the matrix. To prevent damage due to freezing in cold climates an ethylene glycol antifreeze

is mixed with the water. This modifies the thermal properties of the coolant. The temperature of the coolant is limited by its boiling point which may be increased by pressurising the system. The pressurised system has to be designed such that it is strong enough to withstand the pressure. If the flow of water around the system is not solely induced by thermsyphon action then a pump may be included; the pump will operate more effectively in a pressurised system where the likelihood of cavitation is lessened.

The radiator in a water cooled system being made of non-ferrous metal (usually brass and copper) is an expensive component. It is easily damaged and is isolated from vibration of the engine by flexible rubber connections. Failure of the water cooling system usually arises as a result of a leak from one of these connecting hoses. Control of the temperature of a water cooling system is simple and is provided by a thermostatic water flow valve, usually with a bypass to prevent stationary pockets of the coolant evaporating and causing local overheating. The large capacity of water contained in the water jacket, in addition to material comprising the water jacket, results in a lengthy warm up time from a cold start. A weight penalty is also incurred as a result of this. The water in the water jacket does have the advantage of providing a damper against vibration of the walls of the cylinder.

With regard to reliability the water cooled engine does not have a very good record. Mackerle[4] states that statistics show that 20% of all engine failures are due to faults in the water cooling system. The air cooled engine has the advantages over the water cooled engine of lower weight, higher running temperature, quicker warm up time, lower air flow, and simplicity of production, operation and reliability.

Its major shortcoming is its higher noise level. In addition to lacking a water jacket to damp noise radiated from the cylinders, air cooled engines are commonly made of aluminium alloys which have a higher thermal conductivity than cast iron, mostly used for water cooled engines, to promote fin efficiency. Aluminium does

not have the noise and vibration damping characteristics of cast iron. Recent trends have, however, been towards lighter engines (in the interests of economy) and aluminium is now commonly used for water cooled engines.

All of the engines produced by British Leyland, both past and present, have been water cooled, the objection to air cooled engines probably being the higher noise level associated with this type of engine. Air cooled engines have been produced by other companies however. In Germany Dr. Eng. F. Porsche designed the well known Volkswagen engine. The Volkswagen Beetle holds the record among European cars for the highest production numbers. Dr. Porsche also designed the air cooled engines for the sports car which carries his name. The success of both of these designs is probably the best reference which can be given to engines of this type. The Tatra Company of Czechoslovakia has produced a great variety of air cooled engines since 1923 for road, rail and aircraft applications. The products of the Tatra company have shown that air cooled engines are not limited to small capacities.

In recent years interest has grown around the use of fluidised bed heat exchangers, the magnitude of gas to immersed surface heat transfer coefficients being of the order of 5 to 10 times[5] those of conventional systems. Much of the research has been on deep beds, which have the disadvantage of producing a high pressure drop, but more recent work has been concerned with the heat transfer coefficients in shallow beds. The appearance of a bubbling fluidised bed led early investigators to believe that the surface heat transfer coefficients were limited by a phenomenon corresponding to the laminar film in conventional convective systems. More recent work by Botterill[6] et al has shown that heat transfer between particles and surfaces is by transient conduction through the gas interface, during the time of point contact. The work of Al-Ali[7] is a useful source of data on heat transfer to immersed plain and finned surfaces in shallow fluidised beds, using the model of Botterill[6], and relevant to engine cooling by this method.

Direct air cooling of engines by the medium of fluidised particles may make air cooled engines more acceptable than at present if it were found that the fluidised bed attenuated the engine noise sufficiently. If this were the case then we should have all of the advantages of air cooled engines without the major disadvantages of noise. The high heat transfer coefficients available with fluidisation would mean less finning of the cylinders and cylinder head, making production easier and also localised hot spots (e.g. around the exhaust valve guides) could be cooled more effectively than in a directly air cooled engine. The disadvantages of cooling the engine in this way are the possibility of the particles entering the engine and causing heavy wear on bearing surfaces and the problem of supplying a flow rate of air between the required limits. Velocity of the gas in a fluidised bed may vary by a ratio[5] of up to 8 to 1 and so the fan could conceivably be driven by the crankshaft through a viscous coupling. When not fluidised the particles would act as a thermal insulation, decreasing the warm up time from a cold start, if the temperature control system was engineered to accommodate this.

Conclusions and Recommendations

It would appear at this stage that direct cooling of an engine by fluidisation would give the advantages of direct air cooling possibly without the disadvantages associated with air cooled engines of radiating higher noise levels. It would be necessary to build a prototype engine to study the level of attenuation of noise possible with this system.

EXHAUST CLEANING

To date the most successful exhaust treatment technique used commercially has been air injection into the exhaust system. To meet extremely low emission levels proposed for the late 1970's it is likely that additional exhaust treatment devices will be needed. Both catalytic and thermal exhaust reactors have the

potential for very low emissions.

Thermal Reactor

One of the currently used methods to reduce hydrocarbon and carbon monoxide emissions is air injection into the exhaust system as described by Steinhagen[8] et al.

Oxides of nitrogen are not reduced, in fact they may be increased if sufficiently high exhaust temperatures result from the combustion of the carbon monoxide and hydrocarbons with the added air, or if the injected air enters the cylinder during the overlap period. To achieve a high degree of oxidation of the hydrocarbons and carbon monoxide, a high exhaust temperature coupled with sufficient oxygen, and a long enough residence time is needed to complete the combustion. If a flame is established the heat generated by the combustion of the carbon monoxide and hydrocarbons keeps the reaction going.

Because of its abundance, the carbon monoxide in the exhaust gases provides most of the combustion generated heat. Quite often carbon monoxide concentrations of several percent are measured. On the other hand, hydrocarbon emissions are only a few hundred parts per million. As a result thermal reactors are developed most easily for rich carburation. Brownson and Stebar[9] have studied thermal reactor performance for a reactor coupled to a single cylinder co-operative fuel research engine. In their work an exhaust mixing tank of 2.4 litres was used for some of their tests. They determined that the basic factors governing combustion of carbon monoxide and hydrocarbons in the exhaust gas are composition of the reacting mixture, temperature and pressure of the mixture, and residence time of the mixture or time available for reaction.

Graph 2.1 shows the hydrocarbon and carbon monoxide emissions as a function of air/fuel ratio and injected air flow rate. The emission concentration results were corrected for the added air. Injected air flow rate is indicated as a percentage of the engine air volume flow rate. The insulated 2.4 litre mixing tank

was used.

The minimum hydrocarbon concentrations occurred at rich mixtures. When too much air was injected, especially at lean mixtures, excessive cooling of the exhaust increased hydrocarbon concentrations to above those with no air. Thus the normal oxidation process was apparently inhibited by this cooling. The effect of air injection on carbon monoxide concentration was somewhat different. Exhaust carbon monoxide was uniformly low at most rich air fuel ratios. A small increase in carbon monoxide occurred at fuel/air ratios slightly richer than stoichiometric. For stoichiometric mixtures and leaner, carbon monoxide was very low. Best results occurred for rich mixtures with air injection at 20 - 30% of inlet air flow. The leanest air fuel ratio for best emission reduction was 13.5:1. Normally engine operation at such a mixture would reduce fuel economy by 10%.

To further study the peculiar shape of the carbon monoxide curve with air injection, a quartz window was installed in the exhaust system. For each air injection rate tried, a blue white luminous flame was observed for all mixture ratios to the left of the small carbon monoxide peak up to the rich mixture where the large carbon monoxide increase occurred near 11:1. The very low emissions with rich mixtures and air injection arose from a 'fire' in the exhaust system. For mixtures leaner than the small carbon monoxide peak, non-luminous oxidation occurred and carbon monoxide emission reduction was relatively poor.

At each air/fuel ratio there exists one minimum air injection rate that provides maximum emission oxidation. Minimum air flow is desired in order to reduce pump power requirement, and hence size and cost. Graph 2.2 shows the optimum air injection rate for the data of graph 2.1 for both hydrocarbon and carbon monoxide emissions. It is apparent that air injection was not highly effective in reducing carbon monoxide emission unless luminous burning occurred. This did not happen when the mixture ratio provided by the carburettor was chemically correct or leaner.

Graph 2.3 shows the result of a small (44K) decrease in exhaust temperature,

at 14:1 air fuel ratio. As a result of the temperature decrease, luminous burning could not be achieved, and minimum carbon monoxide concentration required a 90% air flow rather than 20%. A result such as this demonstrates the possible dependence of the required air injection rate on ambient temperature, and prior engine operation (state of warm up). Conversely this data also shows that small changes in engine condition might produce large changes in air injection effectiveness.

Exhaust system insulation may be necessary to achieve high reaction rates in engines with well cooled exhaust ports. Insulation also helps to reduce emission concentrations during warm up by accelerating warm up rate.

At mixtures significantly leaner than stoichiometric in the range of 16 to 17.5:1 air injection is not needed to supply oxygen; in fact it would only cool the exhaust to too low a temperature for any reaction to take place. On the other hand at such lean mixtures only extremely good heat conservation can produce temperatures high enough for appreciable reaction. Warren[10] has studied this lean region and has concluded that with improved carburation it is possible to achieve surge free operation at 17 to 17.5:1 and leaner. When this can be achieved both hydrocarbon and carbon monoxide emissions are reduced to extremely low values (hydrocarbons less than 50 parts per million and carbon monoxide less than 0.1%, Federal Emission Tests) if exhaust temperature is kept high enough through good insulation. Unfortunately oxides of nitrogen are high at air fuel ratios of 17:1. Even leaner operation is necessary to reduce all three emission components. Promising work has been done on stratified charge engines by Honda in particular (Environmental Protection Agency[11] 'Automobile Emission Control - the state of the art as of December 1972').

Graph 2.4 shows the effect of temperature and reactor volume on exhaust hydrocarbon concentration at an oxygen input concentration of 3%. Reactor volume may be viewed as the volume of the exhaust system which is insulated and at the high temperature needed for reaction. Note that if the exhaust

temperature were 760°C only twice the conventional system volume would be needed for virtually complete combustion. On the other hand, if the temperature were only 650°C eight times the volume would achieve only a 76% decrease in concentration. A pair of conventional exhaust manifolds has a volume of about 2.5 litres.

Increasing the exhaust system volume increases the residence time during which reactions can occur. This is a benefit provided the added surface area does not result in excessive cooling. Thus when large volume exhaust manifolds are used they must be well lagged.

The importance of reactor residence time in connection with gas temperature and composition was shown theoretically by Schwing[12] for exhaust system oxidation of carbon monoxide and hydrocarbons. His results show how the extent of oxidation is determined by a balance between rate of reaction and residence time and the energy liberated by combustion. Schwing's[12] approach can be used as a design base for thermal reactors which are well mixed. Levenspiel[13] gives a fundamental discussion of reactor engineering and Blenk et al[14] and Patterson[15] give applications of these fundamentals to a multicylinder engine thermal reactor system.

Graph 2.5 shows the volume advantage which Brownson[9] found when he added increased insulated exhaust volume at a mixture ratio of 14.5:1. In this case carbon monoxide and hydrocarbon concentration reduction are sought.

Significant hydrocarbon reductions were noted as volume was increased. No carbon monoxide concentration reduction was found for this non-luminous oxidation mixture ratio. Graph 2.6 shows that at a rich mixture of 12.3:1 both carbon monoxide and hydrocarbons were reduced to virtually zero with 2.4 litres of added insulated volume. In addition to this the minimum air injection rate requirement was decreased as added volume increased. Without insulation at 12.3:1 no decrease was noted in either emission constituent in spite of the volume increase. This result suggests that the exhaust oxidation process occurring in the

unmodified engine was in the port and immediately downstream thereof. The increased surface area of the added uninsulated volume downstream allowed enough cooling to stop the reactions that might otherwise have proceeded within this added volume had the exhaust temperature been sufficiently high.

In conclusion, increasing the residence time of the exhaust by increasing volume improves both the carbon monoxide and hydrocarbon oxidation effectiveness of air injection and reduces the air flow rate required provided that heat losses are low. This conclusion applied to both rich and lean mixtures and, as Warren[10] demonstrated if surge free operation can be maintained at a weak enough setting, no air injection is needed.

The exhaust reactors mentioned so far have taken the form of a well insulated exhaust system in which the exhaust gas is maintained at a high temperature for an extended period of time. Combustion of the carbon monoxide and, to a lesser extent, hydrocarbons, provides additional heat to maintain and propagate the combustion process. If this heat were conducted backwards against the direction of flow of the exhaust gas, then the process could reasonably be expected to be further assisted. This is the logic behind the proposal to use a fluidised bed as an exhaust thermal reactor. The process of gas combustion in fluidised beds is well reported, in addition to papers and established texts (Davidson and Harrison[16], and Kuni and Levenspiel[17]) on the thermal and fluidic properties.

Several papers have reported very high thermal conductivities in the vertical direction. They mostly agree on what is defined as 'effective thermal conductivity' of a fluidised bed. One of the earliest papers on fluidised bed conductivities was that of Shrikhande[18]. Shrikhande[18] worked with very tall columns and obtained values for the thermal conductivity at 12 cm intervals, for different rates of heat transfer through the bed. Linear temperature profiles were found and from this it was possible to define an 'effective thermal conductivity' as that which enabled the heat transfer to be described by Fourier's Law. This

conductivity increased linearly for an increase in fluidising velocity. Conductivities ranging from 63 to 450 kW/mK were reported for glass beads of varying diameters.

Similar results were published by Lewis, Gilliand and Girovard.[19] Conductivities ranging from 2 to 430 kW/mK were noted. Measurements of conductivities in the radial direction (horizontal) produced values of only about 2% of those in the axial (vertical) direction. In this work a honeycomb baffle was placed halfway down the bed and although this did not affect conductivities above and below the baffle it did produce a sharp discontinuity in the bed. This baffle would have stopped the vertical movement of solids.

The work of several Russian workers has been published by Zabrodsky.[20] These tend to agree with the aforementioned work but one interesting point emerges. The Russian workers recorded bed temperatures at very close intervals and found that there was not a linear gradient near the bottom of the bed. From this they concluded that the effective thermal conductivity was much less at the bottom of the bed.

The most noticable aspects of these works is the very high conductivities. Contributions from the fluidising medium are very small in comparison.

A comprehensive study of gas combustion in fluidised beds is given by Broughton.[21] He attempted unsuccessfully to obtain combustion with separate injections of gas and air, combustion only occurring above the surface. This illustrates poor gas stream mixing in the bed. With pre-mixed gas streams Broughton[21] studied temperature variation down the vertical axis of the bed. It was found that the temperature was constant down the greater length of the bed, but near the distributor plate the temperature increased to a maximum and then decreased towards the plate. Broughton[21] obtained successful pre-mixed combustion with particles of less than 1 mm diameter until he reached a diameter of 0.3 mm diameter. To explain this he used Davidson's[22] model to show that with very small particles a high proportion of the feed gas passes rapidly through the

bed in the bubble phase and does not mix within the bed. This bypass would also remove some of the heat from the bed.

An interesting paper presented by Elliott and Virr[23] at the Third International Conference on Fluidised Bed Combustion, outlines initial studies at the University of Aston in Birmingham. They argued that shallow beds are preferable to deep beds since this would reduce the heat loss from the bed container. Because of this, their work was involved in studying how a shallow bed could be used without combustion occurring above the bed surface. All of this work was with pre-mixed air-gas supplies, separate gas injection being rejected on the grounds that deep beds would be required for complete combustion. Initiation of bed combustion was obtained by igniting the air-gas mixture just above the surface and allowing recirculation of the particles to warm up the bed.

Exploratory studies into the possibility of reducing atmospheric pollution by fluidised combustion have shown the advantages to be gained. Oxides of nitrogen were of the same low level as reported by Jarry[24] et al, and near stoichiometric conditions carbon monoxide/carbon dioxide ratios of less than .002 have been reported. This represents a considerable improvement on the conventional gas burner. Tests were performed by Cole and Essenhigh[25] to find at what bed temperature a fresh air gas mixture could be injected with an initiation of combustion. It was found that this would occur at temperatures as low as 400^{o}C. This temperature is very low and it is possible that there were hot spots within the bed sufficient to ignite the mixture, but even so, this work is encouraging in the application considered here.

The greatest problem liable to arise in an attempt to use a fluidised bed as an exhaust thermal reactor is due to the large range of exhaust gas flows which the device must handle. The exhaust gas flow from the engine will be of the order of 100:1 from idle to maximum speed and throttle conditions. The range[5] of gas velocity which can be passed through the bed between incipient fluidisation and the onset of allutriation is of the order of 8:1. This wide range of fluidising

velocities will probably not be efficiently usable, maximum emission concentration reduction being maximised at one particular velocity which may be expected to be above the onset of the bubble phase and below velocities such that gas passes through the bed without reacting. A further problem will be due to the relatively low velocities obtainable resulting in a large distributor area. These problems may possibly be removed by using a rotating fluidised bed where the particles are under the action of a centrifugal force field. Metcalfe[26] has found experimentally that the bed throughput (at the minimum fluidising velocity) increases as the centripetal acceleration to the power of 0.54. These results were only for a range of accelerations of from 5 to 30 gravities. From this a 100 fold increase in throughput requires an increase in rotational velocity of 145 times. Metcalfe also found that the minimum fluidising pressure increases as the square of the rotational speed. Hence at high throughputs the pressure drop in the bed will be very high (145^2 times the pressure drop at idling). Hence, if at idling the bed pressure drop is of the order of 150 mm of water, at the maximum flow rate the pressure drop will be of the order of 3 km of water gauge. Extrapolation over such a wide range may be unreliable but it may be sufficient to conclude that high flow rates may only be obtained at the expense of very high pressure drops. Hence this idea seems to be ruled out.

Using a bed under the action of gravity, a bed of approximately 0.6 m diameter would be required for the 4.2 litre XJ6 engine. This is for the engine running at maximum speed and throttle opening. At idle the bed would not be fluidised unless some system of blanking off some of the area were found. A bed of smaller area could be used to provide a fluidised reactor at low engine speeds and throttle openings and a fixed bed at higher speeds and openings. This would be advantageous in that the unit would be more compact and fluidised combustion would occur in the most troublesome operating conditions i.e. at rich mixture settings when idling producing higher emissions at lower temperatures. The pressure drop would be higher when the bed became packed, but packed beds have

been used on motor vehicles as catalyst supports. Fluidised beds do not operate successfully unless the distributor plate is horizontal. This situation would be difficult to achieve in a motor car.

It may be that the properties of a fluidised bed are such that gas pressure pulsations (as exist in an I.C. engine exhaust system) are attenuated by passing the gas through a fluidised bed. If so this would be an added benefit of such a system.

Conclusion and Recommendations

From the literature it would appear that a fluidised bed would work well as an exhaust thermal reactor because of the high axial conductivity obtainable. It would appear, however, that the engineering problems associated in using such a device in a motor car may prohibit its use. Such a device may be worthy of study for constant speed stationary engines such as used for power generation, or water or gas pumping.

Catalyst Support

Several catalysts have shown the ability to oxidise hydrocarbons and carbon monoxide in the exhaust. Usually a noble metal such as platinum, or an oxide, is needed. Catalysts are often granular alumina pellets with a very high surface area per unit volume, the catalyst material being deposited on the surface of the pellets. Alternatively a ceramic matrix is used, the catalyst being similarly deposited on its surface. The mode of operation of such a catalyst is as for an exhaust thermal reactor, the additional benefit being that the catalyst permits the oxidation reactions to occur at relatively low temperatures.

One problem with catalysts is that they deteriorate with mileage. Often the deterioration is caused by lead compounds in the exhaust which coat the active catalyst surface. The lead in the exhaust comes from the addition of tetra-ethyl lead to the petrol to improve its anti-knock qualities.

Catalysts may use air injection to complete combustion or may operate without air and utilize excess oxygen from lean mixture operation if sufficient heat conservation can be achieved. There is evidence that some catalysts accumulate oxygen during lean mixture operating modes such as cruising. This oxygen then reacts during rich mixture modes such as idling.

Catalytic reduction of oxides of nitrogen is more of a problem. A chemically reducing environment is required and this involves rich mixture operation and a fuel economy problem. Many reducing catalysts have been found to produce ammonia (as reported by Hunter[27] and Bernstein[28]) a pollutant possibly more dangerous than the oxides of nitrogen. All catalysts may emit trace metallic compounds as the catalysts break up in normal driving, and health aspects have to be considered.

Since the catalysts used for control of automotive exhaust emissions operate in a similar manner to exhaust thermal reactors, the possible advantages of using fluidised particles as catalyst supports are the same, i.e. the high thermal conductivity of the fluidised bed should help to maintain the reactions involved. Additionally the high surface area of the particles is available for coating with the catalyst. Some degree of particle cleaning may be afforded by the abrasive action of the particles on their neighbours to reduce contamination of the catalyst with lead from the fuel. Unfortunately the same engineering problems also present themselves.

Conclusion and Recommendations

The same advantages would be gained by using a fluidised bed as a catalyst support system as for an exhaust thermal reactor. Similarly engineering problems may prevent the use of such a device, as they may the use of fluidised bed exhaust thermal reactors.

GRAPH 2.1

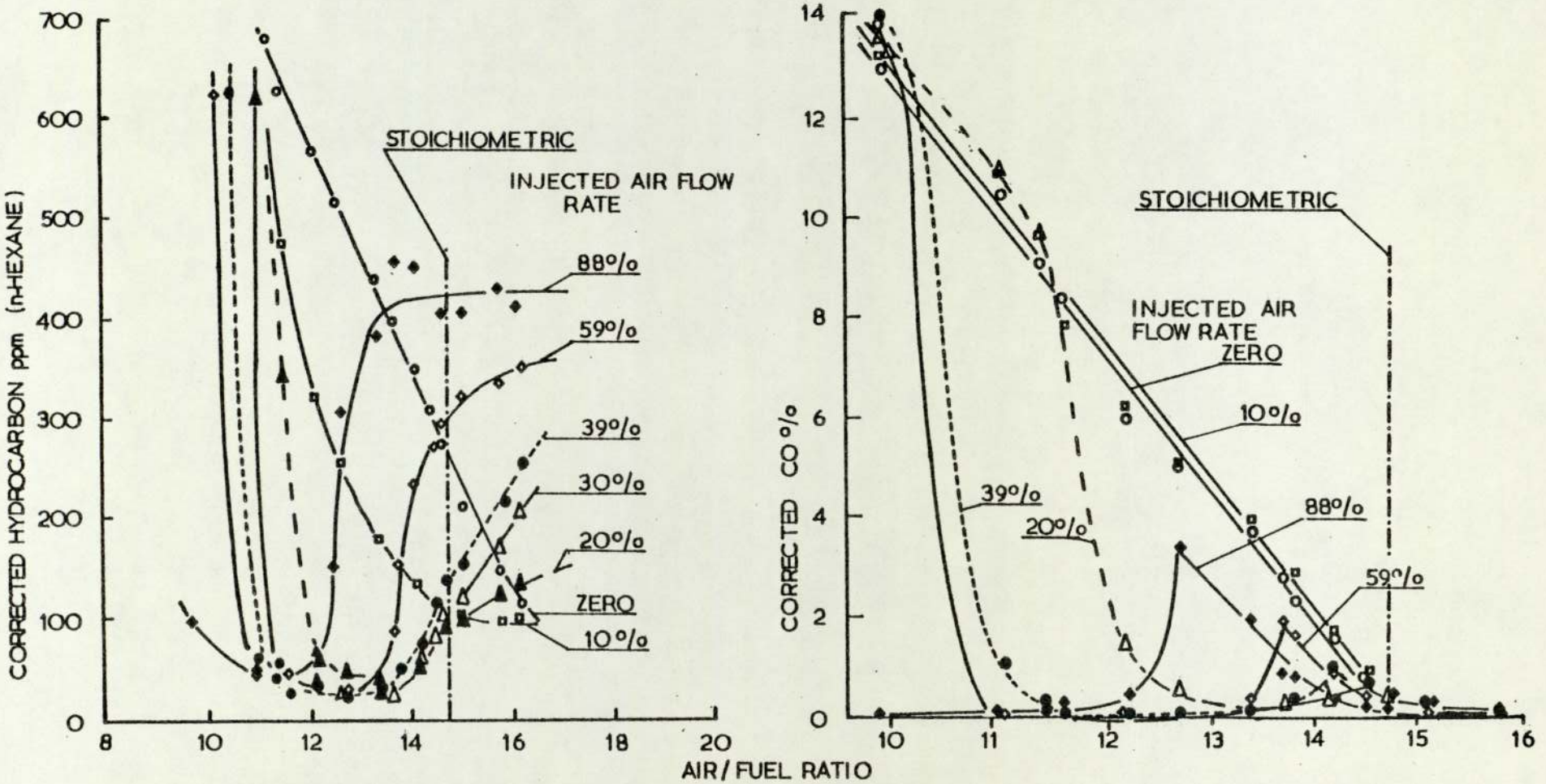

THE EFFECT OF AIR FUEL RATIO AND AIR INJECTION FLOW RATE ON CARBON MONOXIDE AND HYDROCARBON EMISSIONS [FROM THE WORK OF BROWNSON & STEBAR][9]

GRAPH 2.2

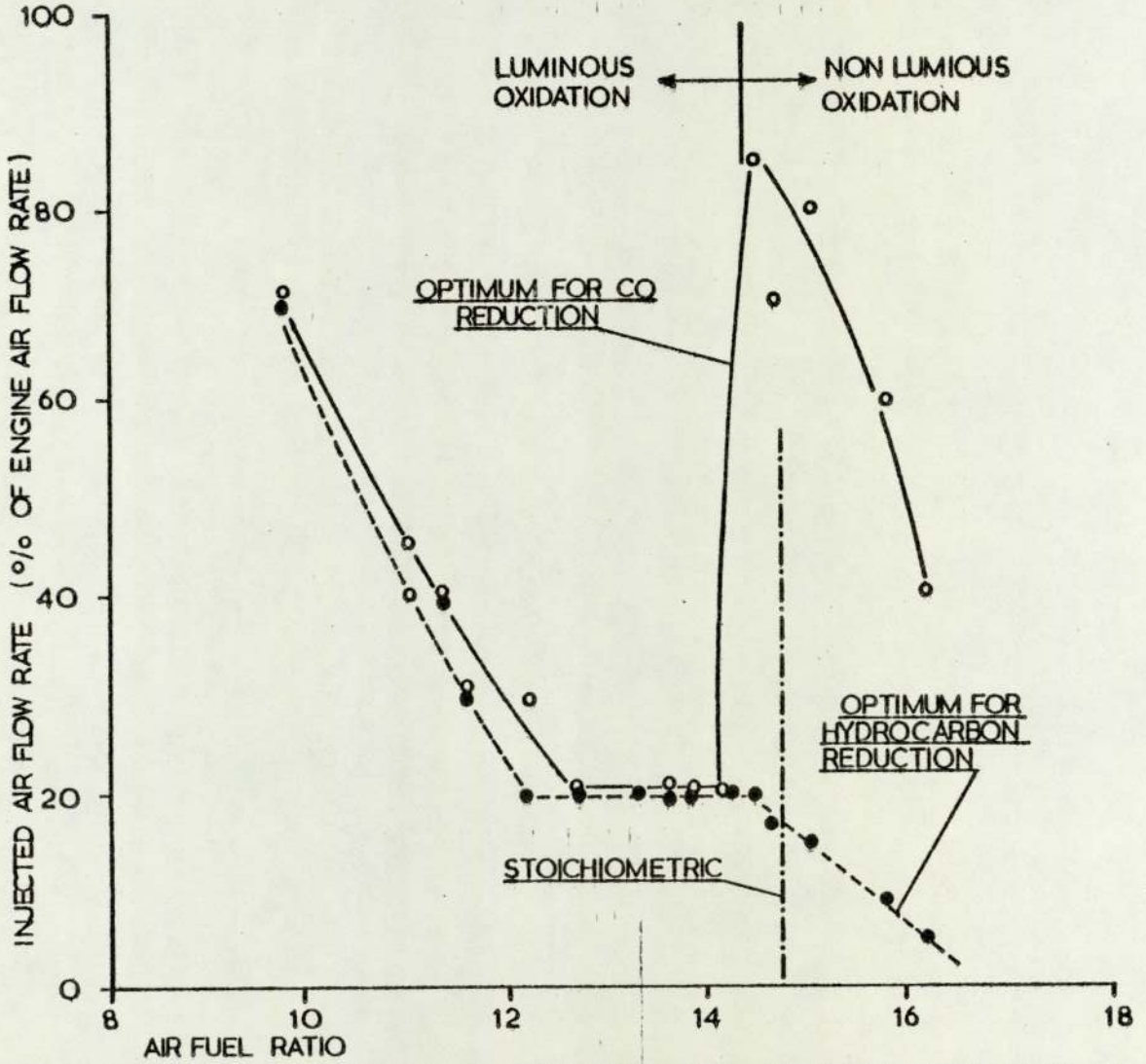

THE EFFECT OF AIR FUEL RATIO AND TYPE OF OXIDATION ON OPTIMUM AIR INJECTION RATE
[FROM THE WORK OF BROWNSON & STEBAR[9]]

GRAPH 2·3

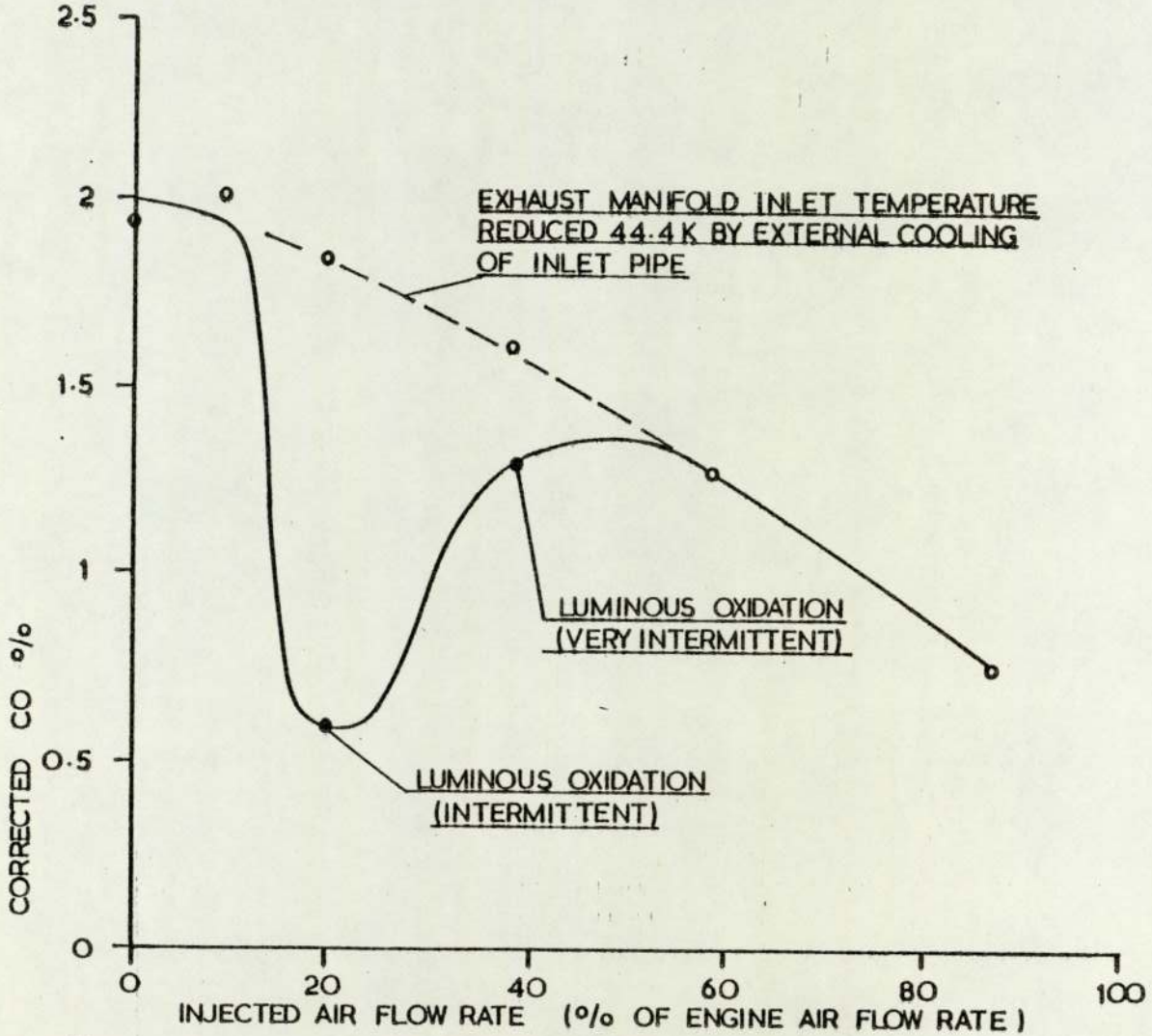

THE IMPORTANCE OF TEMPERATURE IN PROMOTING LUMINOUS COMBUSTION
[FROM THE WORK OF BROWNSON & STEBAR[9]]

GRAPH 2.4

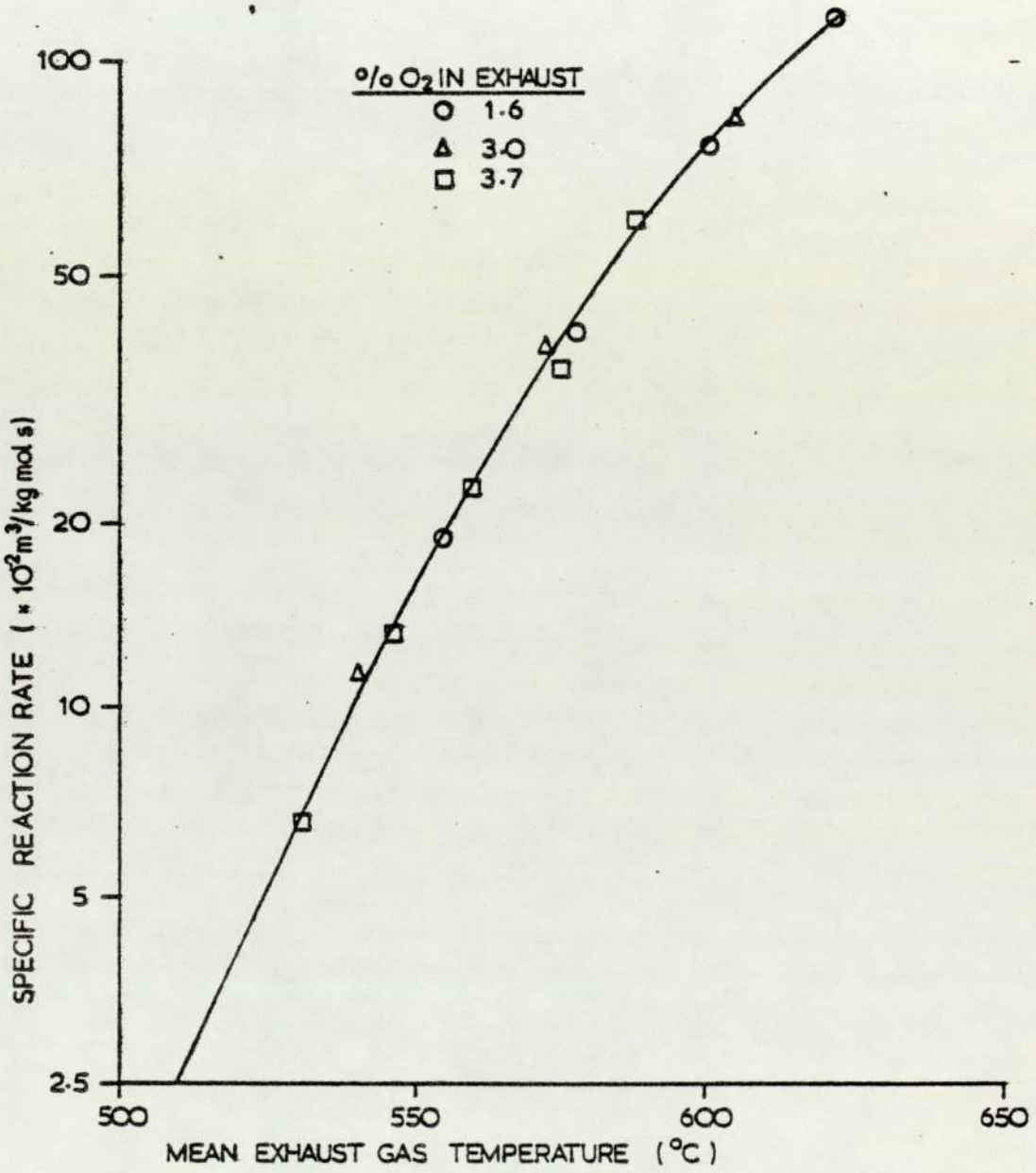

THE EFFECT OF TEMPERATURE ON REACTION RATE

[FROM THE WORK OF WARREN ET AL[10]]

GRAPH 2·5

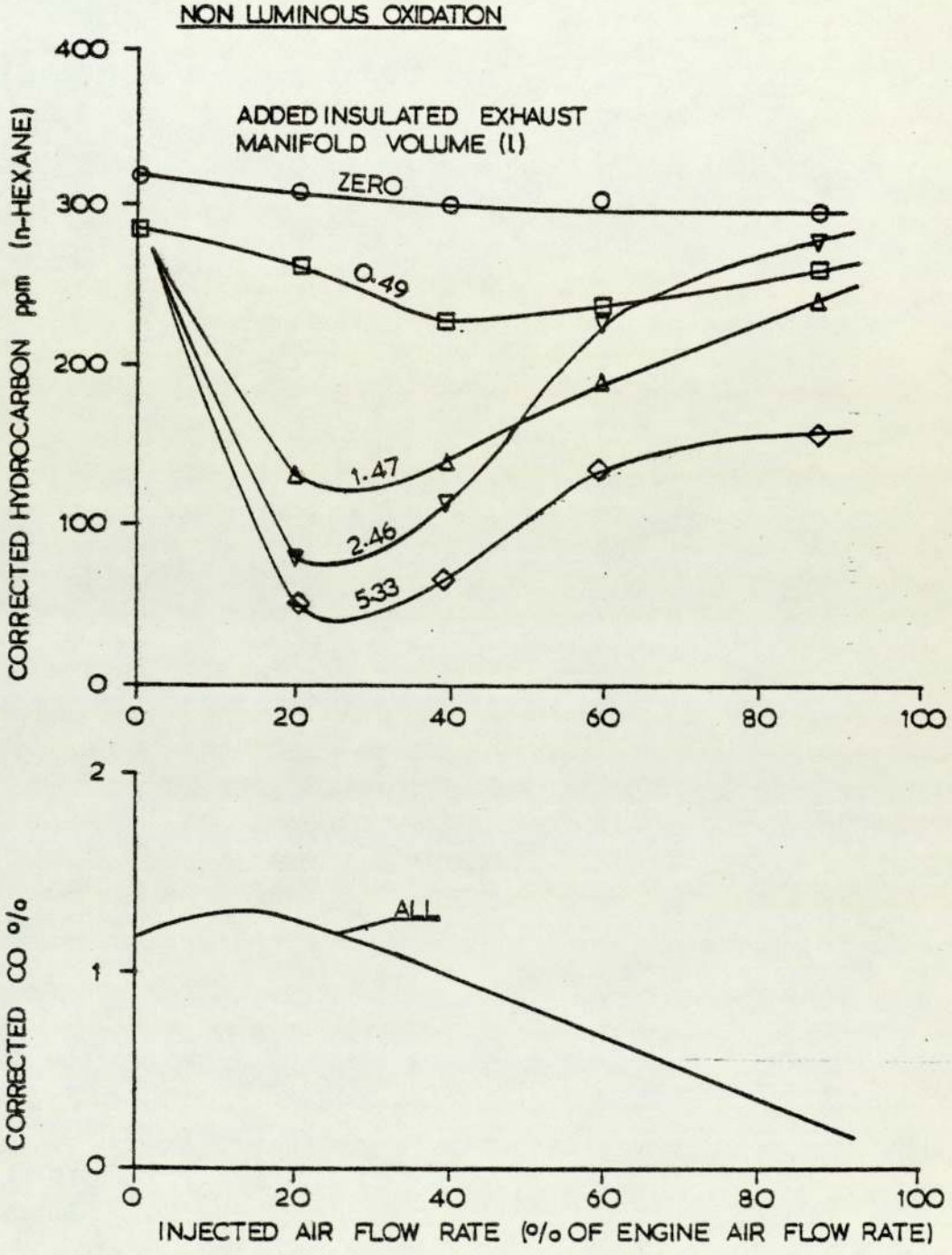

THE EFFECT OF INJECTED AIR FLOW RATE AND ADDED INSULATED EXHAUST MANIFOLD VOLUME ON CARBON MONOXIDE AND HYDROCARBON EMISSIONS AT AN AIR/FUEL RATIO OF 14·5 [FROM THE WORK OF BROWNSON & STEBAR[9]]

GRAPH 2.6

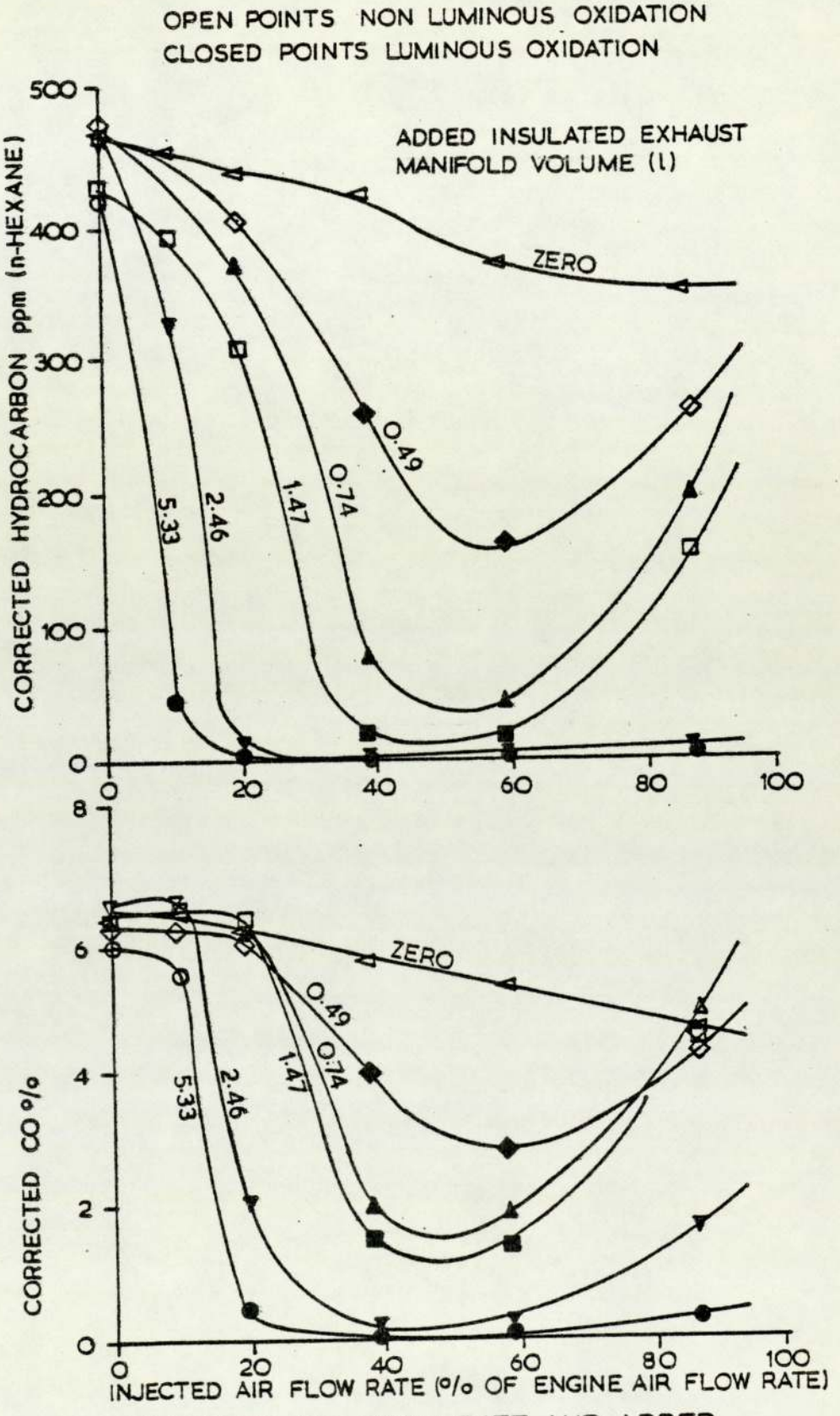

THE EFFECT OF INJECTED AIR FLOW RATE AND ADDED INSULATED EXHAUST MANIFOLD VOLUME ON CARBON MONOXIDE AND HYDROCARBON EMISSIONS AT AN AIR/FUEL RATIO OF 12.3 [FROM THE WORK OF BROWNSON & STEBAR[9]]

CHAPTER 3

REFRIGERATION FOR MOTOR CAR AIR-CONDITIONING

INTRODUCTION

The penalties of air-conditioning the passenger compartment of a motor car are increased manufacturing cost and, if the system is driven by the mechanical power output of the engine, an increase in fuel consumption. Vapour systems, essentially reversed Rankine cycles, have the potential for high coefficients of performance owing to the isothermal modes of heat addition and rejection. Gas cycles such as the air cycle do not have this advantage and are also limited by lower refrigerant side heat transfer coefficients, than are available with two phase flow in the condenser and evaporator of vapour cycles. The two systems considered here are the mechanical vapour compression system, as is used at present, and the absorption cycle. Both cycles are similar except in the method of attaining a pressure difference between the evaporator and condenser. For the mechanical vapour compression system this is achieved by direct compression of superheated vapour in a mechanical compressor, and in the absorption system is achieved by dissolving the refrigerant in a liquid absorbent and pumping this liquid to a high pressure. The refrigerant is driven off from the solution by raising of the temperature in the generator, and the absorbent is throttled back to the absorber.

To reduce the mass flow rate of absorbent required between absorber and generator and the resulting losses due to sensible heat effects, a refrigerant and absorbent of high affinity are required.

The requirements of both systems, with regard to choice of a suitable refrigerant, are similar with the exception of the need for a compatible absorbent of high affinity for the absorption system.

For the vapour compression system the ultimate coefficient of performance is that of a reversed Carnot cycle working between the same two temperatures. For a system with a heat input the ultimate coefficient of performance is that of

a Carnot cycle engine driving a reversed Carnot cycle refrigerator, as calculated by the method of Bosnjakovic[29] and shown by Threlkeld.[30] The temperatures considered for the Carnot engine are those of the generator and absorber source and sink and for the Carnot refrigerator are the temperatures of the medium being cooled and the sink to which heat is rejected from the condenser. Theoretically the coefficient of performance increases with generator temperature. The heat which may be transferred from the engine exhaust gases decreases as the temperature at which this heat is transferred is increased. An optimum coefficient of performance may therefore be expected to exist.

THE CHOICE OF A SUITABLE REFRIGERANT

For convenience and brevity refrigerants are henceforth described by the numbering system of BS4580[31] (1970). Many texts have dealt with descriptions of refrigerants, notably that of Kuprianoff, Plank and Steinle[32] who give comprehensive details and also A.S.H.R.A.E.[33] In this project choice has been limited to established refrigerants, the search for new substances being outside the scope of work. For motor car air-conditioning the first requirement must be safety with regard to toxicity and flammability.

The relative safety of the established refrigerants is published in BS4434[34] and in the A.S.H.R.A.E.[33] handbooks. In BS4434[34] the refrigerants are listed in three groups. Group 1 is described 'Refrigerants in this group are non flammable and may be used in direct expansion equipment where the total charge, adequate in quantity for the refrigeration requirements of the spaces concerned, could escape into the humanly occupied spaces without creating undue hazards'. Included in this list are most of the halogenated hydrocarbons with the notable exception of R30 and R40, but including R11, R12, R13, R13B1, R21, R22, R113, R114, R115, C318, R500, and R502. Water, although not mentioned, must also fall into this category. Group 2 lists refrigerants whose principal objection is their toxicity. Ammonia, R30, R40 and R160 fall into this category. Group 3 refrigerants are

objectionable by virtue of their flammability and include the light hydrocarbons such as butane. Only the refrigerants of the above group 1 are worthy of further consideration in this application. In ANSI Standard[35] B9.1 - 1958 refrigerants are similarly listed in three groups under similar headings. The list of 'safe' refrigerants is as for the British Standard, with the exception that R30 falls into the American group 1.

The American Underwriters Laboratories Classification[36] is based on acute toxicity tests on guinea pigs. Of the refrigerants listed as group 1 by the BSI[34] and ANSI[35], all appear in the higher categories (lowest toxicity) of the Underwriters Laboratories Classification[36]. Group 6 refrigerants (the least toxic) are described as gases or vapours which in concentrations of up to at least 20% by volume for durations of exposure of at least 2 hours do not produce injury, and the group includes R12, R114, and R13B1. Group 4 refrigerants are quoted as being lethal or producing serious injury in concentrations of 2% to 2½% for durations of exposure of 2 to 2½ hours. Refrigerants R21 and R40 fall into this group. Two groups 5a and 5b include R11 and R22.

On the grounds of safety it would seem that any of the refrigerants of group 1 in BS 4434[34] with the exception of R21 are worthy of consideration.

The freezing point of the refrigerant should lie below the lowest temperature expected in the evaporator, or expected to be experienced in climatic conditions in which the car might be used. To ensure that a high heat transfer coefficient is available for heat rejection and that heat is rejected isothermally, the critical temperature should be above the maximum temperature expected in the condenser. With an expected maximum condensing temperature of around 90°C, R13, R13B1, and R115 may be unacceptable as having critical temperatures below 90°C. Refrigerant R113 has a freezing point[34] at -35°C which is probably low enough to be acceptable in all but the worst of climatic conditions, but water, in many other ways a perfect refrigerant, is unacceptable on this point.

The specific enthalpy of evaporation of the refrigerant should be high to reduce the required mass flow rate around the system. Specific enthalpies of evaporation of BS 4434[34] Group 1 refrigerants at $0^{o}C$ are compared on graph 3.1. To illustrate the advantage of water in this respect, it has an enthalpy of evaporation some 16.5 times as high as the present refrigerant R12. Of the refrigerants deemed acceptable so far in this study R22 has the highest enthalpy of evaporation, some 36% higher than R12.

The required volumes of components in the two systems considered is dependent on the specific volume of the refrigerant, and more important the enthalpy of evaporation per unit volume. In this respect R22 is superior to R12 by an increase of 61%, indicating a reduction in compressor swept volume per unit time for the vapour compression system, of the same amount for the same refrigeration load, and a possible cost saving by using a smaller compressor.

The evaporator pressure should not be less than atmospheric to prevent air leaking into the system and reducing the condensing heat transfer coefficient. The condenser pressure should be moderate, to enable the components to be light, and yet of sufficient strength. The saturation pressures of BS4434[34] group 1 refrigerants at $0^{o}C$ and $90^{o}C$ are plotted on graphs 3.2 and 3.3 for comparison.

The requirement of lubrication of the compressor of the vapour compression refrigeration system, entails refrigerant coming into contact with the lubricating oil. To prevent reductions in heat transfer coefficients in the evaporator owing to coating of the surfaces with oil carried over from the compressor, and modification of the refrigerant properties - in particular the reduction of evaporating pressures, the oil and refrigerant should be mutually immiscible. Care must be taken to ensure that the lubricating oil is carefully chosen and/or that effective oil separators are incorporated. The usual method of oil separation is described by Anderson[37]. The addition of an oil separator is an extra cost to be avoided if possible. The absorption system, having moving parts only in a liquid pump, may need no additional lubrication.

From the above analysis of refrigerants it is apparent that as an alternative to refrigerant R12 used at present, R22 may have an advantage. Its drawbacks are higher pressures requiring stronger components, and a lower critical temperature which may entail improving heat transfer in the condenser to maintain a temperature sufficiently lower than the critical for heat transfer to be by condensation.

The coefficient of performance of the vapour compression system, operating between given source and sink temperatures, is limited by the temperature differences required for heat transfer and also by the isentropic efficiency of the compressor. The temperature differences required for heat transfer are dependent on the overall conductances and the air mass capacity rates. The conductances , with two phase or liquid flow in the evaporator and condenser, may be assumed to be limited on the air side and are primarily dependent on the heat transfer surface areas and the air velocities. The compressor isentropic efficiency is limited, in the case of a positive displacement device as used at present, by refrigerant pressure losses at the compressor inlet and outlet. These pressure losses will be a strong function of refrigerant velocity, and the use of a refrigerant of lower specific volume, in reducing these velocities, may result in a higher isentropic efficiency. The compressor volumetric efficiency, a reduction in which increases the required displacement per unit time, decreases as these pressure losses increase, giving a further advantage to the use of a refrigerant having a higher enthalpy of evaporation per unit volume.

THE CHOICE OF SUITABLE ABSORBENT REFRIGERANT COMBINATIONS FOR THE ABSORPTION CYCLE

The requirements of a fluid to act as the working fluid in the vapour compression cycle are similarly relevant to the refrigerant in the absorption cycle.

Probably the most complete literature survey of absorption refrigeration is

that of Ellington[38] et al in 1957. This includes a list of 50 refrigerants considered for this system, together with relevant references. The importance of absorption refrigeration with regard to commercial usage of large plants is stated by Archie[39] as accounting for more than a quarter of the systems sold in capacities of greater than 350 kW, and illustrates the research effort put into such systems.

The traditional fluids used as refrigerant and absorbent are ammonia and water, clearly unsuitable in this application owing to the toxicity of ammonia. These fluids and their use as an absorbent refrigerant pair are well documented generally and the properties of the mixture charted thoroughly by Macriss[40] et al. The most important commercial alternative fluids are water as a refrigerant and a solution of lithium bromide salt in water as an absorbent. This combination has the advantage that the lithium bromide has no vapour pressure and hence carry over of absorbent from the generator is not a problem and no rectification is required as with the ammonia/water system. Limitations of the system are due to the low vapour pressure of water at the evaporator temperature and the resulting possible leaks of air into the system, and the high freezing point of water. The system has found most use in large commercial air-conditioning installations where the danger of freezing is avoided and the need for continual purging of air is a disadvantage outweighed by the other advantages.

Attention to refrigerant/absorbent pairs might be limited for motor car air-conditioning to BS4434[34] Group 1 refrigerants and suitable absorbents.

As mentioned in the introduction, for a high coefficient of performance the quantity of absorbent circulated between the absorber and generator must be kept low in relation to the quantity of refrigerant circulated around the system. This implies a solubility in excess of ideal solubility as defined by Hala[41] et al and a negative deviation from Raoult's Law as defined by the same authors. Unfortunately when a solution is formed in this way heat is generated and this additional heat, known as the heat of solution, has to be rejected in the absorber. In order to evaporate the refrigerant from the absorbent more energy than

indicated by the latent heat of evaporation has to be added at the generator. Buffington[42] proposed that the overriding factor in selecting absorbents should be this negative deviation from Raoult's law. Jacob Albright and Tucker[43] questioned this however and suggest that there may be an optimum, beyond which the irreversibility due to the heat of solution is equal to, or greater than, that due to the sensible heat carried over by the absorbent from the generator to the absorber.

The history of refrigerants in general and absorbent/refrigerant combinations in particular is outlined in two papers by Hainsworth.[44,45] He also lists the desirable properties of the binary combination. The first commercial air-conditioning machine to be put on the market using a halocarbon refrigerant, used R21 and dimethyl ether of tetraethylene glycol and was marketed by Williams Oil-O-Matic Heating Corporation in 1937.

Several papers have been written by Zellhoefer[46,47,48,49] on this and similar machines. Similar refrigerant absorbent combinations have since been studied and the results published by the same author and by Albright[50,51,52] et al. Zellhoefer[46,47,48,49] et al postulated the existence of C-H$\leftarrow$O or C-H$\leftarrow$N bonds of which there is much evidence. Refrigerants having a hydrogen atom in the molecule are superior therefore, and refrigerants R21, R22, R133a, R31, R124a and R134 show high solubilities. In 1959 Mastrangelo[53] published a paper on the solubility of halocarbons in the same absorbent as was used by Williams Oil-O-Matic and a further[54] paper postulating an equation of solubility based on statistical thermodynamic considerations, which is a source of data for calculation of heats of solution in absorption systems using halocarbon refrigerants. Eiseman[55] calculated the performance of an absorption machine using the same absorbent for the six refrigerants having a hydrogen atom and mentioned above. Of the six, refrigerant R22 gave the highest solubility but gave a lower coefficient of performance than R21, which required a lower mass flowrate owing to its higher enthalpy of vapourisation. A disadvantage of R22 was due to the high pumping power required, owing to the large pressure difference

required between the evaporator and condenser. Doubts are expressed as to the temperature stability of R21 at the generator temperature of 111°C and evidence in the form of experimental results published showing the superiority of R22 over R21 in this respect. These results extend up to temperatures of 177°C. The other four refrigerants considered gave lower coefficients of performance owing to reduced solubilities.

The proposed application of absorption refrigeration for the air-conditioning of space stations and spacecraft has been reported. This is an application comparable more closely perhaps with the air-conditioning of motor cars than is domestic or commercial refrigeration. The constraints on the design of safety, being operable in any gravitational attitude and of being light in weight, compact and of small load are similar. The research was carried out by Lockhead Missiles and Space Company and is contained in two reports,by Hale[56] et al and by Sims[57] et al. Their conclusion with regard to choice of a refrigerant/absorbent combination is in agreement with Eiseman[55], and R22 and dimethyl ether of tetraethylene glycol are used in a prototype. With a generator temperature of 177°C a coefficient of performance of 0.59 is reported, considerably higher than calculated by Eiseman[55] and due to the increased generator temperature.

Using the fluids proposed by Hale[56] et al and Sims[57] et al an absorption system suitable for motor car air-conditioning might be made operable.

THE LIMITATIONS OF THE ABSORPTION SYSTEM AND THEIR EXAMINATION

The first limitation to consider with regard to this system is the cooling load which might be produced using the heat energy of the exhaust gas. In chapter 5 this heat energy is measured experimentally and in chapter 8 the cooling load, assuming a generator temperature of 177°C and a coefficient of performance of 0.59 as found by Sims[57] et al, is calculated and compared with the cooling load available with the present system.

Refrigerant R22, shown to have possible advantages over R12, has a lower

critical temperature. Difficulty may be found installing sufficient condenser heat transfer surface and providing sufficient air flow, maintaining the condenser temperature low enough relative to the critical, for the system to operate efficiently using either vapour compression or absorption cycles. This limitation of R22 is studied in Chapter 8 using a mathematical model of the vapour compression system, and the model of the heat rejection system developed in chapter 4.

The removal from the engine of the burden of the compressor will yield extra capacity of the engine cooling system, which might be used for heat rejection from the absorber. This extra capacity whether used directly, or by a reduction of radiator size and the inclusion of a third heat exchanger, will be necessary to reject heat from the absorber.

The dependence of the stability of halocarbon refrigerants on temperature will entail the use of a temperature limiting heat transfer device of some form, which may take the form of a mechanical thermostat, a temperature limiting heat pipe using a non condensible gas as described by Dunn and Reay[58], or by a similar temperature limiting thermosyphon.

Control of the system may be of the form of an on/off switch on this temperature limiting device transferring heat from the exhaust gases to the generator.

The limitations mentioned in the latter three paragraphs are practical problems requiring further investigation if the absorption system appears favourable after examining the limitations outlined in the first two paragraphs.

The advantage to be gained from the absorption system in terms of reduced fuel consumption is quantified in chapter 8.

THE PRESENT SYSTEM

For this project the Jaguar XJ6 is used as a subject and is taken to be a vehicle typical of its type. It is a high performance saloon car having an engine capacity of 4.2 litres and mid-laden mass of just under 2000 kg. The 6 cylinder spark ignition engine is water cooled, coolant being circulated by a centrifugal pump driven from the crankshaft via a vee belt. Control of coolant temperature is by a wax bulb thermostat and radiator bypass which is blanked off as the thermostat opens. The radiator is front mounted and convection from the radiator is assisted by an axial flow fan, driven from the crankshaft, via a vee belt and viscous coupling. For the version of the car considered, the transmission is by a five ratio manual gearbox and dry plate clutch. The air-conditioned version of the car has a vapour compression refrigeration system using R12 as the working fluid. The compressor is a 6 cylinder positive displacement reciprocating device, driven through an electromagnetically loaded clutch from the engine crankshaft via a vee belt. Refrigerant from the compressor passes to a dryer bottle and thence to the condenser, a finned tube heat exchanger mounted in front of the radiator. Expansion of refrigerant is by a thermostatic expansion valve to the evaporator mounted inside the front bulkhead. Control of the air temperature leaving the evaporator is by switching off the current to the compressor clutch when the temperature drops to less than $2^{o}C$. The state of the refrigerant entering the compressor is maintained as having a nominal $2\frac{1}{2}K$ superheat by the thermostatic expansion valve, which senses the temperature and pressure of the refrigerant at the evaporator exit. No other automatic controls are incorporated in the refrigeration system itself, but the system is switched on and off, via the compressor clutch, by the air distribution control system. Pressure overloading of the compressor is precluded by a safety valve as an integral part of the compressor.

Air is sucked over the evaporator at a nominal 0.15 kg/s mass flowrate of dry air, on the maximum fan speed. The maximum refrigeration load and the most

severe climatic conditions may be taken as occurring when operating with the fans at the highest speed and an ambient temperature and relative humidity of 45°C and 50%.

THE VARIABLES INFLUENCING THE AIR-CONDITIONING SYSTEM, AND ITS INFLUENCE ON THE CAR

These variables are those which influence each of the components of the system.

The compressor has a direct effect on both the evaporator load and the coefficient of performance. The displacement per unit time and volumetric efficiency influences the mass flow rate of refrigerant and hence the evaporator load, and the isentropic efficiency is a dependent variable of the coefficient of performance.

The evaporator, and the overall conductance of heat from the air being cooled to the refrigerant, through the evaporator, has an influence on the coefficient of performance by setting the lowest temperature in the cycle. This conductance is a function of the temperature and humidity of the air, the air velocity, and the evaporator geometry.

The condenser and the overall conductance of heat from the refrigerant, through the condenser and to the atmosphere, has a direct influence on the upper temperature of the cycle and hence the coefficient of performance. This conductance is dependent on the air velocity and the condenser geometry.

The air velocity over the condenser is produced by the engine cooling fan and by the forwards motion of the car. This air velocity also influences the radiator heat transfer coefficient, since on leaving the evaporator, the air passes over the radiator. The engine cooling system temperatures are dependent on the radiator overall conductance and the mass capacity rate and temperatures of this air flow. The relative positions of the condenser, radiator, fan cowl and engine cooling fan are shown on figure 3.1. The condenser does not completely cover the

radiator and does not have the advantage of the same air mass flowrate. The fan cowl is fitted with simple rubber flaps to act as non return valves and take advantage of ram air when the car is moving but constrain the air flow, due to the fan, to be through the radiator when stationary. The temperatures of the engine coolant are also dependent on the mass flow rate of coolant between the engine and radiator, the mass capacity rate and radiator coolant side heat transfer coefficient being functions of this.

In addition to providing the tractive effort, which must equal the rolling friction of the tyres and aerodynamic drag, the engine has to supply other loads. These are primarily the transmission losses, the air-conditioning compressor and the engine cooling fan and viscous coupling. The fuel consumption may be calculated as a strong function of brake load and engine speed. By calculating the fuel consumption with and without each of these loads, the fuel consumption contribution of each load may be taken as the difference.

In later chapters each of the variables is quantified and a mathematical model of the system built up. Using this model the complete system is studied and improvements suggested.

FIGURE 3.1

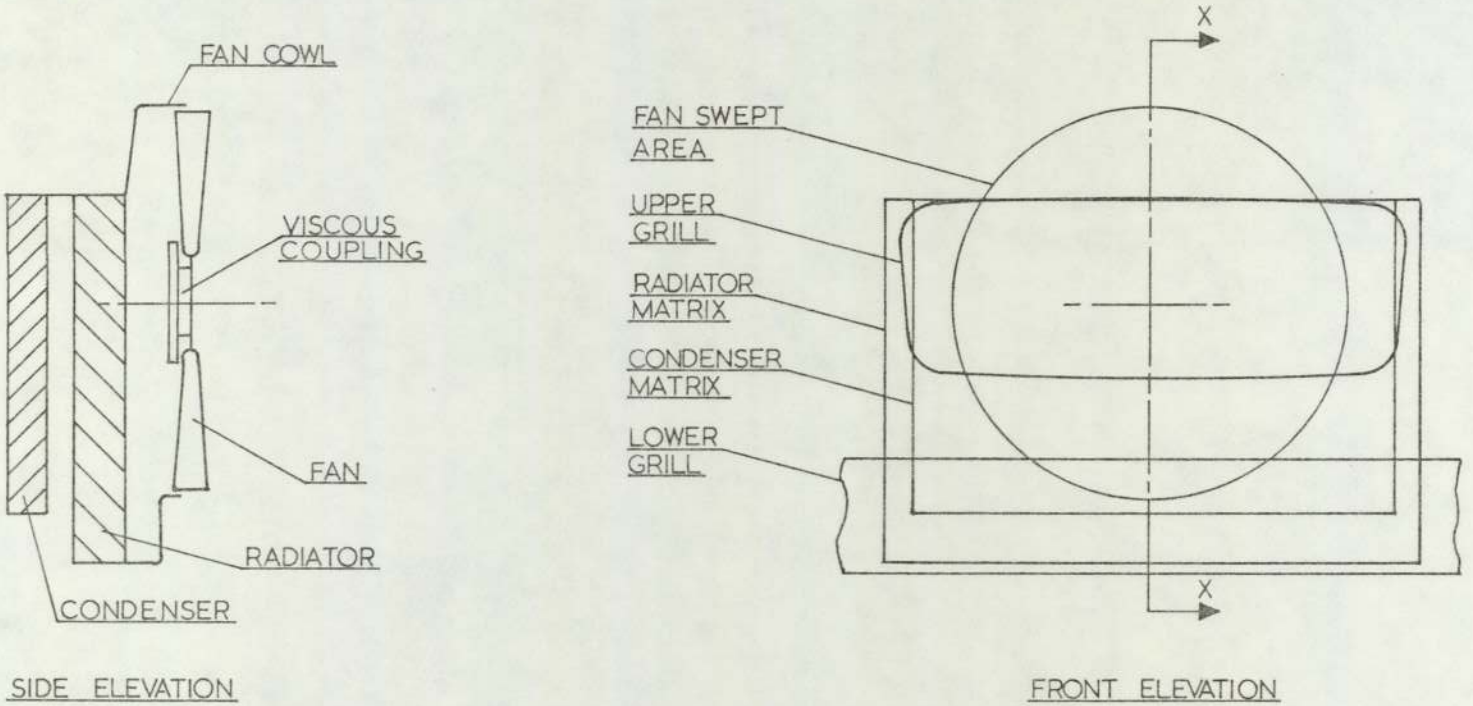

THE RELATIVE POSITIONS OF THE CONDENSER, RADIATOR, FAN AND FAN COWL

GRAPH 3.1

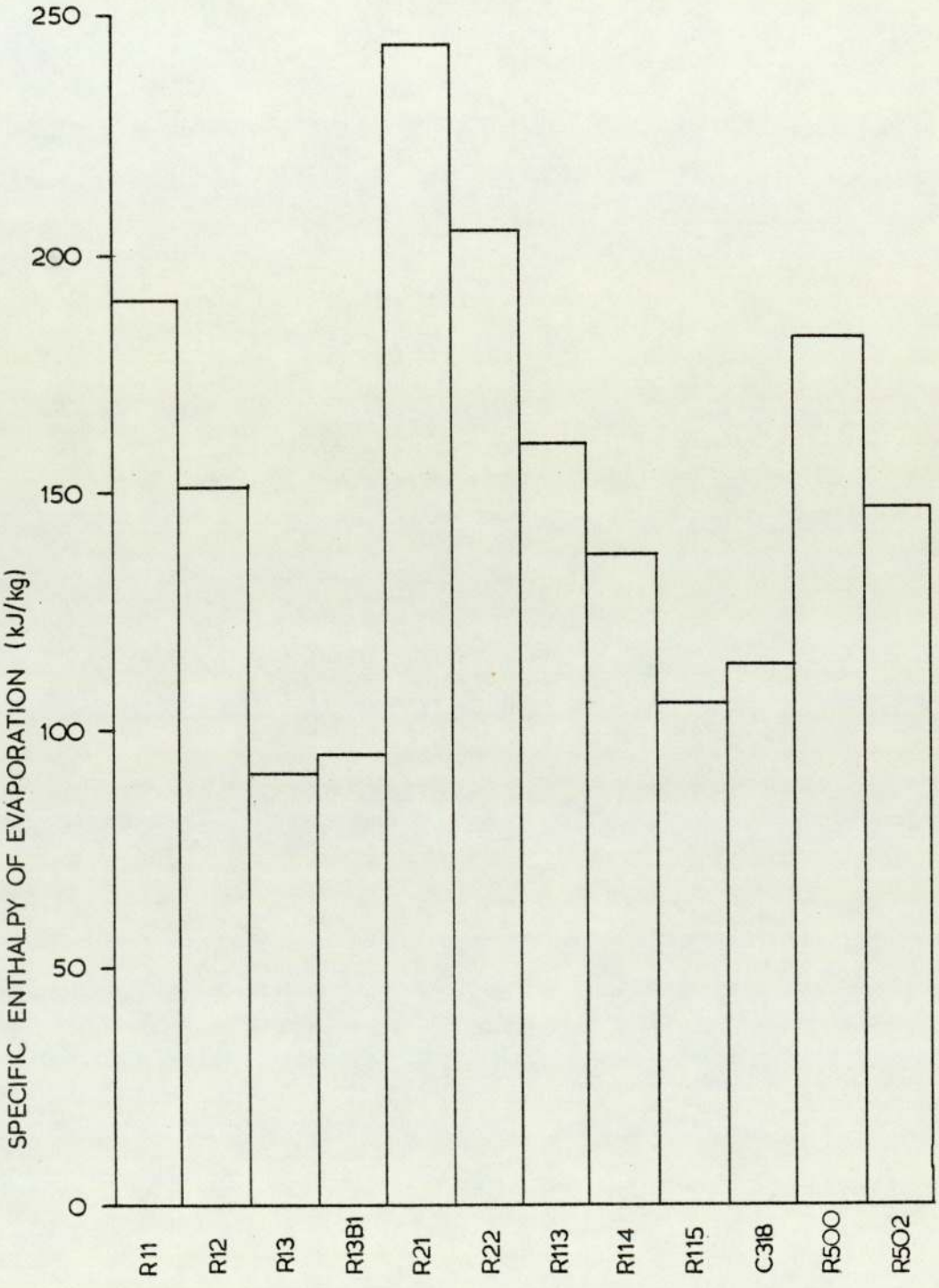

COMPARISON OF SPECIFIC ENTHALPIES OF EVAPORATION OF BS4434[33] GROUP 1 REFRIGERANTS [DATA FROM ASHRAE[32]]

GRAPH 3.2

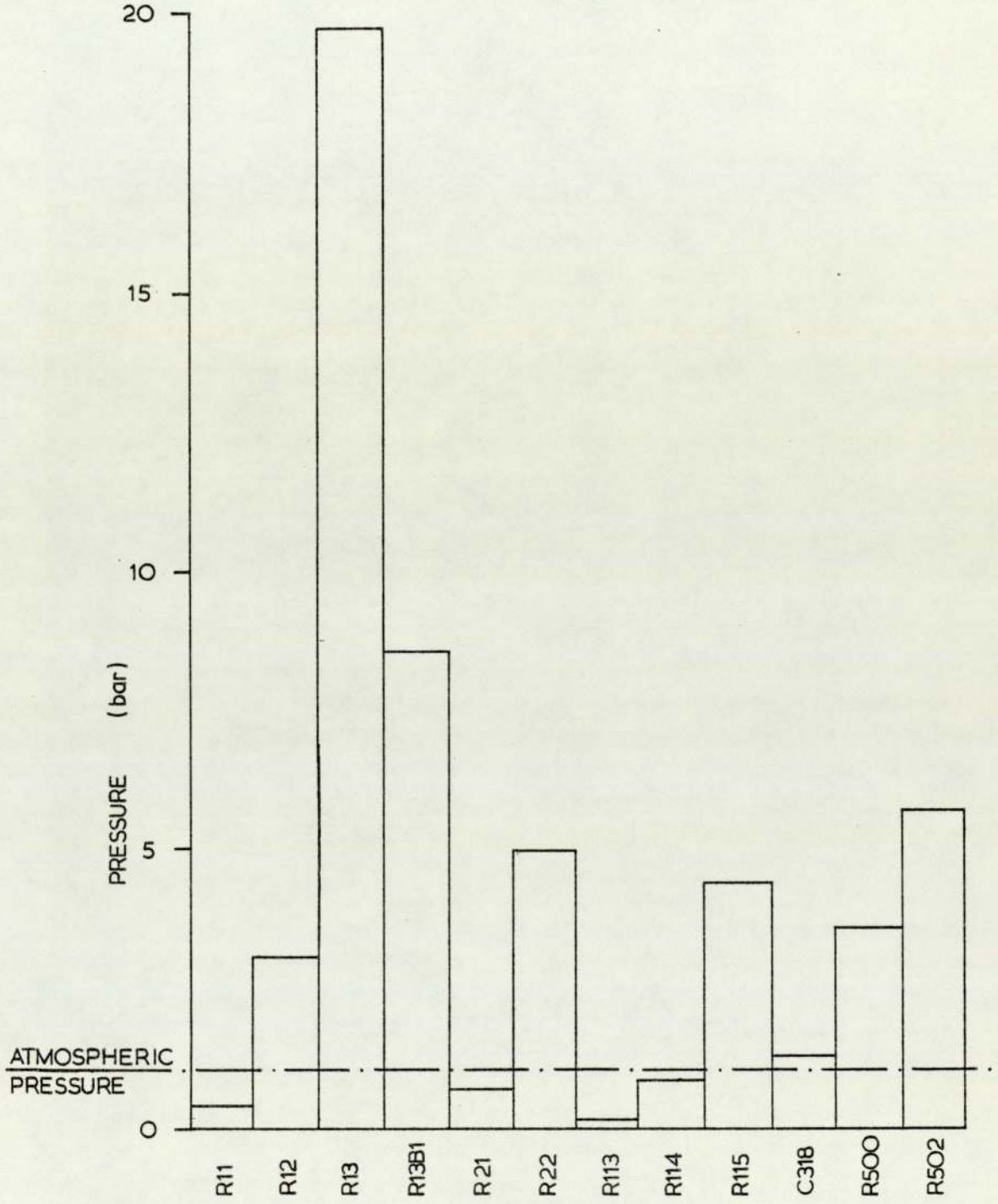

COMPARISON OF SATURATION PRESSURES OF BS 4434[33] GROUP 1 REFRIGERANTS AT 0°C [DATA FROM ASHRAE[32]]

GRAPH 3.3

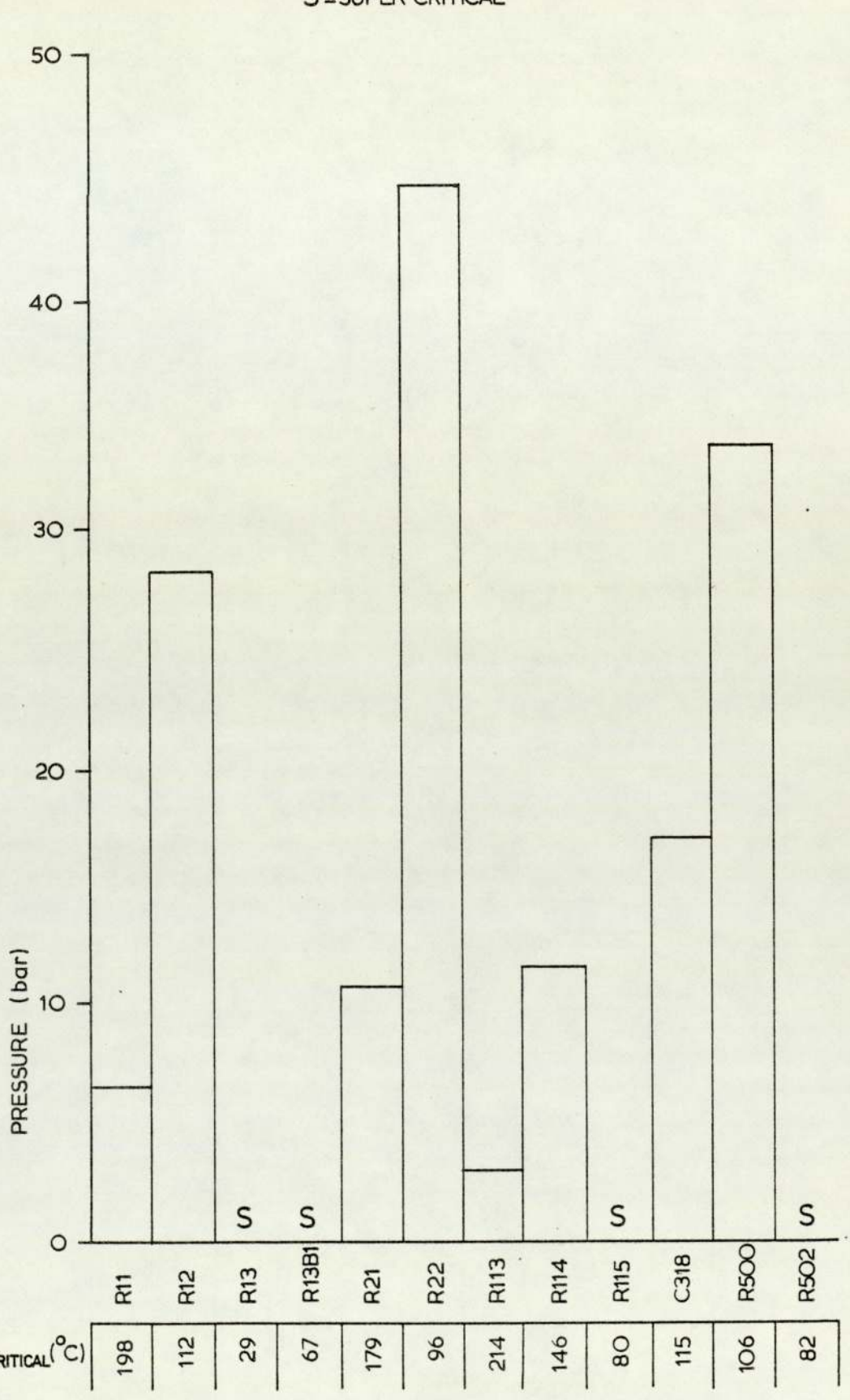

COMPARISON OF SATURATION PRESSURES OF BS 4434[33] GROUP 1 REFRIGERANTS AT 90°C [DATA FROM ASHRAE[32]]

CHAPTER 4

THE MECHANISM OF HEAT REJECTION FROM THE ENGINE AND AIR-CONDITIONING SYSTEM

METHOD OF CORRELATION

As illustrated in chapter 3 the mechanism of heat rejection from both the engine and the air-conditioning system is by forced convection to the atmosphere from extended surface heat exchangers. The velocity of air over these surfaces has an influence on the heat transfer coefficient and also on the mean temperature difference between the air and the heat exchanger surfaces. It is necessary therefore to obtain data on the air velocity over the heat exchangers and on the parameters which control this air flow. The air flow is generated by the forwards motion of the car and by the engine cooling fan.

The forwards motion of the car produces a region at the front where the velocity of the air relative to the car is greatly reduced and the pressure is high. In the region underneath the car the air may be expected to be at a pressure different to atmospheric due to the velocity of the car with respect to the ground. Air passing through the condenser and radiator travels from the high pressure region at the front and is exhausted to the underside of the car. The passage of air in this way must be due to a pressure difference which must equal the frictional pressure drop.

To analyse the system the following assumptions are made:

(a) That compressibility effects may be neglected

(b) That the air flow around the car whilst travelling at some velocity U_v is effectively the same as when the car is stationary with a wind blowing over the car with velocity U_v and the road moving under the car at velocity U_v.

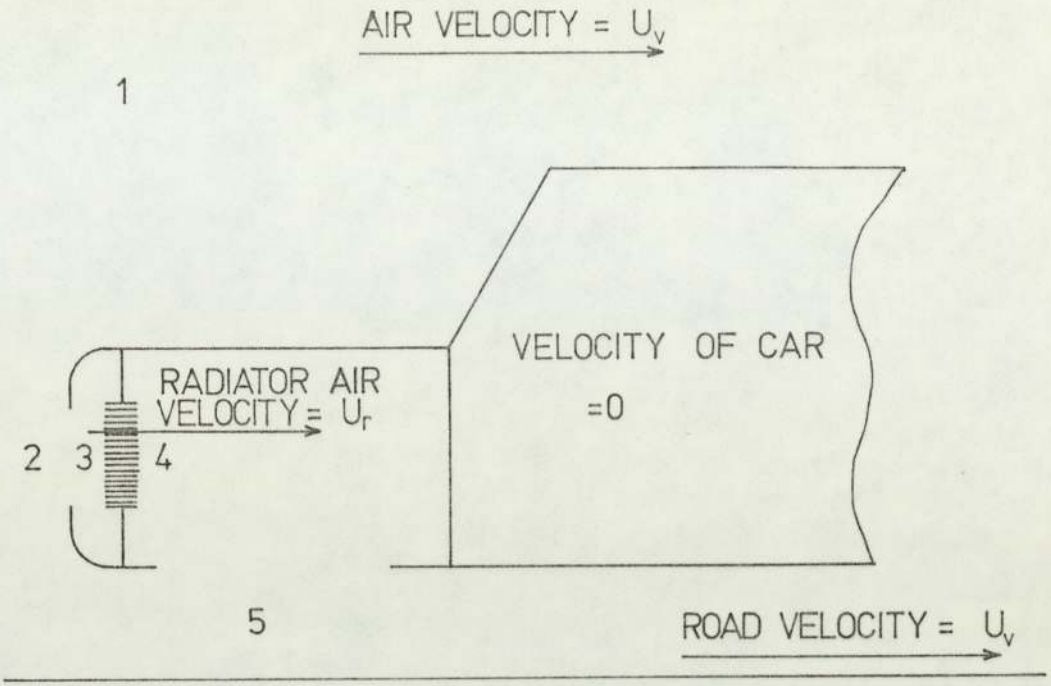

(c) That the pressure at (4) is equal to the pressure at (5) and that the pressure at (5) is independent of the velocity at (4) (i.e. that the volume flow rate from (4) to (5) is small compared with the total volume flow rate past (5) and that there is no constriction between (4) and (5)).

(d) That the pressure at (3) is equal to the pressure at (2) (i.e. the grill does not restrict the air flow).

(e) That the piezometric pressure difference between the free stream at (1) and the underside of the car (5) is directly proportional to the square of the wind and road velocity U_v.

i.e. $$\frac{P_5}{\varrho} = k_v \frac{U_v^2}{2} = \frac{P_4}{\varrho} \qquad 4.1$$

Applying Bernoulli's equation between (1) and (2)

$$\frac{U_v^2}{2} = \frac{U_r^2}{2} + \frac{P_2}{\varrho} \qquad 4.2$$

Applying Bernoulli's equation between (3) and (4)

$$\frac{P_3}{\varrho} = \frac{P_4}{\varrho} + k_r \frac{U_r^2}{2} = \frac{P_2}{\varrho} \qquad 4.3$$

Hence by solving to give U_r in terms of U_v

$$U_r = U_v \sqrt{\frac{1 - k_v}{1 + k_r}} = kU_v \qquad 4.4$$

This suggests a linear relationship between the velocity through the radiator and the car velocity which will later be shown to be the case experimentally. Theoretically the car could be driven with the radiator and condenser removed and k_v calculated from measurement of the air velocity through the radiator orifice. The constant k was however calculated by measurement of U_r and measurement of k_r.

The assumption that the pressure drop across the radiator is proportional to velocity squared is an approximation but variations in k_r with velocity may be compensated for by allowing k_v to vary with U_v. This produces a slightly non linear variation of U_r with U_v in the final relationship when heat exchangers of different pressure/velocity relationships are considered. An alternative would be to assume that k varies slightly with U_v as may be the case, and that k_v is a constant. The former method was chosen for this analysis.

The engine cooling fan has a pressure/volume flow rate characteristic curve which must, at its operating point, be coincident with the pressure/volume flow rate characteristics of the heat exchangers. By measuring these characteristics and by assuming that the velocity is directly proportional to fan speed as suggested by Woods Guide[59] it is possible to calculate the air velocity due to the fan.

Addition of the ram air velocity and the fan air velocity must take account of the influence of the ram air velocity on the fan. For an axial flow fan a low fan speed coupled with a high ram air velocity would produce a turbine effect with the ram air tending to motor the fan. For a paddle bladed centrifugal fan no such reaction is possible. The fan in question was found to behave as the latter case.

The engine cooling fan is driven from the engine crankshaft via a vee belt and a viscous coupling. For a solidly driven fan, the fan air velocity might be assumed to vary linearly as the engine speed, as suggested above. The effect of the viscous coupling is to reduce the fan speed and hence the fan air velocity at car speeds such that the ram air velocity is sufficient to provide adequate cooling. The mechanism by which fan power consumption is reduced may be understood from a simple analysis for which the following assumptions are made:

(a) That the fluid used is newtonian.

(b) That the fluid viscosity does not vary with temperature and hence with power dissipation in the coupling.

(c) That the power consumed by the fan is proportional to the cube of its speed.

(d) That the air velocity is proportional to the speed of the fan.

Free body diagrams involving the fan, viscous coupling and pulley are shown below.

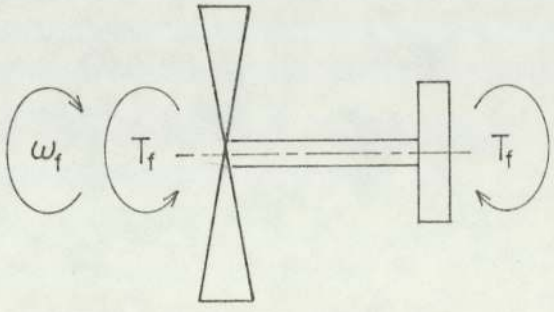

FAN AND OUTER MEMBER OF COUPLING

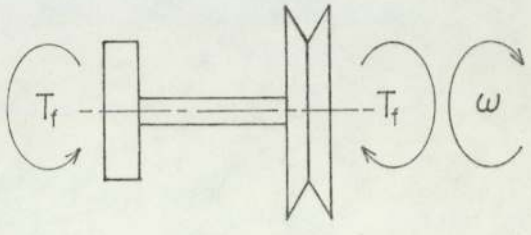

INNER MEMBER OF COUPLING AND DRIVEN PULLEY

From (c): $T_f = k_1 U_r^2$ 4.5

From (a): $k_2 (\omega - \omega_f) = T_f$ 4.6

From (d): $\omega_f = U_r k_3$ 4.7

Solving to give U_r in terms of ω

$$U_r = \frac{k_2 k_3}{2k_1} \left[\sqrt{1 + \frac{4 k_1 \omega}{(k_2 k_3)^2}} - 1 \right] \quad 4.8$$

This is a monotonous relationship (i.e. U_r does not reach a maximum) shown later not to represent experimental data.

Of the assumptions made (b) is the least applicable. As the torque and hence the slip and power dissipation in the coupling increases with speed, the temperature of the fluid increases and its viscosity decreases resulting in increased slip. Equilibrium is reached when the coupling attains a temperature such that heat is generated and dissipated to the airstream at the same rate. Hence a maximum fan speed is reached which cannot be increased by increasing the driven speed of the coupling. To produce a model representing this mechanism completely would require heat transfer data for the coupling and viscosity/temperature data for the fluid. A simple model is sufficient however to predict that at zero driven speed the rate of change of fan speed with driven speed is zero, a factor subsequently used for fitting equations to experimental data.

Air side piezometric pressure drops across extended surface heat exchangers are traditionally correlated as friction factor against Reynolds number. The possible variation in geometry may also be taken into account in terms of non-dimensional geometric ratios. By plotting these dimensionless groups it is possible to see discontinuities in the relationship to suggest a change in the type of flow, i.e. laminar to turbulent. For both the present radiator and condenser, the friction factor has been plotted against Reynolds number and a value of critical Reynolds number obtained. The critical Reynolds number has been assumed to be

independent of changes in the geometry of the heat exchanger, due to variations in fin density or core thickness. This approximation is necessitated by a lack of experimental data at low values of Reynolds number.

Heat transfer and pressure drop data, in terms of j factor and friction factor, are correlated against Reynolds number and the ratio of passage length to mean diameter, for the radiator. The manufacturer's design data[60] is used for calculation of the condenser pressure drop and air side heat transfer coefficient.

For the coolant side heat transfer coefficient of the radiator the familiar Nusselt number, Prandtl number, Reynolds number relationship is used with an experimentally derived constant.

The refrigerant side heat transfer coefficient for the condenser is dealt with in chapter 8.

CONDENSER AIR VELOCITY MEASUREMENTS IN SITU

A hot wire anemometer was developed and calibrated for this purpose. The device and the method of calibration are described in Appendix A1.

Using the hot wire anemometer the air velocity over the condenser was measured under the following conditions.

a) Car stationary, viscous coupling locked

b) Car moving, fan removed

c) Car stationary

d) Car moving in first, second, third, fourth and fifth gears

The tests with the car stationary were carried out with the car indoors to remove the influence of crosswinds. The tests on the moving car were conducted on straight roads at constant speed, the car being driven in both directions. Tests out of doors were not conducted in wet or windy conditions, the wind speed being less than 5 m/s in all cases. Atmospheric pressures were noted during the tests and efforts made to ensure that the nickel wire was kept clean using a soap solution.

RESULTS

The experimental data and computed velocities are listed in Appendix A2.

The plotted data of velocity against engine speed with the viscous coupling locked lie closely about a straight line as shown on graph 4.1. This line was fitted by the method of least squares and constrained through the origin. The gradient of the curve with the viscous coupling unlocked and the car stationary is assumed at zero engine speed to be as for the straight line with the viscous coupling locked, as discussed earlier. Hence a curve of the form:

$$U_{cFan} = A(1 - B\omega^n) \qquad 4.8$$

(where A, B, and n are constants) was fitted to the data by the method of least squares, and found to give a good representation as shown on graph 4.2.

The points plotted for air velocity against road speed with the fan removed were similarly fitted to a straight line constrained through the origin. The fit of this line, as shown on graph 4.3, lends validity to the analysis of the variation of ram air velocity with road speed.

With the car moving and the unlocked viscous coupling driving the fan the combined effect of ram air velocity and fan generated velocity are evident. It was found that the data could be described by an equation of the form:

$$U^2_{cTotal} = U^2_{cFan} + U^2_{cRam} \qquad 4.9$$

Functions of this form are shown plotted with the data on graphs 4.4 to 4.8 inclusive, and deviations from the data tabulated in appendix A2. The logic for this method is that both the fan and the ram effect impart kinetic energy to the air and the function illustrates the effect of adding the kinetic energy from each source. The independence of the kinetic energy imparted by the fan, from the ram air velocity suggests that the fan behaves as a centrifugal fan, as discussed earlier.

By using the function above an equation was developed for the condenser face air velocity:

$$U_c^2 = (Ag_1\omega (1 - B (g_1\omega)^n))^2 + (Cg_2\omega)^2 \qquad 4.10$$

where U is the face velocity, A, B, and C are constants derived from the experimental data, g_1 is the fan pulley gear ratio, g_2 is the car gear ratio and ω is the engine speed. Using this equation it is possible to calculate the condenser air face velocity given any combination of g_1, g_2 and ω. It is also possible by varying the value of B to study the effect of varying the viscosity of the fluid in the viscous coupling, since the slip and B are both dependent on this viscosity.

Using the developed equations the condenser air face velocity has been plotted against road speed in miles/hour on graph 4.9, and against engine speed in rev/min on graph 4.10.

A further ramification of the fitted equations for condenser air face velocity is that knowing the fan power consumption at one speed it is possible to calculate the power consumption of both the fan and viscous coupling as a function of engine speed and pulley ratio.

As above:

$$U_{cFan} = A\omega g_1 (1 - B (\omega g_1)^n) \qquad 4.11$$

and

$$U_{cFan} = A\omega_f \qquad 4.12$$

$$\text{hence: slip} = \omega g_1 - \omega_f = B (\omega g_1)^{n+1} \qquad 4.13$$

Assuming that the torque varies as the square of the fan speed:

$$T_f = k\omega_f^2 = k(\omega g_1)^2 (1 - B(\omega g_1)^n)^2 \qquad 4.14$$

$\therefore$ Power dissipated by coupling

$$= k B(\omega g_1)^{n+3} (1 - B(\omega g_1)^n)^2 \qquad 4.15$$

Power dissipated by fan

$$= k(\omega g_1)^3 (1 - B(\omega g_1)^n)^3 \qquad 4.16$$

Total dissipation by fan and coupling

$$= T_f \omega g_1 \qquad 4.17$$

$$= k(\omega g_1)^3 (1 - B(\omega g_1)^n)^2 \qquad 4.18$$

Using data obtained by the manufacturer[61], of torque against volume flow rate at a fixed fan speed, for an identical fan with the same tip clearance but using a different cowl, the value of k was calculated. As seen from the manufacturers data plotted on graph 4.11, the torque does not vary with volume flow rate over the range of flow rates for which the fan may be used. Using this value of the constant k in the above equations the power dissipation by the fan and coupling are plotted on graph 4.12. Also plotted for comparison is the power which would be consumed were the fan solidly driven, showing the dramatic effect the coupling has in reducing power consumption at high speeds.

MEASUREMENT OF FAN PRESSURE/VOLUME FLOW RATE CHARACTERISTICS

A test rig owned by Smiths Industries of Witney was used to establish data on the present engine cooling fan and fan cowl. This rig is adaptable for the testing of engine cooling fans or extended surface heat exchangers of the type used for car radiators, air-conditioning condensers, car interior heating matrices etc. The rig consists of three chambers of approximately 2m by 2m by 2m. Air enters the first chamber through an aperture. This chamber is fitted with pressure tappings to register the static pressure. Air flows from this chamber through one of a range of nozzle orifices (designed to BS1042 part 1[62]) to the second chamber. Each of the nozzle orifices is provided with a rubber bung, the nozzle selected being the only one unblocked. From the second chamber the air passes through a duct to the third chamber. This duct has a centrifugal fan, driven from

a Ward-Leonard set, and a remotely operated sluice connected in series, to generate and/or control air flow. The third chamber is similarly provided with static pressure tappings as is the first. Air from the third chamber is exhausted to atmosphere through an apperture.

The element to be tested is fitted to either of the appertures on the first or third chamber and by manipulation of the rig fan speed and the sluice, the required volume flow rate may be set and read off an inclined manometer connected to a suitable nozzle orifice. The piezometric pressure drop is read from an inclined manometer connected to the static pressure tappings on the same chamber to which the element being tested is fitted. A mercury barometer and mercury in glass thermometer were provided for the measurement of atmospheric pressure and ambient temperature.

The fan cowl was secured outside the aperture in the third tank and an air-tight seal effected with adhesive tape. The fan was mounted on the shaft of a d.c. electric motor, driven from a Ward-Leonard set, and fitted with an electronic impulse tachometer.

Two tests were carried out:

a) With the ram air flaps unsealed

b) With the ram air flaps sealed with adhesive tape.

In each case the driven speed was maintained at 1,000 rev/min and the volume flow rate varied between zero and the maximum in noted steps, the piezometric pressure difference across the fan being noted at each step. The ambient temperature and barometric pressure were read during the tests. A hand held smoke generator was used to study the air flow pattern around the fan and cowl.

The measured pressures were corrected to standard temperature and pressure by assuming that the piezometric pressure difference varies as the density, as given by Woods[59]. The two sets of results are shown on graph 4.13 to show the absence of leakage through the ram air flaps when unsealed. The curves drawn through the data points for the flaps unsealed are cubic splines for the

purpose of interpolation.

The form of the curve is as may be expected, the rate of pressure rise decreasing as the flow is reduced until the pressure recovers and the flow becomes less stable.

A sketch showing the airflow around the fan is shown in figure 4.1. This is the airflow pattern expected for a centrifugal fan and not an axial flow fan, lending validity to the method of correlating ram air velocity and fan air velocity. This effect may be promoted by the position of the electric motor acting as a bluff body downstream of the fan, but a similar configuration exists in the car with the engine in the same position and somewhat larger than the electric motor.

EVALUATION OF THE FRICTION FACTOR OF THE PRESENT RADIATOR AND CONDENSER TO ESTABLISH VALUES OF THE CRITICAL REYNOLDS NUMBERS

Velocity/piezometric pressure drop data were established experimentally for the radiator and condenser, as fitted to present air-conditioned cars, using the flow rig which was used for the tests on the engine cooling fan. The condenser and radiator in turn were affixed over the aperture in the first (air inlet) chamber and the volume flow rate increased whilst readings were taken of piezometric pressure drop. Atmospheric pressure and ambient temperature were read during the tests.

From the results, values of friction factor and Reynolds number were calculated. The experimental and calculated results data are tabulated in appendix A2. The air velocity was calculated from the volume flow rate and free (minimum) flow area. The mean diameter was calculated for the radiator as a series of triangular passages whose base length equals the fin pitch minus fin thickness and perpendicular height equals the coolant tube spacing. For the condenser the mean diameter was calculated as for a series of parallel plates. The fin geometries of the radiator and condenser are shown on figs. 4.2 and 4.3.

In calculating the velocity and mean diameter for the condenser, no account was taken of the refrigerant tubes. Figures 4.2 and 4.3 show the dimensions of the radiator and condenser.

The friction factor is plotted against Reynolds number on a log-log plot on graph 4.14. Discontinuities exist for both the radiator and condenser at Reynolds numbers of 227 and 329 respectively. At lower Reynolds numbers the form of the functions approximate to rectangular hyperbolas as would be expected for laminar flow. In this laminar region for the radiator the line fitted by the method of least squares has the equation:

$$f = \frac{50.217}{Re^{1.095}} \qquad 4.19$$

The expected equation for an infinitely long smooth circular pipe is:

$$\frac{16}{Re} \qquad 4.20$$

indicating a friction factor of approximately 3.1 times as high as calculated from theory.

For the condenser the equation fitted in the laminar flow region is constrained to have a gradient of -1 on the log-log plot and is

$$f = \frac{85.7}{Re} \qquad 4.21$$

The expected equation for infinitely long flat plates is:

$$f = \frac{24}{Re} \qquad 4.22$$

which indicates that the friction factor is approximately 3.6 times as high as calculated from theory. For both the radiator and condenser the divergence from theory is largely due to the short length (core thickness) of the airflow passages, and also to the existence of louvres on the radiator and tubes and crinkled fin edges on the condenser.

This being the case, the influence of the length to mean diameter ratio on the value of the critical Reynolds number may be considerable as may be other

dimensionless geometric ratios describing the louvres and tubes.

The factors believed to influence the magnitude of the friction factor in laminar flow are also believed to account for the low values of critical Reynolds number when compared to values of 2300 from the literature for smooth circular pipes. A low critical Reynolds number and the resultant turbulent flow at low velocities is desirable in a heat exchanger to promote high surface heat transfer coefficients. To make this an advantage the heat exchanger should be operated with a velocity sufficiently high to ensure that the Reynolds number is higher than the critical value.

DETERMINATION OF THE RADIATOR COOLANT-SIDE HEAT TRANSFER COEFFICIENT

Experimental data[60] from a series of tests carried out by the radiator manufacturer on radiators of similar design to that used on the present car were made available for this project. This data is tabulated in appendix A2. Two sets of test data were used for evaluation of the coolant-side heat transfer coefficient, each of these sets of data giving a variation of coolant and air flow rates for particular radiator dimensions.

Overall conductance was calculated using the equation due to Stevens[63] given by Rohsenow and Hartnett[64] for cross flow heat exchangers. By assuming fluid mixing on the coolant side the calculation is greatly simplified, and the air off temperature is only used for calculation of the bulk temperature and fluid properties, which for both coolant and air was taken as the arithmetic mean. Errors arising from the assumption of coolant mixing are less significant if the coolant temperature change is small, which is the case in practice but not at the high air flow rates and low coolant flow rates in some of the experimental results. A constant fin efficiency on the air side is assumed.

The overall conductance is the inverse of the sum of the resistances and assuming a zero resistance for the copper of the tubes the resistances considered

are those on the coolant side and the air side. McAdams[65] gives the following equation for the forced convection heat transfer coefficient inside a smooth circular tube.

$$Nu = 0.023 \ Re^{0.8} \ Pr^{0.4}, \text{ where } Re > 10^5 \qquad 4.23$$

For both the air side and water side, the heat transfer coefficients are assumed to vary as the mass velocity to the power of 0.8 as given in this equation.

Hence:

$$\frac{1}{U_{OVERALL}} = \frac{C_1}{m_{water}^{0.8}} + \frac{C_2}{m_{air}^{0.8}} \qquad 4.24$$

This equation was fitted separately to the data for the two radiator tests by the method of least squares to find the value of C_1. The data and fitted equations are plotted on graphs 4.15 and 4.16. The resultant coolant side equation became:

$$Nu = 0.0138 \ Re^{0.8} \ Pr^{0.4} \qquad 4.25$$

- for the two row 1.59 mm fin pitch radiator, and

$$Nu = 0.0136 \ Re^{0.8} \ Pr^{0.4} \qquad 4.26$$

- for the three row 2.12 mm fin pitch radiator, assuming indexes of 0.8 and 0.4 for the Reynolds number and Prandtl number respectively. Properties were calculated from the data of Mayhew and Rogers[66] at a temperature of 80°C. The agreement between these figures indicates that the method and result of the calculations is a good approximation. A mean value of the constant of 0.0137 was subsequently used. Although water was used in these tests on the radiators, the dimensionless equation is assumed to be applicable to other fluids and was subsequently used for a water antifreeze mixture as used in the car. The properties of a 45/55 water antifreeze mixture were obtained from the antifreeze manufacturers[67], and were also taken at 80°C.

CORRELATION OF AIR SIDE j AND f FACTORS WITH REYNOLDS NUMBER AND FIN GEOMETRY

For the radiators tested by the radiator manufacturer[60] and tabulated in Appendix A2, the following dimensionless equations were fitted:

$$f = A_1 Re^{b_1} (L/d)^{c_1} \qquad 4.27$$

$$j = A_2 Re^{b_2} (L/d)^{c_2} \qquad 4.28$$

where d is the mean diameter and L is the core thickness, and A_1, b_1, c_1, A_2, b_2, c_2 are constants. Properties of air and water were calculated using polynomials fitted to data from Mayhew and Rogers[66] and for both were taken at the arithmetic mean bulk temperatures. The overall conductance was calculated using the equation due to Stevens[63] as for the determination of radiator coolant side heat transfer coefficient. The water side heat transfer coefficient was calculated using the Nusselt number, Prandtl number, Reynolds number relationship developed earlier. The thermal resistance of the tubes was assumed to be zero. The fin efficiency was calculated iteratively using the relationship

$$\eta_{fin} = \frac{\tanh x}{x} \qquad 4.29$$

$$\text{where } x = W_f \sqrt{\frac{h}{2t\,k}}$$

where:

W_f is the fin width measured between the tubes,

h is the surface heat transfer coefficient,

k is the thermal conductivity of the fin material,

t is the fin thickness.

The conductivity of the copper fins was taken to be constant, and a value of 400W/mK given by the manufacturers[60] used. The mean diameter was calculated for the air passages by the method described earlier. The characteristic length L

is taken to be the core thickness. The area of flow is the minimum open area of the matrix as before.

The resultant calculated values of j and f are plotted against Reynolds number on graphs 4.17 and 4.18. Also shown are the fitted equations at the values of (L/d) used. The fitted coefficients of equation 4.27 are:

$A_1 = 3.122$

$b_1 = -0.40$

$c_1 = -0.33$

and for equation 4.28 are:

$A_2 = 1.478$

$b_2 = -0.48$

$c_2 = -0.47$

The R.M.S. deviations of j and f are 8.4% and 5.8% respectively. Comparison with the equation fitted for turbulent flow through the present radiator using data obtained at Smiths Industries gives a mean deviation of 14.5% from that data over the range of Reynolds number of 500 to 5000. This is probably due both to the inadequacy of the equation in Reynolds number and (L/d) to represent the data and also the scatter of the data.

From the experience gained by measuring the velocity/pressure drop relationship for the present radiator and condenser at Smiths Industries laboratory, an expression of the form:

$$f = (A_3 + B_3 Re^n)\ (A_4 + B_4\ (L/d)^m) \qquad 4.30$$

where A_3, B_3, n, A_4, B_4, and m are constants, would give a more accurate fit to experimental data. The data currently available on this particular pattern of radiator is insufficient in both quantity and quality to permit this.

For turbulent flow through a smooth circular pipe of infinite length and a Prandtl number of 1:

$$\frac{f}{j} = 2 \qquad 4.31$$

For the relationship established here for j and f the higher ratio of approximately 6 is probably due to the losses at the exit from the air passages. This multiple of 3 is consistant with the earlier comparison of the friction factor with a simple theoretical analysis in the laminar region.

The expected similarity between j and f suggests that a similar relationship to equation 4.30 would also provide a better representation of j.

CONDENSER AIR SIDE PIEZOMETRIC PRESSURE DROP AND HEAT TRANSFER COEFFICIENT

Experimental data, on the pattern of heat exchanger used as a condenser, made available by the manufacturer[60] is insufficient in quantity, for analysis by the method used for the radiator. Design data from the same source[60] on this unit was made available in graphical form. The following is an algebraic representation of this data.

$$h = 1.716 \times R/F \times U_c^{0.57} \qquad 4.32$$

$$P = 8.284 \times R/F \times U_c^{1.74} \qquad 4.33$$

where P is the pressure drop in N/m^2, R is the number of tube rows, F is the fin pitch, and h is the heat transfer coefficient in W/m^2 of face area. U_c is the condenser face velocity.

COMPARISON OF RADIATOR AND CONDENSER AIR VELOCITIES

As shown in chapter 3, the physical layout of the radiator, condenser, fan cowl, and engine cooling fan is such that the radiator completely covers the fan cowl, but the condenser of smaller area does not. This configuration renders analysis of the air flow impossible except on the basis of potential flow. Potential

flow analysis in this situation would be exceedingly complex and probably yield results of poor accuracy. The method of analysis used here is based on the following assumptions:

a) The velocity of air flowing through that portion of the radiator shadowed by the condenser is the same as for the condenser.

b) The piezometric pressure drop experienced by the fan is that due to the radiator and condenser in series with an air velocity equal on each.

c) The volume flow rate, pressure rise characteristics of the engine cooling fan are unaffected by the close proximity of the radiator matrix.

Following these assumptions and using the data obtained with the hot wire anemometer, the friction factor/Reynolds number relationship was developed from the manufacturer's data on the radiator, the velocity/pressure drop design data on the condenser, and the data obtained on the engine cooling fan. The condenser velocity was found to be 15.5% greater than the radiator velocity. This is as might be expected from the layout of the components.

Using the same method, a mathematical model was developed to calculate the radiator and condenser air velocities for any combination of fin pitches and core thicknesses. The model was extended to include the effects of ram air velocity, calculated from equation 4.4. The ratio of condenser air velocity to radiator air velocity is assumed to remain constant and to be an effect of the component layout. This model is included in Appendix A5 in the form of a computer program. An improvement, especially with regard to the influence of ram air velocity, would result from measurement of the radiator air velocity using a similar hot wire anemometer covering the area of the radiator matrix.

An improved hot wire anemometer, giving a more accurate mean velocity over the area of flow and/or a matrix of point velocities, is suggested and described in appendix A1. This may be a useful instrument for the development of engine cooling fans and fan cowls.

RESULTS OBTAINED BY THE CAR MANUFACTURER FOR THE AIR FLOW RATE THROUGH THE RADIATOR

Volume air flow rates through the radiator of the car have been measured by the sponsor with the car stationary and the viscous coupling locked. The method adopted was to attach a sharp edged circular duct to the front of the car and sealed such that all of the air passing through the radiator passed first through this duct. The air velocity was measured at the entrance to the duct using a vane anemometer and was assumed to be uniform over the cross section. The vane anemometer which gives a direct reading of velocity has since been calibrated in a wind tunnel, of cross-section approximately ten times the diameter of the anemometer, against a pitot static tube giving a reading of kinetic head on a Chattock gauge. A plot of the radiator air velocity using the results thus corrected, against engine speed is shown on graph 4.19 and the corrected results tabulated in appendix A2. The resultant air volume flow rate, at a fan speed equal to that used when testing the fan volume flow rate/pressure rise characteristic, is apparently greater than the fan can achieve against a zero pressure head. Two reasons for this discrepancy are that the close proximity of the radiator has an influence on the fan characteristics and/or the assumption that the velocity profile at the entrance to the duct is uniform. The latter reason is the most credible and invalidates the test except as a method of comparing two systems.

A method which would yield more accurate data on volume air flow rate is to use a conical inlet duct as recommended by The Fan Manufacturers' Association[68]. The advantage of this device is that the flow rate is calculated from a pressure head on an inclined manometer, the density of air, and an established coefficient. A disadvantage which remains is that the nozzle produces an increased head against which the fan has to work. It would be possible to use a rig similar to that owned by Smiths Industries and used for the fan, radiator, and condenser tests. Such a rig would, however, be expensive, cumbersome, and only be usable with the vehicle stationary.

FIGURE 4.1

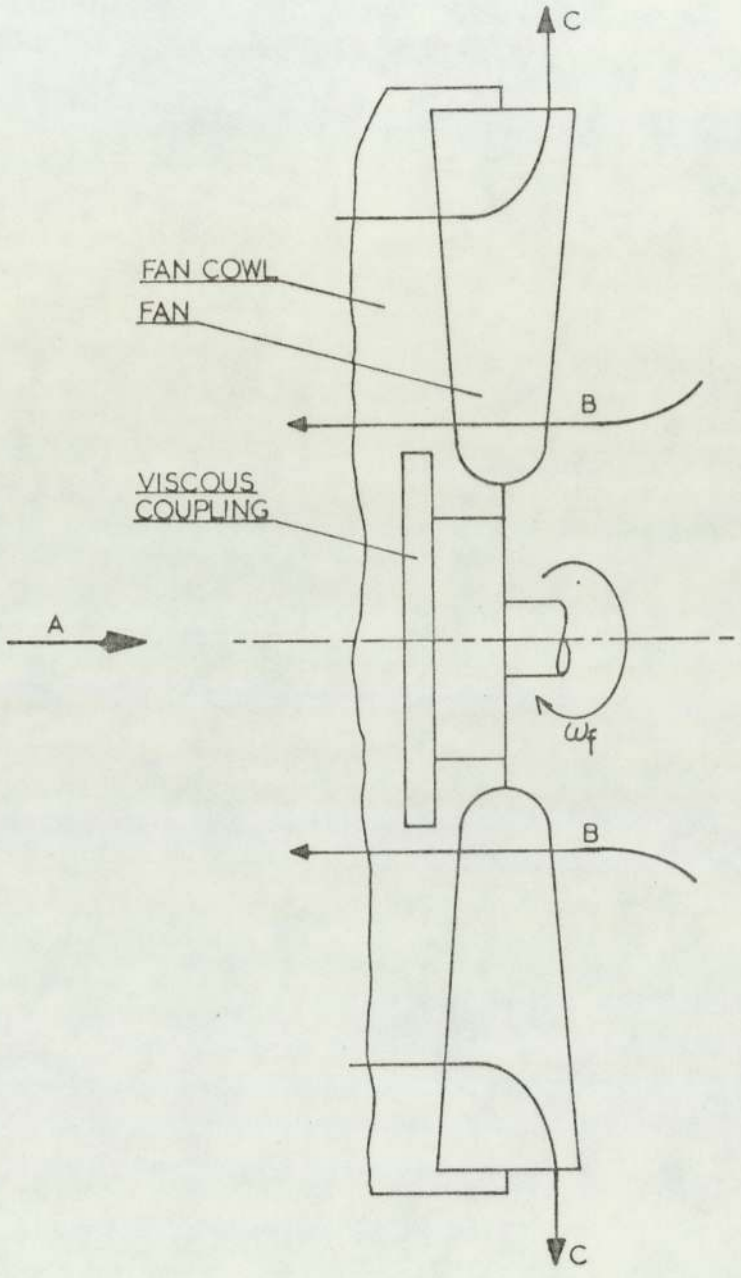

THE OBSERVED
AIR FLOW AROUND THE
ENGINE COOLING FAN

A VOLUME AIR FLOW
B LOW VELOCITY REVERSE FLOW
C HIGH VELOCITY RADIAL FLOW

FIGURE 4·2

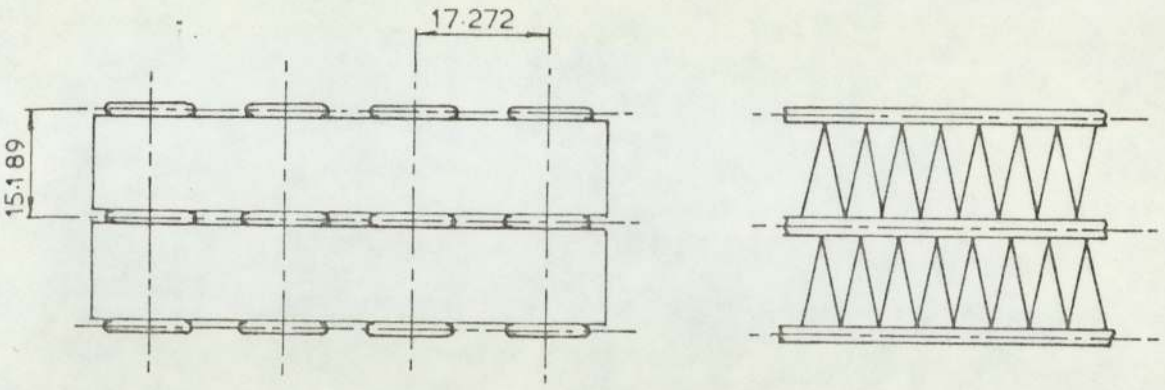

THE CORE ASSEMBLY

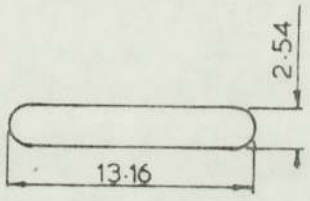

THE COOLANT TUBE

TINNED COPPER 0·127 WALL THICKNESS

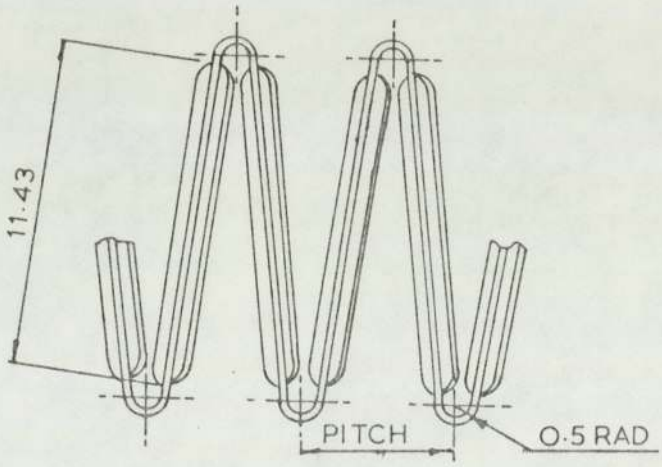

FIN COPPER 0·0533 GAUGE

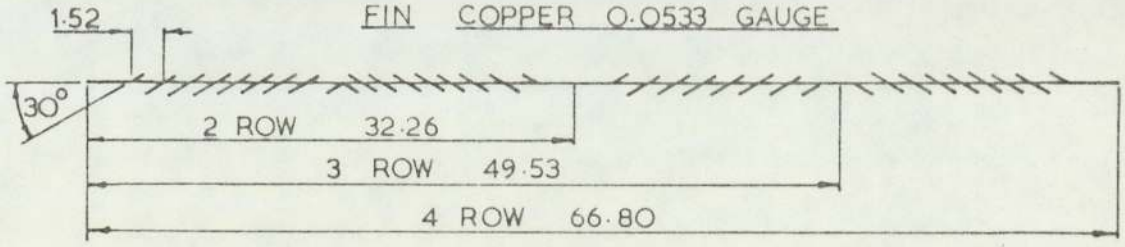

MARSTON RADIATORS'[60] SUPAPACK I RADIATOR

CORE GEOMETRY

DIMENSIONS IN mm

FIGURE 4.3

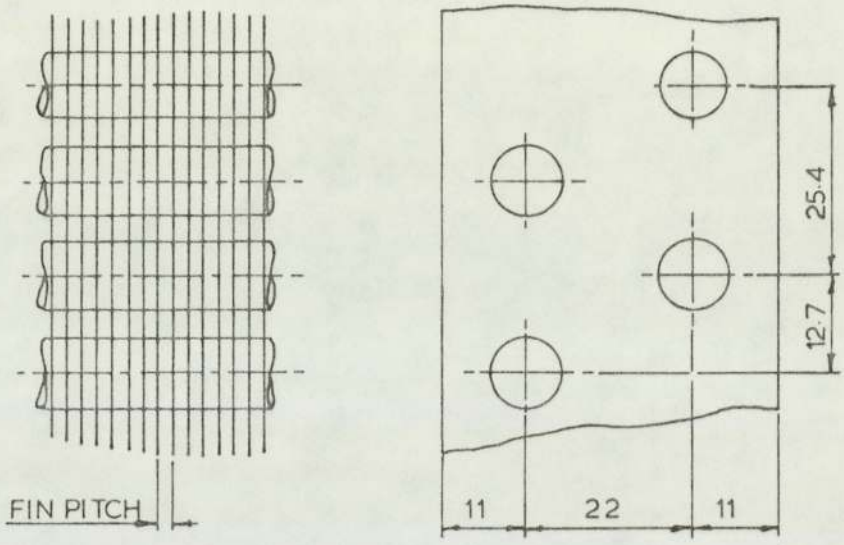

FINS-ALUMINIUM 0.152 THICK

TUBES COPPER 9.52 DIA 0.508 WALL THICKNESS

THE CONDENSER GEOMETRY (FROM REFERENCE 60)

DIMENSION IN mm

GRAPH 4.1

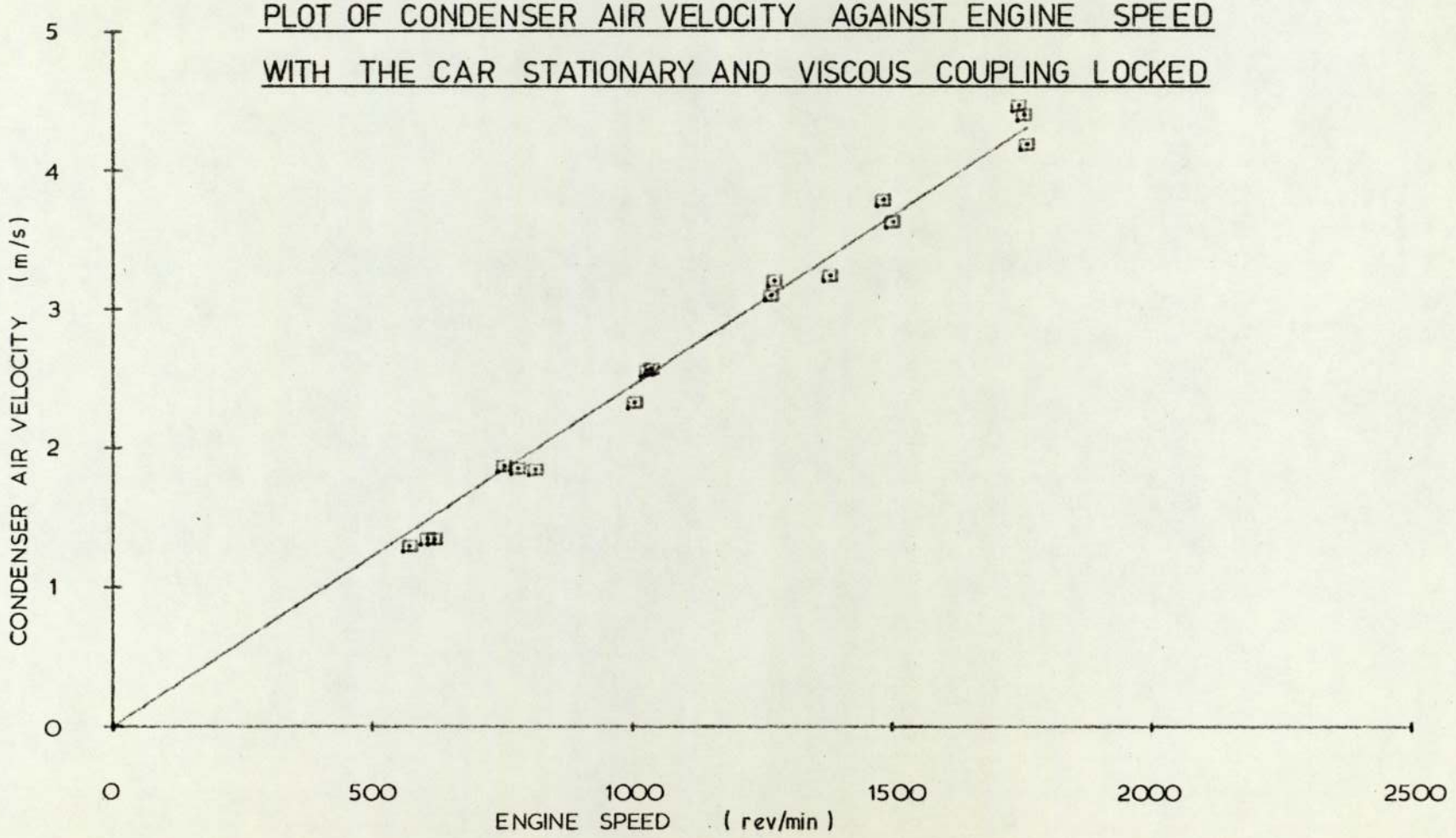
PLOT OF CONDENSER AIR VELOCITY AGAINST ENGINE SPEED
WITH THE CAR STATIONARY AND VISCOUS COUPLING LOCKED
CONDENSER AIR VELOCITY (m/s)
0
1
2
3
4
5
0
500
1000
1500
2000
2500
ENGINE SPEED (rev/min)

GRAPH 4.2

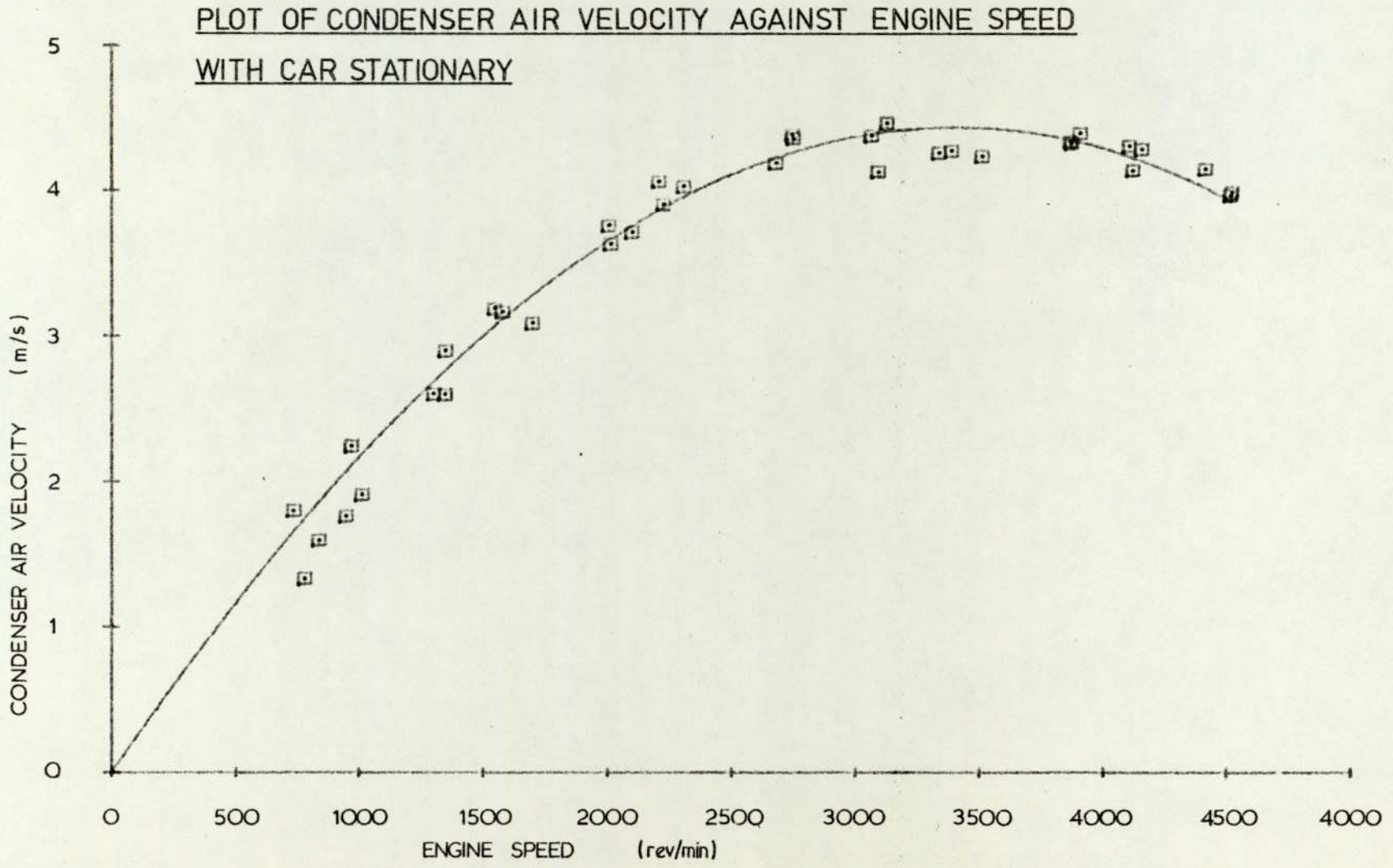
PLOT OF CONDENSER AIR VELOCITY AGAINST ENGINE SPEED
WITH CAR STATIONARY
CONDENSER AIR VELOCITY (m/s)
0
1
2
3
4
5
0
500
1000
1500
2000
2500
3000
3500
4000
4500
4000
ENGINE SPEED (rev/min)

GRAPH 4.3

PLOT OF CONDENSER AIR VELOCITY AGAINST ROAD SPEED WITH FAN REMOVED

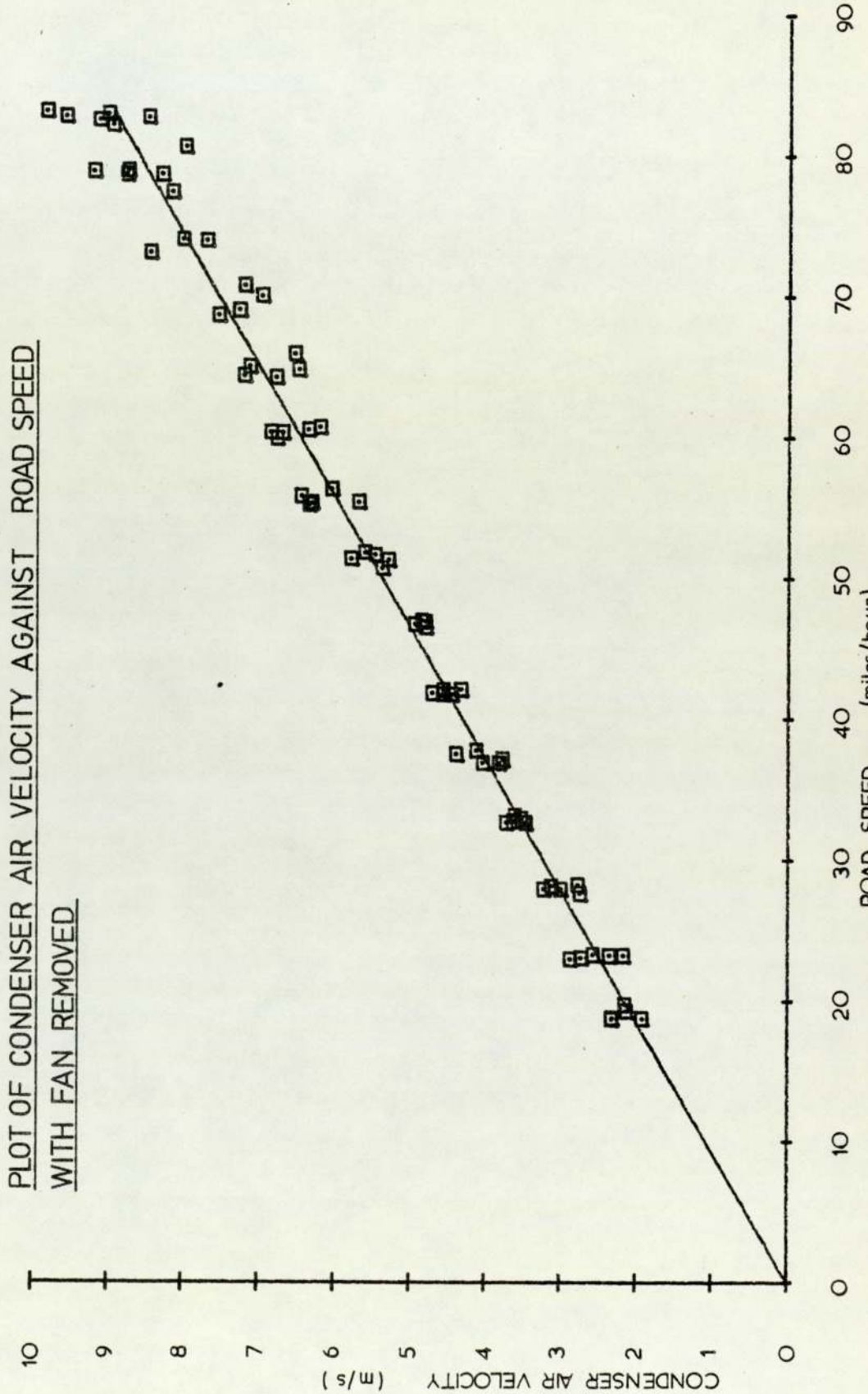

GRAPH 4.4

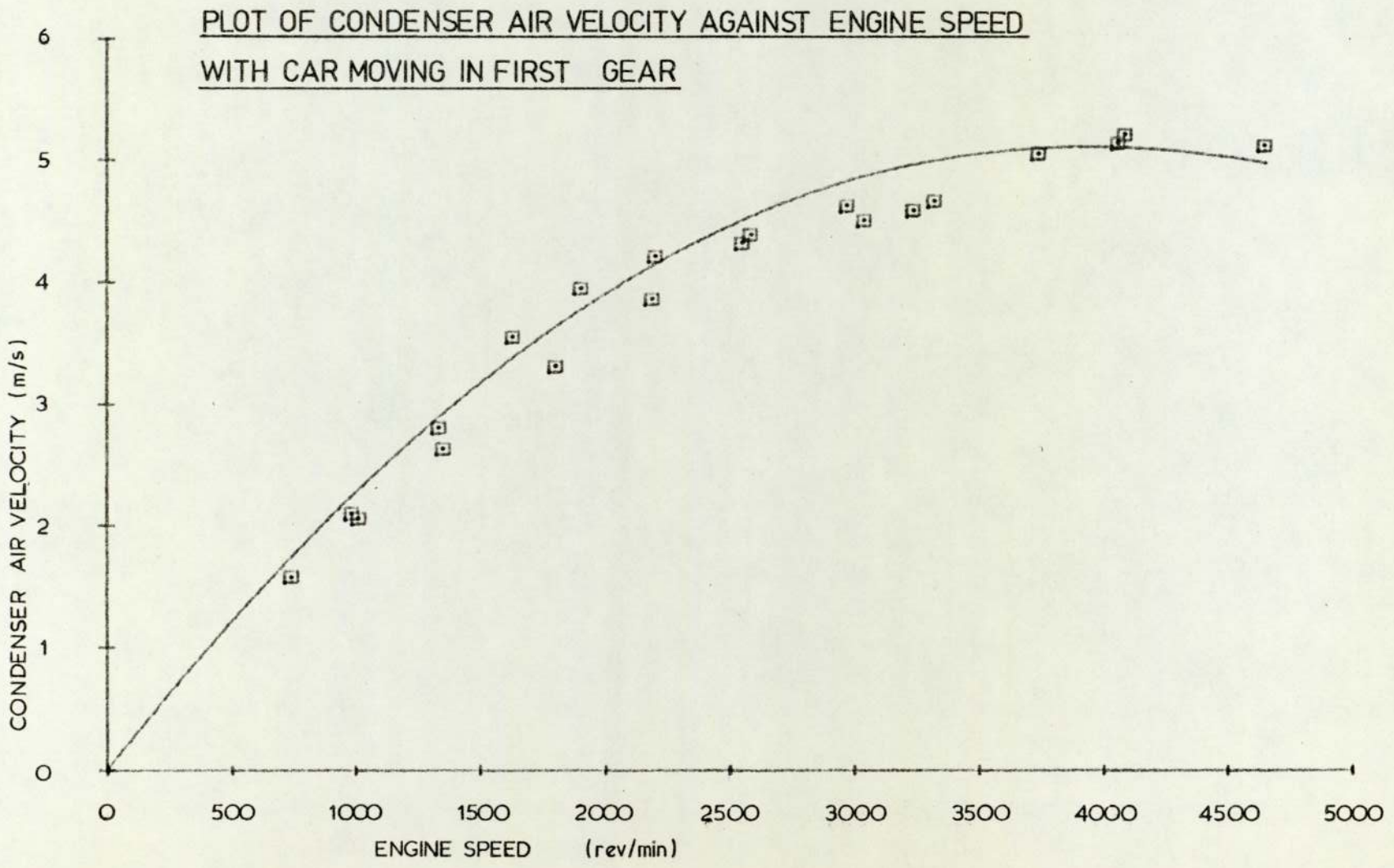
PLOT OF CONDENSER AIR VELOCITY AGAINST ENGINE SPEED
WITH CAR MOVING IN FIRST GEAR
CONDENSER AIR VELOCITY (m/s)
0
1
2
3
4
5
6
0
500
1000
1500
2000
2500
3000
3500
4000
4500
5000
ENGINE SPEED (rev/min)

GRAPH 4.5

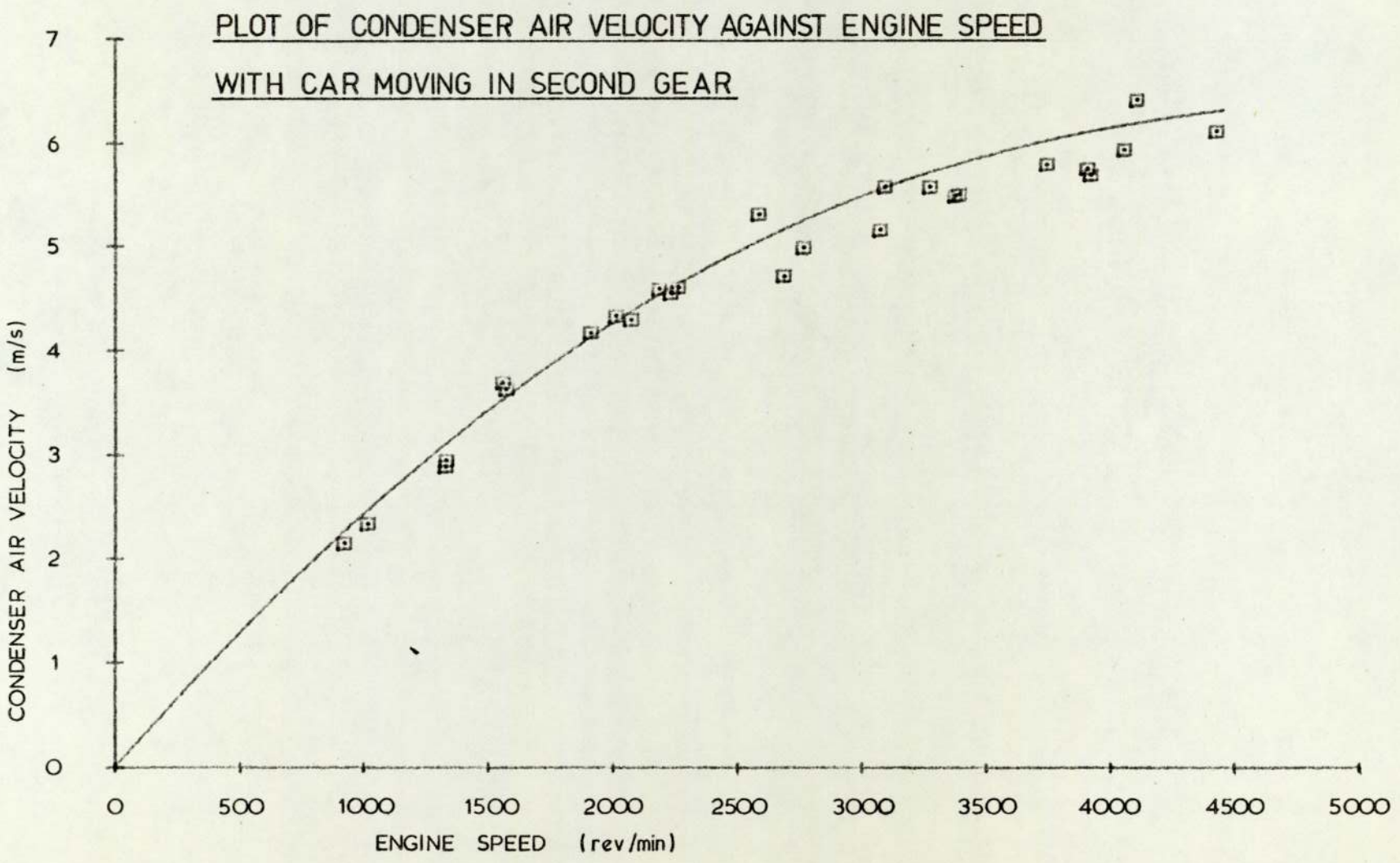
PLOT OF CONDENSER AIR VELOCITY AGAINST ENGINE SPEED
WITH CAR MOVING IN SECOND GEAR
CONDENSER AIR VELOCITY (m/s)
0
1
2
3
4
5
6
7
0
500
1000
1500
2000
2500
3000
3500
4000
4500
5000
ENGINE SPEED (rev/min)

GRAPH 4.6

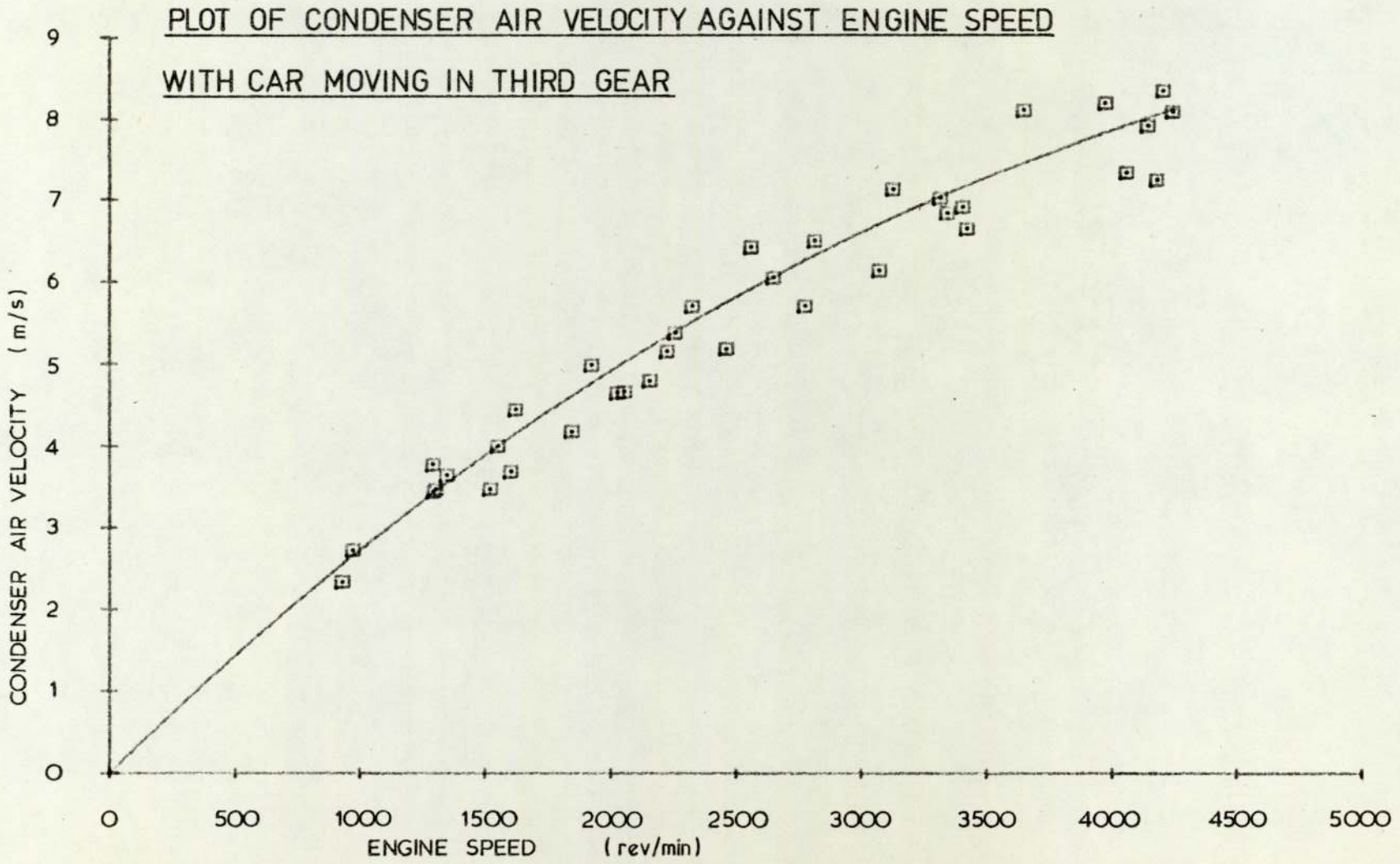
PLOT OF CONDENSER AIR VELOCITY AGAINST ENGINE SPEED
WITH CAR MOVING IN THIRD GEAR
CONDENSER AIR VELOCITY (m/s)
0
1
2
3
4
5
6
7
8
9
0
500
1000
1500
2000
2500
3000
3500
4000
4500
5000
ENGINE SPEED (rev/min)

GRAPH 4.7

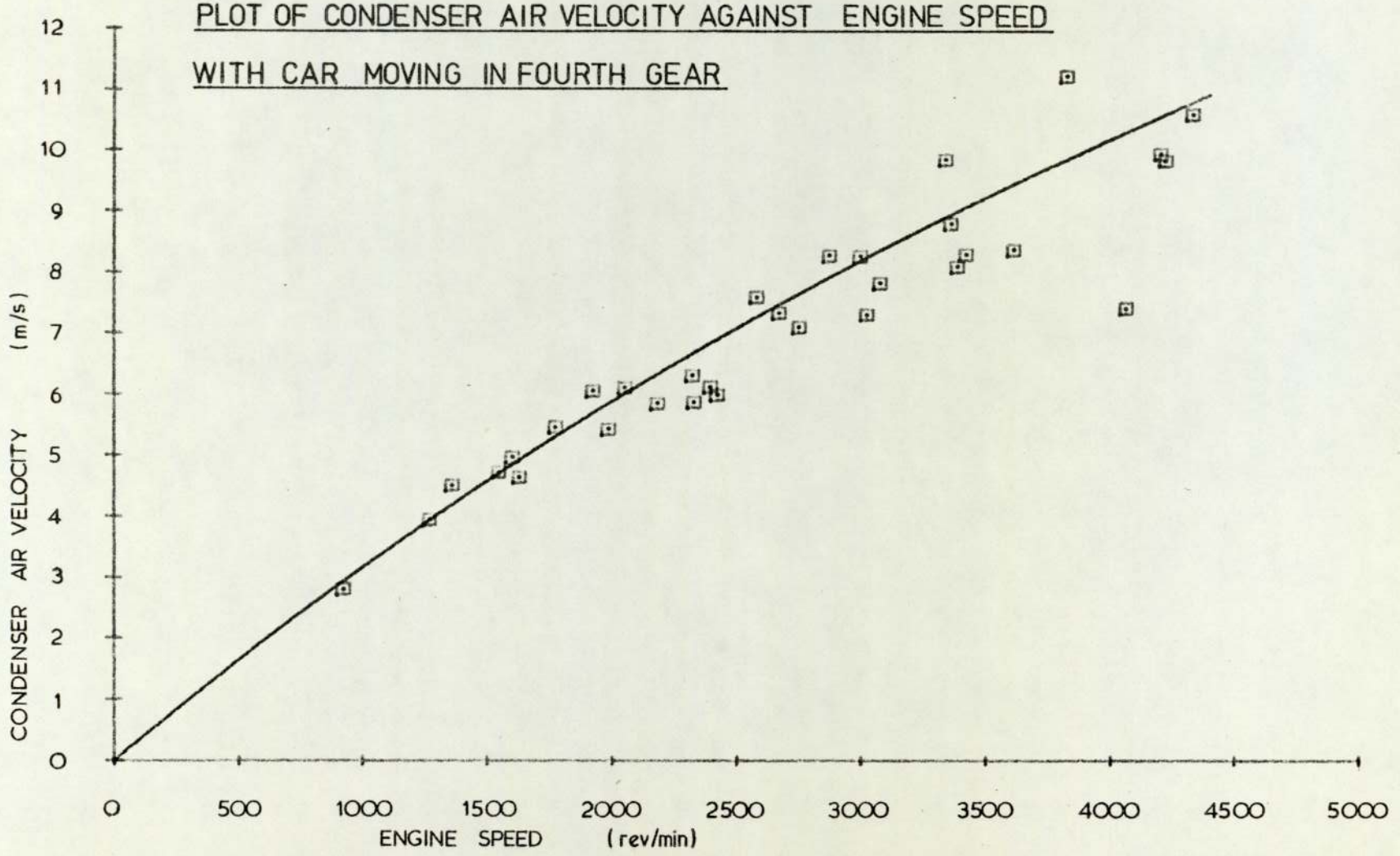
PLOT OF CONDENSER AIR VELOCITY AGAINST ENGINE SPEED
WITH CAR MOVING IN FOURTH GEAR
CONDENSER AIR VELOCITY (m/s)
0
1
2
3
4
5
6
7
8
9
10
11
12
0
500
1000
1500
2000
2500
3000
3500
4000
4500
5000
ENGINE SPEED (rev/min)

GRAPH 4.8

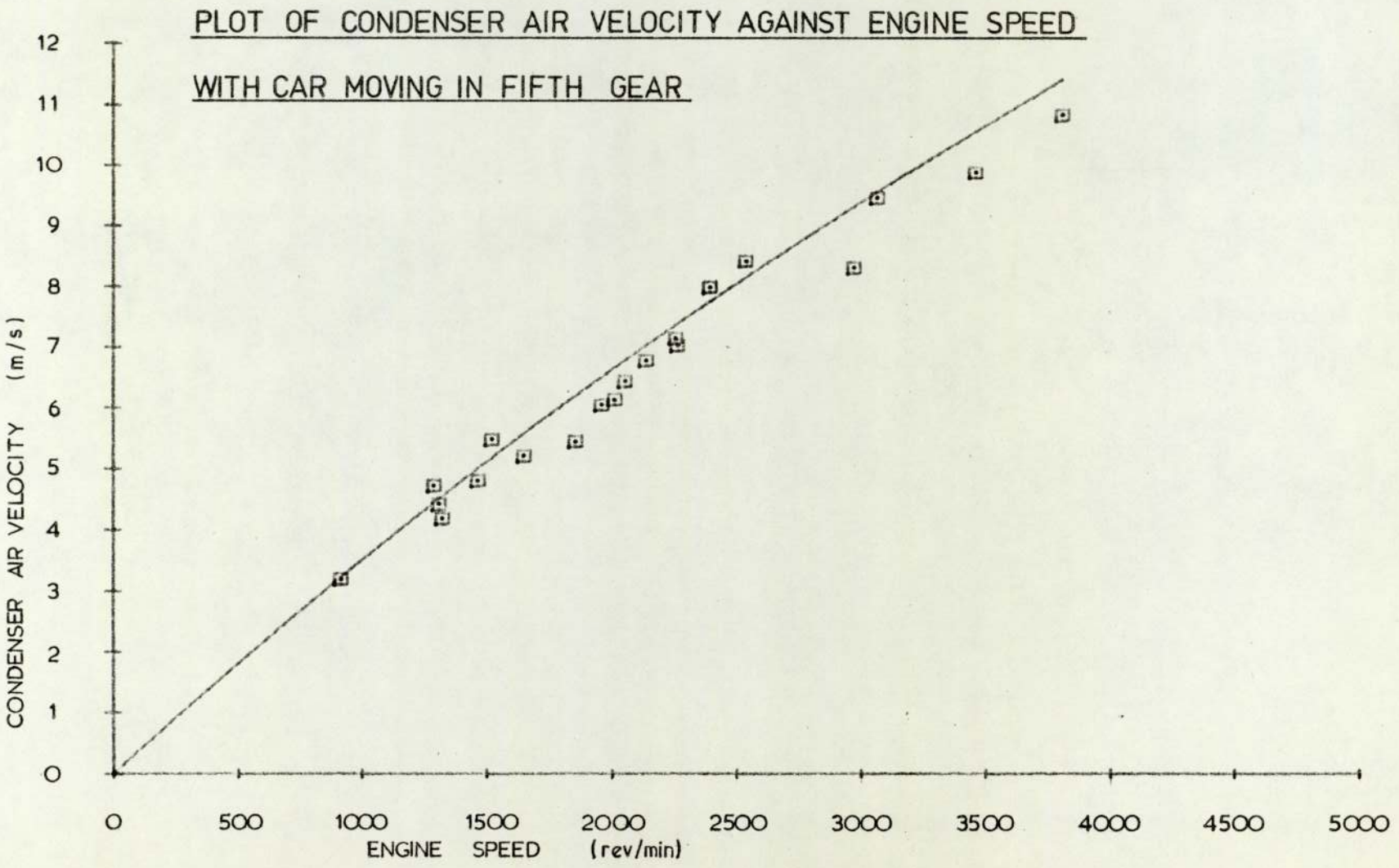
PLOT OF CONDENSER AIR VELOCITY AGAINST ENGINE SPEED
WITH CAR MOVING IN FIFTH GEAR
CONDENSER AIR VELOCITY (m/s)
0
1
2
3
4
5
6
7
8
9
10
11
12
0
500
1000
1500
2000
2500
3000
3500
4000
4500
5000
ENGINE SPEED (rev/min)

GRAPH 4.9

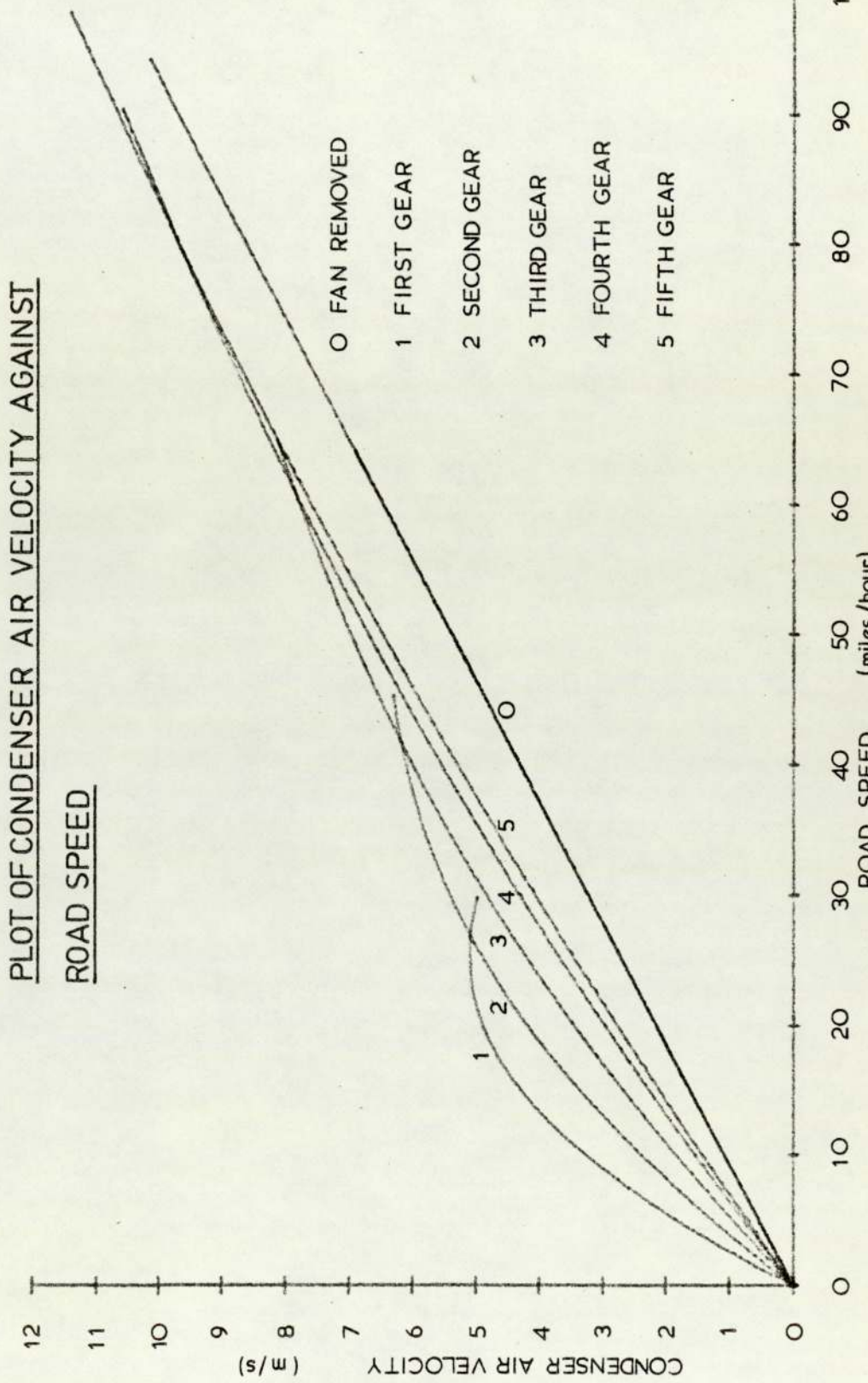
PLOT OF CONDENSER AIR VELOCITY AGAINST
ROAD SPEED
CONDENSER AIR VELOCITY (m/s)
ROAD SPEED (miles/hour)
0 FAN REMOVED
1 FIRST GEAR
2 SECOND GEAR
3 THIRD GEAR
4 FOURTH GEAR
5 FIFTH GEAR
0
1
2
3
4
5
0
10
20
30
40
50
60
70
80
90
100
1
2
3
4
5
6
7
8
9
10
11
12

GRAPH 4.10

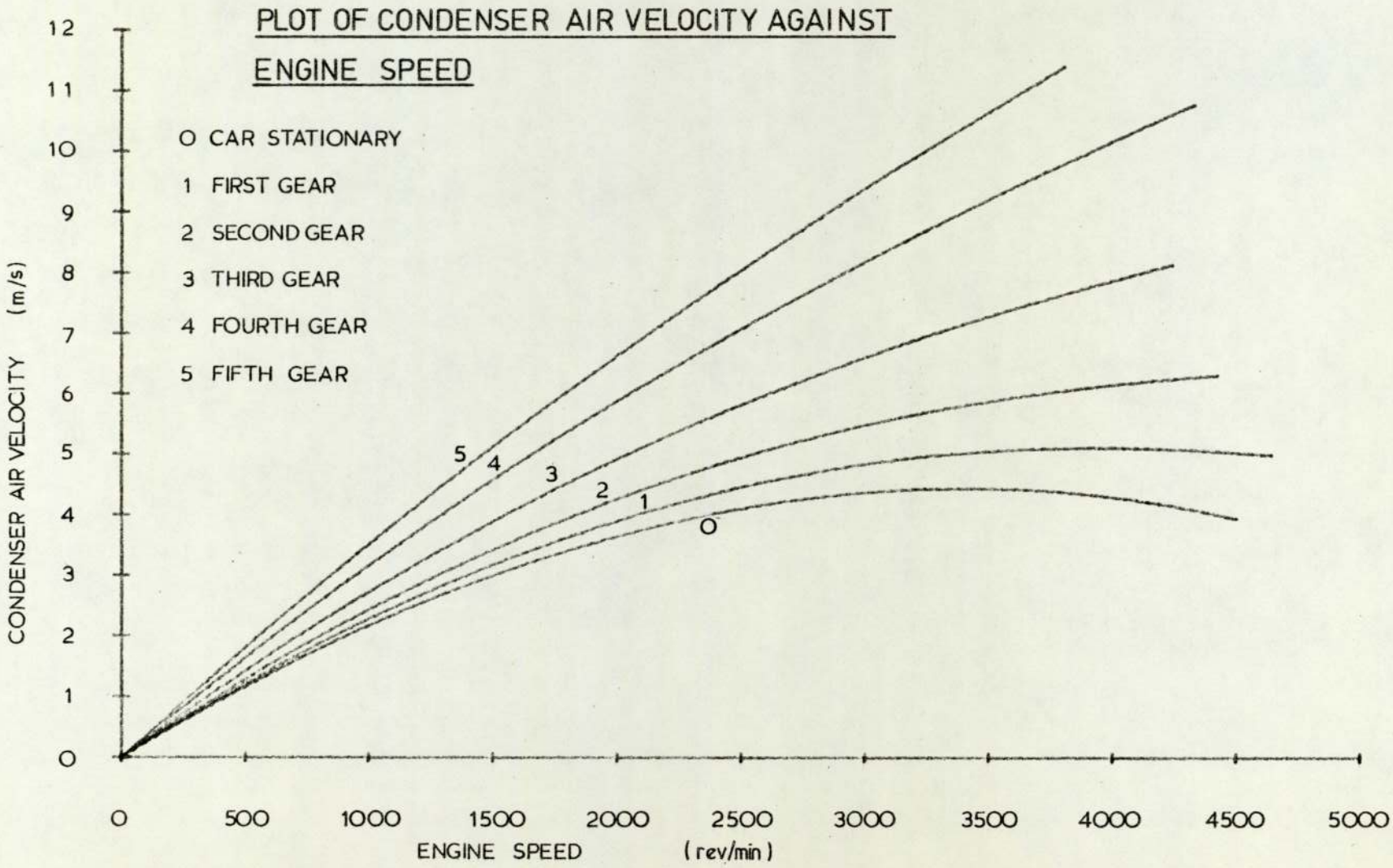
PLOT OF CONDENSER AIR VELOCITY AGAINST ENGINE SPEED
O CAR STATIONARY
1 FIRST GEAR
2 SECOND GEAR
3 THIRD GEAR
4 FOURTH GEAR
5 FIFTH GEAR
CONDENSER AIR VELOCITY (m/s)
0
1
2
3
4
5
6
7
8
9
10
11
12
0
500
1000
1500
2000
2500
3000
3500
4000
4500
5000
ENGINE SPEED (rev/min)

GRAPH 4.11

PLOT OF THE POWER CONSUMPTION OF THE ENGINE COOLING FAN AT 1000 rev/min FAN SPEED [FROM REFERENCE 61]

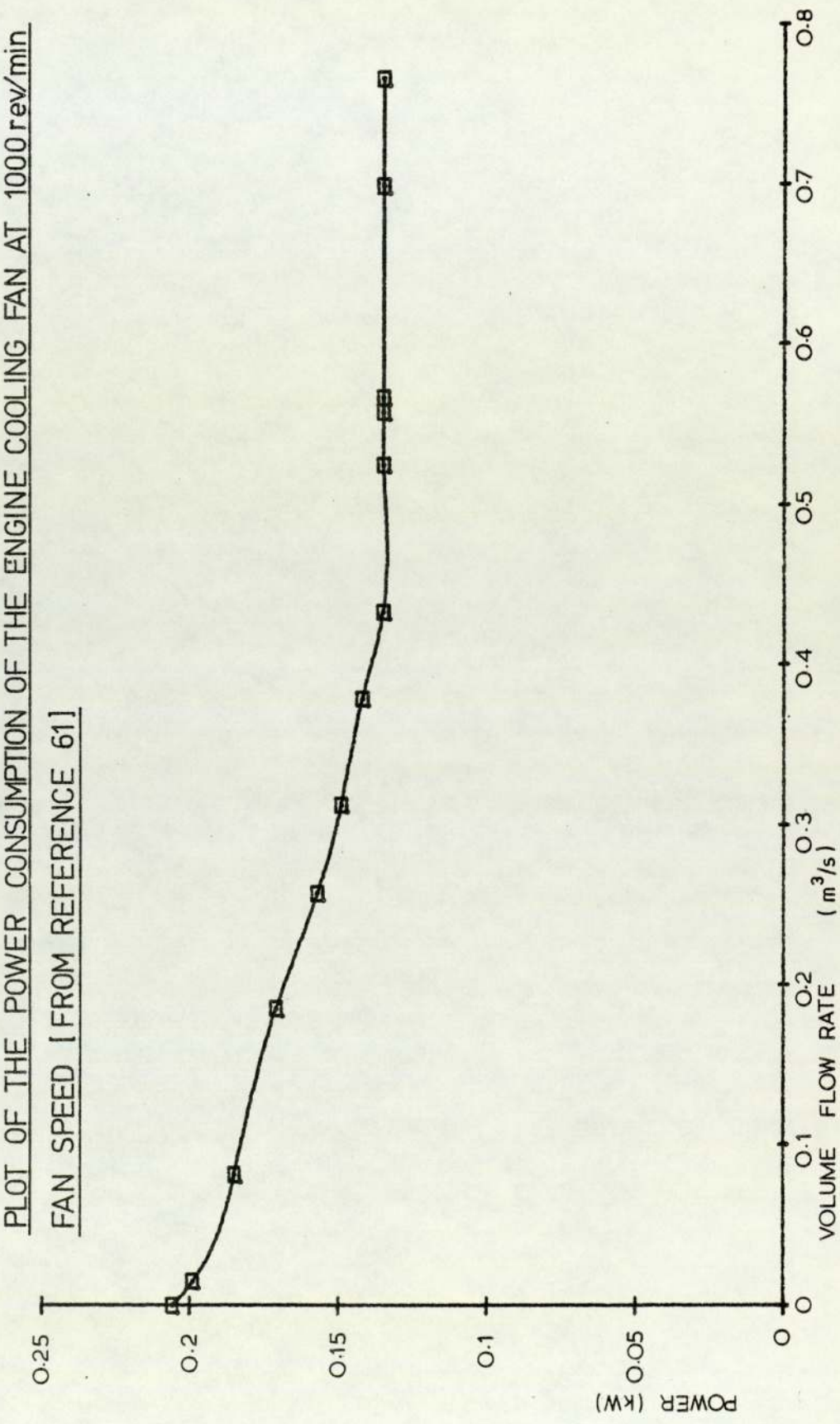

GRAPH 4.12

PLOT OF POWER CONSUMPTION BY FAN AND VISCOUS COUPLING AGAINST ENGINE SPEED

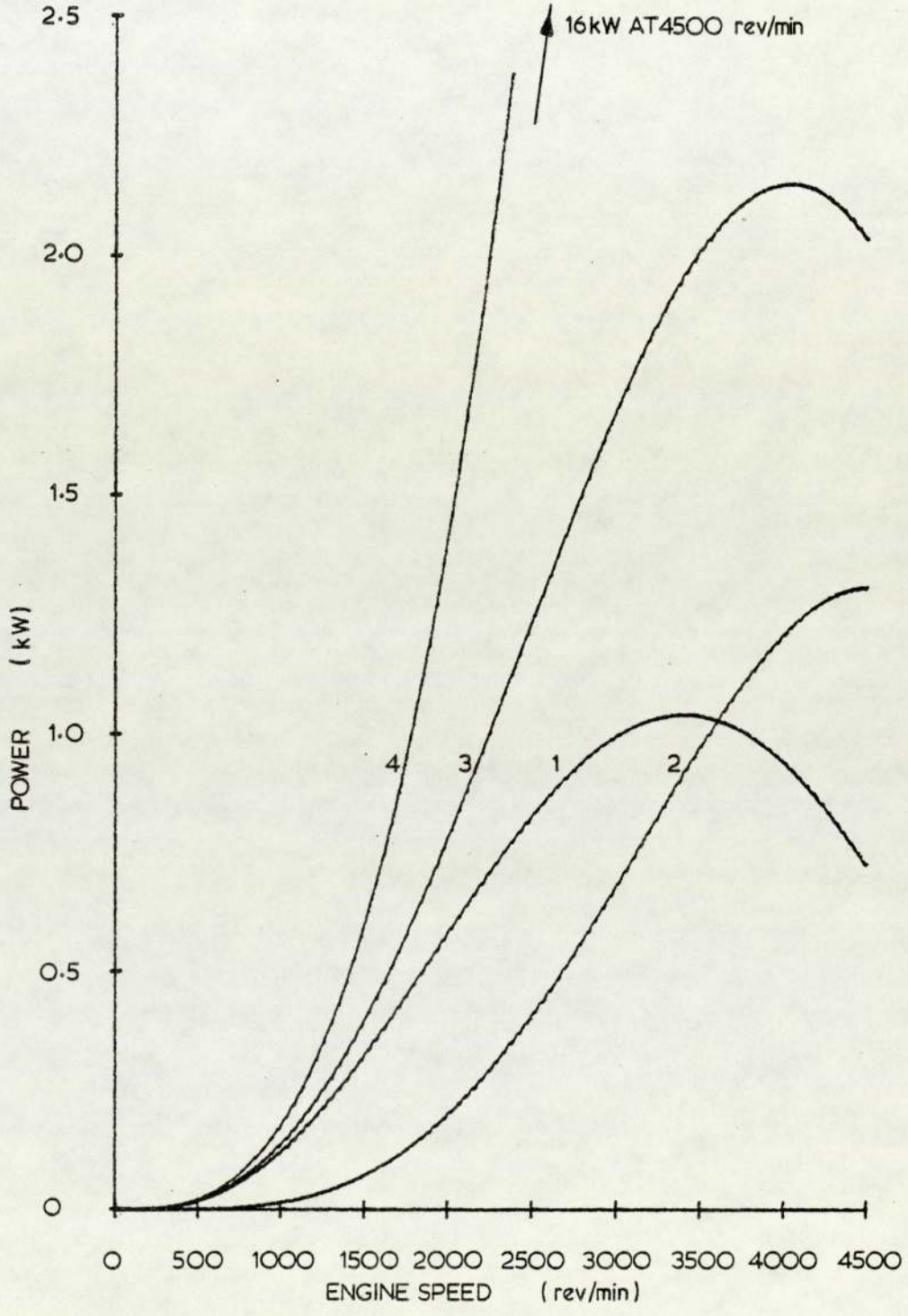

1 POWER TO FAN

2 POWER TO VISCOUS COUPLING

3 TOTAL POWER CONSUMPTION

4 POWER CONSUMPTION OF FAN WITH SOLID DRIVE

GRAPH 4.13

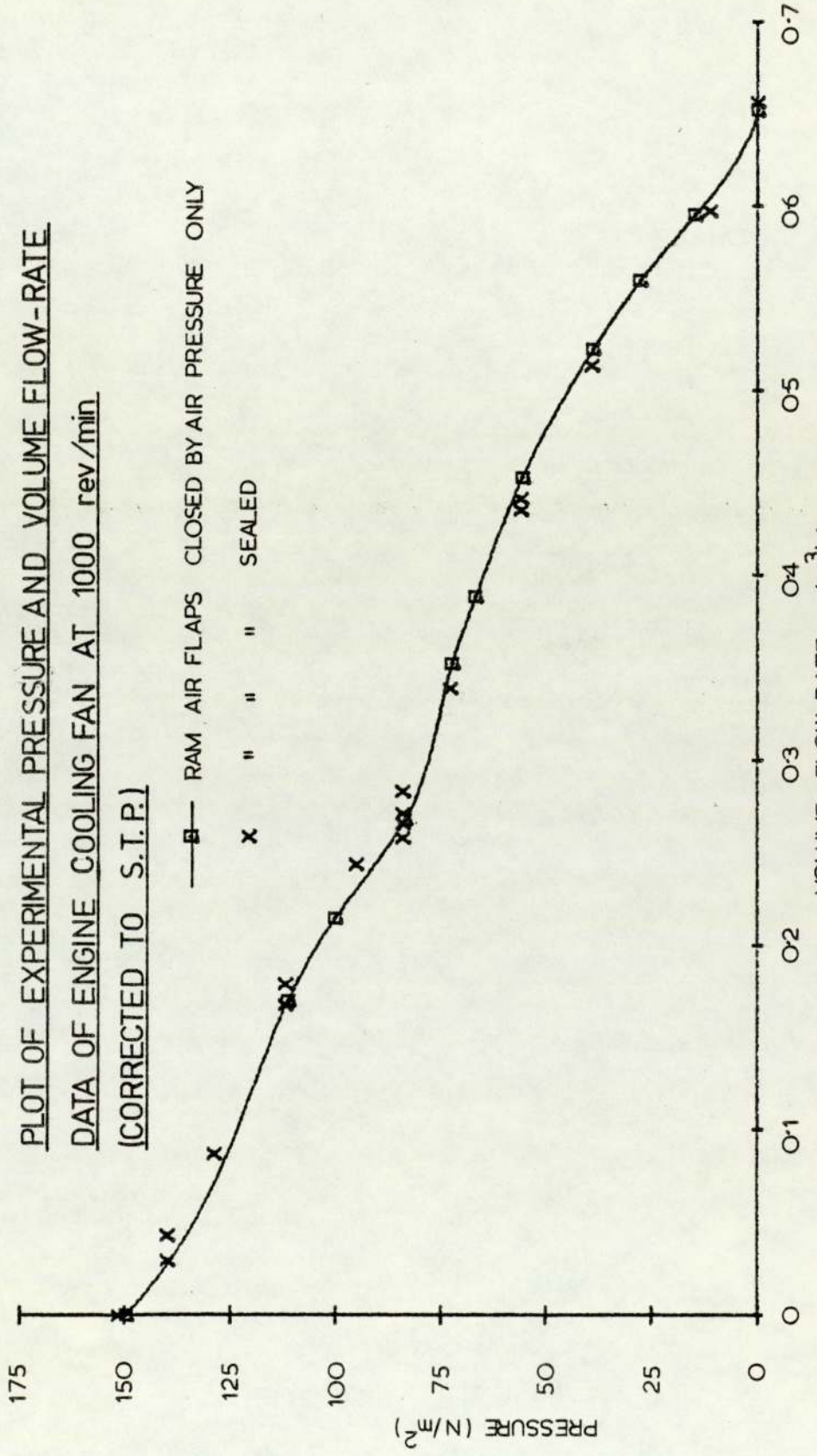
PLOT OF EXPERIMENTAL PRESSURE AND VOLUME FLOW-RATE
DATA OF ENGINE COOLING FAN AT 1000 rev/min
(CORRECTED TO S.T.P.)
RAM AIR FLAPS CLOSED BY AIR PRESSURE ONLY
" " " SEALED
PRESSURE (N/m²)
VOLUME FLOW RATE (m³/s)
0
25
50
75
100
125
150
175
0·1
0·2
0·3
0·4
0·5
0·6
0·7

GRAPH 4.14

LOG-LOG PLOT OF f AGAINST Re FOR JAGUAR XJ6 RADIATOR (MARSTON RADIATOR'S SUPACK I), AND CONDENSER (MARSTON RADIATOR'S SHIPLEY FINCOIL)

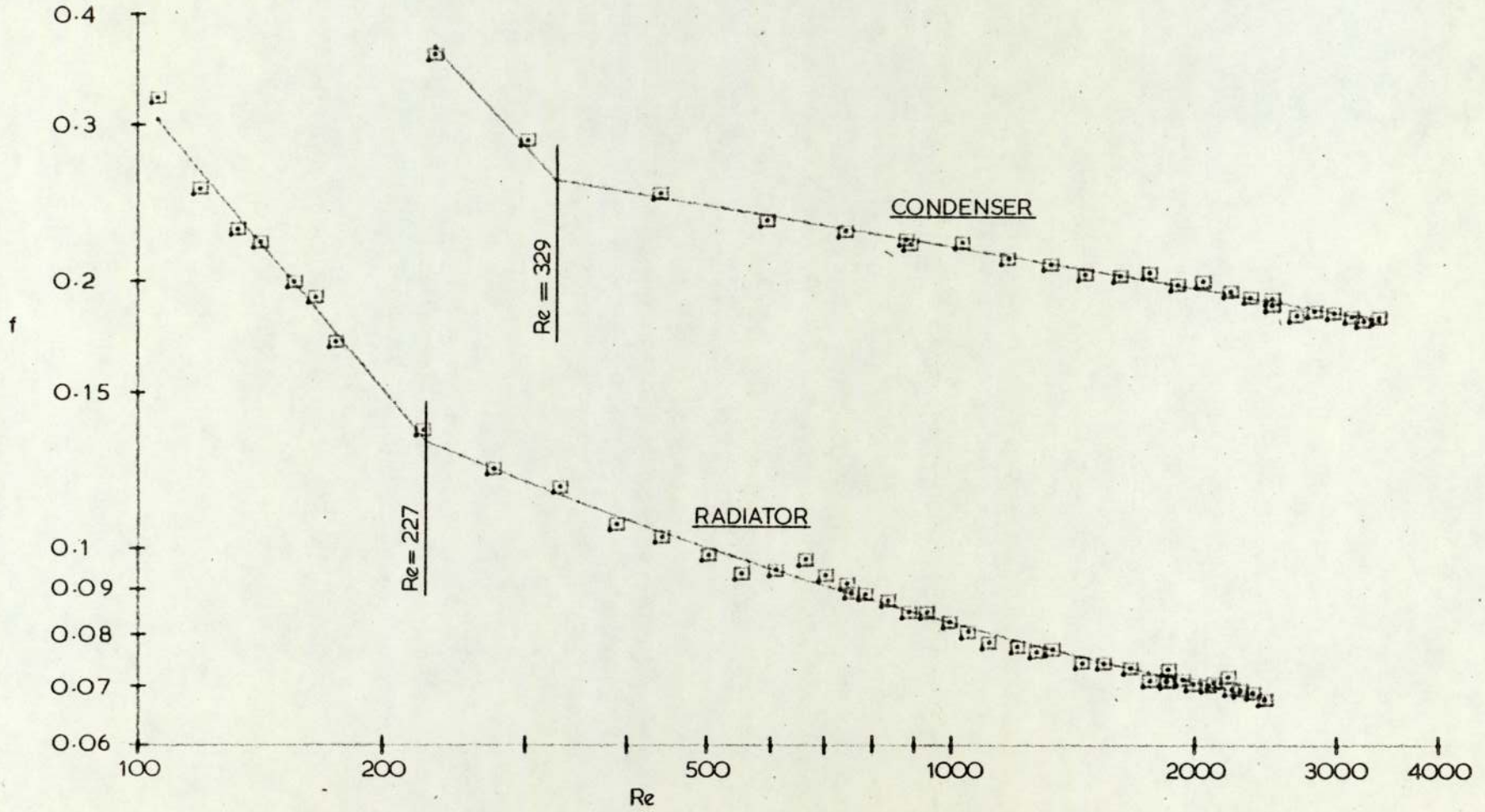

GRAPH 4.15

PLOT OF OVERALL CONDUCTIVITY AGAINST AIR MASS FLOW RATE

'MARSTON RADIATORS SUPAPACK I' TEST CORE

2·12mm FIN PITCH
87 TUBES IN ROWS OF 3
HEADER DISTANCE 0·4572m
CORE WIDTH 0·4531m
CORE THICKNESS 49·53mm

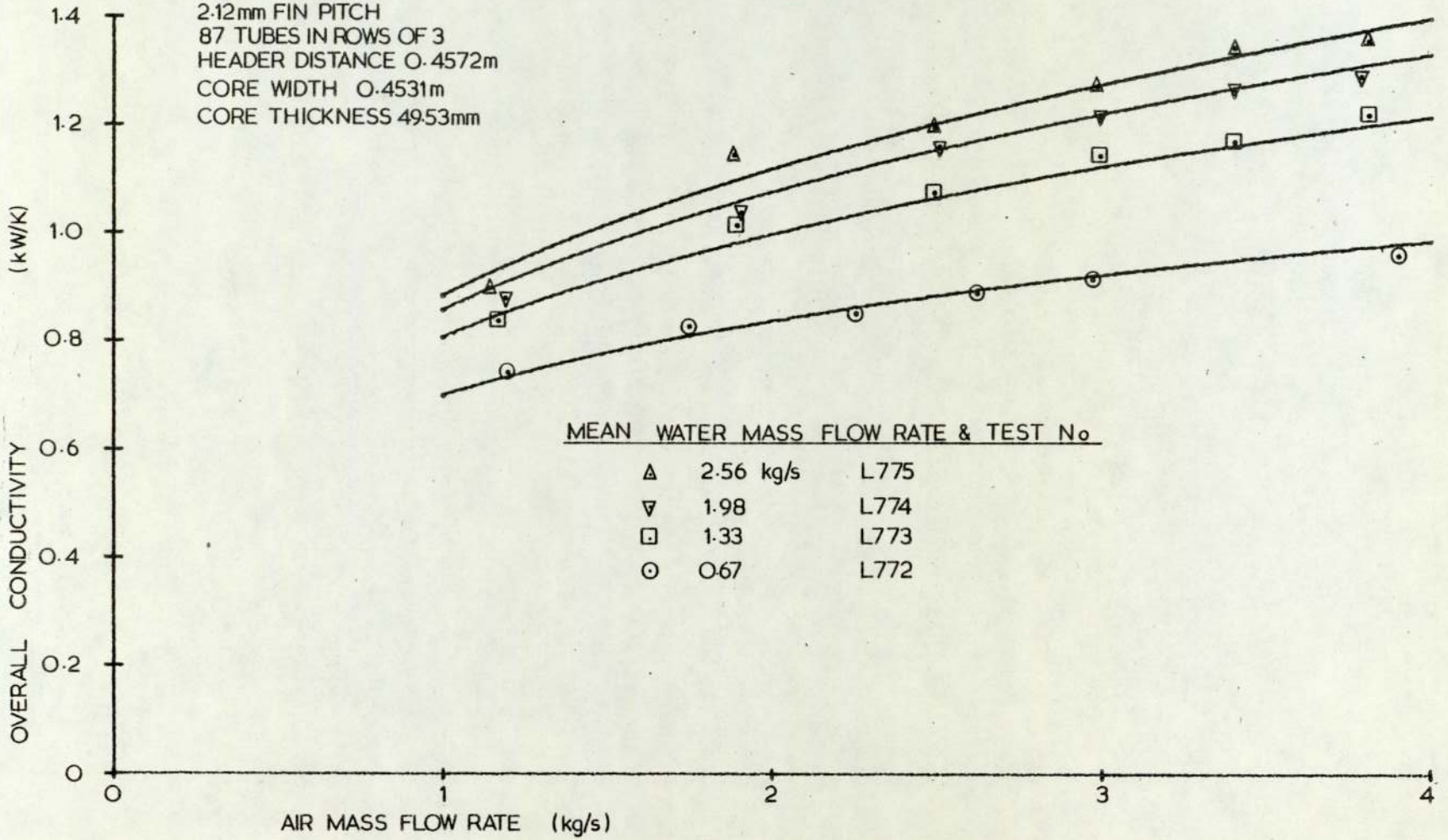

MEAN WATER MASS FLOW RATE & TEST No

△	2·56 kg/s	L775
▽	1·98	L774
□	1·33	L773
○	0·67	L772

GRAPH 4.16

PLOT OF OVERALL CONDUCTIVITY AGAINST AIR MASS FLOW RATE

'MARSTON RADIATORS SUPAPACK 'I' TEST CORE

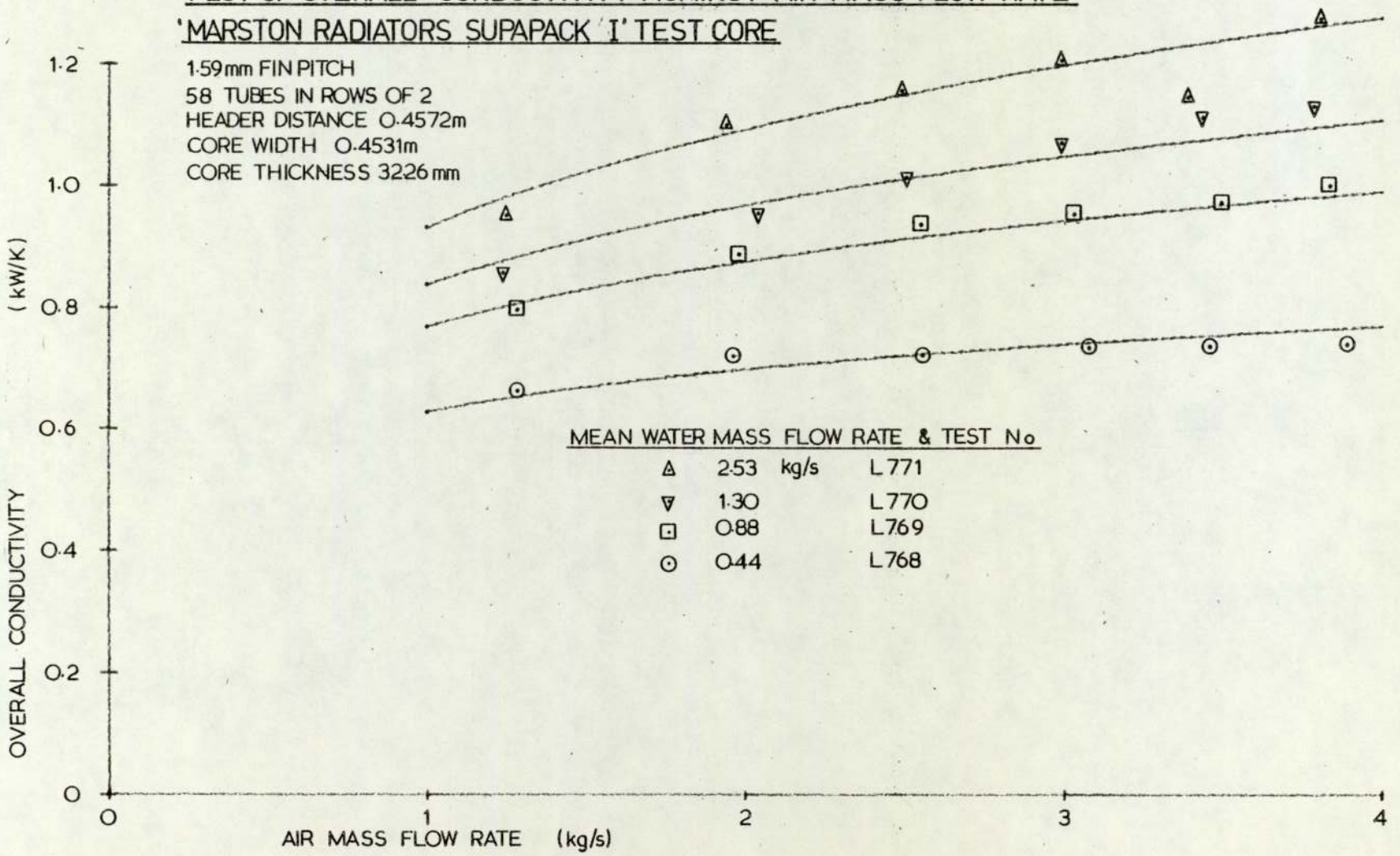

GRAPH 4.17

LOG-LOG PLOT OF j AGAINST Re FOR VARIOUS RATIOS OF L/De
AIR SIDE OF MARSTON RADIATOR'S SUPAPACK I RADIATORS

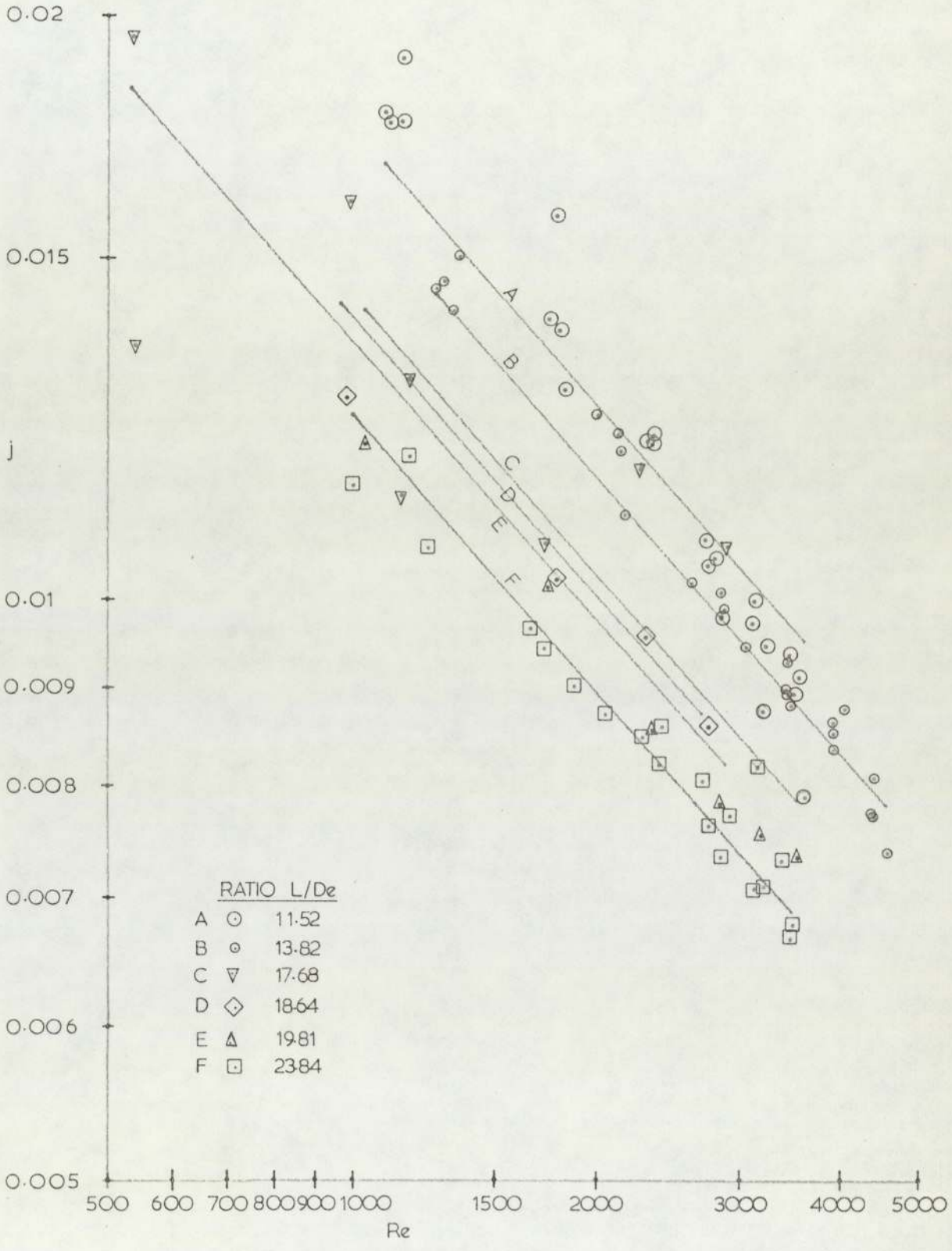

GRAPH 4.18

LOG-LOG PLOT OF f AGAINST Re FOR VARIOUS RATIOS OF L/De
AIR SIDE OF MARSTON RADIATOR'S SUPAPACK I RADIATORS

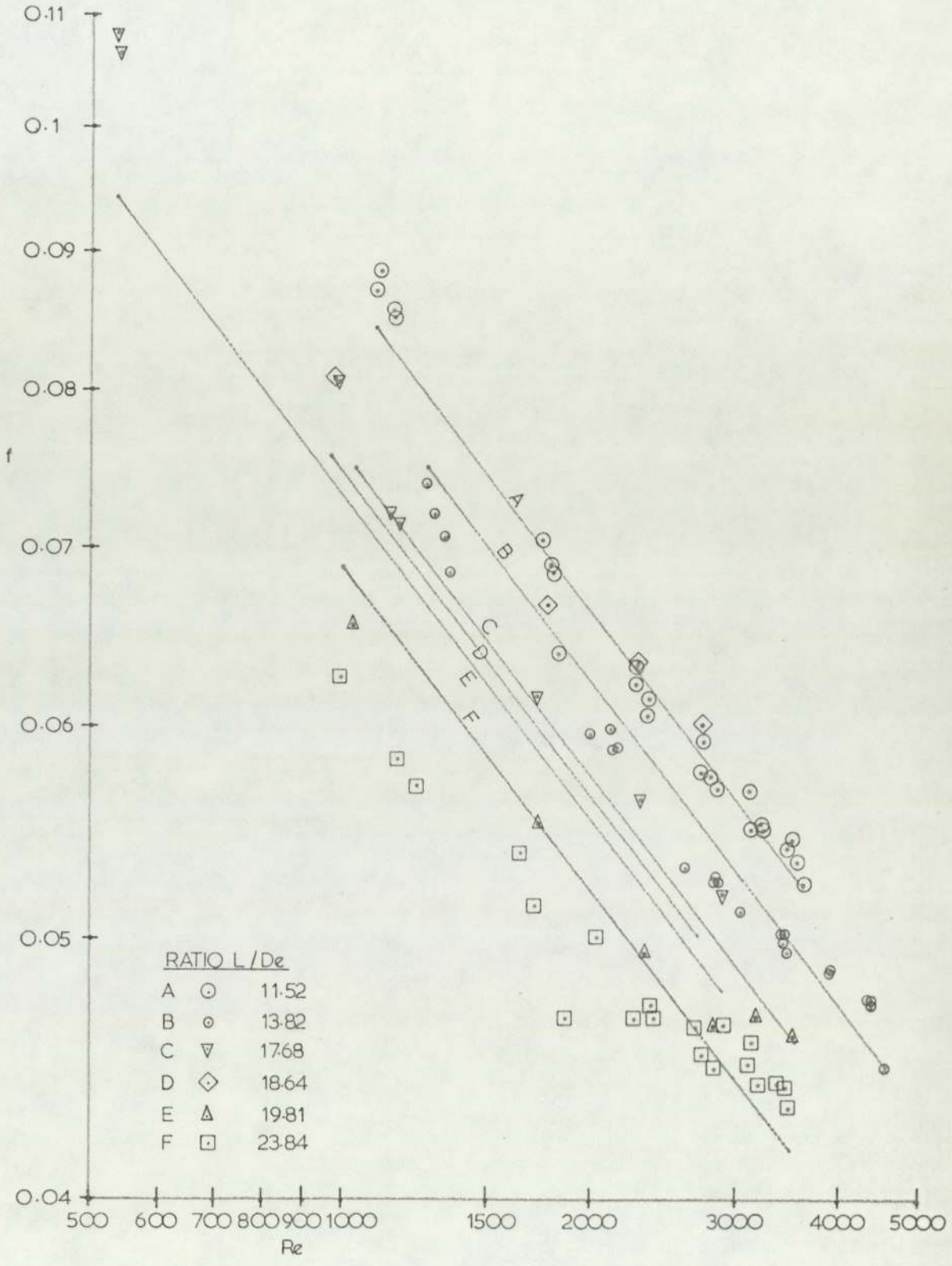

GRAPH 4.19

PLOT OF RADIATOR AIR VELOCITY AGAINST ENGINE SPEED.
AIR VELOCITY MEASURED USING A CALIBRATED VANE ANEMOMETER AT THE INLET OF A SHARP EDGED DUCT. DUCT VELOCITY DISTRIBUTION ASSUMED UNIFORM

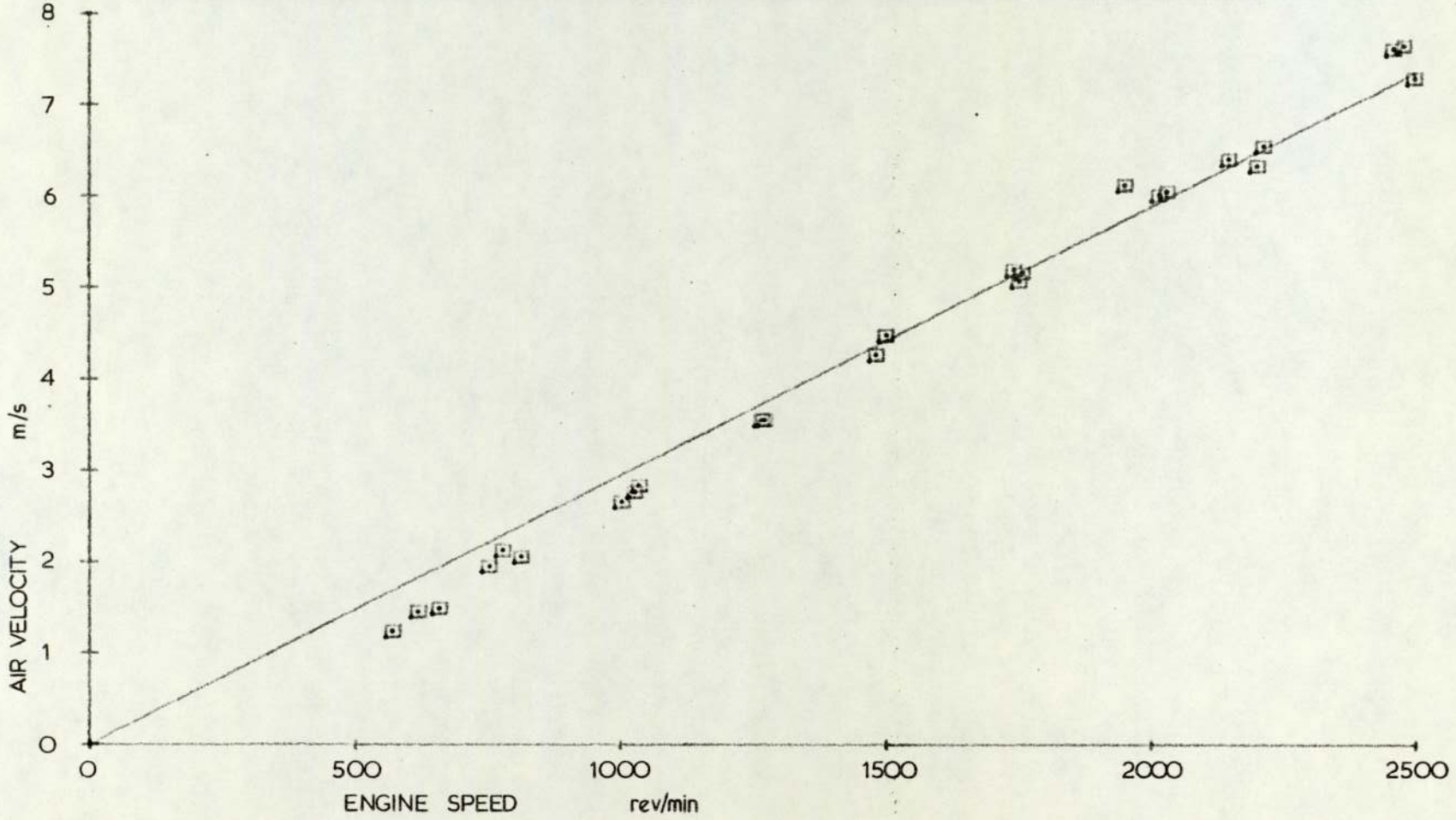

CHAPTER 5

MASS AND ENERGY TRANSFERS TO AND FROM THE ENGINE OF THE NON AIR-CONDITIONED CAR

INTRODUCTION

For the purpose of this work the engine is assumed to be a system which takes in chemical fuel and produces mechanical work, and hot exhaust gas, and rejects heat to a coolant flowing from the radiator, through the system and back to the radiator. In considering the energy and mass transfers, their magnitudes are assumed to be functions of the engine speed and mechanical power only, except in the case of the coolant flow rate, which is dependent on its temperature on leaving the system, and also on the coolant side friction factor of the radiator. Hence it is assumed that the enthalpy increase of the coolant as it passes through the system is independent of the temperature of the coolant either entering or leaving the system. This is justified by the large temperature difference between the cooling water and the combustion gases, in relation to small possible variations in the mean coolant temperature. Similarly it is assumed that the enthalpy of the exhaust gases is unaffected by small changes in coolant temperature. Other energy transfers (i.e. by radiation and convection and also heat transferred in the oil cooler) are unaccounted.

The energy and mass transfers to and from the system have been quantified for the purpose of this work as:

Coolant flow rate = f (engine speed, coolant outlet temperature, and radiator friction)

Exhaust gas enthalpy = f (engine speed, and brake power)

Exhaust gas mass capacity rate = f (engine speed, and brake power)

Heat rejected to coolant = f (engine speed, and brake power)

Fuel flow rate = f (engine speed, and brake power)

For the purpose of quantifying the latter four dependent variables, an engine was set up on a test bed and instrumented, and a series of tests carried out.

The speed of the engine is dependent on road speed and overall gear ratio. The mechanical power delivered at the road wheels is dependent on the aerodynamic and frictional drag, gradient and vehicle acceleration, the aerodynamic drag being dependent on the shape of the car and its velocity, and the frictional drag being dependent on the coefficient of rolling friction for the tyres and the vehicle mass. In driving up a gradient the power requirement is also a function of the vehicle mass and the gradient. The additional power required to accelerate the car is directly proportional to its mass and acceleration. The power delivered at the wheels may be termed the road load. The power produced by the engine is therefore the sum of the road load, transmission losses, and the loads produced by the auxilaries, i.e. the engine cooling fan, alternator, power steering pump, etc. With the exception of the cooling fan the power consumption of the auxilaries is small (i.e.$<$ 1 kw), the maximum alternator output being approximately 250W and the power steering pump working against a pressure only when the steering wheel is being turned, and a spool valve closed to divert the fluid to the steering rack.

For the calculation of the road load and transmission losses data had previously been obtained by the sponsor.[76] Power consumption of the engine cooling fan and viscous coupling is as given by the function developed in chapter 4.

Coolant is pumped from the radiator to the engine by a centrifugal pump which is an integral part of the front timing cover. The pump rotor is directly coupled to the pulley, driven from the crankshaft, which drives the cooling fan viscous coupling. Coolant from the engine flows back to the radiator through a thermostatic valve. This valve is arranged to divert flow from a bypass hose (bypassing the radiator) to the radiator, as the coolant temperature increases. Data on coolant flow rates with the thermostat propped fully open and the bypass hose blanked off were previously obtained by the sponsor.[77] No data is available on

the influence of thermostat opening on flow rate and hence a linear variation is assumed. This is justified in examining the limits of the cooling system performance since the limit is imposed at coolant temperatures such that the thermostat is fully open.

DETERMINATION OF FUEL FLOW RATE AND ENGINE ENERGY TRANSFERS IN THE LABORATORY

The Test Rig

A standard 4.2 l Jaguar XJ6 engine was solidly mounted on a test bed in a laboratory.

The exhaust gases from the engine passed through a large expansion chamber to reduce resonance effects and then through a 100 mm diameter pipe to a stack. A fan in the stack provides a small draught to prevent a build up of flammable gas and also reduce the pressure drop in the system. When running, the maximum exhaust pressure measured in the engine manifold was found to be less than 150 mm water gauge.

The engine was cooled by water in a pressurised closed circuit, heat being transferred from a motor car radiator immersed in a water bath. Water from a reservoir was pumped into the bath and returned via a forced draught cooling tower. The standard engine thermostat was retained and circulation of water through the engine and radiator was assisted by the standard engine coolant pump.

Oil from the engine sump was circulated by a mains electric pump through a shell and tube heat exchanger, and a paper element filter and back to the sump. The oil flow rate was adjustable by means of a gate valve at the pump outlet. The coolant side of this heat exchanger was fed by water from the reservoir, and regulated by a valve.

The dynamometer was fed with water from the same reservoir, regulating gate valves being installed upstream of the brake and on the brake outlet itself.

Connection to the brake was via flexible, convoluted, rubber hose. It was found necessary to install an additional pump to supplement the supply pressure available to the brake. This was installed upstream of the inlet regulating valve.

Fuel was supplied to the engine from a tank and via a filter. The tank was mounted above the engine to provide a gravity feed and an S.U. electric fuel pump fitted in addition to ensure a sufficient delivery when the supply from the tank was cut off and the engine fed from a measuring cylinder.

The ignition system and starter motor were supplied with current from a 12 volt lead-acid accumulator. No charging system was used whilst tests were in progress, the accumulator being recharged between tests.

The throttles were connected to a quadrant, bolted to the cylinder head. A return spring was fitted to the butterfly spindle of each carburettor to prevent movement through backlash in the linkage. The quadrant was provided with a thumbscrew such that it could be locked in any position.

The Engine Tested

The engine, prior to testing, was completely dismantled and examined for defects. On rebuilding, any worn or suspect components were replaced. The engine specification was as built for the 1973 British market and described in the manufacturer's workshop manual[69] and spares catalogues[70] for that year.

The only auxiliary driven from the crankshaft was the engine coolant water pump. In the absence of the power steering pump, which is pivoted to adjust the tension of the water pump vee belt, a jockey pulley was fitted.

Mechanical power transmission was taken from the engine flywheel to an adaptor plate and universally joined shaft to the dynamometer.

The induction system was adapted for the inclusion of a viscous air flow meter by modification of the air filter box. This box was connected via a 63.5 mm inside diameter rubber pipe, 150 mm long to the air meter, which has, as an integral component, a felt air filter. The standard air filter elements were excluded.

Prior to testing, new spark plugs and contact breaker points were installed with the gaps set to the manufacturer's recommended figures. The ignition timing was set statically with the aid of a 12 volt bulb and the accumulator, the setting being to the manufacturer's recommendation[69]. Setting of the carburettor butterfly valves was achieved by measurement of the air flow to each carburettor using a vane anemometer, giving a direct reading of velocity, and a duct tapered to fit 1 mm inside the intakes. With the engine idling at 750 rev/min a velocity reading for each carburettor was taken and the throttle linkage adjusted until the two readings were identical. The fuel/air mixture strength was set with the engine idling at 750 rev/min to give 2.75% carbon monoxide (as a volumetric fraction of the dry products) measured at the separate exhaust manifolds, receiving exhaust gas, from the three cylinders supplied by each carburettor. This setting was recommended by the personnel[71] of the manufacturer's engine development department.

No choke was fitted to the engine for cold starting purposes, a rich mixture being produced for this purpose by manually lowering the main jet of one carburettor against its spring, without adjustment of the mixture strength adjusting screw.

Instrumentation

The engine was coupled to a hydrodynamic dynamometer (Heenan and Froude type DPX3) for the measurement of brake power output. The static balance of this dynamometer was checked prior to use.

A proximity detector registering six steel pegs in an aluminium wheel was mounted on the front of the crankshaft, the output of the detector being connected to an electronic digital counter for the measurement of engine speed. The calibration of this counter was checked against the A.C. mains electric frequency of 50 hz and found to be accurate over a 10 second period.

For the purpose of obtaining a continuous reading, found useful when setting the engine speed, an impulse tachometer was wired into the engine ignition system.

Fuel flow rates were measured using a graduated cylinder (with graduations of 100, 200 and 400 ml) and a stop-watch, the accuracy of which was checked against the G.P.O. 'speaking clock'. No error could be found.

The induction air flow rate was measured using a flowmeter with a viscous element, the pressure head across the element and vacuum down-stream of the element being read off a manometer of variable inclination. This equipment was manufactured by Ricardo and Co. and designated by them, type H and having a recommended flow rate limit of 165 l/s.

The temperature of the air entering the viscous flow meter was read off a mercury in glass thermometer.

Coolant temperatures were measured independently at the inlet and outlet by bare, unsheathed chromel-alumel thermocouples. Coolant flow rates were read off a variable area flow meter manufactured by GEC Elliot Limited (type number 35K).

Fuel inlet temperatures were measured using chromel-alumel thermocouples in the carburettor float chambers. Care was taken to ensure that the leads which passed through the float chamber air vents did not prevent free movement of the floats.

Exhaust gas temperatures were measured at the cylinder head/manifold interface by 1 mm diameter, stainless steel sheathed, chromel-alumel thermocouples. These were installed through drilled holes in the exhaust manifold in positions such that approximately 50 mm of the sheaths were exposed directly to the exhaust gas.

Other temperatures monitored throughout the tests but not noted were the coolant temperature at the thermostat (monitored to prevent overheating) and the temperature of the lubricating oil in the sump (monitored in order to maintain a

constant temperature by manual adjustment of the water flow rate through a shell and tube oil-cooler).

All of the thermocouples were connected via a selector switch to a digital voltmeter manufactured by Solartron (type A200) and having a resolution of 1 μV and range of 1 μV to 1.2 kV. The maximum error is stated as ±0.005% on all ranges except the lowest where this increases to ±0.01%. All of the thermocouples except those for measurement of exhaust gas temperatures were connected through independent ice cold junctions.

The percentages by volume of dry gas, of carbon monoxide and carbon dioxide, were measured using a non-dispersive infra-red meter manufactured by Horiba (type Mexa 300). This meter was calibrated using prepared gases marketed by the same company. The meter was connected through a condensing coil immersed in cold water, and a silica-gell drying bottle, to a three way valve connecting the meter, in turn, to either of the manifolds receiving gas from the front or rear three cylinders, or downstream from the point at which the pipes from each of these manifolds merge.

A vane anemometer in a duct was used to measure the relative air flow to the two carburettors, in order to balance these.

Method of Testing

Tests were performed both with the dynamometer connected to the engine, and disconnected to represent idle performance. With the dynamometer disconnected readings were taken at engine speeds of 500 to 4500 rev/min, in steps of 500 rev/min. With the dynamometer connected, readings were taken at the same speeds and with the brake load adjusted in steps up to the maximum. The maximum power settings were limited by the maximum available from the engine or by the maximum which the brake could absorb under stable conditions.

At each setting of the brake load and/or engine speed, the engine was run until the water inlet and outlet, and thermostat temperature appeared to have

reached constant values. The oil flow rate through the oil cooler was adjusted to maintain a sump temperature of 90 to 95°C. The readings taken were as listed in the experimental results tables in appendix A3. The results are tabulated separately at each speed, the zero load readings being the first result in each table. These results were not obtained during the same test run as the rest of the results in each table.

Results

Temperatures were calculated from the thermocouple readings using the calibration equation contained in B.S.4937 part 4 [72] (1973). In the case of the exhaust temperatures, cold junction compensation was made by adding to the measured potential the potential relating to ambient temperature. From this sum the temperature was calculated.

In calculating the air inlet mass flow rate, compensation was made for changes in temperature and pressure, as they influence density and viscosity, away from the calibration temperature of 20°C and pressure of 760 mm of mercury. The variation in viscosity of air with temperature was calculated from a cubic regression to the data tabulated by Mayhew and Rogers [66], over the temperature range of 0 to 100°C. The manufacturer's calibration equation was used as a basis and is:

$$\text{vol}/(\text{ft}^3/\text{min}) = 16.0 \times \text{head}/(\text{inches water gauge})$$

For the calibration of fuel mass flow rate the relative density of petrol is taken as 0.744 from the data of Spiers [73].

For the calculation of the water flow rate a cubic was fitted to data read off the calibration chart supplied with the flow meter. This calibration was subsequently checked by weighing a constant water flow through the instrument over a time interval measured with the same stop-watch used in the measurement of fuel flow rate. Water flow rates used were at either end of and in the middle of the instrument's range. The maximum deviation of the calibration equation was

found to be at the lowest reading and to be less than 1.5%. Values of the enthalpy of liquid water were calculated from values of the specific heat taken from Mayhew and Rogers[66] by fitting a quadratic and integrating.

The mass flow rate of the exhaust gas was calculated as the sum of the air and fuel flow rates. The constituent proportions of the exhaust gas were calculated by assuming combustion to give products of nitrogen, carbon monoxide, carbon dioxide, and superheated steam. The enthalpy of the products was calculated at the arithmetic mean of the gas temperatures measured, above a datum of 250^{o}C, by integration of the equations, for the specific heat of these gases, given in Hamblin[74]. The mass capacity of the exhaust gases at 250^{o}C was also calculated using these equations. The calculated results are also tabulated in appendix A3.

Presentation of Results

Each of the four quantities required as functions of mechanical power output and engine speed may be assumed to vary in a similar manner as the exhaust gas mass flow rate. The exhaust gas mass flow rate was plotted against engine speed at idle as shown in graph 5.1. If the energy available per unit mass of combustible mixture (and hence exhaust gas) were constant then this graph would represent a measure of friction power against engine speed. Friction losses include coulomb friction, viscous friction, and pumping losses, suggesting that the total is the sum of linear, squared and cubed terms. At both high and low engine speeds combustion efficiency is known to be poor, and results in the need for ignition advance. This produces higher mass flow rates at both high and low engine speeds as evidenced by the experimental data. A cubic was found to give a good representation and is forced through the origin on the assumption that friction power and hence mass flow rate approaches zero at zero speed.

The exhaust enthalpy, and mass capacity rate are direct functions of exhaust gas temperature and this quantity has also been plotted against engine speed at

idle, and is shown on graph 5.2. The form of this curve suggests that the exhaust mass capacity rate curve will be of a similar form to the exhaust mass flow rate but with a sharper rise at low engine speeds due to the sharp rise of temperature and hence specific heat at these speeds. Extrapolation from the exhaust gas temperature data down to zero speed, suggests that at zero speed the exhaust gas temperature would be less than the 250°C datum chosen for the exhaust gas enthalpy calculations, resulting in a negative enthalpy at zero speed.

Each of the four quantities to be expressed as functions of mechanical power and engine speed are plotted on graphs 5.3, 5.4, 5.5 and 5.6, at idle. A cubic was fitted to each of these curves on the basis of the above arguments, with the exception of the exhaust enthalpy which appears to represent a straight line. At high speed the upturn of the exhaust gas mass flow rate seems to be balanced by the downturn of the temperature. The plot of heat rejection to the cooling system follows the same pattern as for the exhaust mass flow rate which suggests that the heat transfer coefficient between the hot gases and cylinder walls is a strong function of piston velocity. The sharper gradient at low engine speeds than exists in the mass flow rate plot may be due to the sharply rising temperature of the combustion process as its efficiency increases.

Each of the four quantities are plotted against brake power output at each engine speed on graphs 5.7 to 5.11 inclusive. Each of the quantities are fitted to an equation of the form:

$$AP \times (1 + BP) + C \qquad 5.1$$

where A, B, and C are functions of engine speed. The constant (with respect to mechanical power) C is the function fitted at idle. The constant A, which represents the gradient at zero speed was fitted next, with B fitted last as a perturbation from a straight line.

In the case of heat rejection to the cooling system this quantity does not appear as a strong function of power output. This may be attributed to a fairly constant combustion temperature with increasing power, but a strong function of

heat transfer coefficient with increasing piston speed.

The enthalpy and capacity rate of the exhaust gas and fuel flow rate all increase rapidly with increasing power, as may be expected since the mass flow rate of combustion products similarly increases.

In the case of a few of the readings, the calculated air fuel ratio was such that there was too little oxygen present to oxidise all of the carbon in the fuel. These readings were omitted in the calculation of exhaust enthalpy and mass capacity rate. Doubts as to the setting and correct metering of the carburettors called for the colour of the spark plug electrodes to be examined on completion of the tests. A colour photograph of these is shown on plate 5.1. The chocolate brown colouring of the electrodes and ceramic insulators is indicative of correct mixture strengths in each of the six cylinders.

The expected maximum power output of the engine could not be realised using this rig. It is believed that this was due to the throttling effect of the viscous flowmeter and could have been overcome by supercharging the engine to produce the same vacuum at the carburettor inlets, as could be measured without the viscous flow meter fitted.

At higher engine speeds (above 3000 rev/min) it was found that the dynomometer could not be adjusted to stably hold the engine at a constant speed at full throttle. This may either have been due to a lack of pressure in the water supply or the furred and corroded condition of the brake which has been in service for several years.

The maximum power results of tests carried out on an identical engine at the company's experimental department[75] have been adopted for use in this project. A plot of these results is shown on graph 5.11, against engine speed. A quartic was found to give an excellent least squares fit to this data. On the graphs of fuel flow rate, heat rejection to coolant, exhaust enthalpy, and exhaust mass capacity, the fitted equations are shown extrapolated to this maximum power equation, and also to an engine speed of 5000 rev/min, the maximum recommended speed of the

engine. Tests were not run at this speed in fear of damaging the engine at low brake loads.

ROAD LOAD

The rolling resistance of the tyres has been calculated using tyre friction data obtained by the sponsor[76] from the tyre manufacturer (Dunlop). To this data, in the form of a graph of resistance per unit vehicle weight, has been fitted an equation of the form:

$$= A + BU_v + CU_v^n \qquad 5.2$$

where A, B, C and n are constants. This gives an excellent fit to the data. Using this equation and the mid-laden mass of the vehicle quoted by the manufacturers[76], the power required to overcome this resistance is plotted on graph 5.12. The aerodynamic resistance is added to the rolling resistance and also plotted on this graph. The power dissipated in overcoming the aerodynamic drag is assumed to vary as the cube of the road speed, and was calculated from a figure, gained by experience in tests on this model by the sponsor[76], of the power dissipated at 100 miles/hour.

TRANSMISSION EFFICIENCY

Figures quoted by the manufacturer[76] have been used in calculating transmission efficiencies. These are:

93% for the rear axle

97% for the manual gearbox in direct drive

94% for this gearbox in indirect drive

COOLANT FLOW RATE

Tests on the coolant flow rate have been carried out by the sponsor[77]. For these tests a 4.2 l XJ6 engine was set up on a test bed and connected, as in the vehicle, to a radiator, the radiator being immersed in a tank of water instead of

an air stream. The thermostat was propped fully open and the bypass hose blanked off. The water flow rate was measured using a turbine flowmeter at increments of engine speed, for the Marston's Supapack I radiators fitted to both air-conditioned and non air-conditioned versions of the car. The results of these tests are plotted on graph 5.13. In the absence of further data, the water flow rate with a fully open thermostat is assumed to vary linearly with the ratio of tube length/number. Ideally an additional test could be carried out with the radiator replaced by two header tanks (cut from a radiator) linked by a straight length of large diameter tube which could be assumed to exhibit zero pressure drop along its length. This would set a more realistic upper limit to the water flow rate.

The thermostat fitted to the cooling system of the engine is of the wax capsule type and set to commence opening at 82°C and be fully open at 100°C. The opening of the thermostat has been found by the vehicle manufacturer[78] to be approximately linear with temperature. In the absence of further data the water flow rate is assumed to vary linearly with opening and hence temperature.

On starting the thermostat is known to suffer[79], in the fully closed position, from the pressure on it which prevents it opening until a temperature somewhat higher than 82°C. Since this is a dynamic effect, it is neglected in this project, but borne in mind that pressure balanced thermostats are available.

VARIATION OF ENERGY AND MASS TRANSFERS WITH ROAD SPEED

Using the fitted equations a mathematical model was developed in the form of computer subroutines. These are shown in appendix A5. Using these subroutines the variations of fuel flow rate, heat rejection to engine coolant, exhaust enthalpy and exhaust mass capacity have been plotted on graphs 5.14 to 5.17 inclusive, for the car using the 5 speed manual gearbox with a rear axle ratio of 3.54:1. The power developed by the engine is the sum of the fan and viscous coupling consumption, the aerodynamic drag, the tyre rolling resistance, and the transmission losses.

PLATE 5.1

THE SPARK PLUG ELECTRODES ON COMPLETION OF THE TESTS ON THE ENGINE

Top row, left to right - cylinders 1, 2, 3

Bottom row, left to right - cylinders 4, 5, 6

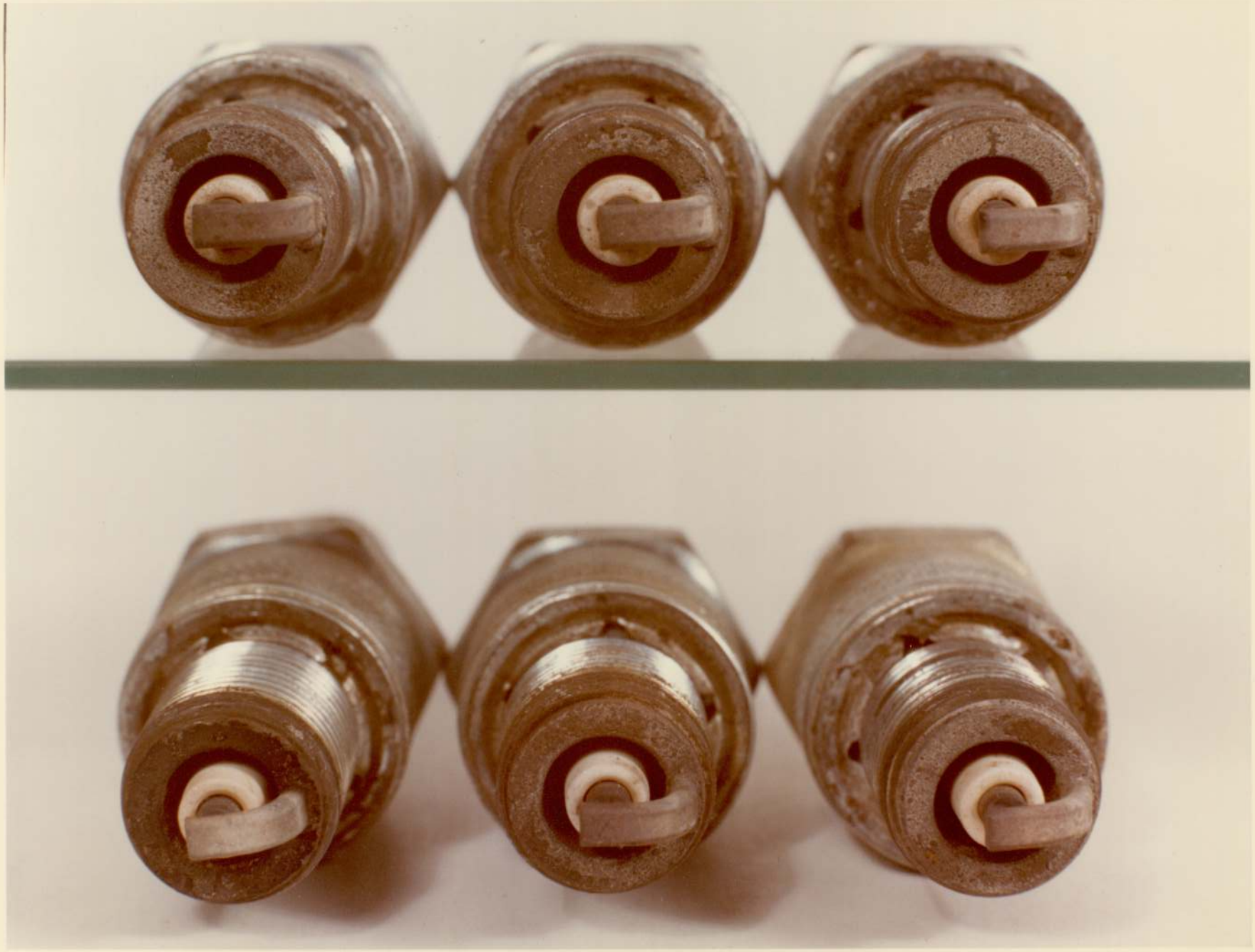

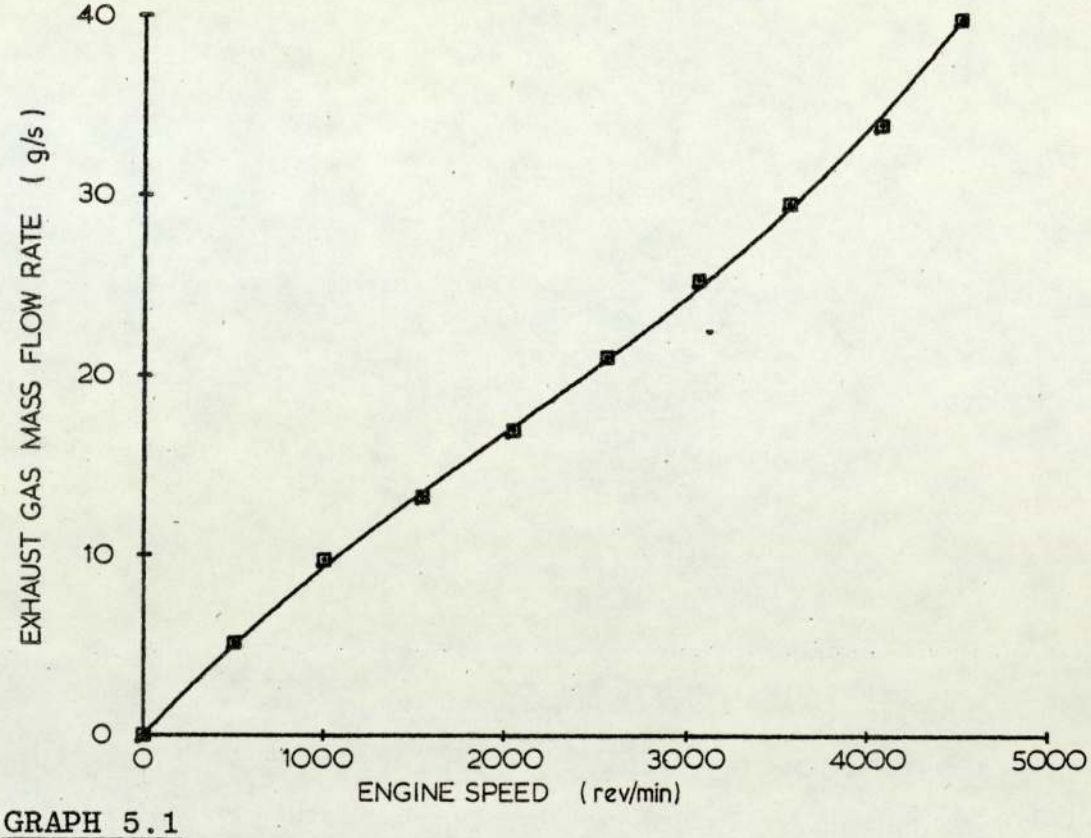

GRAPH 5.1

PLOT OF EXHAUST GAS MASS FLOWRATE AGAINST ENGINE SPEED AT ZERO BRAKE POWER

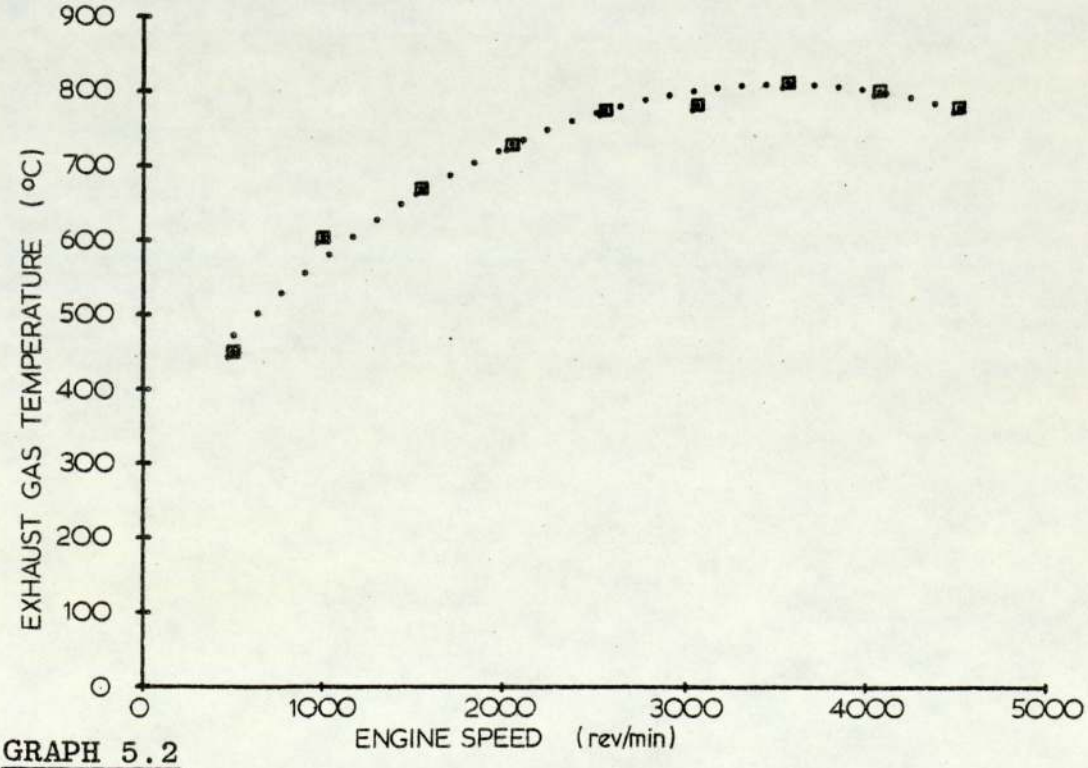

GRAPH 5.2

PLOT OF EXHAUST GAS TEMPERATURE AGAINST ENGINE SPEED AT ZERO BRAKE POWER

GRAPH 5.3

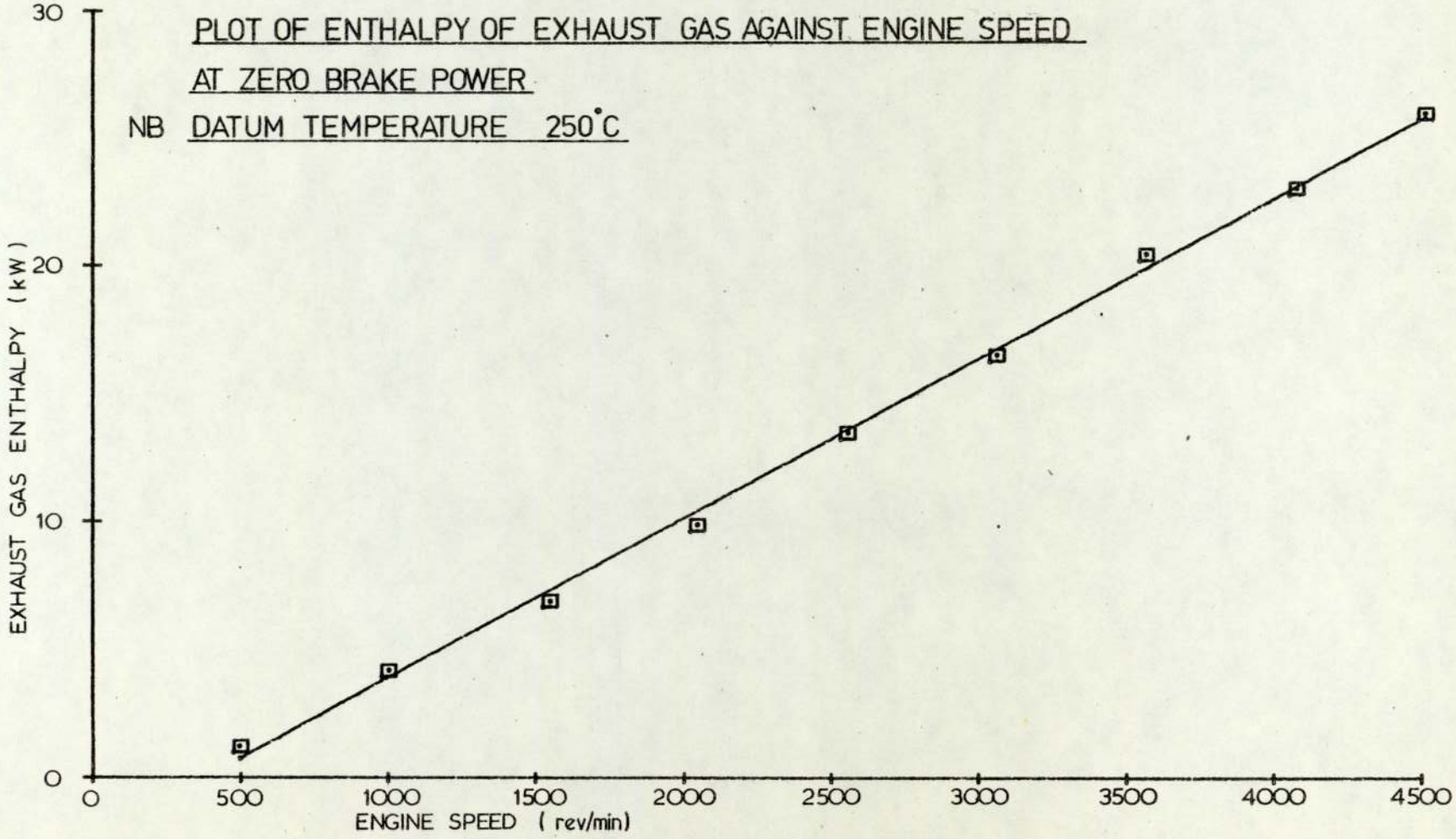
PLOT OF ENTHALPY OF EXHAUST GAS AGAINST ENGINE SPEED
AT ZERO BRAKE POWER
NB DATUM TEMPERATURE 250°C
EXHAUST GAS ENTHALPY (kW)
30
20
10
0
0
500
1000
1500
2000
2500
3000
3500
4000
4500
ENGINE SPEED (rev/min)

GRAPH 5.4

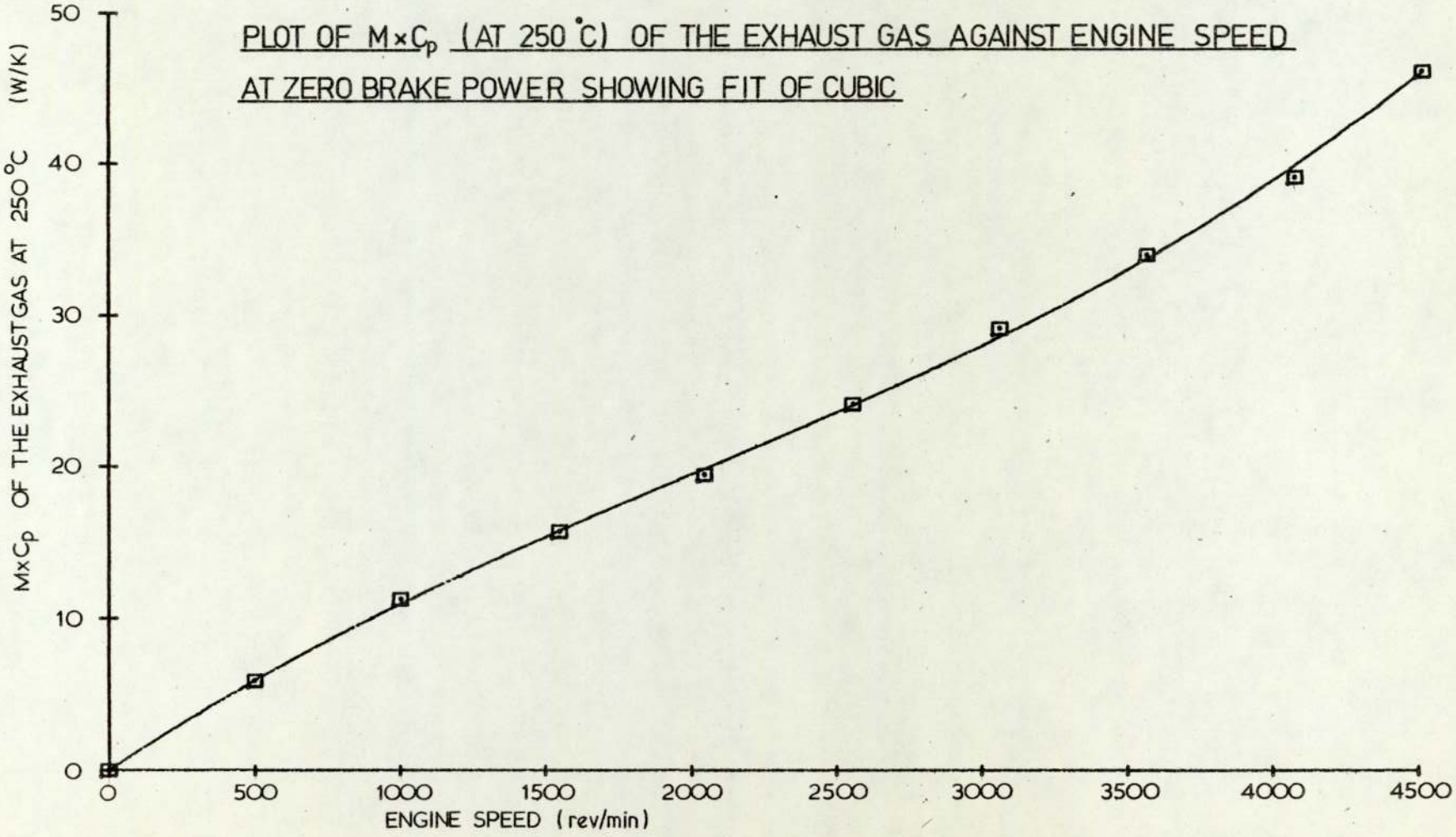
PLOT OF M×Cp (AT 250 °C) OF THE EXHAUST GAS AGAINST ENGINE SPEED
AT ZERO BRAKE POWER SHOWING FIT OF CUBIC
MxCp OF THE EXHAUSTGAS AT 250°C (W/K)
0
10
20
30
40
50
0
500
1000
1500
2000
2500
3000
3500
4000
4500
ENGINE SPEED (rev/min)

GRAPH 5.5

PLOT OF FUEL FLOWRATE AGAINST ENGINE SPEED AT ZERO BRAKE POWER

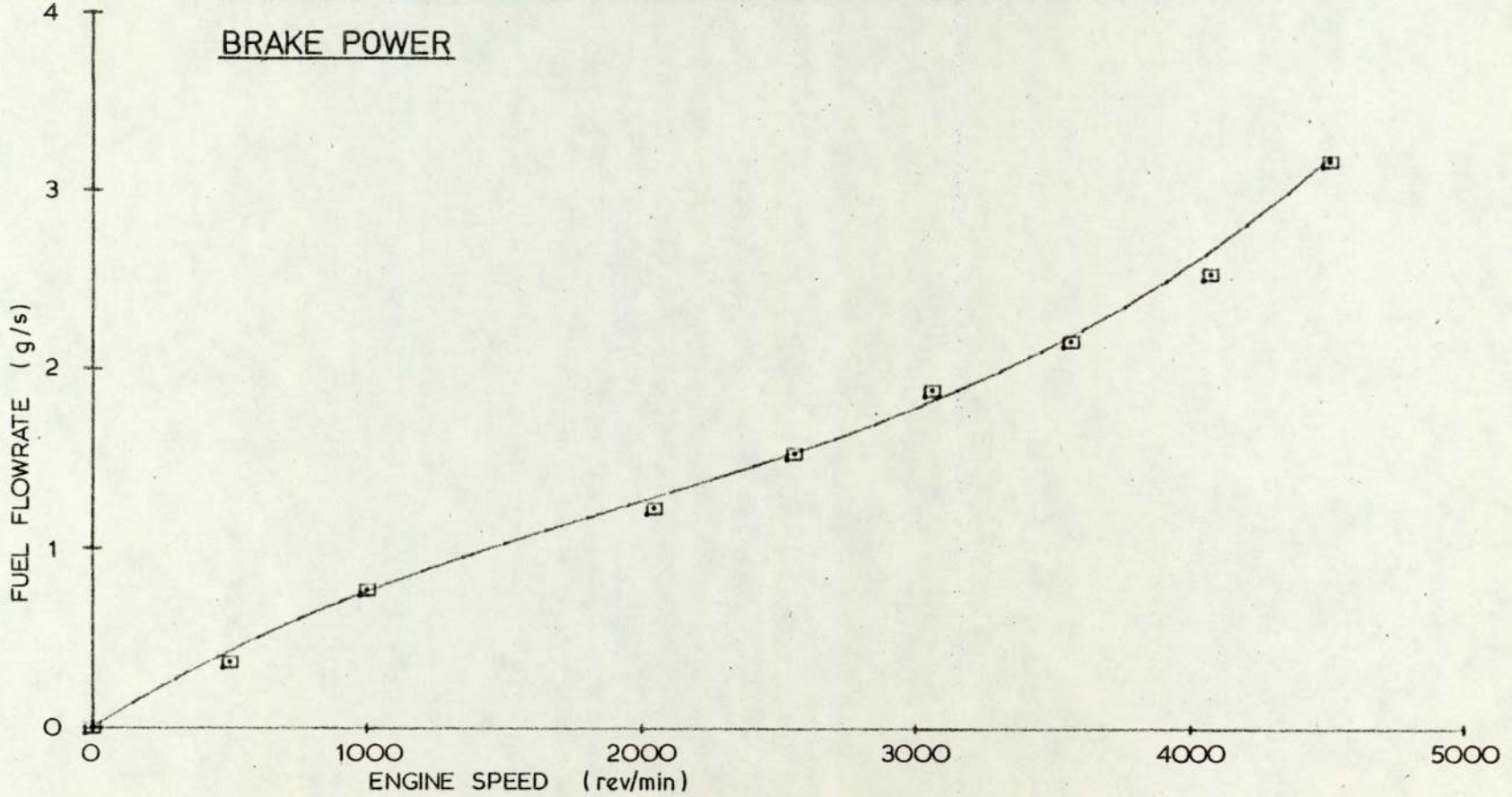

GRAPH 5.6

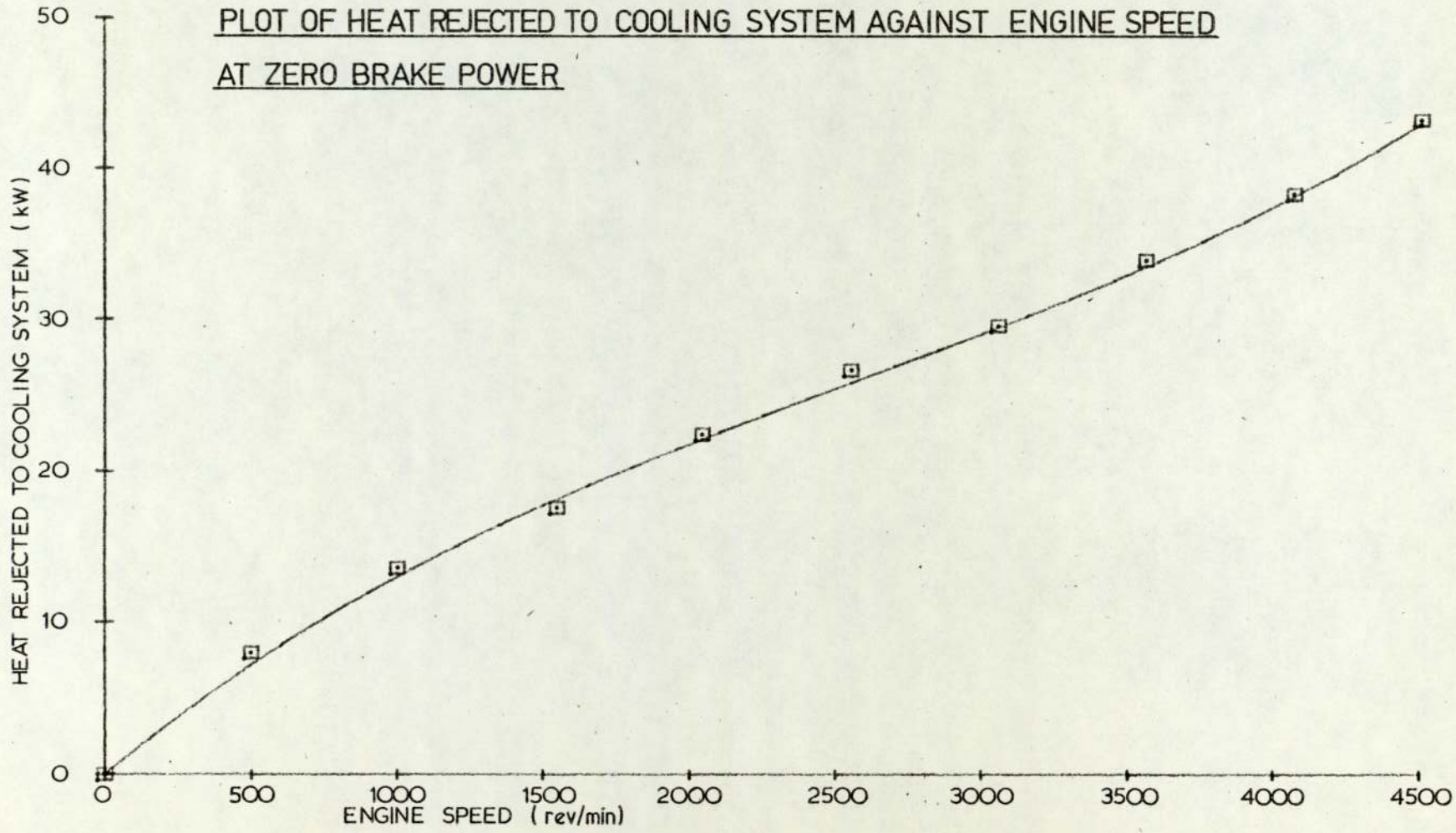
PLOT OF HEAT REJECTED TO COOLING SYSTEM AGAINST ENGINE SPEED
AT ZERO BRAKE POWER
HEAT REJECTED TO COOLING SYSTEM (kW)
0
10
20
30
40
50
0
500
1000
1500
2000
2500
3000
3500
4000
4500
ENGINE SPEED (rev/min)

GRAPH 5.7

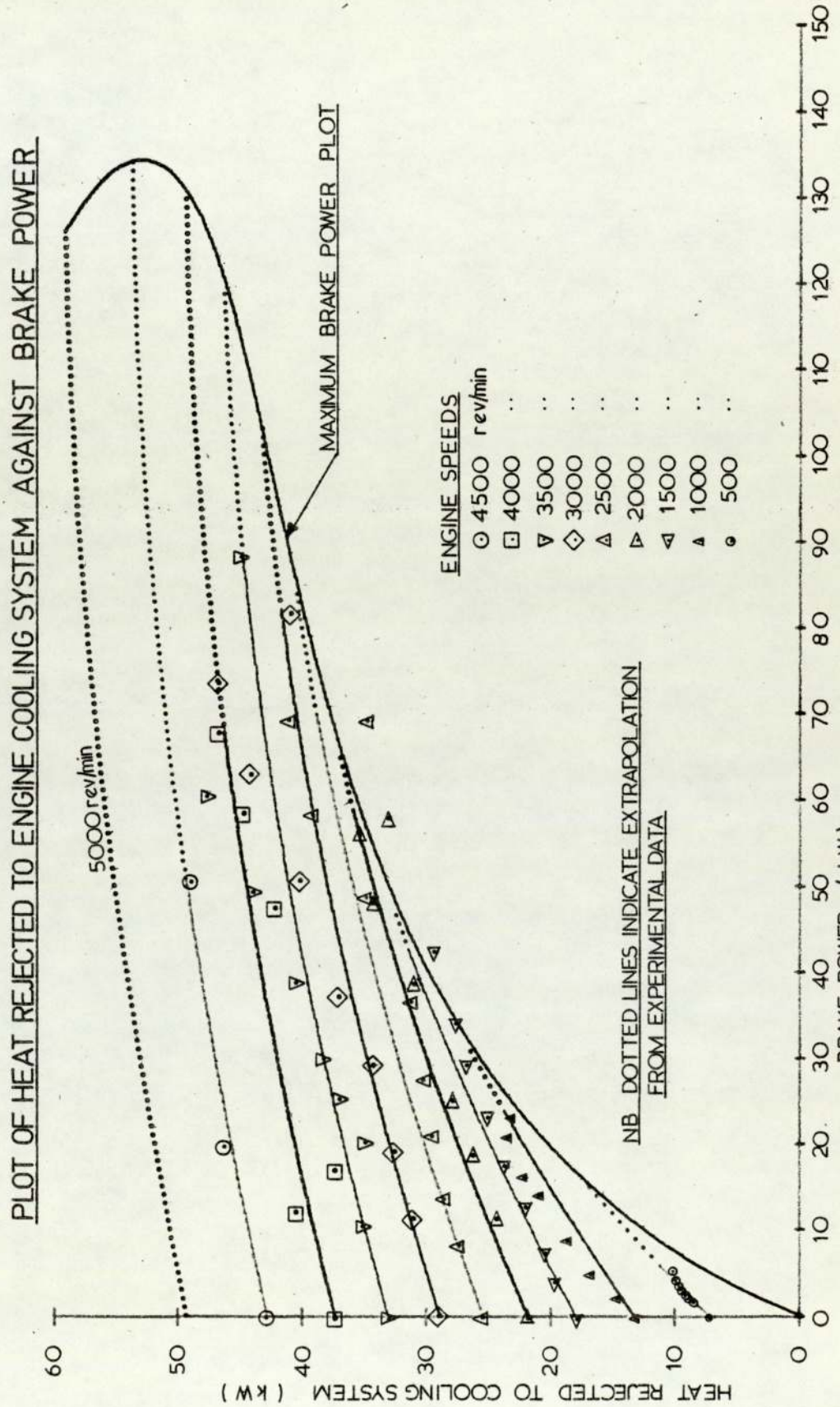
PLOT OF HEAT REJECTED TO ENGINE COOLING SYSTEM AGAINST BRAKE POWER
5000 rev/min
MAXIMUM BRAKE POWER PLOT
ENGINE SPEEDS
4500 rev/min
4000 ..
3500 ..
3000 ..
2500 ..
2000 ..
1500 ..
1000 ..
500 ..
NB DOTTED LINES INDICATE EXTRAPOLATION FROM EXPERIMENTAL DATA
HEAT REJECTED TO COOLING SYSTEM (kW)
BRAKE POWER (kW)
0
10
20
30
40
50
60
70
80
90
100
110
120
130
140
150

GRAPH 5.8

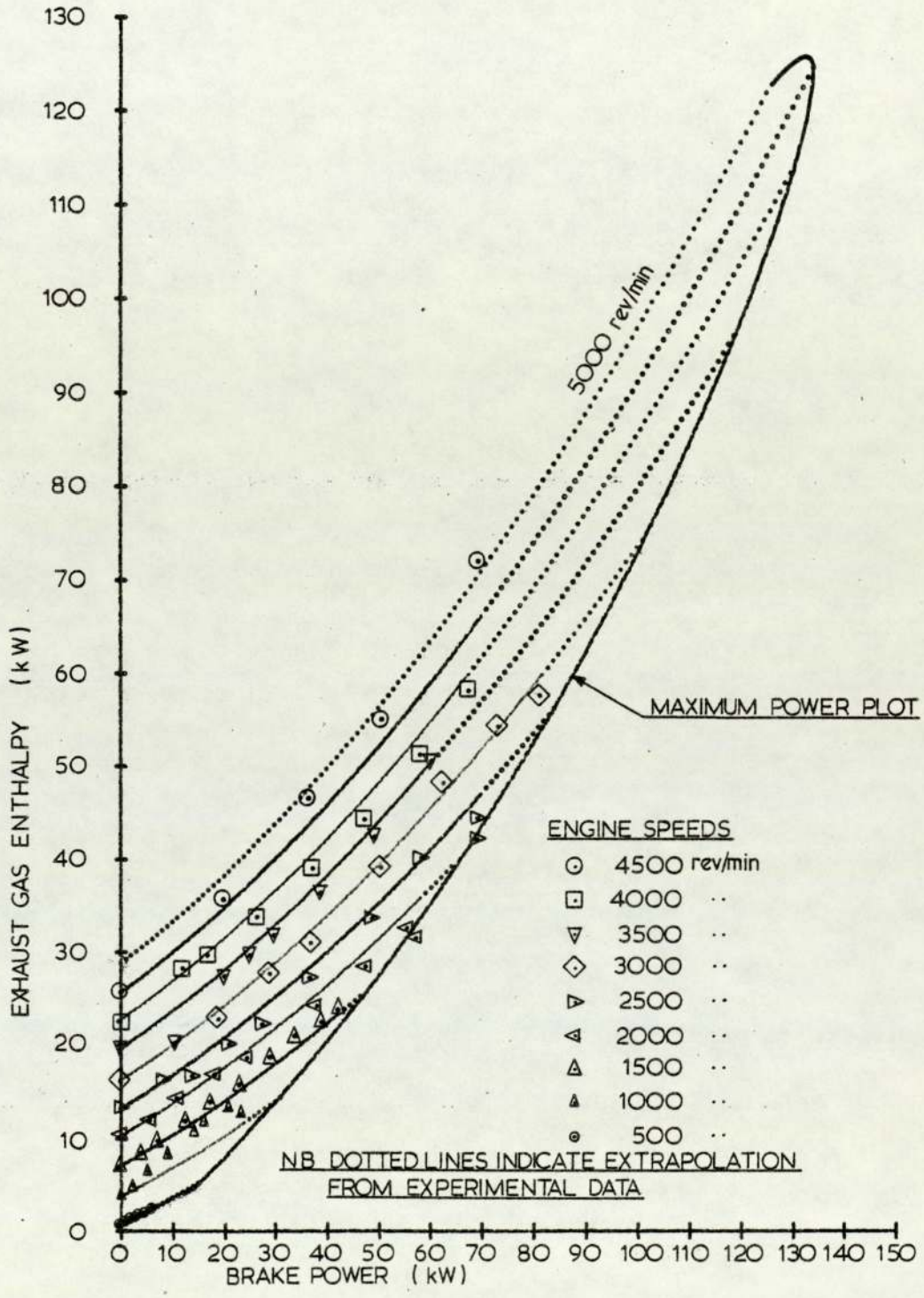

PLOT OF ENTHALPY OF EXHAUST GAS AGAINST BRAKE POWER

NB DATUM TEMPERATURE 250 °C

GRAPH 5.9

PLOT OF $M \times C_p$ (AT 250 °C) OF THE EXHAUST GAS AGAINST BRAKE POWER

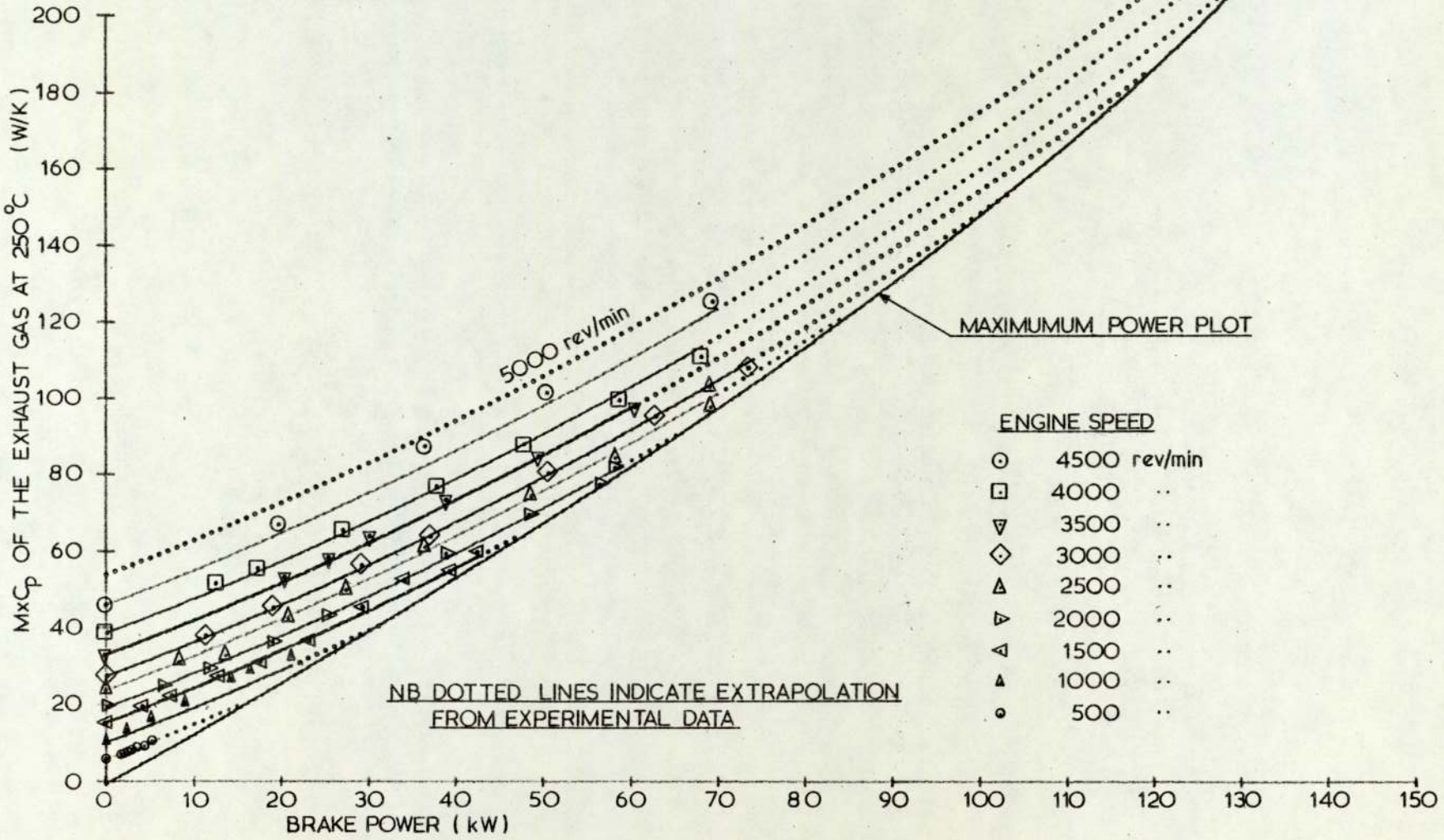

GRAPH 5.10

PLOT OF FUEL FLOW RATE AGAINST BRAKE POWER

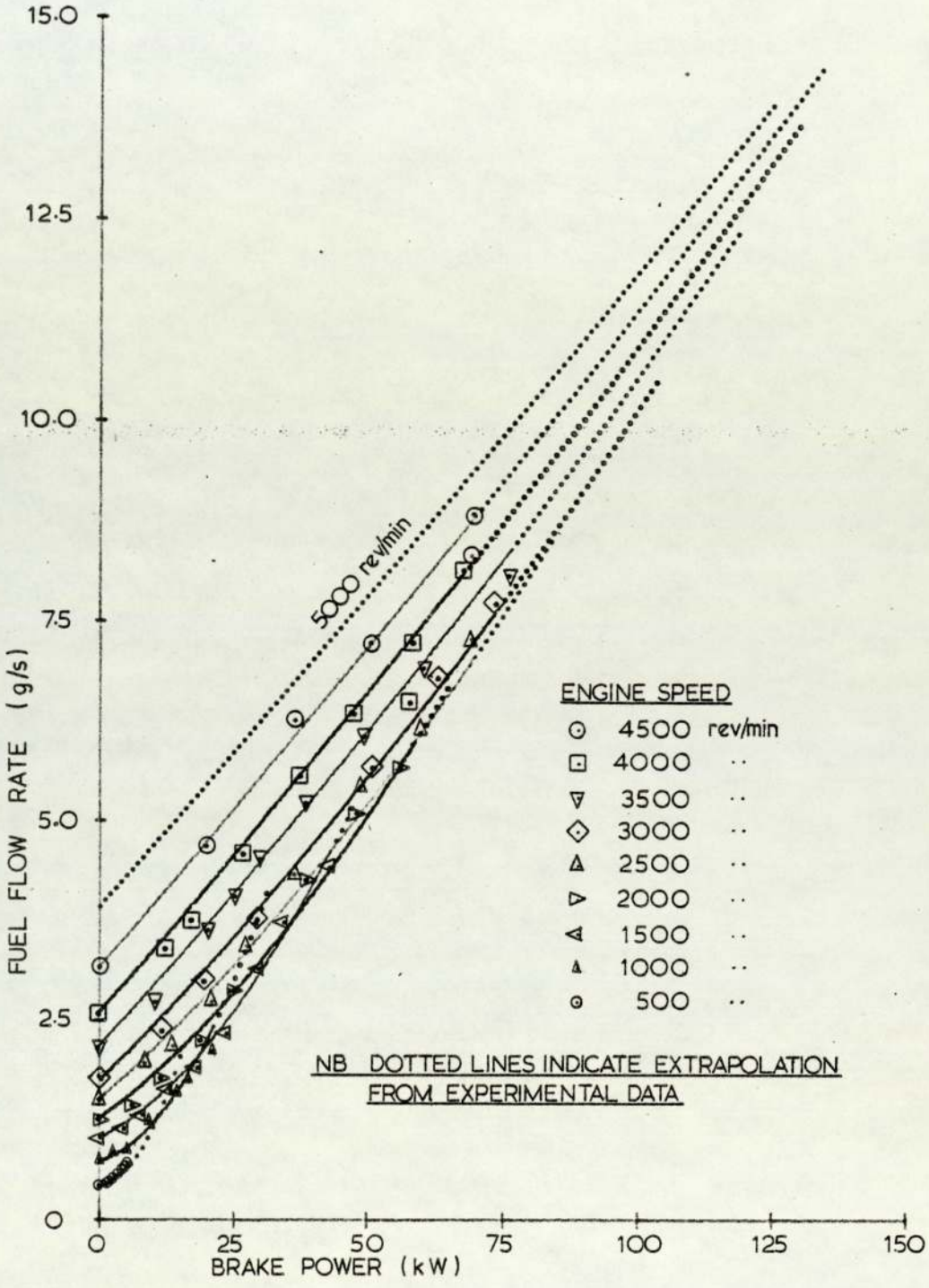

GRAPH 5.11

PLOT OF MAXIMUM BRAKE POWER AGAINST ENGINE SPEED
(FROM TESTS[75] CARRIED OUT IN THE JAGUAR
EXPERIMENTAL DEPT ON 7/7/66)

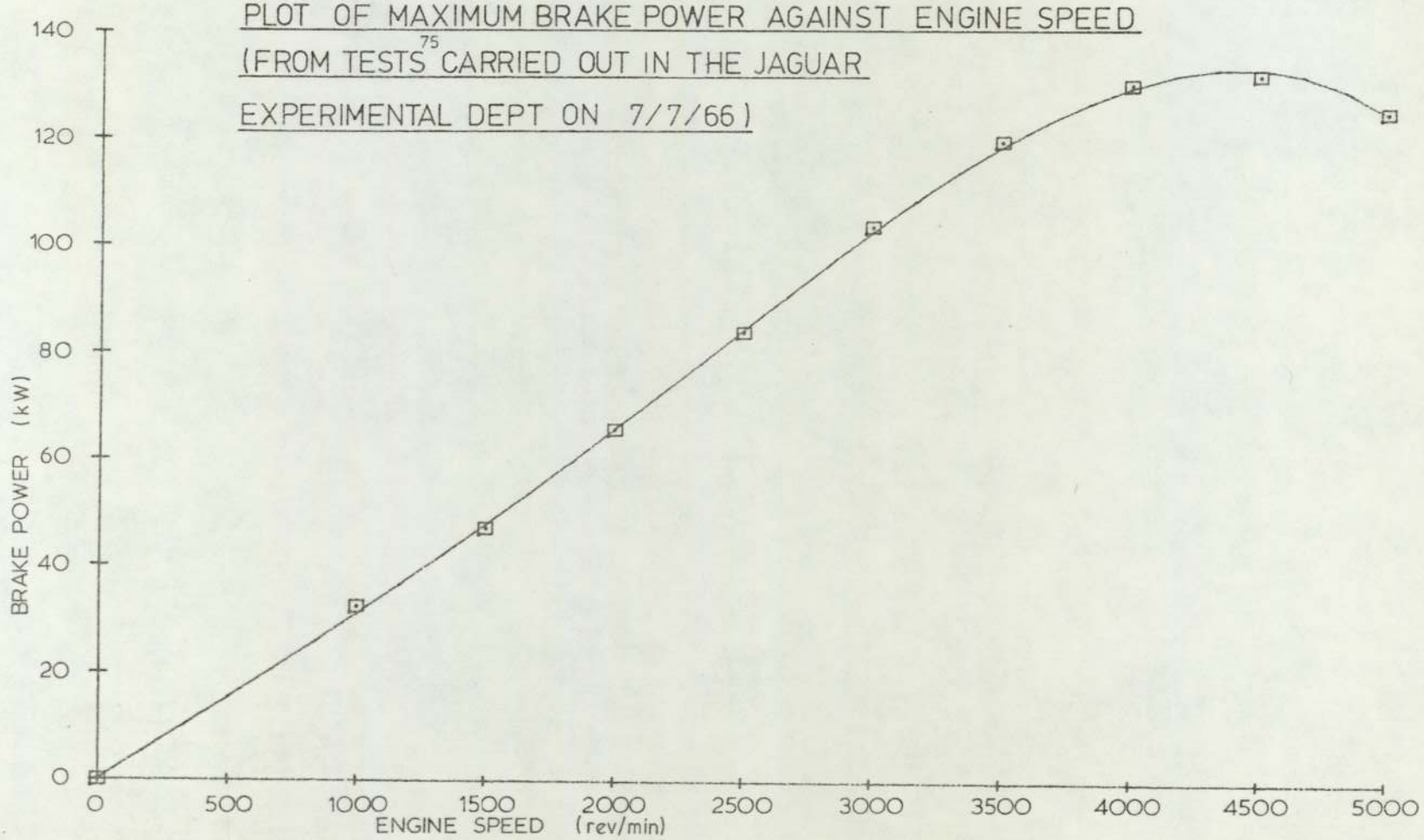

GRAPH 5.12

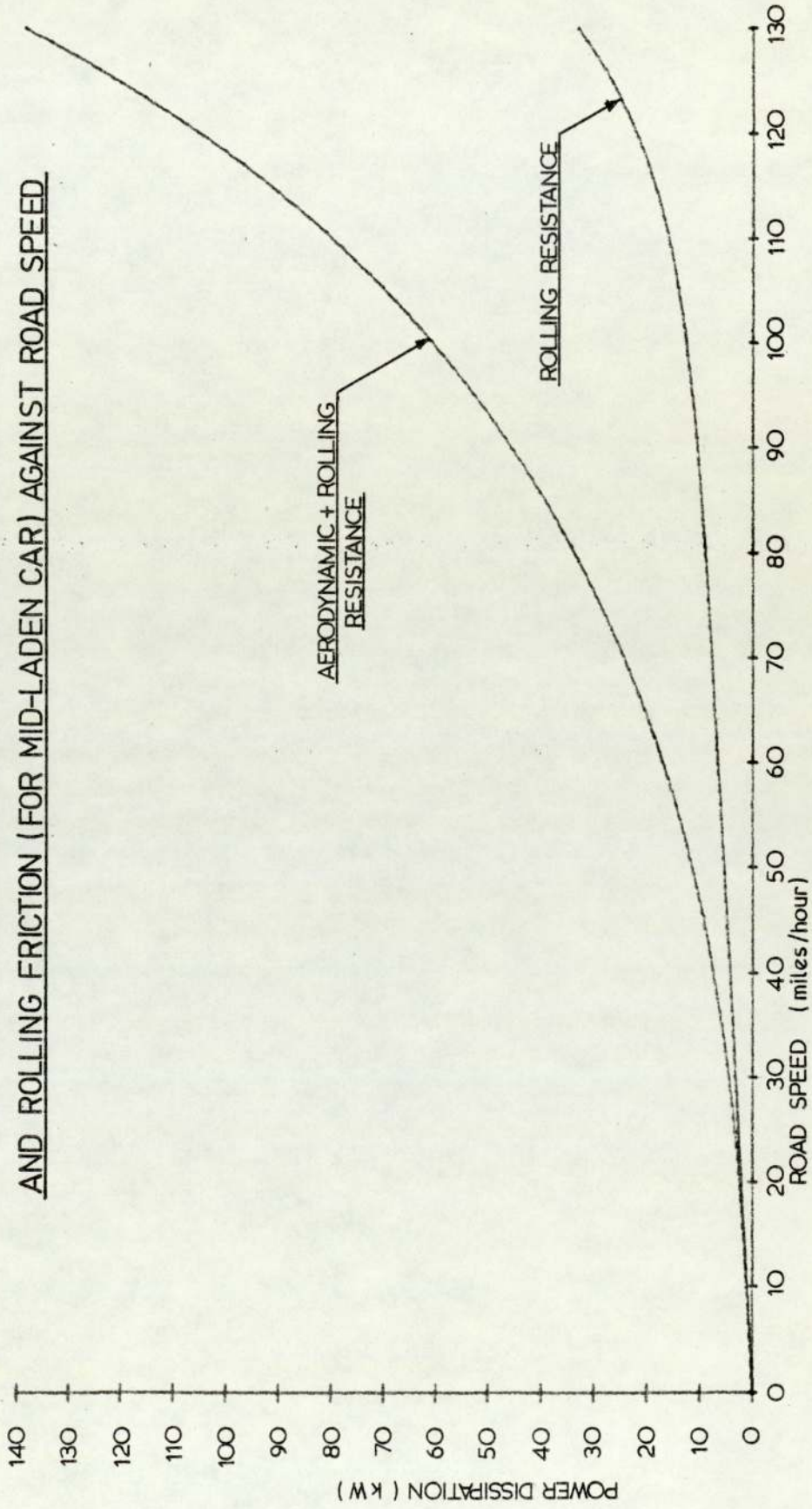
PLOT OF POWER REQUIRED TO OVERCOME AERODYNAMIC
AND ROLLING FRICTION (FOR MID-LADEN CAR) AGAINST ROAD SPEED
AERODYNAMIC + ROLLING RESISTANCE
ROLLING RESISTANCE
POWER DISSIPATION (kW)
ROAD SPEED (miles/hour)
0
10
20
30
40
50
60
70
80
90
100
110
120
130
140

GRAPH 5.13

PLOT OF COOLANT FLOW RATE AGAINST ENGINE SPEED FOR SYSTEM USING MARSTON RADIATORS SUPAPACK I RADIATORS AS FITTED TO AIR-CONDITIONED AND NON-AIR-CONDITIONED VERSIONS OF THE CAR

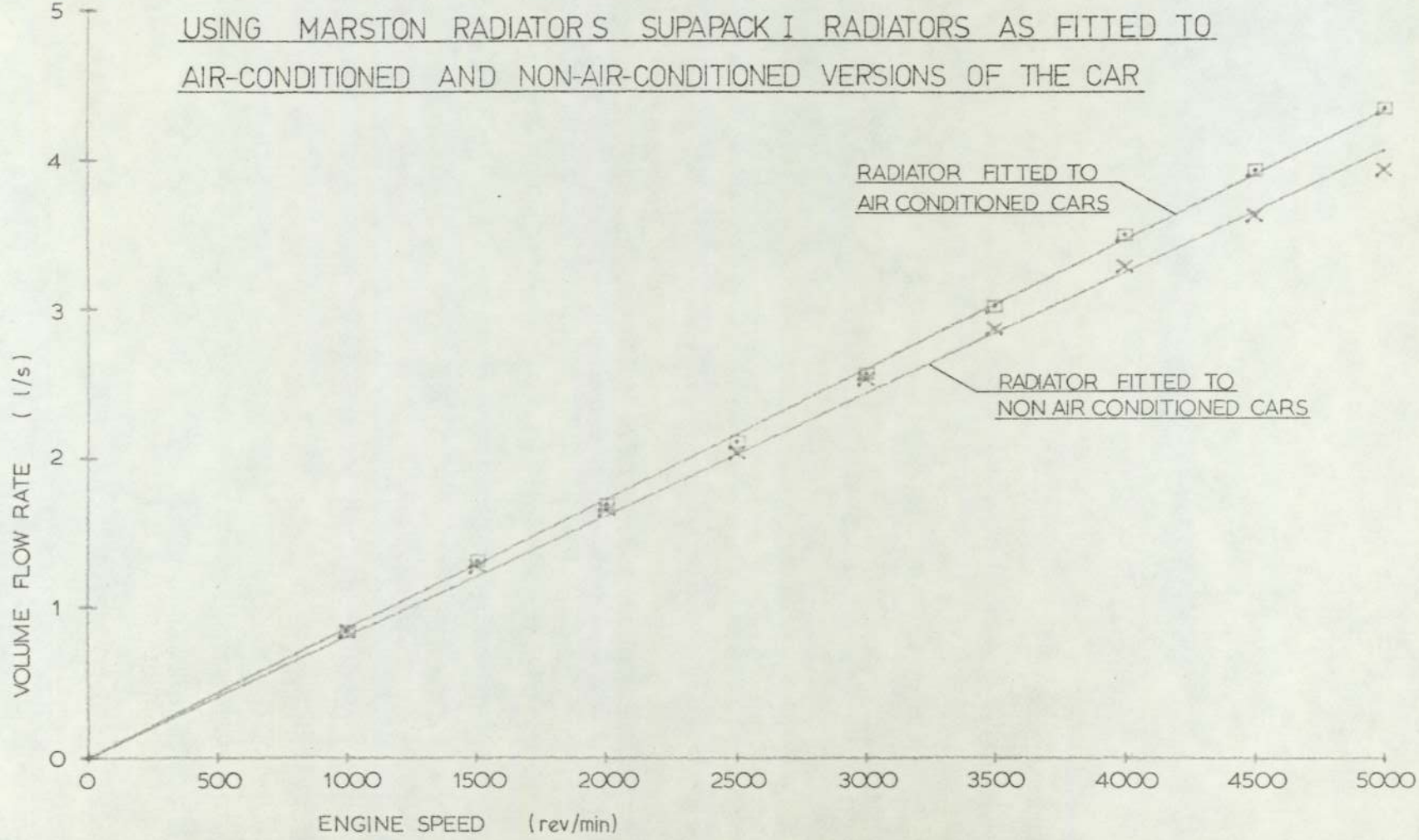

GRAPH 5.14

PLOT OF HEAT REJECTED TO ENGINE COOLING SYSTEM AGAINST ROAD SPEED

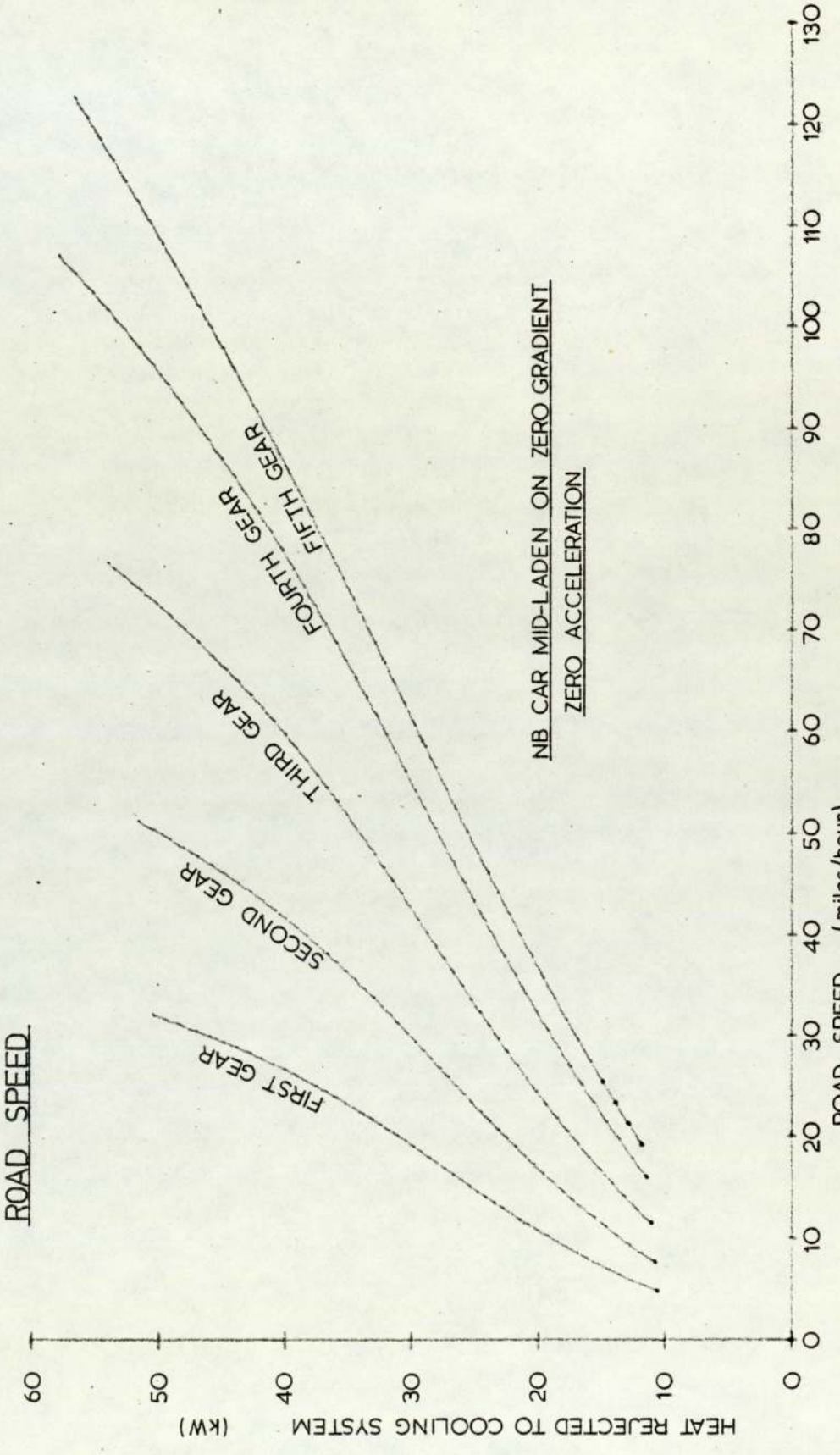

GRAPH 5.15

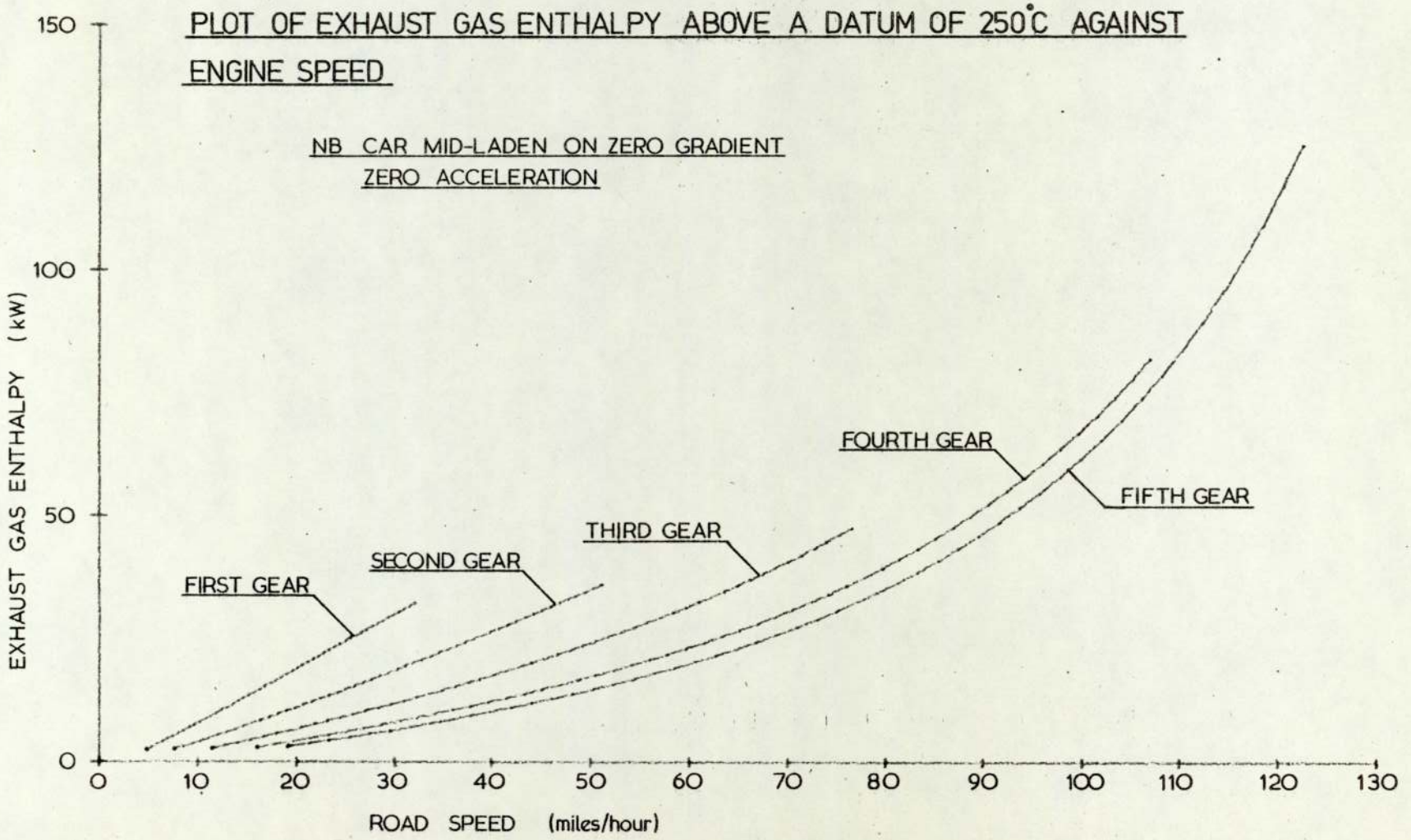
PLOT OF EXHAUST GAS ENTHALPY ABOVE A DATUM OF 250°C AGAINST ENGINE SPEED
NB CAR MID-LADEN ON ZERO GRADIENT
ZERO ACCELERATION
EXHAUST GAS ENTHALPY (kW)
150
100
50
0
FIRST GEAR
SECOND GEAR
THIRD GEAR
FOURTH GEAR
FIFTH GEAR
0
10
20
30
40
50
60
70
80
90
100
110
120
130
ROAD SPEED (miles/hour)

GRAPH 5.16

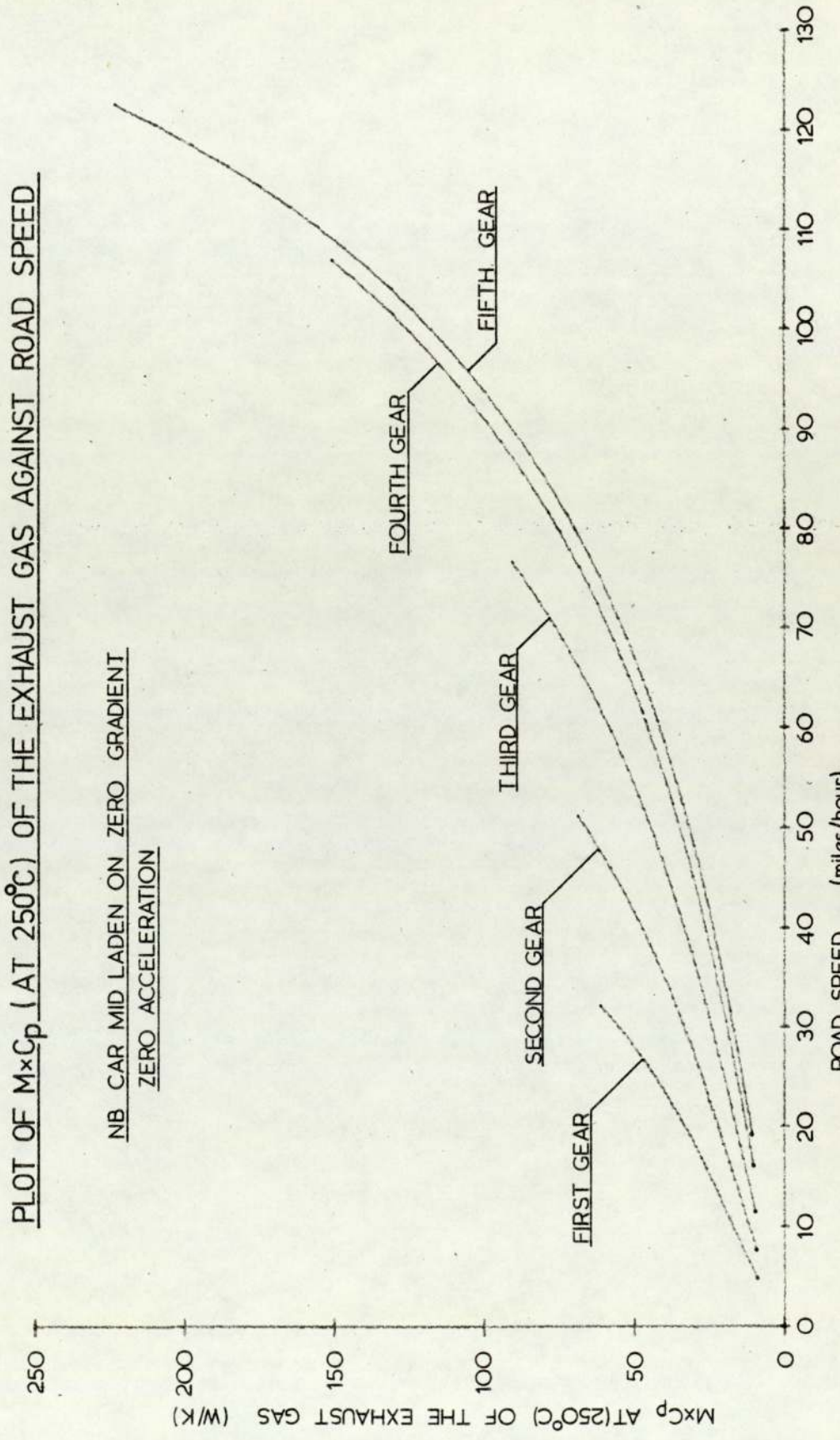
PLOT OF M×Cp (AT 250°C) OF THE EXHAUST GAS AGAINST ROAD SPEED
NB CAR MID LADEN ON ZERO GRADIENT
ZERO ACCELERATION
FIFTH GEAR
FOURTH GEAR
THIRD GEAR
SECOND GEAR
FIRST GEAR
M×Cp AT(250°C) OF THE EXHAUST GAS (W/K)
ROAD SPEED (miles/hour)
0
50
100
150
200
250
0
10
20
30
40
50
60
70
80
90
100
110
120
130

GRAPH 5.17

PLOT OF FUEL FLOW RATE AGAINST ROAD SPEED

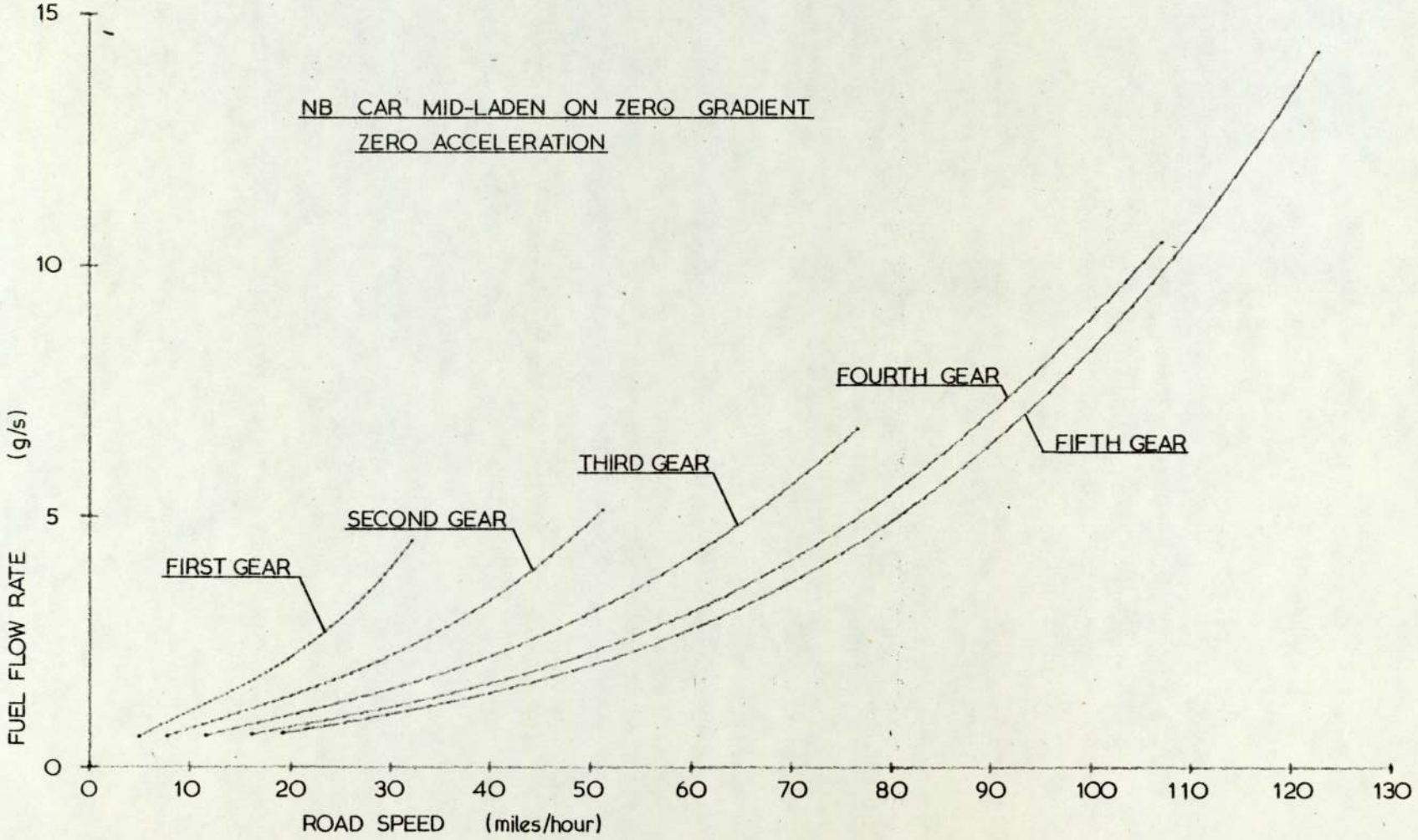

CHAPTER 6

ASPECTS OF THE FUEL ECONOMY AND ACCELERATION OF THE NON AIR-CONDITIONED CAR

THE INFLUENCE OF BRAKE LOADS ON FUEL ECONOMY

Using the model developed in chapter 5 the fractions of the fuel flow attributable to the rolling resistance of the tyres, the aerodynamic drag, and power consumption of the engine cooling fan and viscous coupling have been plotted against road speed, for each of the 5 gear ratios on graphs 6.1, 6.2 and 6.3, and that due to the fan and coupling at idle against engine speed on graph 6.4. Since the rolling resistance is directly proportional to the vehicle weight graph 6.1 may also be considered as the fraction of the total fuel flow attributable to the mass of the vehicle. Since this fraction varies almost linearly with mass the result of weight reduction on fuel economy may be calculated from this graph. It is apparent that a considerable weight reduction is required to produce a significant reduction in fuel flow rate, but this is only for the steady state condition considered. Mass reduction results in an increase of acceleration at a given engine power output above the steady state load, and conversely to achieve a given acceleration a reduction in mass results in a reduction in fuel flow rate. The overall fuel saving which might be achieved given a reduction in vehicle mass, will therefore be greater than predicted from this graph.

The influence of a reduction in drag coefficient may similarly be predicted from graph 6.2. At high speed it is apparent that such savings may be very significant, the result of a 20% reduction in the drag coefficient resulting in a 12% reduction in fuel consumption at speeds above 100 miles/hour.

The saving of fuel by an increase in cooling fan efficiency is also significant as may be predicted from graphs 6.3 and 6.4, but only at high engine speeds. The figure for an idle speed of less than 1300 rev/min is less than 1%. At the present idle speed of 750 rev/min the fan and coupling increase the fuel consumption by only 0.15%. The most significant fuel saving to be gained from the cooling fan

system would result from the use of a constant speed fan - independent of engine speed. This would need to be sized to take account of low speed driving as well as idling. An electric or hydraulic system would have the additional advantage of being easily controlled thermostatically, an on/off system for the former and proportional control for the latter. The electrical load of an electric cooling fan needs to be high even given a fan of high efficiency, and a hydraulic system would probably be expensive. Possibly the cheapest way of providing a constant speed fan would be to include a centrifugal governor in the present viscous coupling to move the plates further apart as the fan speed rises. The effect of a constant speed cooling fan on engine temperature is considered in chapter 7. The fan at present used has an efficiency of approximately 30%. For the present engine driven system a 60% efficient fan would give a fuel saving of approximately 2% at 70 miles/hour in fifth gear, given that the viscous coupling was changed to give the same slip/speed characteristics as at present. Of the three possible economies considered above the cooling fan is probably the item to yield a return most readily.

THE EFFICIENCY AND RATIOS REQUIRED OF A STEPLESSLY VARIABLE TRANSMISSION

Using the model developed in chapter 5, the fuel flow rate at constant engine brake loads up to the maximum has been plotted on graph 6.5. At low brake loads it is apparent that for a given brake load there is an engine speed at which the fuel flow rate reaches a minimum. The locus of these minima has also been plotted. At very low brake loads this minimum does not exist and at high loads the minimum is at the engine speed for which the load is the maximum which the engine can achieve. The spark ignition engine, by virtue of the method of power output regulation, i.e. intake throttling, may be expected to give maximum economy at full throttle when the pumping losses are least. At low engine speeds for this engine, the influence of throttle opening on fuel air mixing

is probably the reason why maximum economy is achieved at part throttle openings. The desirability of turbulence in the inlet manifold for improved fuel economy is well known.

Also plotted on graph 6.5 is the fuel flow in each gear ratio for the mid-laden car in steady state on a zero gradient. It is immediately obvious that the gear ratios do not lie anywhere near the optima for fuel economy.

The selection of ratios for a fixed ratio gearbox inevitably results in a compromise between economy and high acceleration. The high costs of fuel have recently encouraged interest in steplessly variable transmissions. Use of such a transmission may allow for the engine to be run at an optimum speed for economy and acceleration. Steplessly variable transmissions inevitably suffer lower efficiencies than their fixed ratio counterparts owing to greater complexity and slip in the mechanism. Whilst a particular steplessly variable transmission has not been studied, the required ratios and efficiency of such a system to compete on the basis of fuel economy and acceleration have been calculated using the model developed in chapter 5.

Optimised gear ratios against road speed are shown on graph 6.6. For the engine to give maximum economy the engine is made to run at 750 rev/min at road speeds up to that for which the engine brake load gives a minimum fuel flow rate for that engine speed. The engine speed of 750 rev/min was chosen as the lowest speed at which the engine will run smoothly. At road speeds higher than this the engine is constrained to run at the speed which produces a minimum fuel flow rate. This pattern continues until the minimum fuel flow rate which can be achieved is by running the engine at a speed such that maximum power is being developed. The maximum speed of the car is achieved with the engine running such that its speed is that which produces the maximum power available.

Maximum acceleration is obtained by maintaining the engine speed such that maximum power is being produced.

The graph of gear ratio against road speed shows the ratio required for transmission efficiencies of 50 to 100% in steps of 10%. To give the overall transmission efficiency this figure must be multiplied by the 93% efficiency, assumed to still exist for the rear axle. The present fixed gear ratios are also shown for comparison. For this graph the gear ratio has been assumed to be variable down to a zero ratio. Such a ratio would in theory give an infinitely high torque at the road wheels and in practice would have to be limited. Depending on the mechanism chosen, the use of a clutch of some kind may be required for starting. This would be the case for mechanical steplessly variable transmissions in which complete velocity reduction is not possible. The minimum gear ratio required for smooth traction at starting speeds may be taken as that of the current first gear ratio. Under such conditions and with the exclusion of down hill running the ratio of maximum to minimum gear ratios would be of the order of 10.5 to 1 for a 100% efficient system and 7 to 1 for a 50% efficient system.

The optimum fuel flow rates for transmission efficiencies of 100% down to 50% have been plotted on graph 6.7. Also on this graph is the present fuel flow rate for each of the current gear ratios for comparison. To clarify this, the efficiency required, for an optimised system to compete with the present gearbox, has been plotted against road speed on graph 6.8. It is apparent that a transmission with an efficiency as low as 75% may give an improved overall consumption.

Maximum acceleration has been plotted against road speed for steplessly variable transmissions of 100% efficiency down to 50% efficiency on graph 6.9. In calculating vehicle acceleration no account has been taken of the angular acceleration of the road wheels, transmission or engine components, and the results should be used for comparison only between the two systems. As for the fuel flow rate the minimum efficiency required for the steplessly variable transmission to compete has been plotted on graph 6.10. An efficiency as low as 75% would again be worthy of consideration.

A further advantage of the steplessly variable unit is that due to the lower engine speeds, heat rejection from the engine to the cooling system is reduced. This is shown by graph 6.11 where the heat rejected to the coolant has been plotted against road speed, for the zero acceleration case.

For both economy and acceleration an overall transmission efficiency of 75% seems to be the minimum worthy of consideration. For both cases lower efficiencies at low speeds would not deter the use of such a system. At high speeds and high powers, the level of heat rejection from the transmission and the problem of providing sufficient heat transfer surface may be difficult to overcome and is a further indication that the higher efficiency of the transmission, if of varying efficiency, should be at the top of the speed range.

Given a steplessly variable transmission the requirement of the engine to operate at all power/speed combinations, and to do so without producing exhaust pollution, or high noise and vibration levels is an unnecessary constraint on its design. This may in the future make the diesel engine or the stratified charge spark ignition engine more favourable than at present. An engine designed for use with a steplessly variable transmission would doubtless compete with the present engine/transmission system with lower efficiencies than are suggested to be needed by this analysis.

Prior to the cessation of production of constant displacement steam engines for cars, one of their major advantages was the smoothness of their acceleration. This must be among the major advantages also of an internal combustion engined car with a steplessly variable transmission.

THE CONTROL SYSTEM REQUIRED FOR A STEPLESSLY VARIABLE TRANSMISSION

The arrangement of a control system for a car with a steplessly variable transmission should be such that there would be no problem for a driver used to driving cars with conventional manual or automatic transmissions.

The conventional accelerator pedal effectively calls a power output from the engine, although the relationship between throttle opening and power is also a function of engine speed. The suggested control system for a car with a steplessly variable transmission would be similar. The displacement of the accelerator pedal would call for a finite power output from the engine. The control system by either analogue or digital means would calculate the required engine speed and throttle opening required. The engine speed would be set by comparing the speed of the road wheels with the required engine speed. On the result of this comparison a gear ratio would be calculated. The throttle opening and gear ratio would then be set by servo-mechanisms operated by the control system. Lifting of the pedal would effectively call a negative power output from the engine, and as with the present system use the pumping losses in the engine as a braking system. Particularly if rear wheel traction were retained, the amount of power absorbed by lifting the pedal fully should be limited. The separate braking system, operated from a separate pedal should be retained and be completely independent of the transmission/ engine control system.

Such a control system could be linked to also control the fuel injection system and the ignition system rather than controlling these from the dual inputs of engine speed and manifold depression.

The time constant of the control system would need to be short to avoid making the car both unattractive and possibly dangerous. This requirement may point in favour of an analogue rather than a digital system, although recent advances in electronics have made the digital system feasible.

GRAPH 6.1 PLOT OF FRACTION OF FUEL FLOW RATE ATTRIBUTABLE TO THE ROLLING RESISTANCE OF THE TYRES

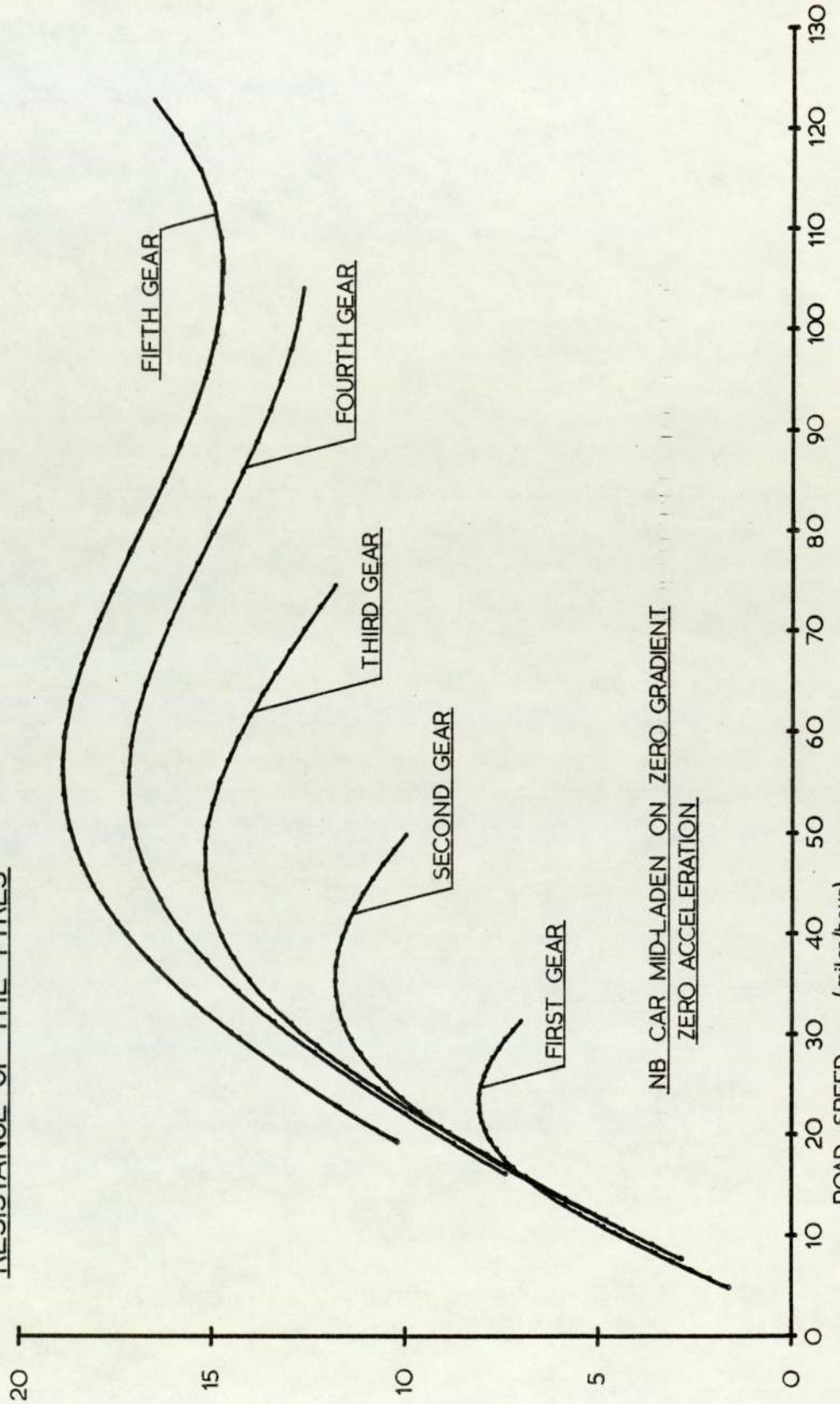

GRAPH 6.2

PLOT OF FRACTION OF TOTAL FUEL FLOW ATTRIBUTABLE TO AERODYNAMIC DRAG AGAINST ROAD SPEED

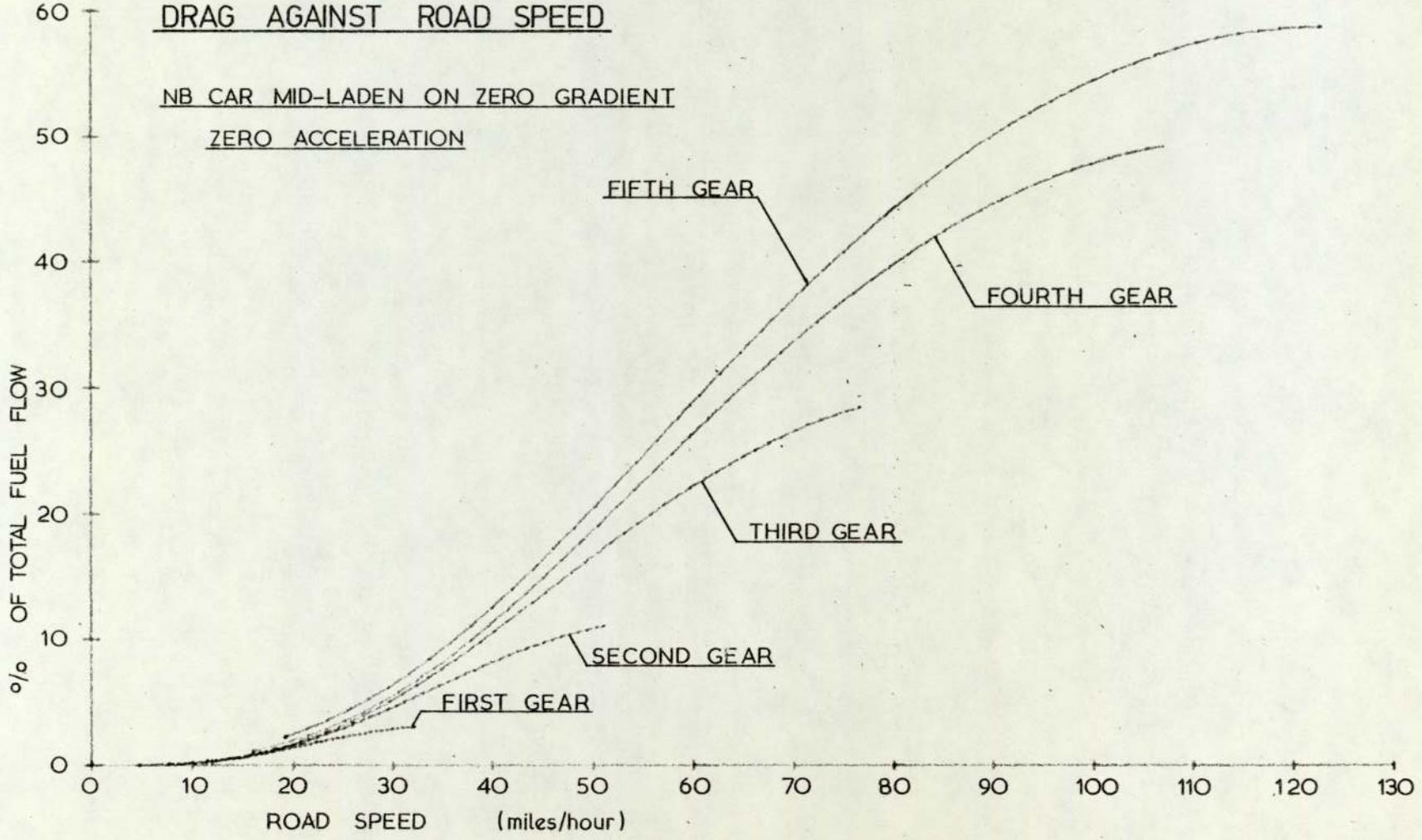

GRAPH 6.3

PLOT OF FRACTION OF TOTAL FUEL FLOW ATTRIBUTABLE TO THE ENGINE COOLING FAN AND VISCOUS COUPLING AGAINST ROAD SPEED

NB CAR MID LADEN ON ZERO GRADIENT

ZERO ACCELERATION

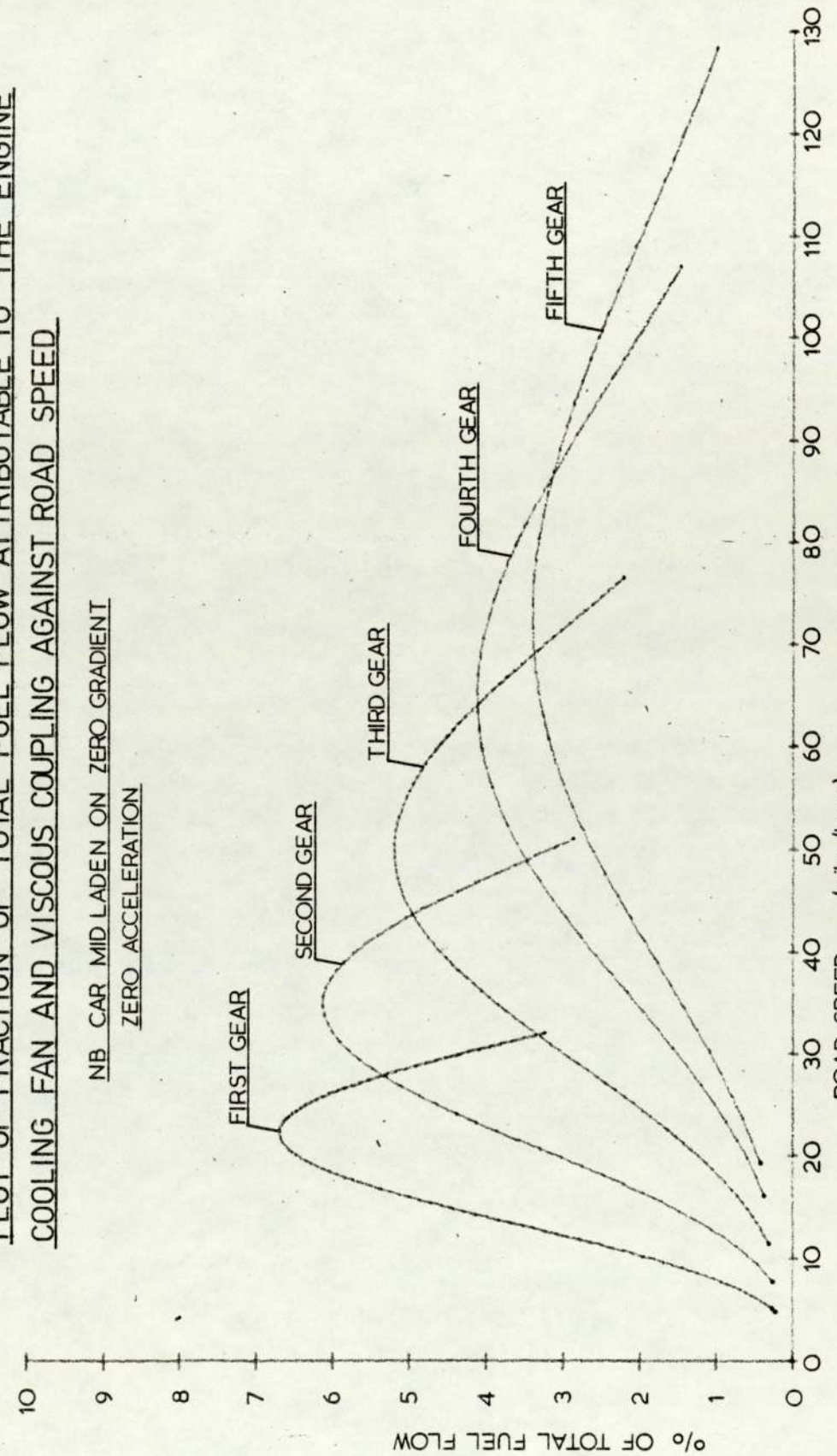

GRAPH 6.4

PLOT OF FRACTION OF TOTAL FUEL FLOW ATTRIBUTABLE TO THE ENGINE COOLING FAN AND VISCOUS COUPLING AGAINST ENGINE SPEED

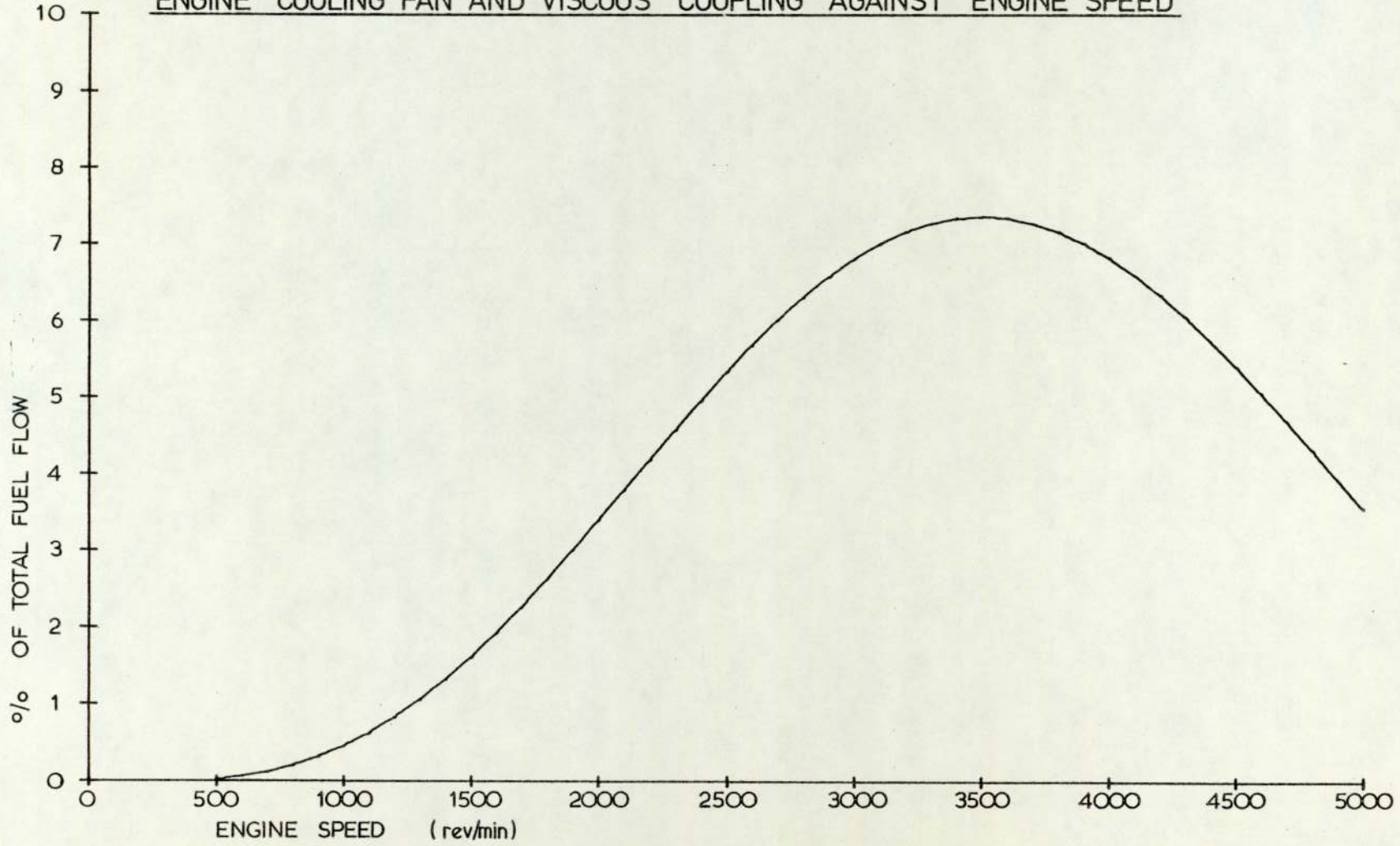

GRAPH 6.5

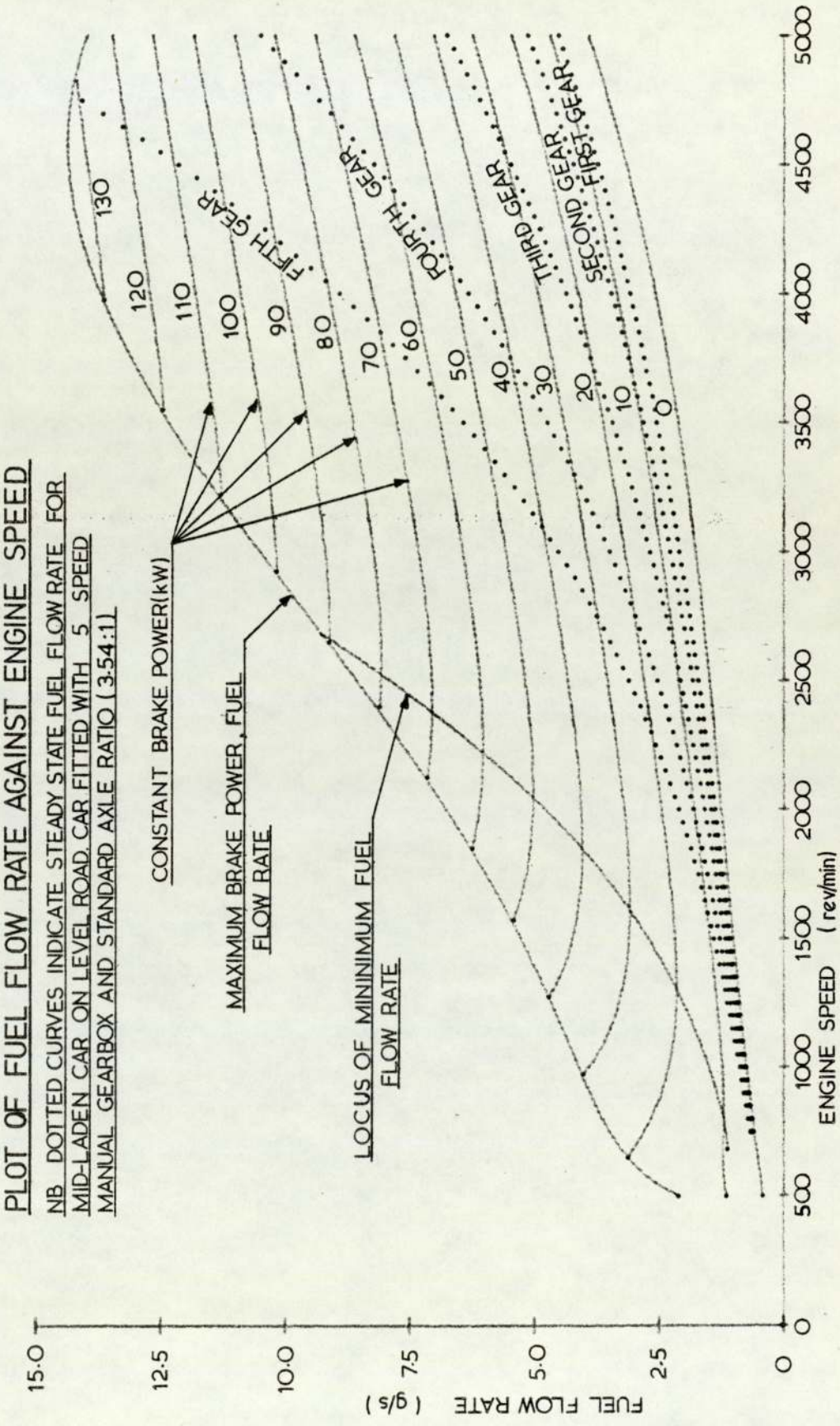
PLOT OF FUEL FLOW RATE AGAINST ENGINE SPEED
NB DOTTED CURVES INDICATE STEADY STATE FUEL FLOW RATE FOR MID-LADEN CAR ON LEVEL ROAD. CAR FITTED WITH 5 SPEED MANUAL GEARBOX AND STANDARD AXLE RATIO (3.54:1)
CONSTANT BRAKE POWER(kW)
MAXIMUM BRAKE POWER, FUEL FLOW RATE
LOCUS OF MININIMUM FUEL FLOW RATE
FIFTH GEAR
FOURTH GEAR
THIRD GEAR
SECOND GEAR
FIRST GEAR
130
120
110
100
90
80
70
60
50
40
30
20
10
0
FUEL FLOW RATE (g/s)
15·0
12·5
10·0
7·5
5·0
2·5
0
0
500
1000
1500
2000
2500
3000
3500
4000
4500
5000
ENGINE SPEED (rev/min)

GRAPH 6.6

PLOT OF CURRENT AND OPTIMISED STEPLESSLY VARIABLE GEAR RATIOS AGAINST ROAD SPEED

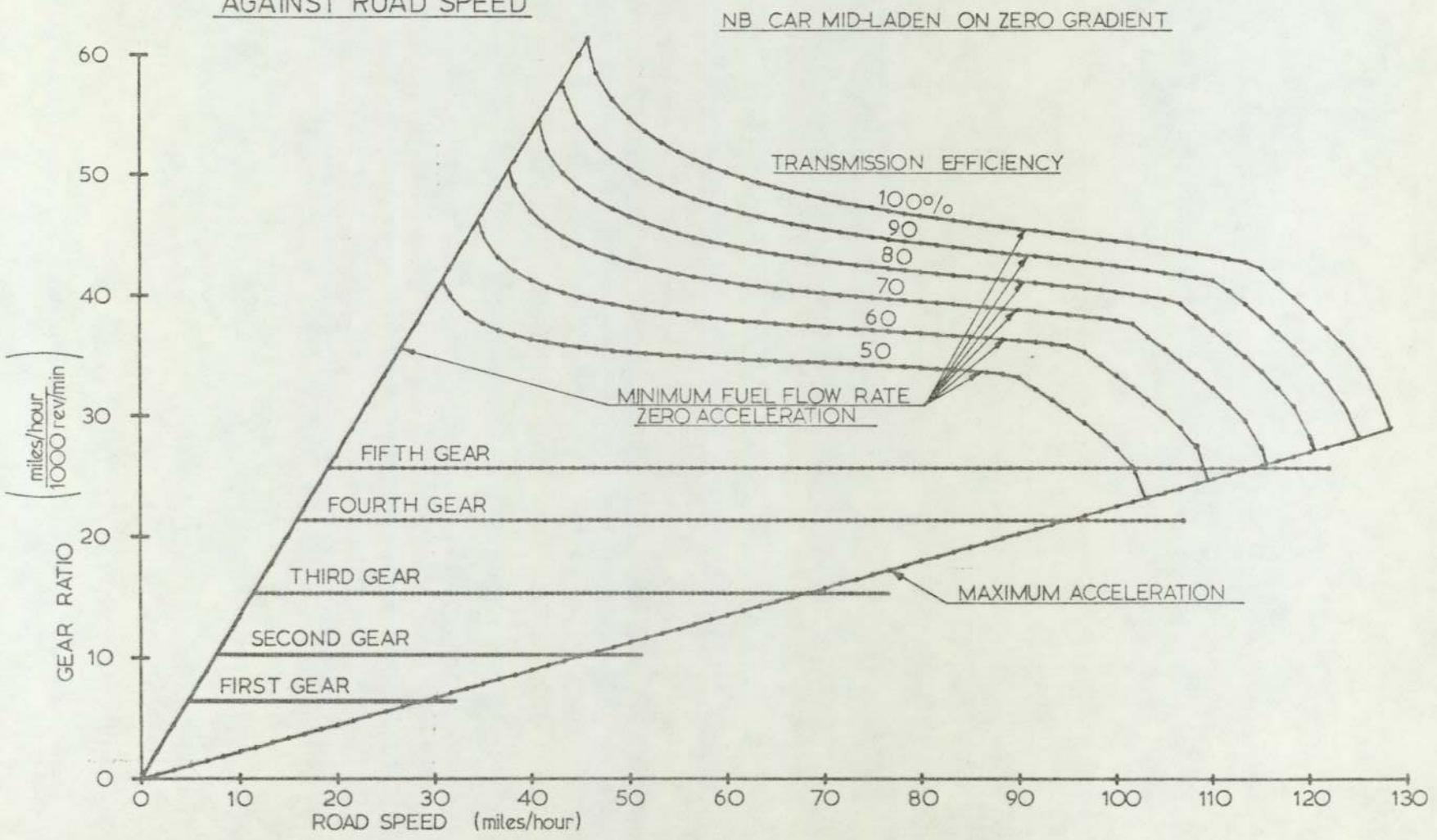

GRAPH 6.7 PLOT OF FUEL CONSUMPTION AGAINST ROAD SPEED USING AN OPTIMISED STEPLESSLY VARIABLE TRANSMISSION AND THE CURRENT GEARBOX

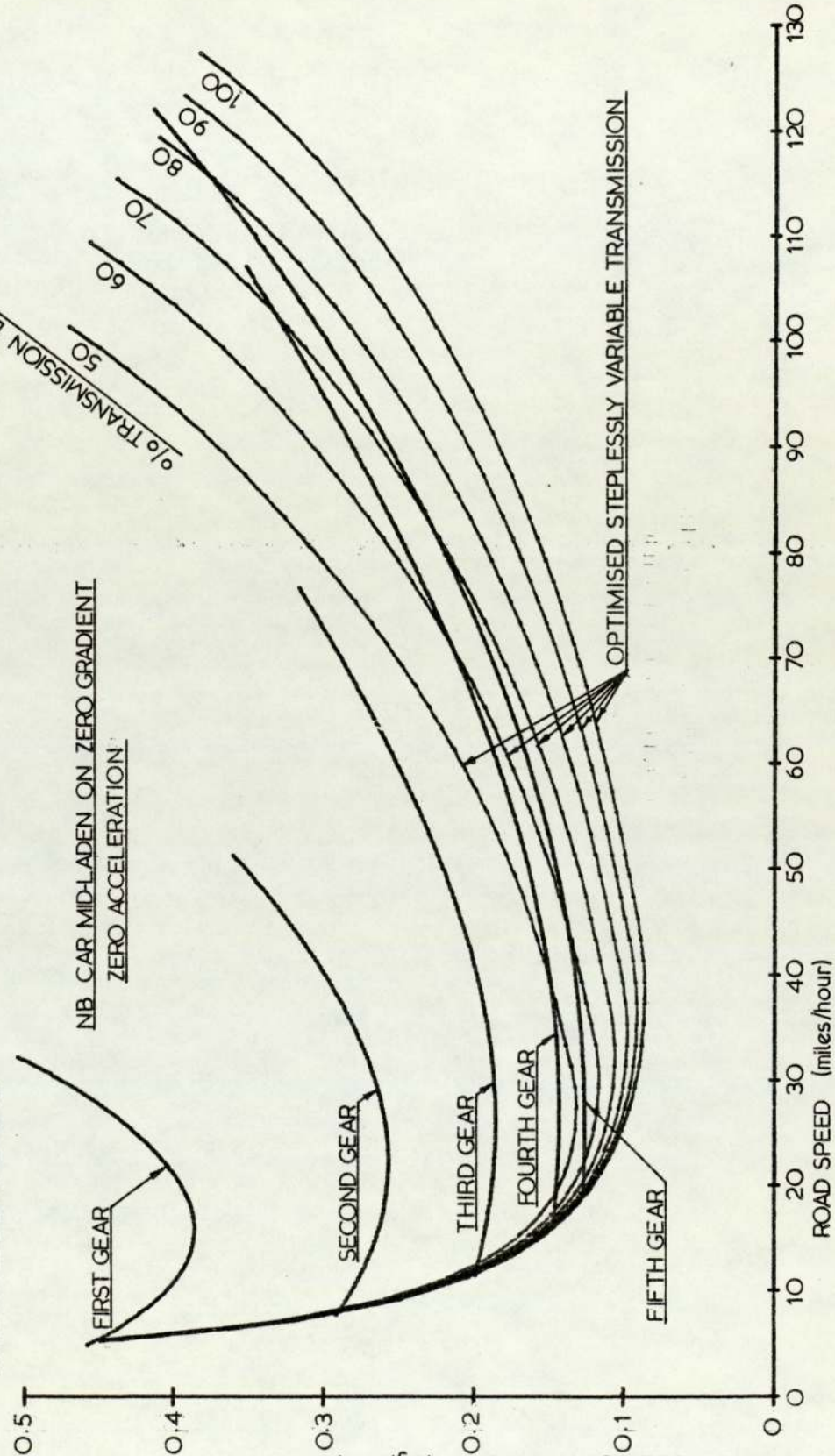

GRAPH 6.8

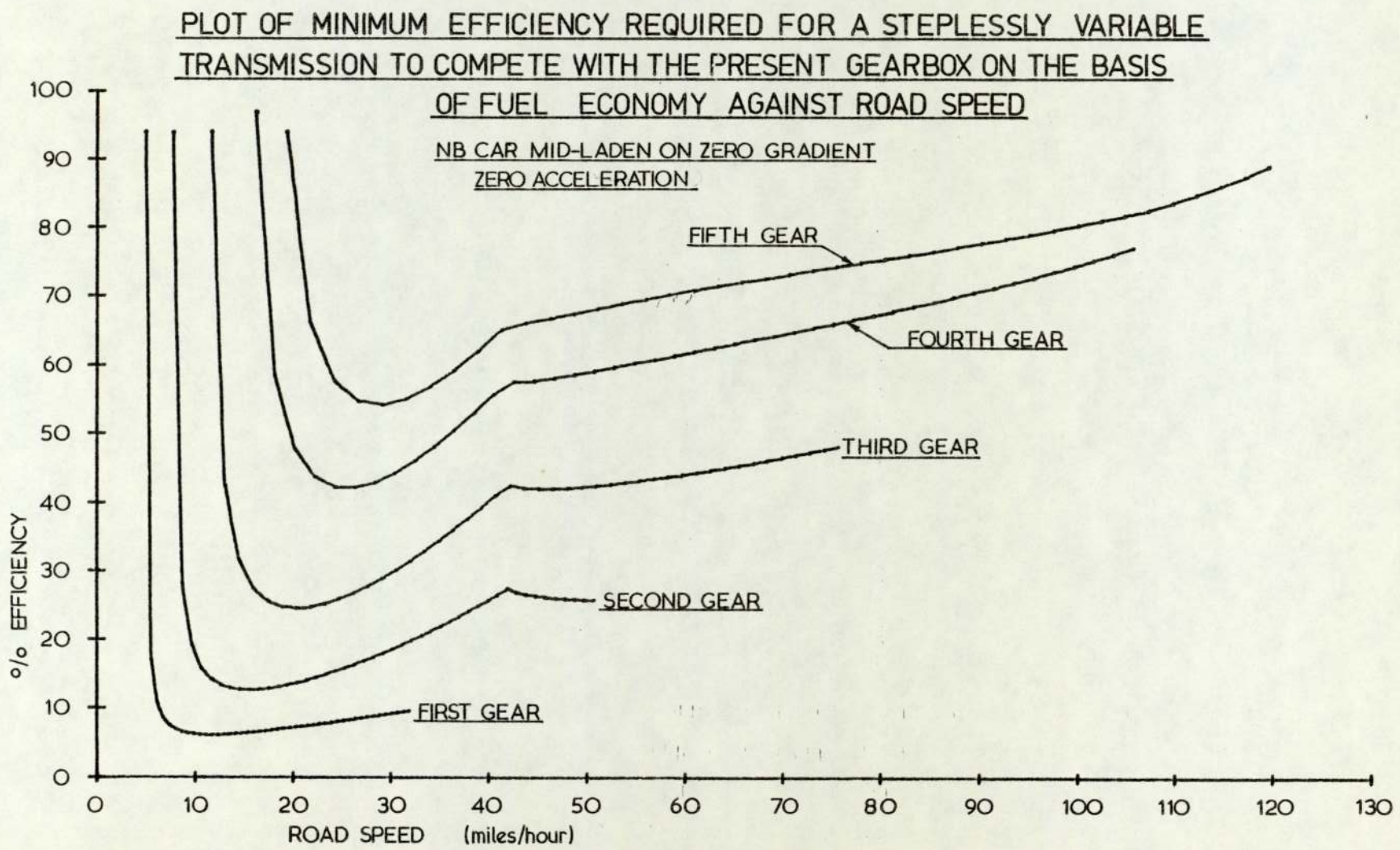
PLOT OF MINIMUM EFFICIENCY REQUIRED FOR A STEPLESSLY VARIABLE TRANSMISSION TO COMPETE WITH THE PRESENT GEARBOX ON THE BASIS OF FUEL ECONOMY AGAINST ROAD SPEED
NB CAR MID-LADEN ON ZERO GRADIENT
ZERO ACCELERATION
FIFTH GEAR
FOURTH GEAR
THIRD GEAR
SECOND GEAR
FIRST GEAR
% EFFICIENCY
ROAD SPEED (miles/hour)
0
10
20
30
40
50
60
70
80
90
100
110
120
130

GRAPH 6.9

PLOT OF MAXIMUMUM ACCELERATION USING AN OPTIMISED STEPLESSLY VARIABLE TRANSMISSION AND THE CURRENT GEARBOX AGAINST ROAD SPEED

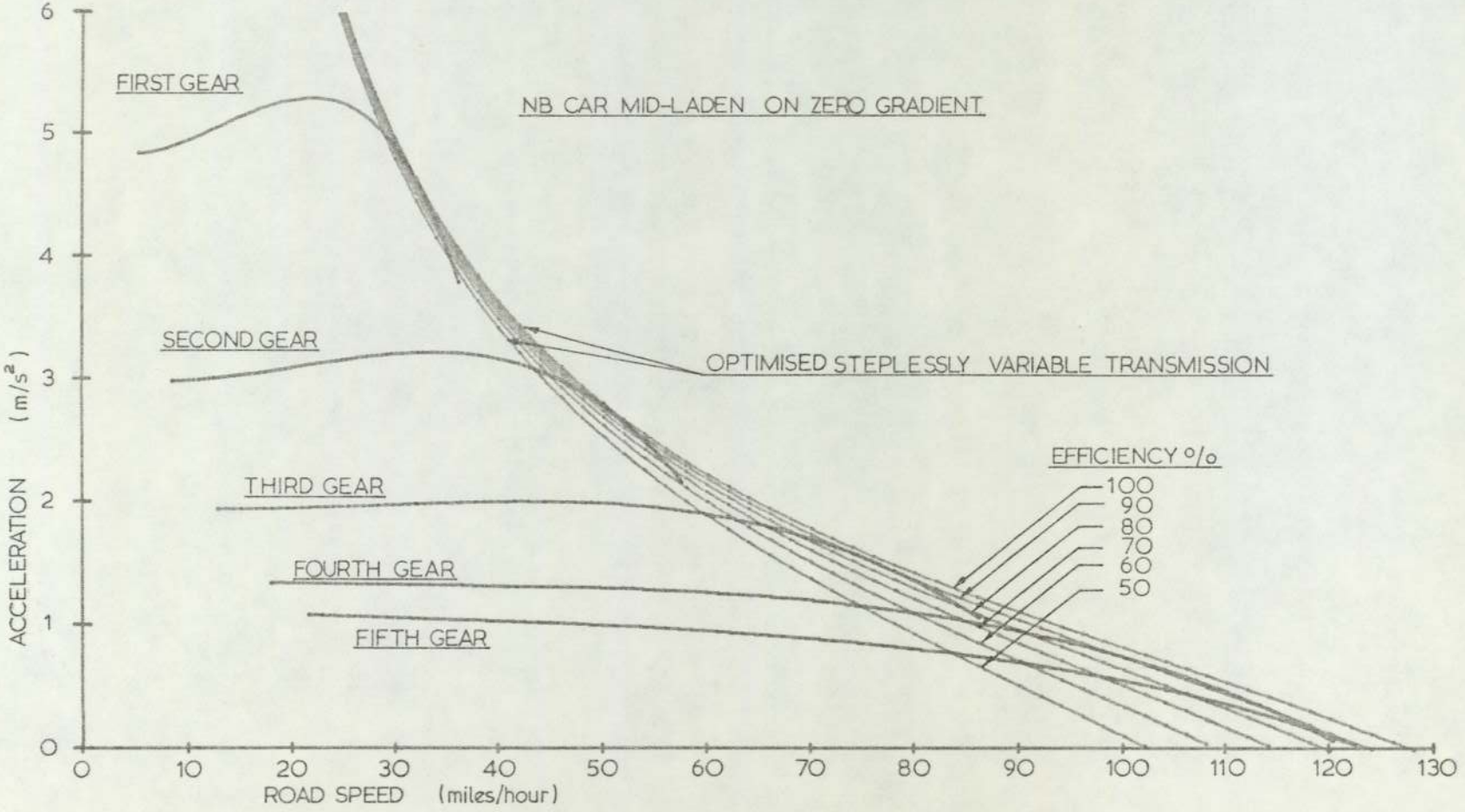

GRAPH 6.10

PLOT OF MINIMUM EFFICIENCY REQUIRED FOR A STEPLESSLY VARIABLE TRANSMISSION TO COMPETE WITH THE PRESENT GEARBOX ON THE BASIS OF MAXIMUM ACCELERATION

NB CAR MID-LADEN ON ZERO GRADIENT

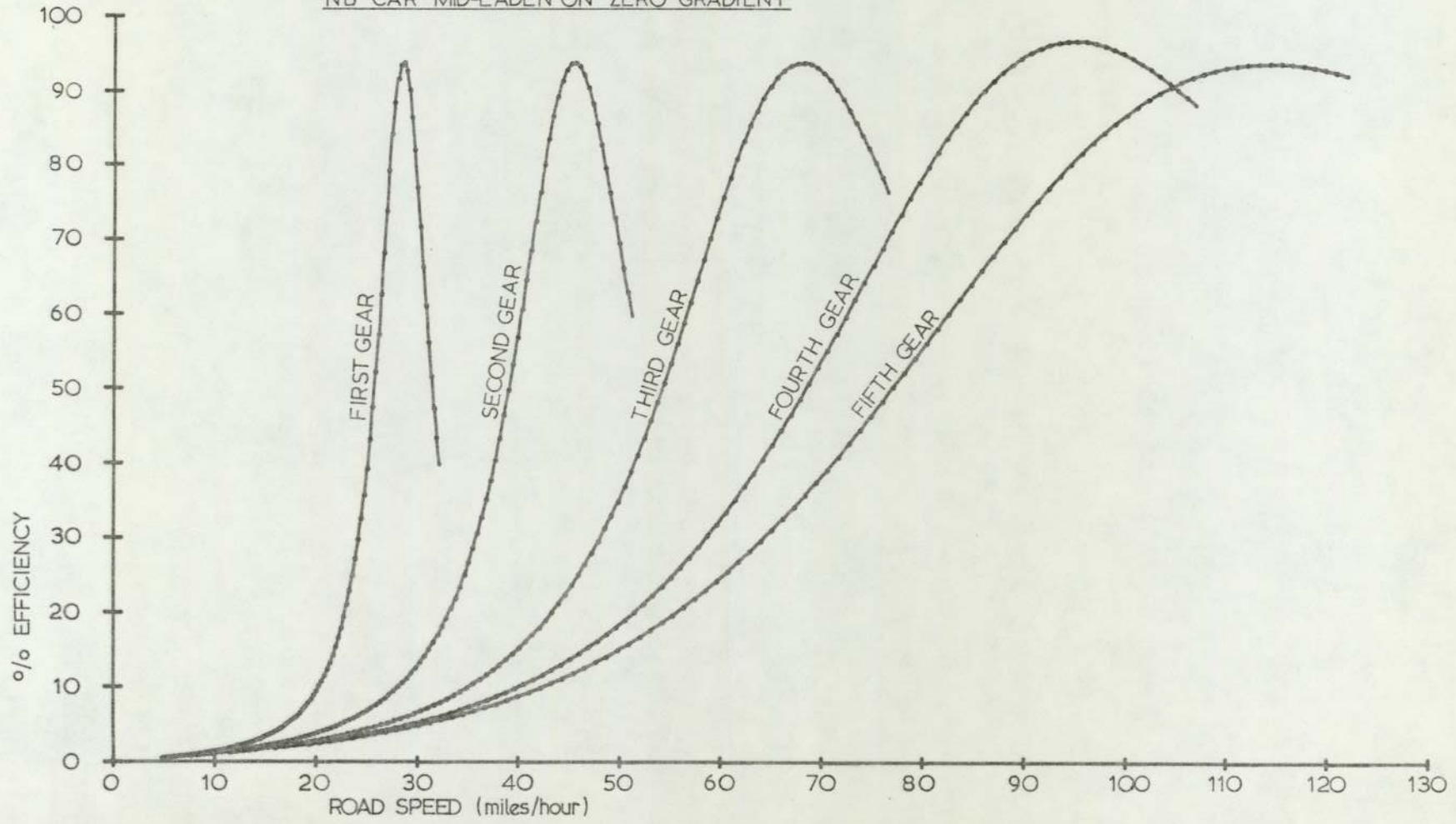

GRAPH 6.11

PLOT OF HEAT REJECTED TO ENGINE COOLING SYSTEM AGAINST ROAD SPEED USING AN OPTIMISED STEPLESSLY VARIABLE TRANSMISSION AND CURRENT GEARBOX

NB CAR MID-LADEN ON ZERO GRADIENT
ZERO ACCELERATION

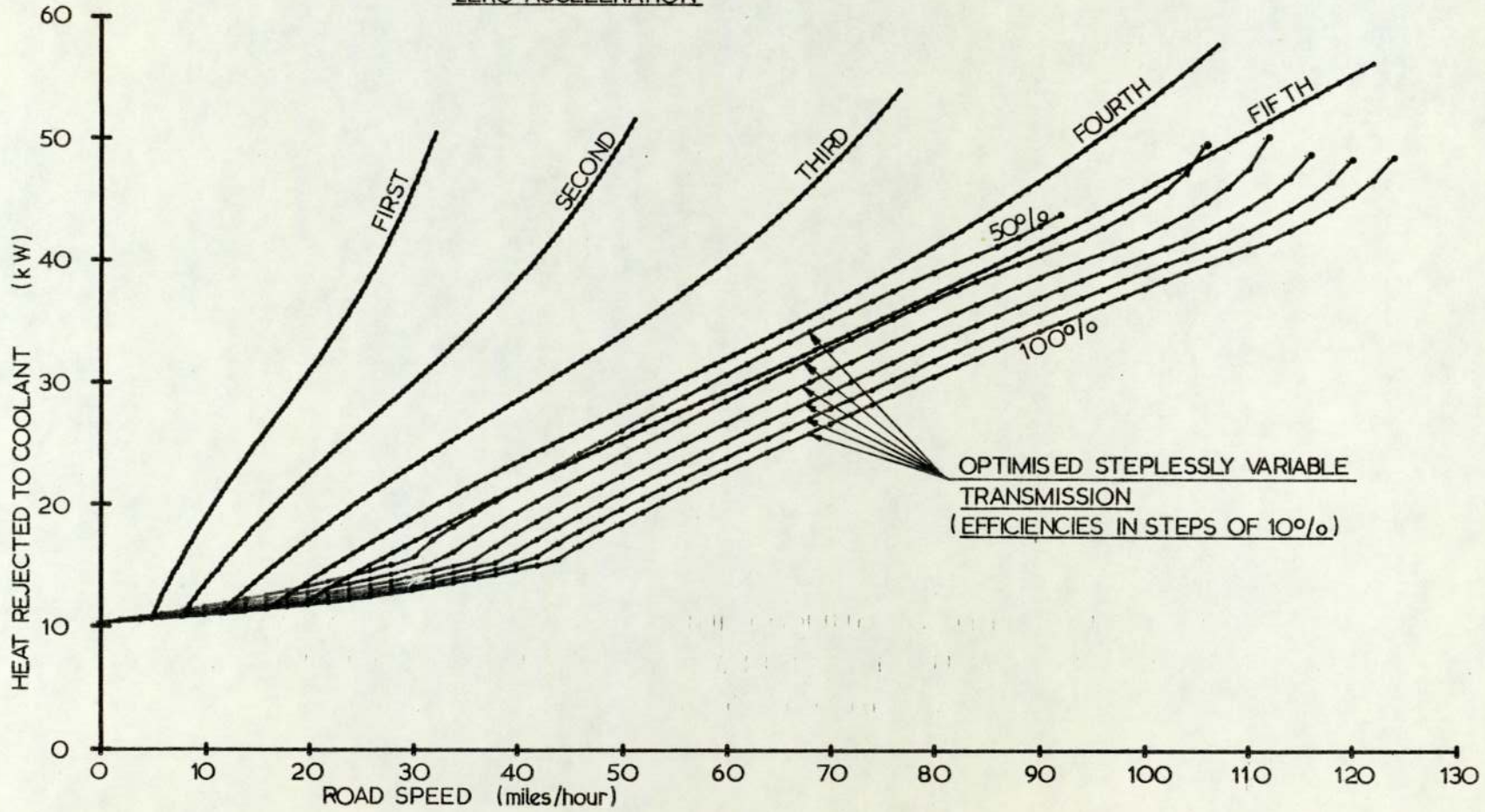

CHAPTER 7

THE ENGINE COOLING SYSTEM

THE MODEL OF THE ENGINE COOLING SYSTEM

The model of the engine cooling system assumes steady state operation, obviating the need for data on the thermal capacity of the system components and calculations involving unsteady state heat transfer. The model in the form of a computer program is contained in appendix A5.

The heat flux to the coolant is calculated from the model described in chapter 5. The model thus takes account of engine speed and engine brake power output, which equals the road load divided by the transmission efficiency, plus the power consumption of the engine cooling fan and viscous coupling.

The radiator air velocity is calculated from the model described in chapter 4 which takes account of the air velocity components due to ram pressure and to the fan, the fan volume flow rate/pressure characteristics being described by cubic spline equations to experimental data. The radiator and condenser piezometric pressure differences are found from equations 4.27 and 4.33 respectively.

The coolant flow rate is calculated by the method described in chapter 5.

The radiator air off temperature is a function of the air mass flow rate, the air on temperature, and the specific heat capacity of air. The latter is calculated from an equation fitted to the data of Mayhew and Rogers[66], as was used in chapter 4 for the calculation of radiator heat transfer data from the experimental results of the radiator manufacturer.

The coolant side heat transfer coefficient for the radiator is found from equations 4.25 and 4.26 with a constant which is a mean of the two given, the properties of the coolant being calculated by the method described in chapter 4.

The radiator air side coefficient is calculated from equation 4.28, the properties of air being calculated by the method described in chapter 4. The radiator fin efficiency is calculated from equation 4.29. The equation due to Stevens[63] and given by Rohsenow and Hartnett[64] for a cross flow heat exchanger is

used, with fluid mixing on the coolant side assumed, as discussed in chapter 4, for the calculation of coolant temperatures.

At temperatures above 100°C at which the thermostat is assumed to be fully open the coolant mass flow rate is a function of engine speed only. By assuming an initial top hose temperature of 100°C a more accurate top hose temperature is calculated. If this is more than 100°C then the thermostat is fully open and an iterative procedure is used to calculate the coolant temperatures. This is necessitated by the variation in coolant properties with temperature. If the first result indicates that the top hose temperature is less than 100°C then a Newton-Raphson iterative procedure is used to calculate the water mass flow-rate and coolant temperatures. The iteration is of coolant mass flow rate, the top hose temperature being calculated as a function of this.

RESULTS CALCULATED FROM THE MODEL

To study the cooling system all of the results calculated are for vehicles without thermostats in an ambient temperature of 45°C, taken to be the maximum design temperature. The effect of the thermostat is to produce a minimum top hose temperature of 82°C.

Graphs 7.1, 7.2 and 7.3 show the results from the model for the non air-conditioned car. The fan cowl used on the non air-conditioned car is slightly different to that of the air-conditioned version, a factor not taken into account in the model.

Graph 7.1 shows the influence of engine speed on cooling system temperature with the engine idling, for both water and a 45/55 mixture of water and antifreeze as a coolant. The reduced coolant side heat transfer coefficient, due to the properties of the water antifreeze mixture[57] in comparison with water, results in higher coolant temperatures. This is partially compensated for by the increased boiling point of the water antifreeze mixture[57], which as for water is calculated at the blow off pressure (1.034 bar above atmospheric). Graphs 7.2 and

7.3 show coolant temperatures for the non air-conditioned car using water and the same water/antifreeze mixture. The comparison between the coolants is similar. It is apparent that under no steady state condition does the coolant temperature reach its boiling point except when using the water/antifreeze mixture and idling at an engine speed in excess of 4,900 rev/min. This is not a condition in which the car may be expected to be used.

Graph 7.4 shows the variation in cooling system temperatures for the air-conditioned car against engine speed. The water antifreeze mixture is used and the air-conditioning system is not running, resulting in a radiator air on temperature equal to ambient. Graph 7.5 shows the cooling system temperatures for the same vehicle under similar conditions except with the car moving and is plotted against road speed in miles/hour. Comparison between the air-conditioned car and the non air-conditioned car indicates that coolant temperatures of the air-conditioned car are higher than the non air-conditioned version, even with the air-conditioning system not running. This suggests over cooling in the non air-conditioned car, if the cooling system of the air-conditioned car with the air-conditioning running is effective. This is examined in chapter 8. The body shell of both cars being the same the radiator face area for both versions is conveniently the same. The number of radiator tubes and fin pitch are reduced on the non air-conditioned car. Reduction of fin pitch may not be necessary.

The influence of radiator fin pitch and tube rows for the engine idling at 750 rev/min is shown for the non air-conditioned car on graph 7.6 and for the air-conditioned car on graph 7.8.

The resultant Reynolds number accompanying these radiator variations are plotted on graphs 7.7 and 7.9 and indicate the limits above which laminar flow may be avoided. The optimum radiator design is that which functions adequately and costs least. It may be assumed that radiator cost is a strong function of the number of tube rows and a weaker function of the number of fins.

The influence of radiator face air velocity for the non air-conditioned car and for the air-conditioned car is shown on graphs 7.10 and 7.11 respectively. In both cases a considerable increase in velocity is needed to produce a significant reduction in coolant temperature, and this would be at the expense of increased fan power and noise.

The influence of coolant mass flow rate on coolant temperature is shown on graphs 7.12 and 7.13 respectively for the non air-conditioned and air-conditioned versions at an idle speed of 750 rev/min. In each case the coolant mass flow rate may be increased to produce a decrease in coolant temperature, and this with little influence on power consumption and no influence on noise level. Hence a larger water pump (or running the pump at a higher speed) may make a smaller radiator possible or a decrease in the number of fins and/or tube rows. An optimum total cost of pump and radiator may be achieved on this basis.

Graphs 7.14 and 7.15 show the effect of using a constant speed fan having the same driving torque and producing the same velocity as the current fan at a 750 rev/min idle. The fuel economy advantage and a suggested practical means of achieving the constant speed are considered in chapter 6. Obviously at the current idle speed of 750 rev/min the temperatures are as for the current system. In low gears the temperature of the top hose is increased but driving in these low gears is unlikely for any length of time. In the higher gears the difference from the present system is very small.

The effect of a constant speed fan has only been examined for the non air-conditioned version of the car. This might be extended and found advantageous for the air-conditioned car also, although the effect on the air-conditioning system may be a reduced coefficient of performance and an increased compressor load, which may outweigh the advantage of the reduced fan load. In view of the small effect of the fan on the cooling system in the higher gears, this is unlikely.

The influence of changes in the condenser geometry on engine cooling system temperatures is shown on graph 7.16. It is apparent that for the range of

changes shown the effect is small. The influences of such changes on the condenser air side Reynolds number and the refrigeration system are considered in chapter 8.

Graph 7.17 shows the influence of changes in the condenser fin pitch and tube configuration on the engine cooling system temperatures when the air-conditioning system is turned off, at an idling engine speed of 750 rev/min and also when moving at 70 miles/hour in fourth gear. The curve at idle extends to the maximum brake load which the engine can supply at this engine speed. The influence of moderate loads, as may be due to auxiliary devices, is small.

GRAPH 7.1

PLOT OF COOLING SYSTEM TEMPERATURE AGAINST ENGINE SPEED

NON AIR-CONDITIONED CAR ENGINE IDLING

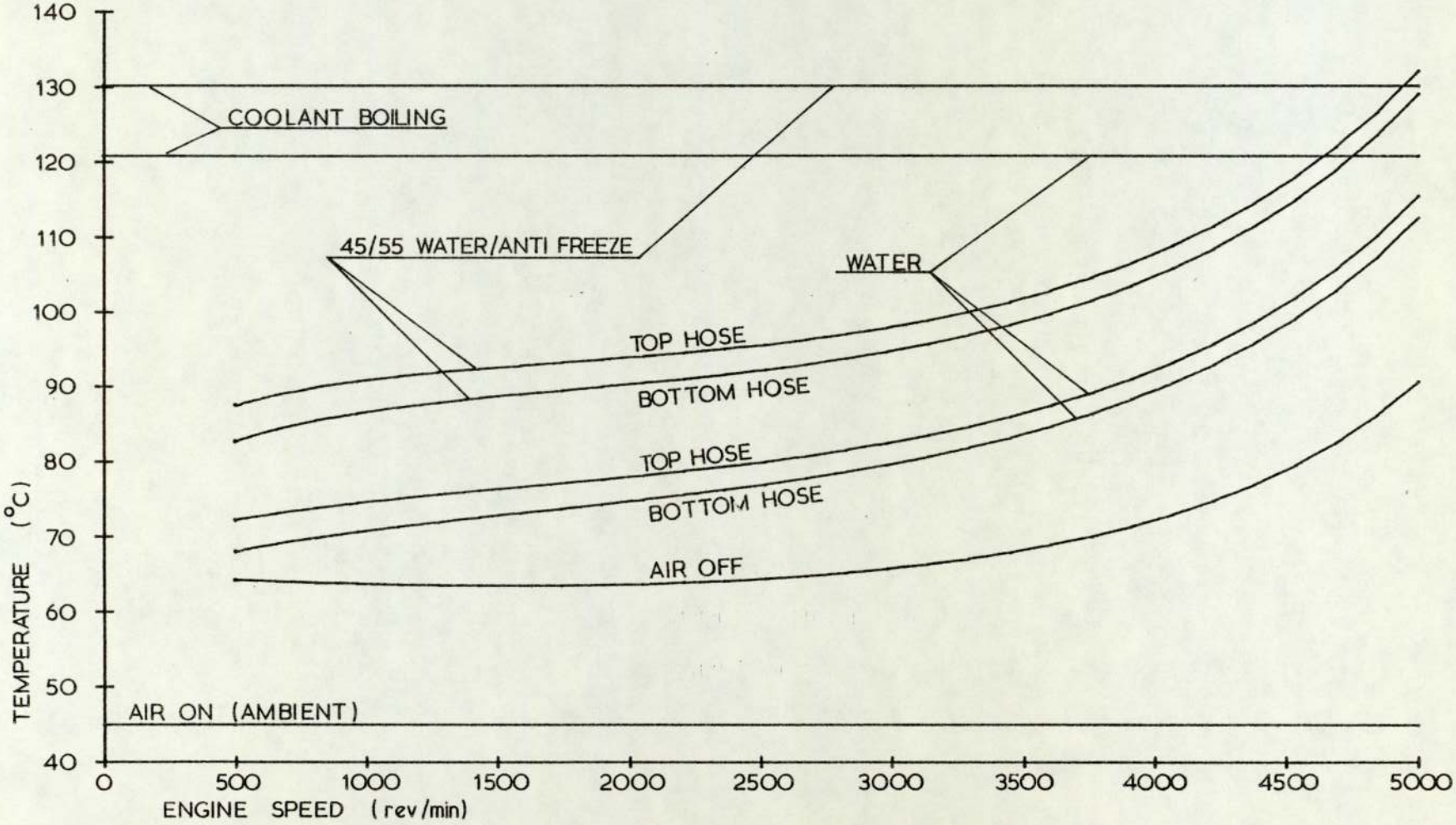

GRAPH 7.2

PLOT OF COOLING SYSTEM TEMPERATURE AGAINST ROAD SPEED

NON AIR CONDITIONED CAR SYSTEM FILLED WITH WATER

CAR MID LADEN ON ZERO GRADIENT

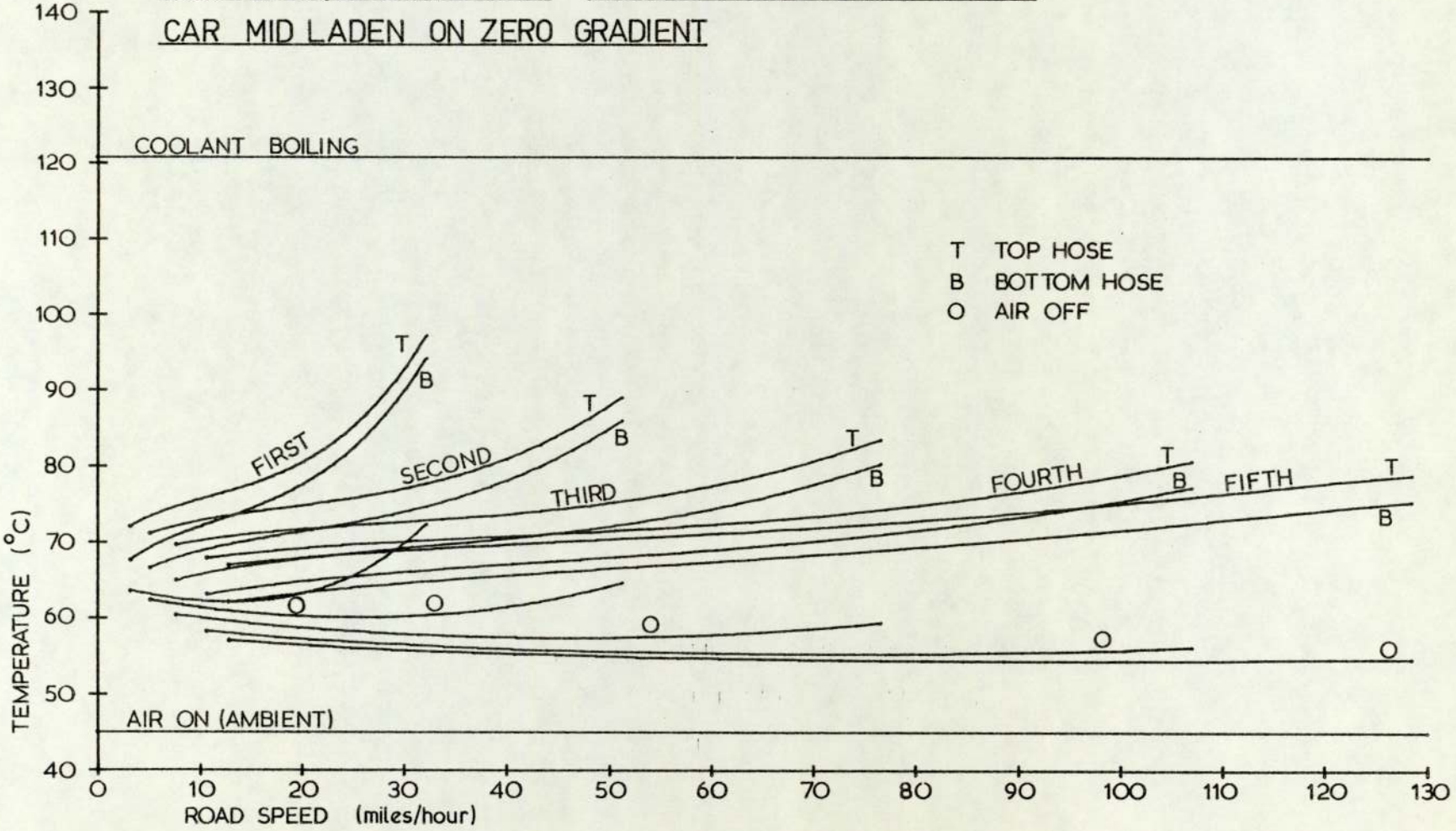

GRAPH 7.3

PLOT OF COOLING SYSTEM TEMPERATURE AGAINST ROAD SPEED

NON AIR-CONDITIONED CAR MID LADEN ON ZERO GRADIENT

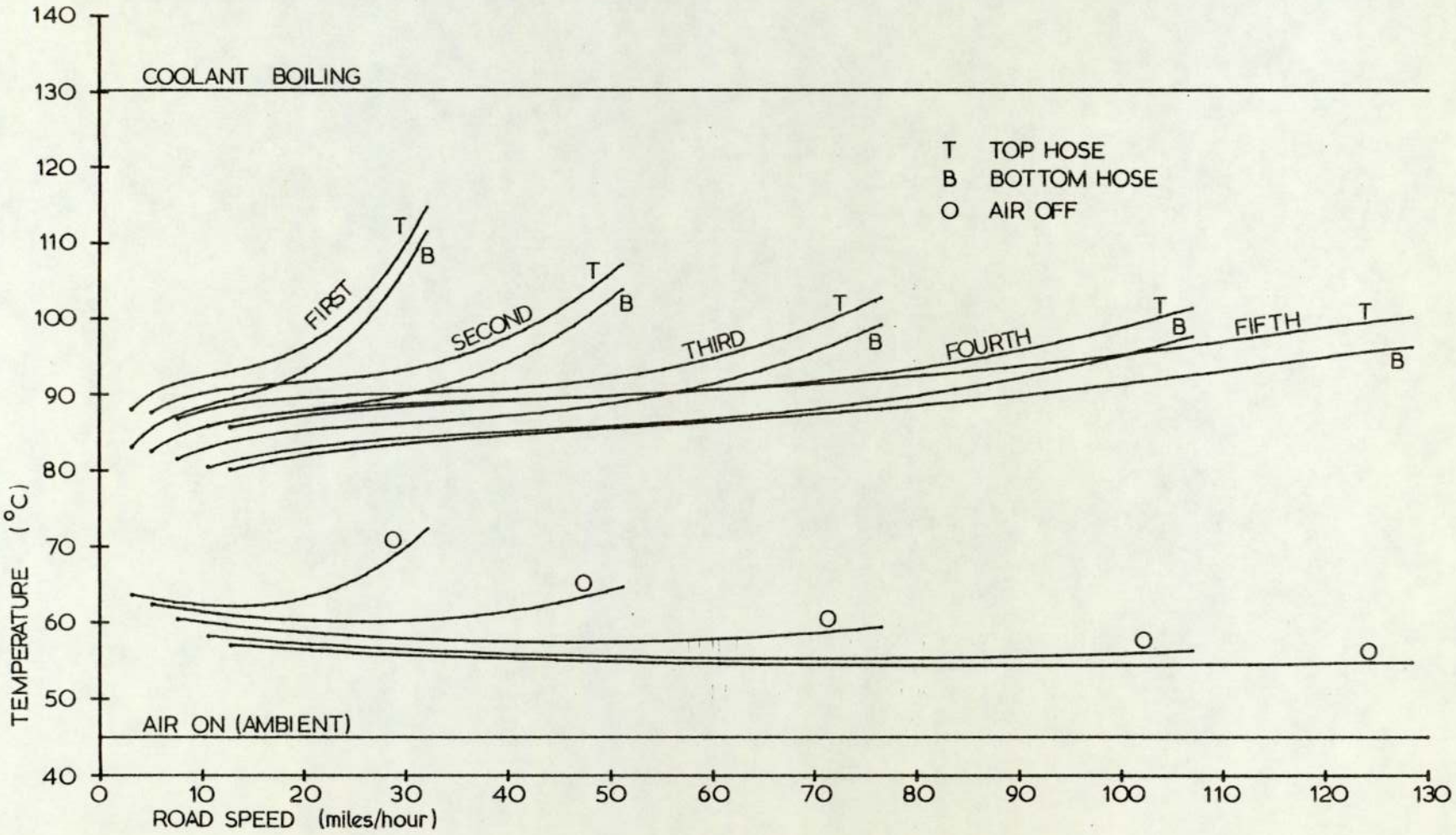

GRAPH 7.4

PLOT OF COOLING SYSTEM TEMPERATURE AGAINST ENGINE SPEED

AIR-CONDITIONING SWITCHED OFF

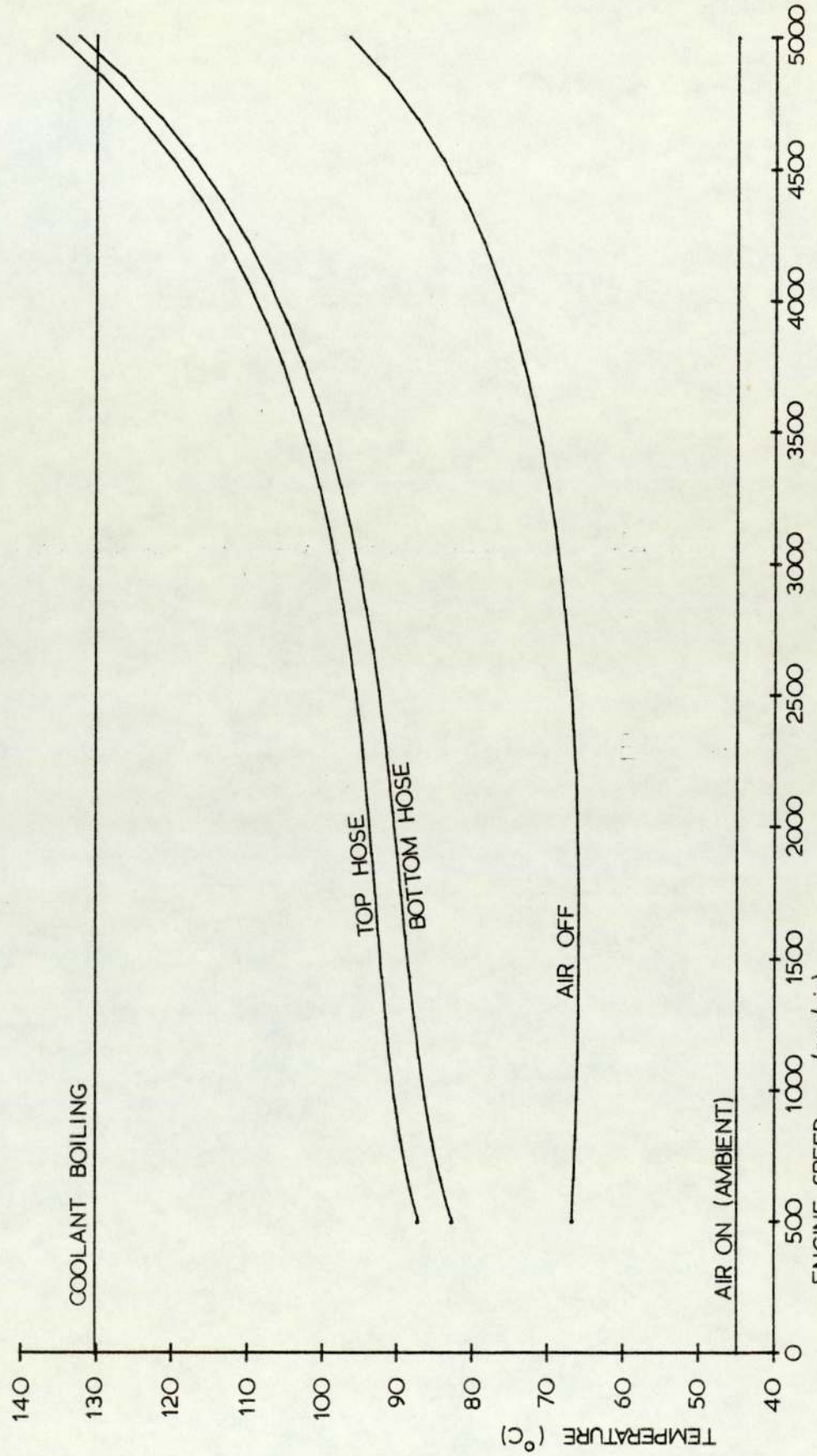

GRAPH 7.5

PLOT OF COOLING SYSTEM TEMPERATURES AGAINST ROAD SPEED

AIR CONDITIONING SWITCHED OFF. CAR MID LADEN ON ZERO GRADIENT

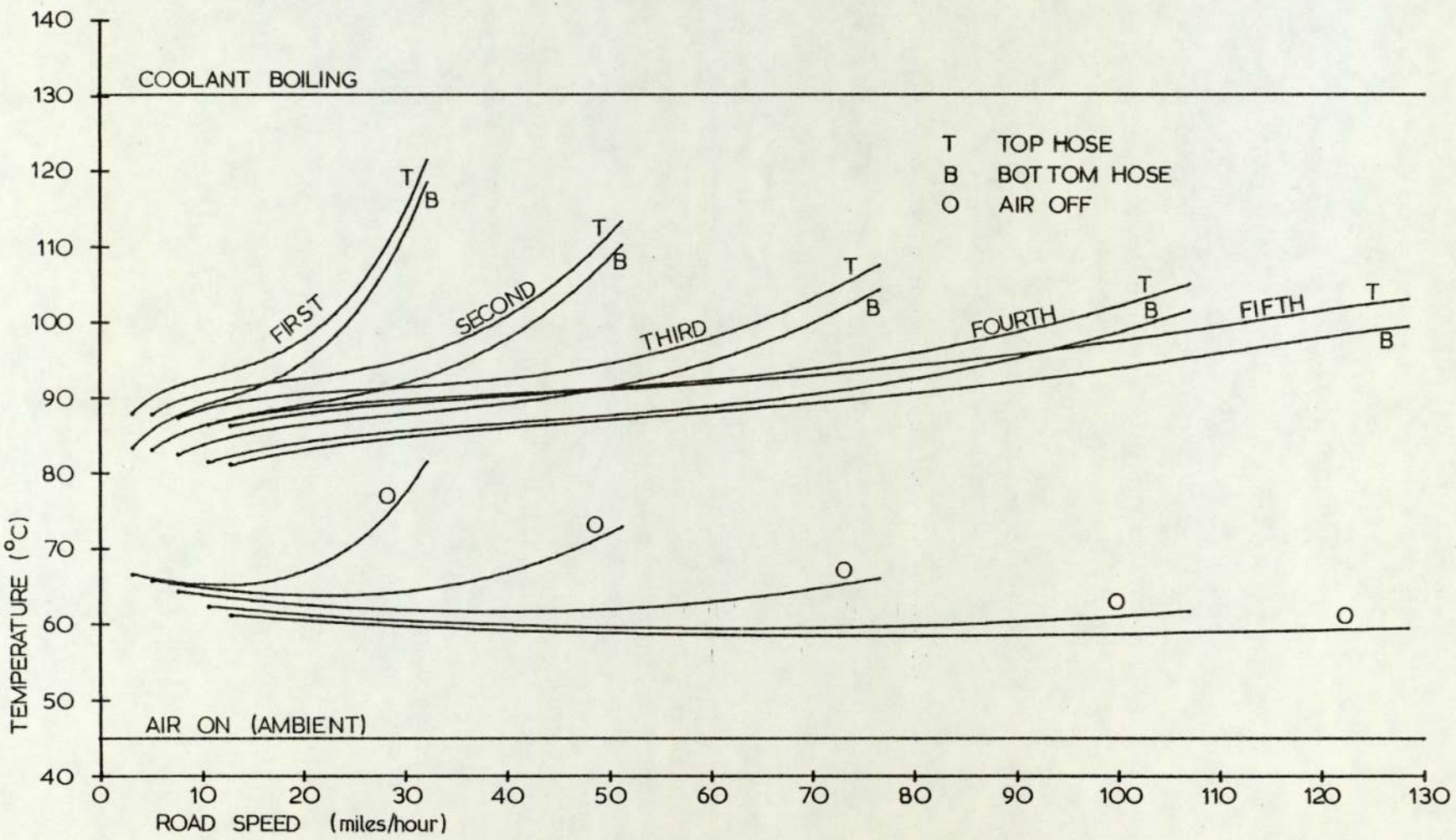

NON AIR-CONDITIONED CAR. ENGINE IDLING AT 750 rev/min

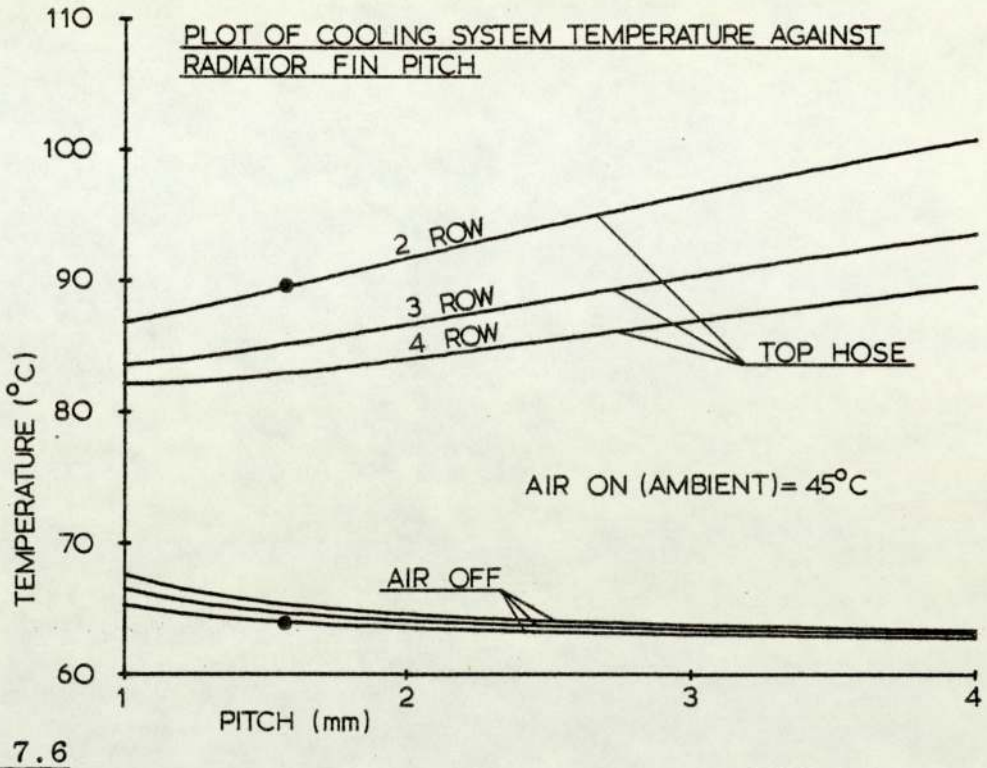

GRAPH 7.6

● PRESENT GEOMETRY

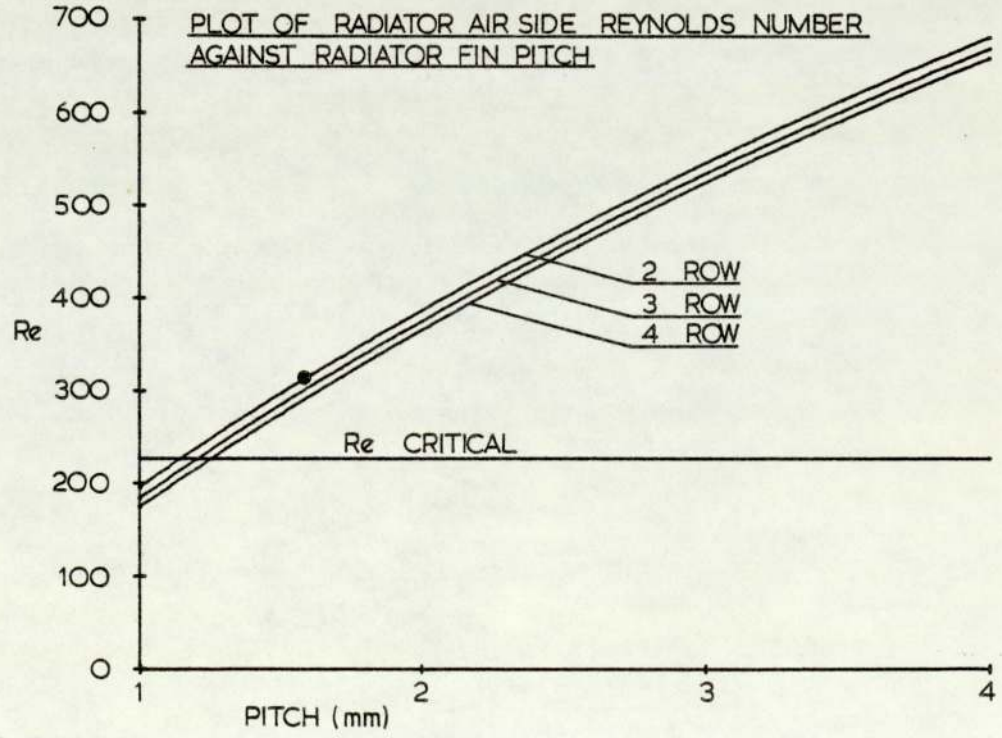

GRAPH 7.7

ENGINE IDLING AT 750 rev/min

AIR-CONDITIONING SWITCHED OFF

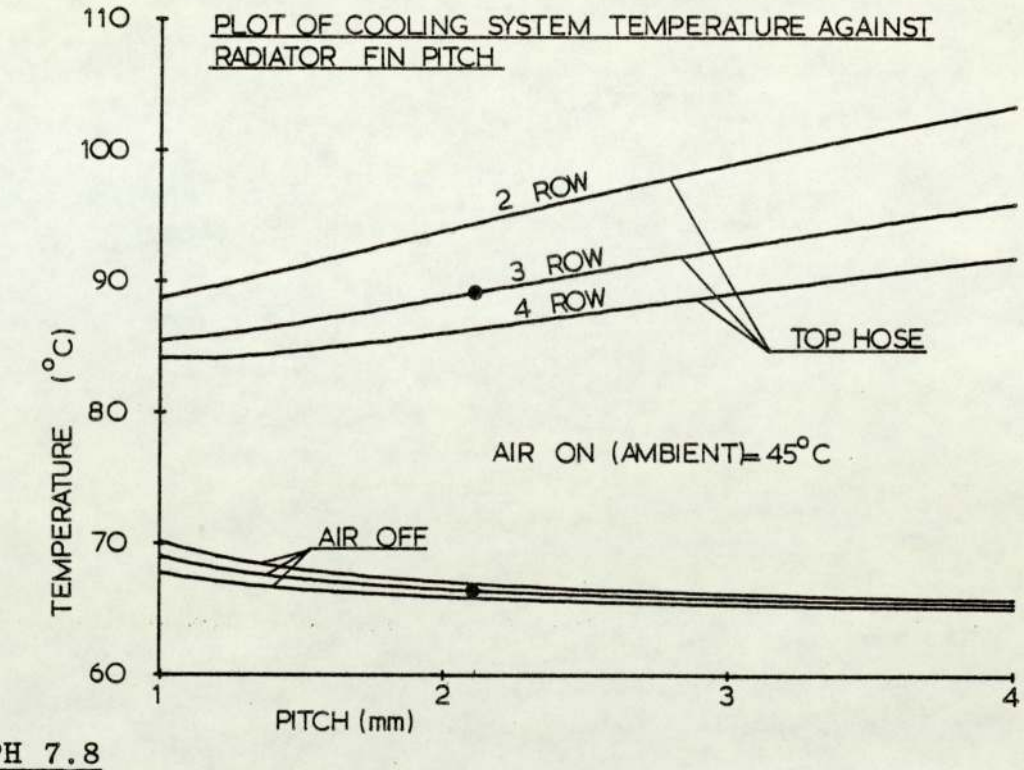

GRAPH 7.8

● PRESENT GEOMERY

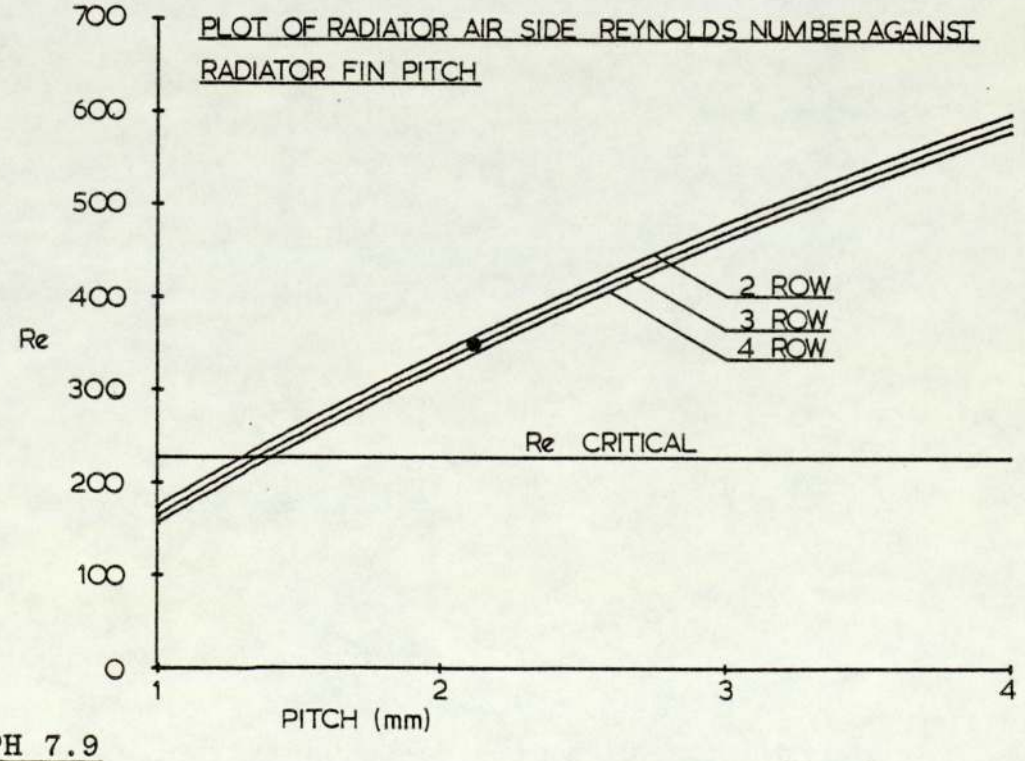

GRAPH 7.9

GRAPH 7.10

PLOT OF COOLING SYSTEM TEMPERATURE AGAINST RADIATOR AIR FACE VELOCITY

NON AIR-CONDITIONED CAR. ENGINE IDLING AT 750 rev/min

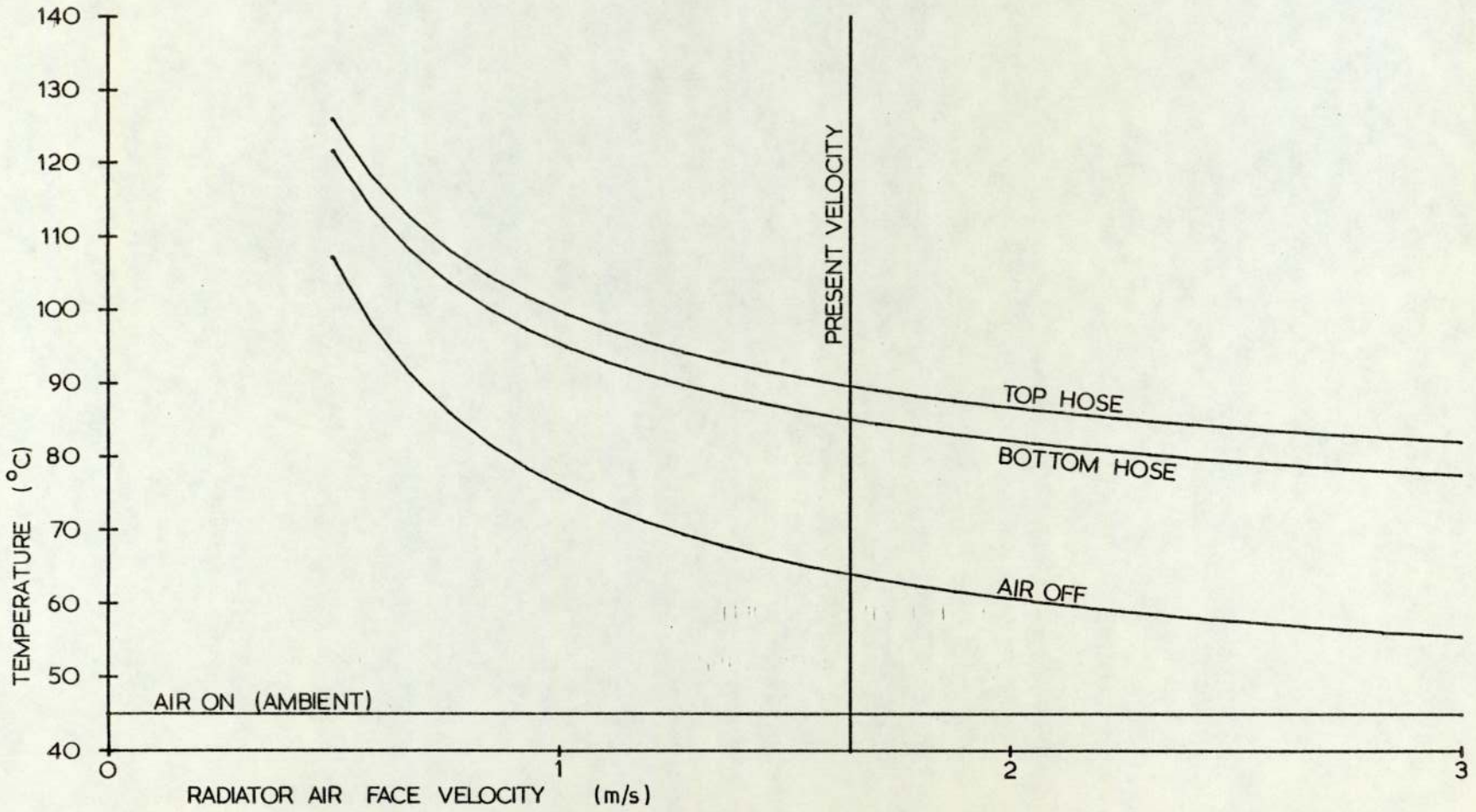

GRAPH 7.11

PLOT OF COOLING SYSTEM TEMPERATURE AGAINST RADIATOR AIR FACE VELOCITY

AIR-CONDITIONING SWITCHED OFF. ENGINE IDLING AT 750 rev/min

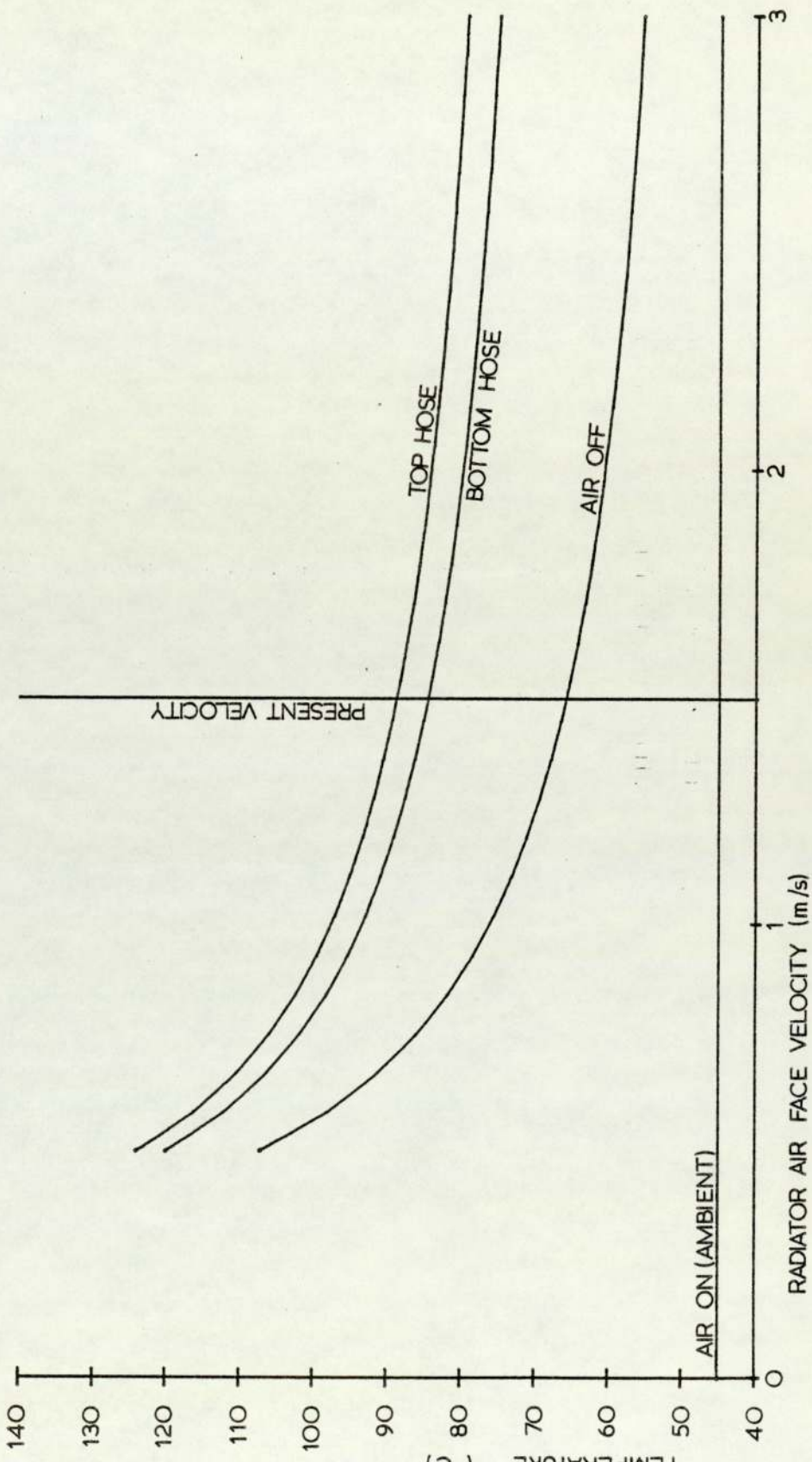

GRAPH 7.12

PLOT OF COOLING SYSTEM TEMPERATURE AGAINST COOLANT MASS FLOW RATE

NON AIR-CONDITIONED CAR. ENGINE IDLING AT 750 rev/min

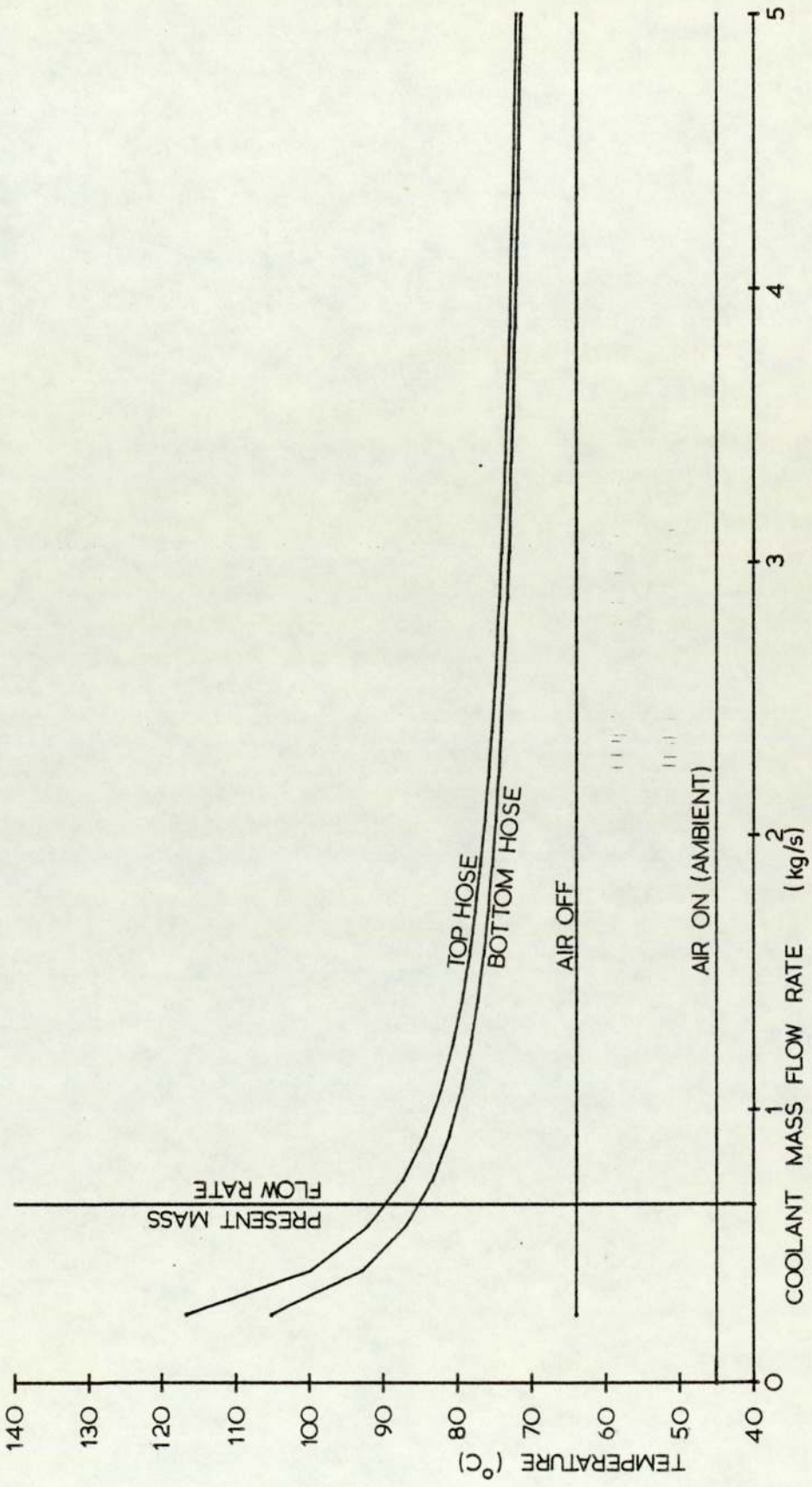

GRAPH 7.13

PLOT OF COOLING SYSTEM TEMPERATURE AGAINST COOLANT MASS FLOW RATE

AIR-CONDITIONING SWITCHED OFF. ENGINE IDLING AT 750 rev/min

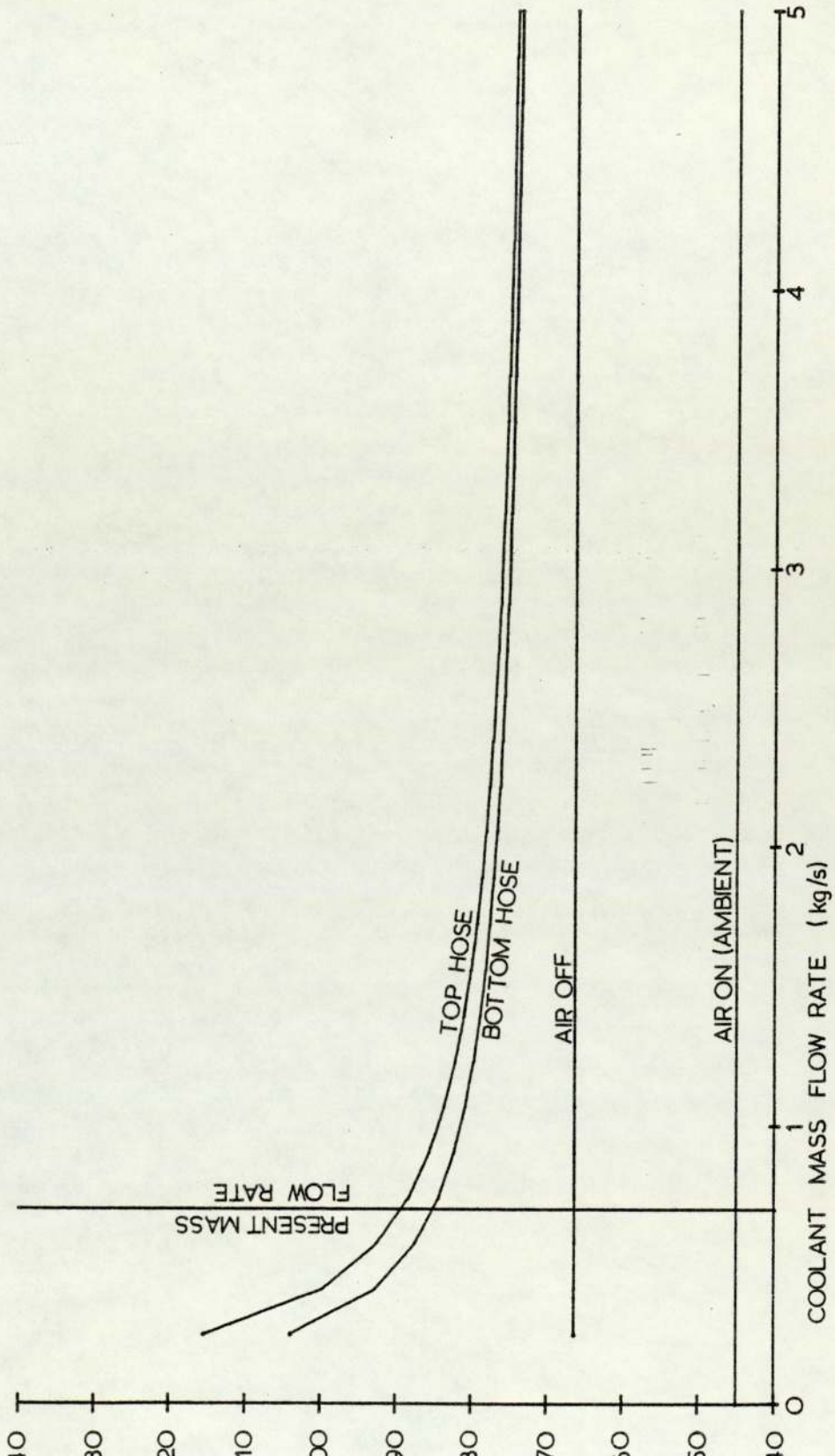

GRAPH 7.14

PLOT OF TOP HOSE TEMPERATURE AGAINST ENGINE SPEED

NON AIR-CONDITIONED CAR.

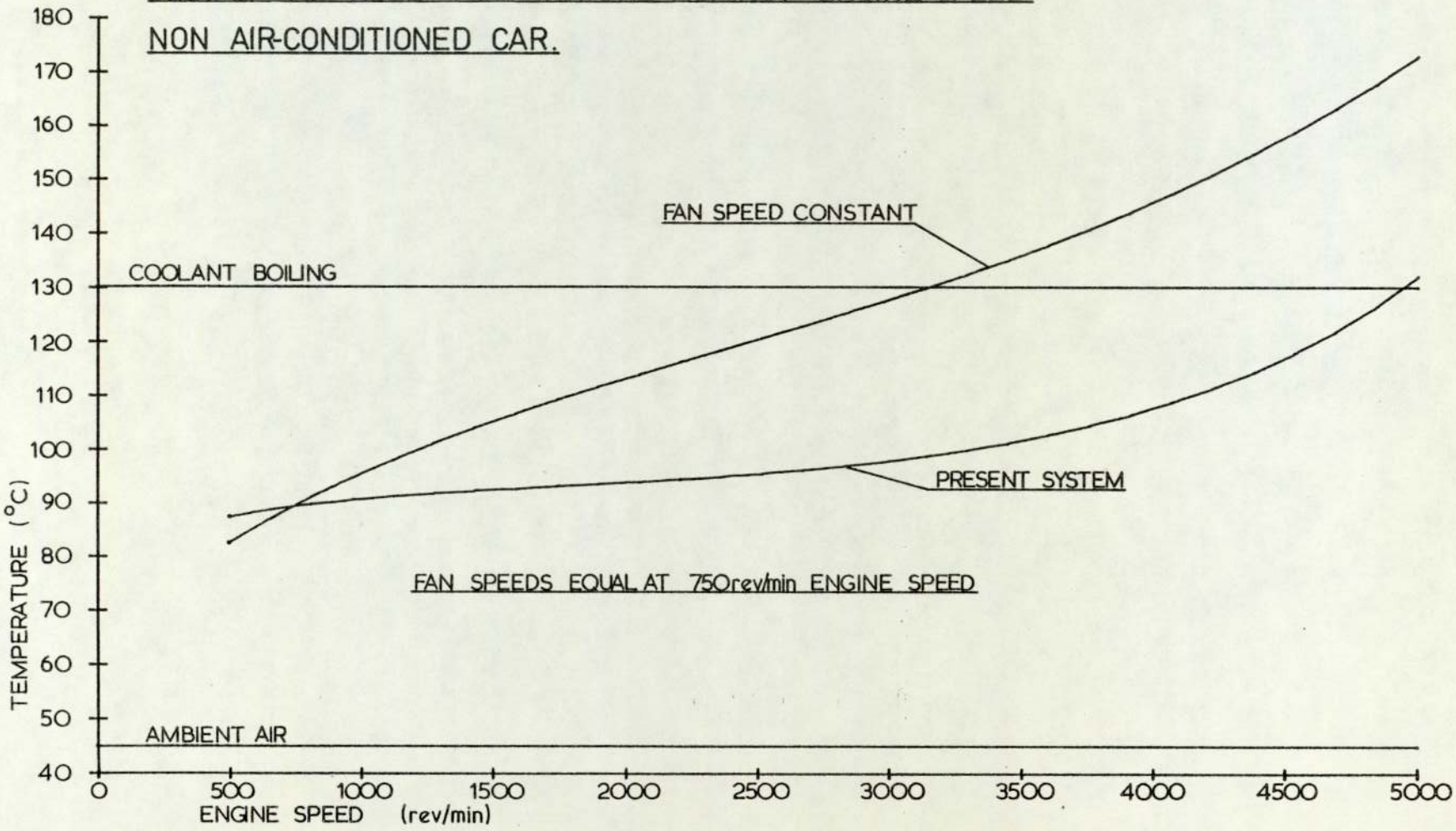

GRAPH 7.15

PLOT OF TOP HOSE TEMPERATURE AGAINST ROAD SPEED
NON AIR-CONDITIONED CAR

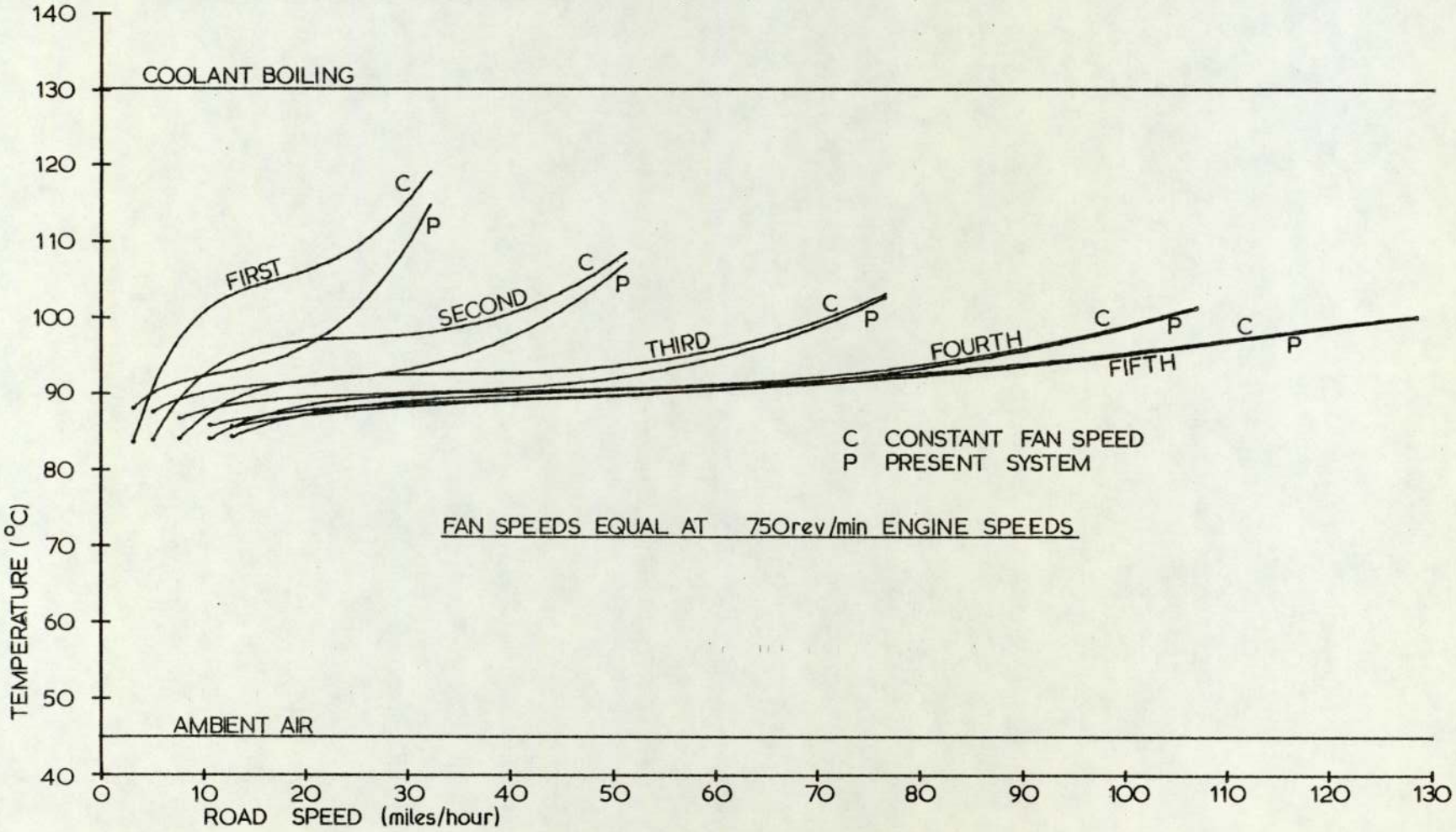

GRAPH 7.16

PLOT OF COOLING SYSTEM TEMPERATURE AGAINST CONDENSER FIN PITCH

AIR-CONDITIONING SWITCHED OFF. ENGINE IDLING AT 750 rev/min

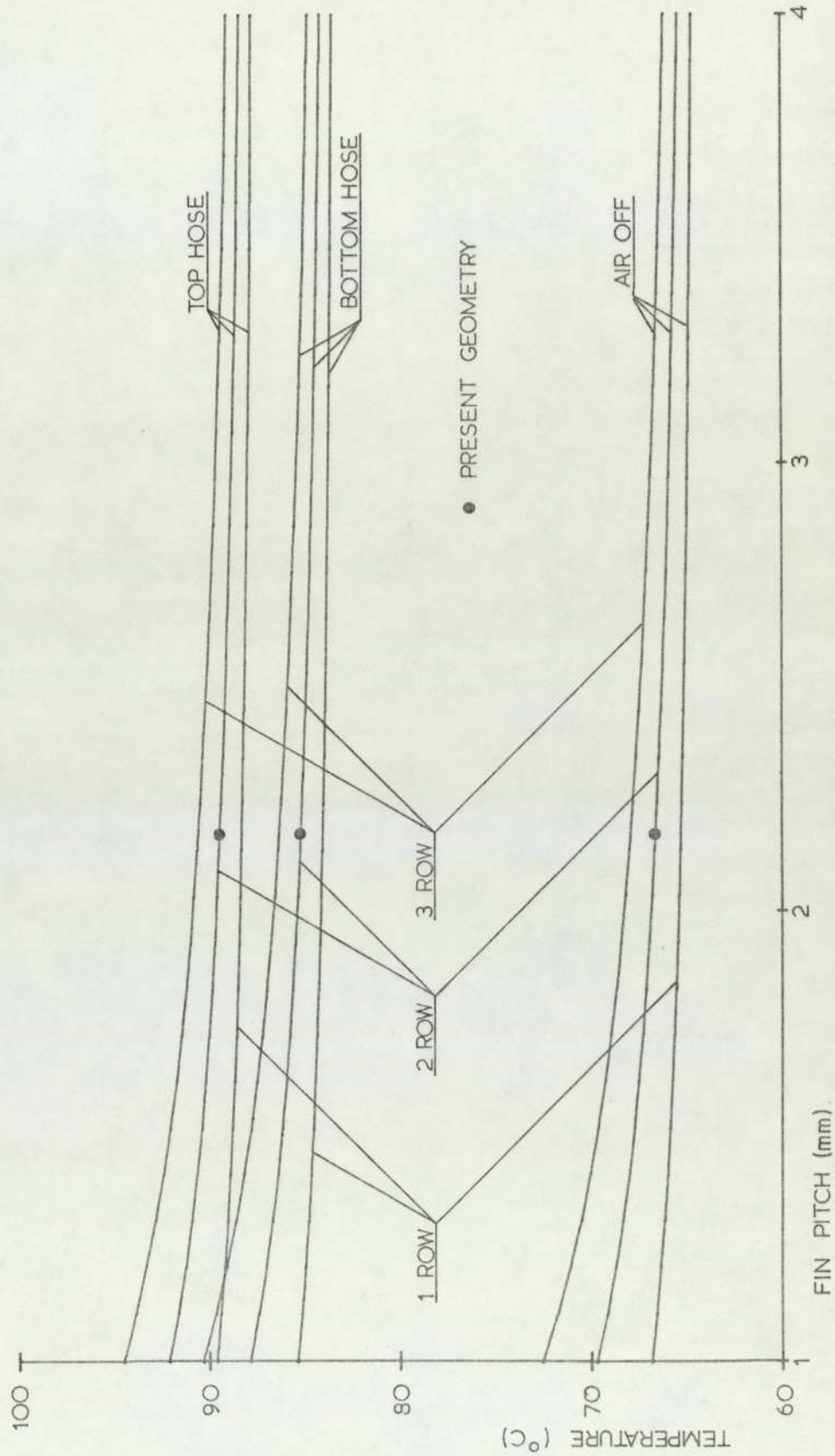

GRAPH 7.17

PLOT OF COOLING SYSTEM TEMPERATURE AGAINST AUXILIARY BRAKE POWER

AIR-CONDITIONING SWITCHED OFF

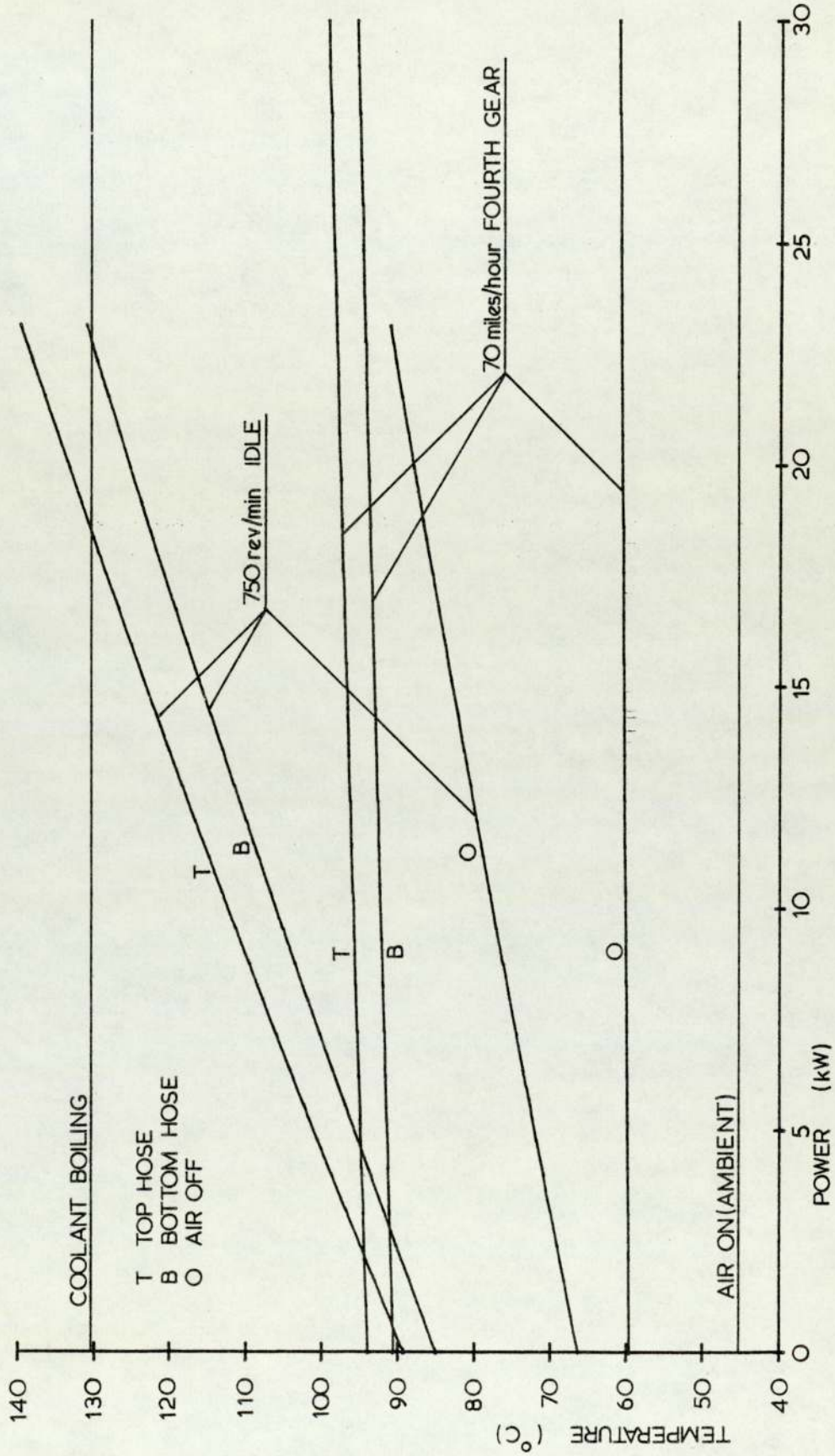

CHAPTER 8

THE REFRIGERATION SYSTEM

THE COMPRESSOR

The compressor, manufactured by General Motors Limited, is a 6 cylinder, reciprocating, positive displacement unit, driven from a swash plate through an electromagnetically engaged clutch. The inlet and exhaust valves of each cylinder are comprised of shim steel strips cantilevered across the ports. Data available from the compressor manufacturer is included in appendix A4. Compressor performance may be described by the volumetric, isentropic, and mechanical efficiencies and by the displacement and volumetric compression ratio. Using values read off the manufacturer's data sheet, an attempt was made to calculate the mechanical efficiency. The results were inconclusive, in some cases a mechanical efficiency greater than one being indicated. A mechanical efficiency of unity was assumed, in ignorance of contrary data, as for such a mechanism it may be expected to be high. For the purpose of a mathematical model, polynomials were fitted to this data for the volumetric and isentropic efficiency, and these efficiencies assumed to be functions of compressor speed only.

THE EVAPORATOR

This is a conventional, extended surface, counter flow heat exchanger, manufactured by Sunstrand Limited. The refrigerant enters the unit after being split into six streams in a header, each stream having ten horizontal passes. The manufacturer's graphical data relevant to the conductance of the unit is contained in appendix A5, and gives conductance as a function of the entering air enthalpy per unit mass of dry air, the refrigerant temperature, the air velocity and the dimensions of the unit. For the purpose of a mathematical model, functions were fitted to data read off these graphs and a computer subroutine written to calculate the refrigerant temperature, given the entering air enthalpy per unit mass of dry air, the air mass flow rate, and the cooling load. The velocity is based

on a constant density of the air, being that at $3^{o}C$ (the nominal controlled air off temperature). This subroutine is included in appendix A5.

THE CONDENSER

The condenser, manufactured by Marston Radiators Limited, is an extended surface, cross flow heat exchanger, the present unit having two tubes with fifteen horizontal passes.

The air side heat transfer coefficient is discussed in chapter 4. The refrigerant side heat transfer is by three stages; gas cooling, condensing, and liquid sub cooling. For the purpose of the mathematical model the condenser is assumed to consist of three separate cross flow heat exchangers whose total face area and tube length are equal to the actual face area and tube length. The refrigerant side heat transfer coefficients are calculated for gas cooling and liquid cooling using the Nusselt number, Reynolds number, Prandtl number relationship given by McAdams[65] for circular tubes, and Reynolds numbers greater than 10^{5}. The heat conductances calculated this way are large compared with the air side conductances and the dependence on overall conductance minimal. The condensing heat transfer coefficient is expected to be very large and is ignored in the calculation of overall conductance. The hypothetical heat exchangers for gas cooling and liquid sub cooling are assumed to behave as cross flow heat exchangers with fluid mixing on the refrigerant side, the equation due to Stevens[63] being used for the calculation of temperatures, as for the radiator in chapter 4. This assumption is only completely true for a single tube but considered to be a valid approximation in this case.

The mean temperature difference between the air and the refrigerant, in the hypothetical condensing heat exchanger, is calculated as the logarithmic mean.

The final form of the mathematical model of the refrigeration system involves calculation of the face areas required for gas cooling and condensation. For liquid sub cooling the final refrigerant temperature is required, given the heat

exchanger face area. The subroutines for these calculations are included in appendix A5.

THE CONTROL OF THE REFRIGERATION SYSTEM

The state of the refrigerant entering the compressor is controlled by a thermostatic expansion valve. The mechanism of this device is as described by Anderson.[37] The refrigerant temperature and pressure sensed by the valve are both at the evaporator outlet; the alternative of sensing the pressure at the evaporator inlet requiring compensation for the refrigerant pressure drop in the evaporator. The valve maintains a nominal $2\frac{1}{2}$K superheat at the compressor inlet.

Icing of the evaporator is prevented by a thermostatic switch, which switches off the current to the compressor clutch. The switch is activated by a vapour charged thermal element in the airstream leaving the evaporator and the current, and hence the system, are switched off at a temperature of 2^{o}C and on again when the temperature rises to 4^{o}C.

System pressure in excess of 30.3 bar (gauge) is precluded by a safety valve fitted to the compressor.

THE PRESENT REFRIGERATION CYCLE

The temperature of the evaporating refrigerant is set by the thermostatic expansion valve which admits refrigerant to the evaporator at a temperature such that the superheat on entering the compressor is as prescribed. The temperature which is set, is dependent on the refrigeration load and the evaporator conductance. The specific enthalpy of the refrigerant entering the compressor, being a function of temperature and pressure, is hence also set by the expansion valve.

The mass flow rate of refrigerant is the product of the compressor displacement per unit time, the density of the refrigerant entering the compressor, and the volumetric efficiency.

The pressure difference between the condenser and evaporator is set by the expansion valve in attaining the required evaporator temperature. The specific enthalpy of the refrigerant leaving the compressor is a function of the isentropic efficiency, the specific entropy at inlet, and the inlet and outlet pressures. For a given condenser pressure, and hence compressor outlet and condensing temperatures, the temperature of the refrigerant, at the condenser exit, may be reduced to some level which may approach the ambient air temperature but must be some finite difference above ambient. From the condenser outlet the refrigerant is throttled to the evaporator inlet, the throttling process being isenthalpic.

As the condenser pressure is increased the volumetric efficiency of the compressor decreases and hence the mass flow rate, owing to the finite clearance volume which must exist in the compressor.

Equilibrium is reached when the properties at the compressor inlet and outlet are such that the enthalpies at the condenser outlet and evaporator inlet are equal.

At low compressor speeds, the refrigerant mass flow rate may be such that the evaporator air off temperature is above that at which the thermostatic switch disengages the compressor clutch. Under these conditions the design refrigeration load is not achieved. At higher compressor speeds the increased refrigerant flow rate may produce an evaporator load in excess of that required and the thermostatic switch will then stop the cycle when the evaporator air off temperature drops to the prescribed level. The air flow over the evaporator then increases the evaporator temperature and the drive is restored when the air off temperature has risen sufficiently. The frequency, at which the cycle is started and stopped, is dependent upon the thermal capacity of the evaporator, and the temperature and thermal capacity of the refrigerant, which continues to be throttled from the condenser to the evaporator. If the thermal capacity of the evaporator is reduced then this frequency is increased and in the limit the

compressor may be considered a variable speed unit, its maximum speed being that when the clutch is engaged. In practice a higher frequency of engagement of the clutch may produce intolerable wear and fatigue.

REFRIGERANT PROPERTIES

Thermodynamic properties of refrigerants 12 and 22, for the purpose of the mathematical model, are calculated from equations supplied by Du Pont de Nemours and Company[80]. Temperatures, as functions of the specific enthalpies of the saturated liquids, are calculated from polynomials, fitted to data generated by the subroutines, and are valid approximations between reduced temperatures of 0.7 and 0.96. These subroutines and functions are included in appendix A5.

Viscosity and conductivity of the liquid and superheated refrigerants are calculated in the model as functions of temperature only, using polynomials fitted to data given by A.S.H.R.A.E.[33].

Specific heat capacities of the liquid refrigerants are calculated from differentiated polynomials, fitted to temperature/saturated liquid specific enthalpy data generated from the subroutines, and are assumed to be functions of temperature only. They are valid for temperatures from $0^{o}C$ up to reduced temperatures of 0.96. These functions are included in appendix A5.

The specific heat capacity of the superheated refrigerant is calculated, at the condenser pressure, as the difference between the specific enthalpies relating to the compressor inlet entropy and the saturated vapour, divided by the temperature difference between these states. The error resulting from extrapolation to the compressor exit temperature is small, since the rate of change of specific heat capacity with temperature, at a constant pressure in the superheated region, is small.

The transport properties are used only for calculation of refrigerant side heat transfer coefficients, which are not controlling.

CALCULATION OF THE ENTHALPIES OF THE COOLED AIR

A computer subroutine was written for this purpose and gives the enthalpy per 1kg of dry air as a function of temperature and relative humidity. Equations, fitted to the data of Mayhew and Rogers[66], over a range of temperature of $0^{o}C$ to $100^{o}C$ are used. This subroutine is contained in appendix A5.

THE MATHEMATICAL MODEL OF THE REFRIGERATION SYSTEM

This model is designed for the calculation of properties and the mass flow rate of the refrigerant, the compressor and refrigeration loads, and the temperature of the air onto the radiator, at given engine and car speeds and climatic conditions.

The refrigeration system is assumed to be operating in a steady state, the effect of the compressor clutch cycling being to reduce the mass flow rate of refrigerant as if the compressor speed were reduced. Heat transfer coefficients on the refrigerant side in the condenser are however calculated as time average coefficients rather than those due to the hypothetical reduced mass flow rate. This assumption obviates the necessity for computation involving unsteady heat transfer.

The mathematical model of the refrigeration system is included in appendix A5 in the form of a computer program.

The refrigeration system is assumed to operate in one of three ways, depending upon the prevailing speeds and climatic conditions. The design cooling load is taken as producing an evaporator air off temperature of $3^{o}C$ (the nominal thermostatic switch operating temperature) and relative humidity of 100%.

N.B. Numbers on the diagrams refer to the states of the refrigerant as in the computer program and the text.

In the text:

m_r = Radiator air mass flow rate

m_R = Refrigerant mass flow rate

L_C = Compressor load = $m_R (h_3 - h_2)$

L_E = Evaporator load = $m_R (h_2 - h_7)$

$L_{E,D}$ = Evaporator design load as defined above

T_o = Ambient (condenser air on) temperature

$\overset{\vee}{T}_5$ = The condensing temperature assuming an infinite coefficient of performance (i.e. $h_3 = h_2$) and an infinite condenser air mass capacity rate

P_B = The compressor safety valve blow off pressure

A = The condenser face area

A_5 = The condenser face area attributable to cooling of the superheated gas

A_6 = The condenser area attributable to condensation

(i)

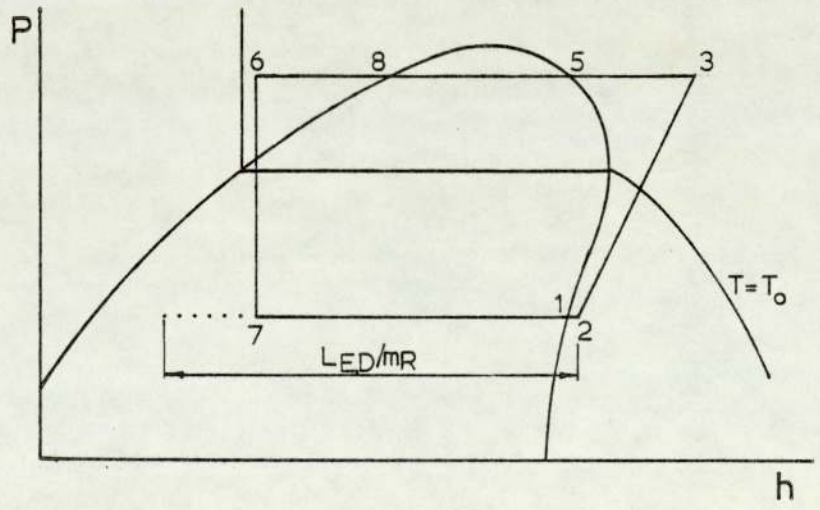

The dotted line represents the change in h in the evaporator necessary to achieve $L_{E,D}$.

In this case m_R is such that $L_{E,D}$ cannot be achieved owing to the limitation that refrigerant in the condenser cannot be cooled to a temperature lower than T_o.

(ii)

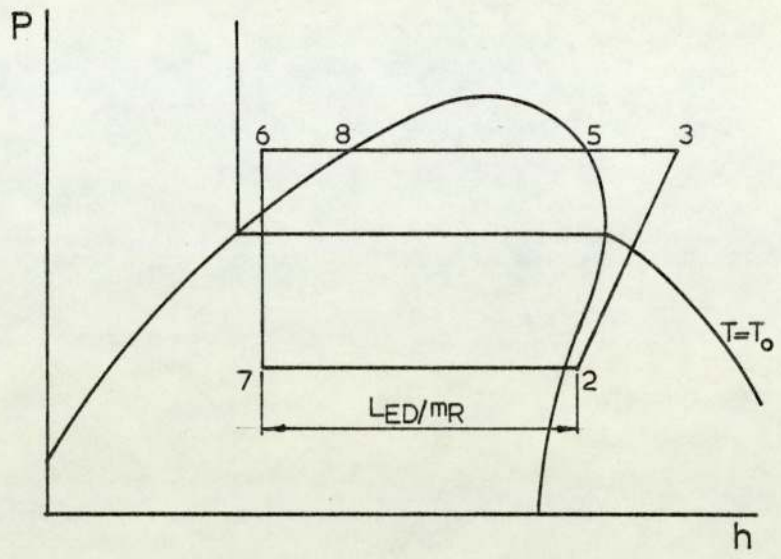

$L_{E,D}$ is achieved.

m_R is reduced.

(iii)

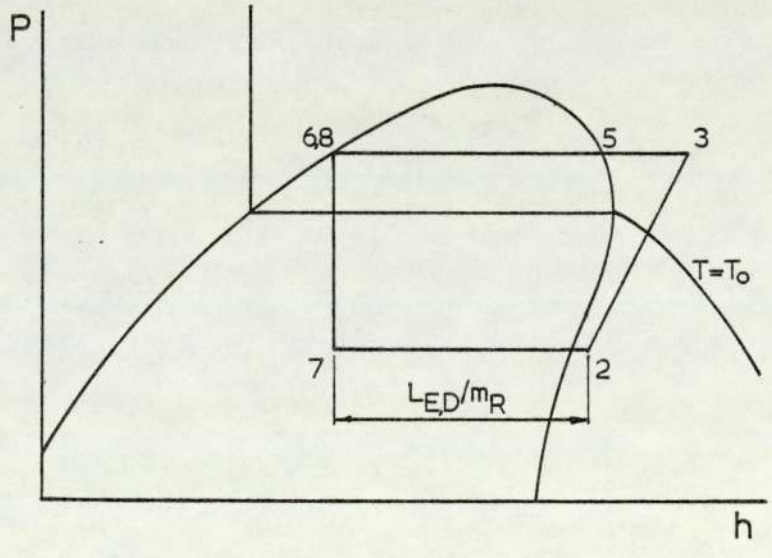

$L_{E,D}$ is achieved.

m_R is reduced such that refrigerant leaves the condenser as saturated liquid, partial condensation not being possible.

Method of calculation

h_6 is initially calculated as that of the saturated liquid at T_o. T_1 is calculated, as is necessary to produce $L_{E,D}$, on consideration of the evaporator conductance. P_1, T_2, η_v and hence h_2 and m_R are calculated. After calculation of h_7 from $L_{E,D}$, m_R and h_2, h_7 is compared with h_6. If h_6 is greater than h_7 then L_E is iteratively decreased until $h_6 = h_7$.

$\check{T}_5$ is calculated and also an initial T_5 assuming that h_6 is that of the saturated liquid and equal to h_7. If $\check{T}_5$ is greater than T_5 then the initial value of T_5 is set to equal $\check{T}_5$.

P_5 is calculated and compared with P_B. If P_5 is greater than P_B then P_5 is set to equal P_B and the resulting T_5 is calculated. h_6 is recalculated as that of saturated liquid at T_5 and m_R is decreased to give $L_{E,D}$, with h_7 equal to h_6.

s_2 and h_2 are calculated and hence h_3 and T_3 on consideration of η_{isen}.

A_5 and A_6 are calculated. If L_E is equal to $L_{E,D}$ and A_5 plus A_6 is less than A then the system operates as in (iii). If not, or if L_E has already been reduced, the system operates as in (i) or (ii).

Hence if the system is operating as in (iii):

m_R is iteratively decreased until A_5 plus A_6 is equal to A.

If the system is operating as in (i) or (ii):

P_5 is iteratively increased until liquid sub cooling takes place. A minimum, h_6 is found as a function of T_5. If h_6 is greater than h_7 then the system operates as in (i), and if not then (ii).

If the system is operating as in (i):

L_E, T_1, h_6, and h_7 etc., are iteratively calculated until h_6 is equal to h_7.

If the system is operating as in (ii):

m_R is iteratively decreased until h_6 is equal to h_7.

The radiator air on temperature is calculated iteratively, as the result of a specific enthalpy increase to the radiator air flow equal to $m_R(h_3 - h_6)/m_r$.

THE LIMITATIONS OF THE MODEL

The assumption of steady state operation is invalidated by the method of controlling the refrigeration load to prevent evaporator icing and also by the effect of changing engine speed during normal driving. The former invalidation is not a limitation in the climatic conditions chosen in which to examine the system (i.e. an ambient temperature and relative humidity of 45°C and 50%) since the design cooling load is never achieved.

Calculations involving a reduction in the mass flow rate of refrigerant give an estimate only of the parameters calculated, with the exception of the refrigeration load. The accuracy of the estimate increases as the frequency of cycling of the compressor clutch. The calculation of refrigeration load however, may be expected to retain a reasonable degree of accuracy at low cycling frequencies.

The assumption of volumetric efficiency being dependent only on compressor speed is made on the basis that the manufacturer's data is that of conditions representative of the use of the device. In practice the volumetric efficiency must reduce with pressure ratio and also be a function of temperature, a maximum pressure ratio being reached when the volumetric efficiency reduces to zero. The volumetric efficiency therefore has an influence on the condensing and evaporating temperatures, the refrigerant mass flow rate, and the refrigeration and compressor loads.

The assumption of isentropic efficiency being dependent on compressor speed only, is similarly only valid if the manufacturer's data is that of conditions

representative of the use of the device. The isentropic efficiency is decreased by pressure losses, at the inlet and exhaust valves, and reduces as the mass flow rate and volumetric efficiency increase. The isentropic efficiency is also therefore a function of pressure ratio and temperature. The influence of isentropic efficiency on the cycle produces a negligible effect on the refrigeration load but a considerable effect on the compressor load.

No account is taken of pressure losses in the heat exchangers or pipe work. Pressure losses in the heat exchangers during condensation or evaporation make these modes of heat transfer non isothermal. Pressure losses, in the pipes linking the heat exchangers and the compressor, effectively reduce the isentropic efficiency of compression. Pressure losses, in the pipes linking the heat exchangers and the expansion valve, have no effect on the system and are compensated for by the thermostatic expansion valve.

On the calculator used (a Hewlett-Packard 9830) the program running time was long and consequently the tolerances, placed on the results from iterative procedures, were large. The calculation of condensing temperature, as giving a minimum specific enthalpy at the exit from the condenser, suffers particularly.

RESULTS FROM THE MODEL OF THE REFRIGERATION SYSTEM

In all cases, the climatic conditions are taken as an ambient temperature and relative humidity of 45^{o}C and 50% respectively. With an evaporator dry air mass flow rate of 0.15 kg/s, as measured by the car manufacturer[2], the design refrigeration load is then 16.89 kW.

The Present System

The refrigeration and compressor loads are plotted against engine speed at idle on graph 8.1 and against road speed on graph 8.2. The resulting refrigeration system temperatures and pressures are plotted on graphs 8.3 to 8.6 inclusive. At idle the compressor safety valve exhausts the system at an engine speed greater

than 3400 rev/min, in the climatic conditions considered. The exact speed has not been calculated but is certainly outside the range of normal idling conditions. Under no driving conditions does the system pressure reach the set pressure of the safety valve.

In the climatic conditions considered, the design refrigeration load is never achieved and consequently the compressor clutch is never disengaged. The refrigeration load is limited by the rate of displacement of the compressor. This rate of displacement of the compressor may be increased, by increasing the pulley ratio or the displacement, but would result in an increased compressor load and engine brake load. The compressor load at idle, as a fraction of the maximum brake load which the engine can achieve, has been plotted on graph 8.7. Increasing the rate of displacement of the compressor, at a given idle speed, would increase this fraction and may result in the engine stalling under extreme climatic conditions.

The refrigeration load may also be increased by increasing the condenser air mass capacity rate and/or the condenser conductance and/or the evaporator conductance. Results from the model, at the present idle speed of 750 rev/min, indicate that an infinite air mass capacity rate and heat transfer coefficient, giving a condenser outlet temperature equal to that of the ambient air, would increase the refrigeration load by only 4%. Further work may show the influence of condenser air mass capacity rate on the compressor load. The condenser air mass capacity rate at idle may only be increased at the expense of increased fan noise and brake power consumption, unless an improved fan were fitted, the condenser face area increased, or a condenser and/or radiator having lower air side pressure drops but similar conductances used. From the volume/pressure characteristics of the fan, plotted on graph 4.13, the maximum improvement in the condenser air mass capacity rate that might be achieved by reducing pressure drops, without increasing the fan speed, is 32%. An increase in the condenser face area may require modifications to the body and aesthetic appearance of the car.

The influence of condenser fin and tube geometry, at the present idle speed of 750 rev/min, on the refrigeration and compressor loads, is shown on graph 8.8, on system pressures on graph 8.9, and on the condenser air side Reynolds number on graph 8.10. Little improvement can be made to the refrigeration or compressor loads without reducing the air side Reynolds number to the critical, unless the air velocity is increased at the expense of increased fan power consumption and noise. Condenser cost may be assumed to be a strong function of the number of tubes and a weaker function of the fin pitch. Cost reduction is limited by an increase in system pressure, and the compressor safety valve blowing off.

The fuel consumption, attributable to the refrigeration system, has been plotted against engine speed at idle on graph 8.11 and against road speed on graph 8.12. This may be reduced by reducing the compressor load. As stated above the isentropic efficiency of the compressor has a strong influence on compressor load but little influence on the refrigeration load. Compressor load has been plotted on graph 8.13 against isentropic efficiency at the present idle speed of 750 rev/min. The maximum reduction in compressor load, resulting from isentropic compression is 36%. A similar reduction in fuel consumption attributable to the refrigeration system would also result. The isentropic efficiency, being reduced by pressure losses at the inlet and exhaust valves, would be improved by using a vane compressor not requiring these valves.

Savings in the fuel consumption are unlikely to result from changes in the condenser fin and tube geometry for the reasons mentioned above. The influence of an increased condenser air mass capacity rate on the compressor load and hence fuel consumption, might be profitably studied using the model, particularly if an improved fan design is developed. An increase in fan speed will produce an increase in the air mass capacity rate and a reduced compressor load but at the expense of an increased fan power consumption. An optimum fan speed may be found using the model but may result in an intolerable noise level. Furthermore,

this optimum would depend on the climatic conditions and a thermostatic fan speed control system be required, to take account of varying ambient temperature.

Cooling system temperatures have been plotted against engine speed at idle on graph 8.14 and against road speed on graph 8.15. Boiling of the coolant apparently does not occur under normal steady state driving conditions, high engine speeds at idle and in first gear being very unusual. In considering modifications to the refrigeration system, which may increase the compressor load or the radiator air on temperature resulting from an increased condenser load, the effect on the cooling system should be considered.

Comparison of graphs 8.14 and 8.15 with graphs 7.1 and 7.3 indicates that the cooling system of the non air-conditioned car has a cooling capacity greater than required. Cost and fuel consumption savings may result from the reduction of fan size and/or speed and radiator face area and/or geometry.

The Use of Refrigerant R22

In order that R22 may be used in the vapour compression system, resulting in a reduction in sizes of compressor and connecting pipework owing to the improved latent enthalpy of evaporation per unit volume, the condensing temperature may need to be reduced. This temperature may be reduced, without influencing the refrigeration load, by an increase in the condenser air mass capacity rate and/or an increase in the isentropic efficiency of compression, as discussed above for the present system using R12.

The increase in latent enthalpy of evaporation per unit volume of R22 over R12, results in the need for a reduction of compressor displacement rate of 42%, calculated on the basis of an infinite condenser air mass capacity rate, an infinite condenser conductance, and a decrease in the compressor pulley ratio.

The influence of condenser geometry on condensing pressure is shown on graph 8.16 for the present system using R22. The safety valve blow off pressure

has been taken at the same reduced pressure (as a fraction of the critical) as for R12 with the present system. The compressor displacement rate is decreased, by 42% by decreasing the compressor pulley ratio, and increased volumetric and isentropic efficiencies are implied. Apparently R22 may be used with the present system with a decreased compressor pulley ratio if the condenser geometry is changed. The model of the system, with the tolerances placed on iterative procedures has only a limited accuracy for calculation of condensing pressure. The use of a larger calculator or a computer and smaller tolerances are recommended for a further study.

The Absorption System Using Refrigerant R22

The method of producing the pressure difference in the absorption system is likely to produce higher condenser loads, and hence temperatures and pressures, than produced in the vapour compression system. The difficulty of using R22 in the vapour compression system is likely therefore to be worsened in the absorption system and may prevent its use.

Graphs 8.17 and 8.18 show the refrigeration loads available, using the absorption system, against engine speed at idle and road speed respectively. The results are based upon the maximum heat transfer to the generator, at a temperature of 177^{o}C, from the exhaust gases, and a coefficient of performance of 0.59 as found by Sims[57] et al. Comparison with graphs 8.1 and 8.2 shows that the enthalpy of the exhaust gas, at the temperature of the generator of 177^{o}C, is sufficient to provide a competitive refrigeration load at high engine speeds. At low engine speeds a similar refrigeration load is not available, the reduced load at the present idle speed of 750 rev/min being a particular disadvantage.

The potential fuel saving, by utilisation of absorption refrigeration, is as plotted on graphs 8.11 and 8.12.

GRAPH 8.1

PLOT OF EVAPORATOR AND COMPRESSOR LOADS AGAINST ENGINE SPEED

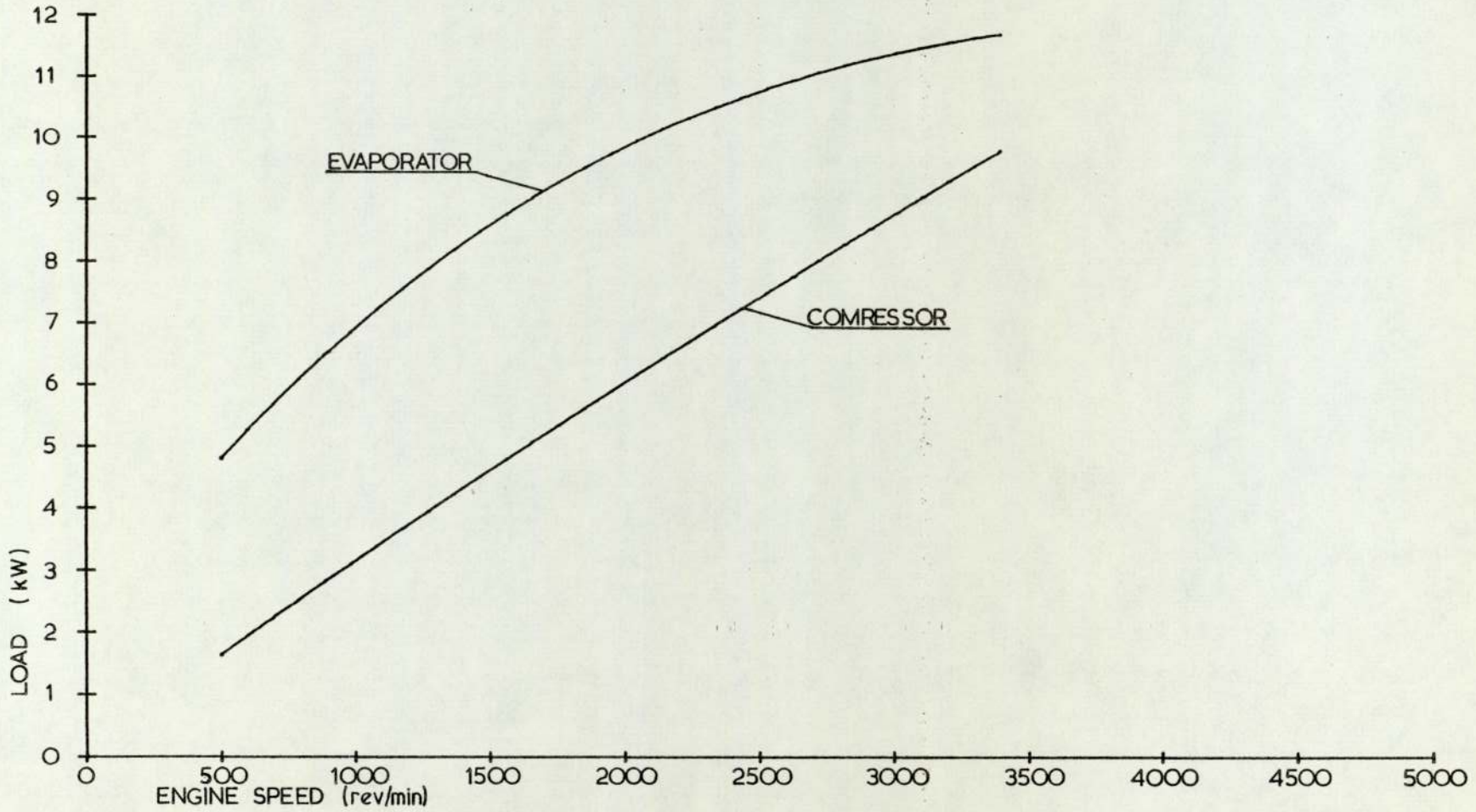

GRAPH 8.2

PLOT OF EVAPORATOR AND COMPRESSOR LOADS AGAINST ROAD SPEED

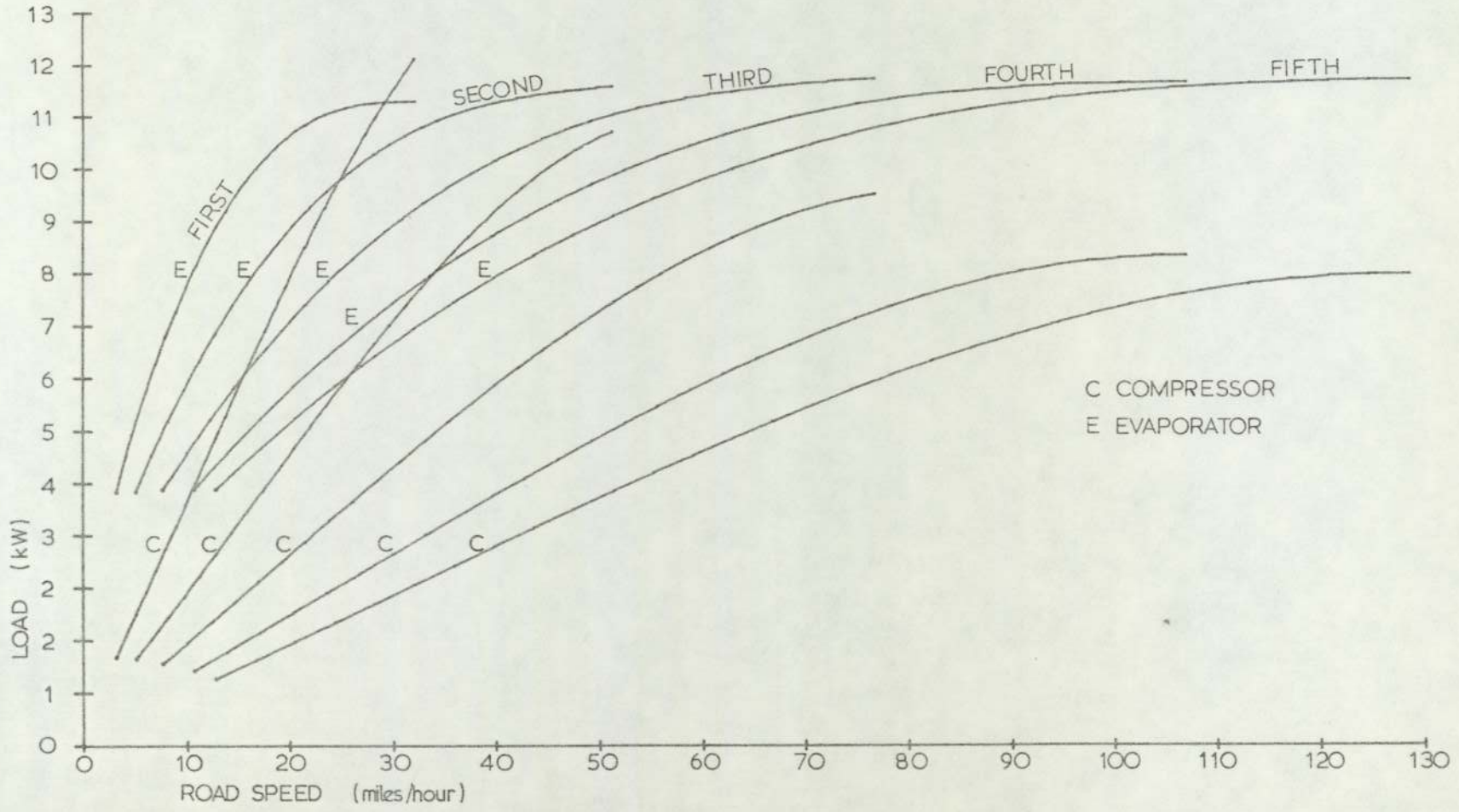

GRAPH 8.3

PLOT OF REFRIGERATION SYSTEM TEMPERATURES AGAINST ENGINE SPEED

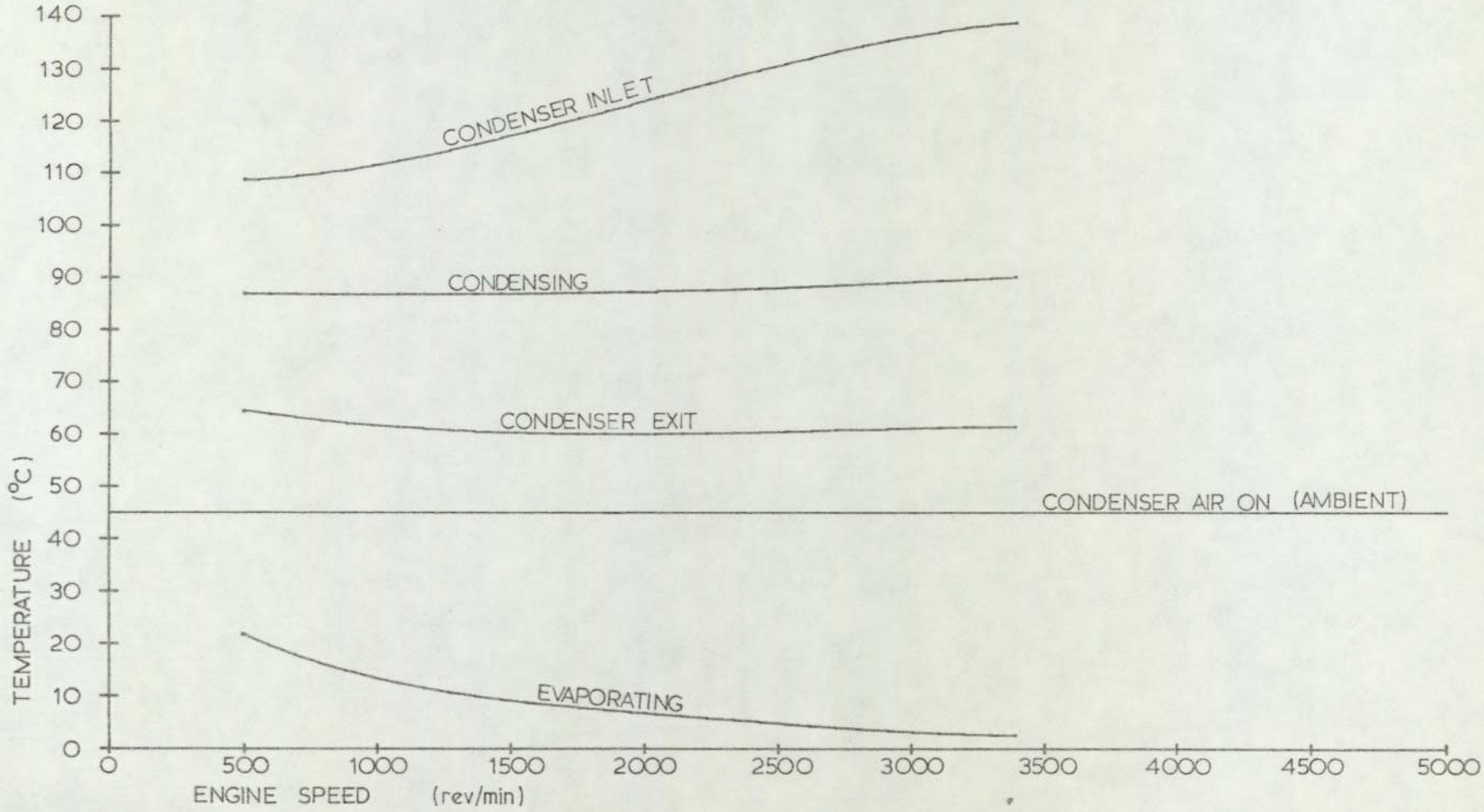

GRAPH 8.4

PLOT OF REFRIGERATION SYSTEM PRESSURES AGAINST ENGINE SPEED

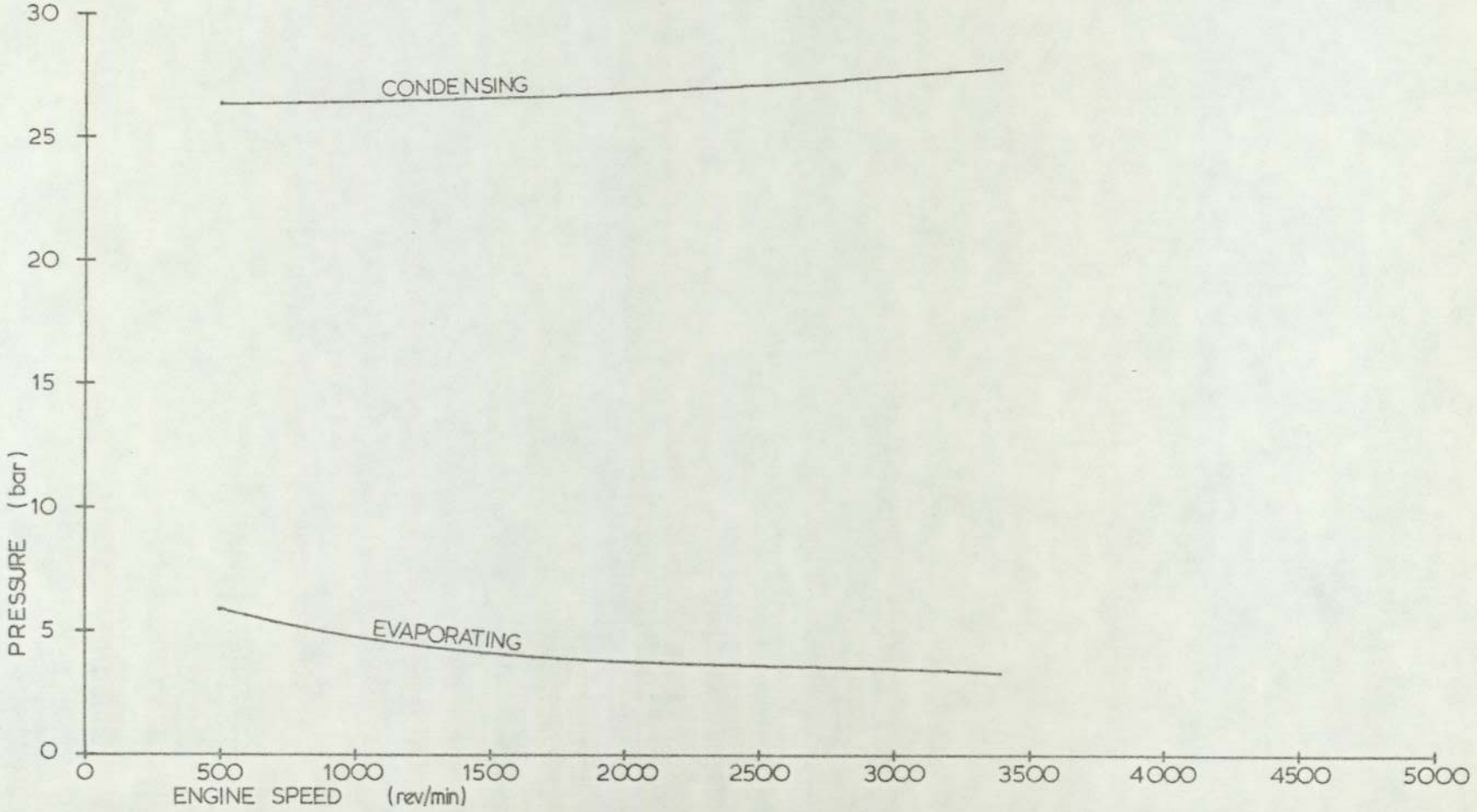

GRAPH 8.5

PLOT OF REFRIGERANT PRESSURES AGAINST ROAD SPEED

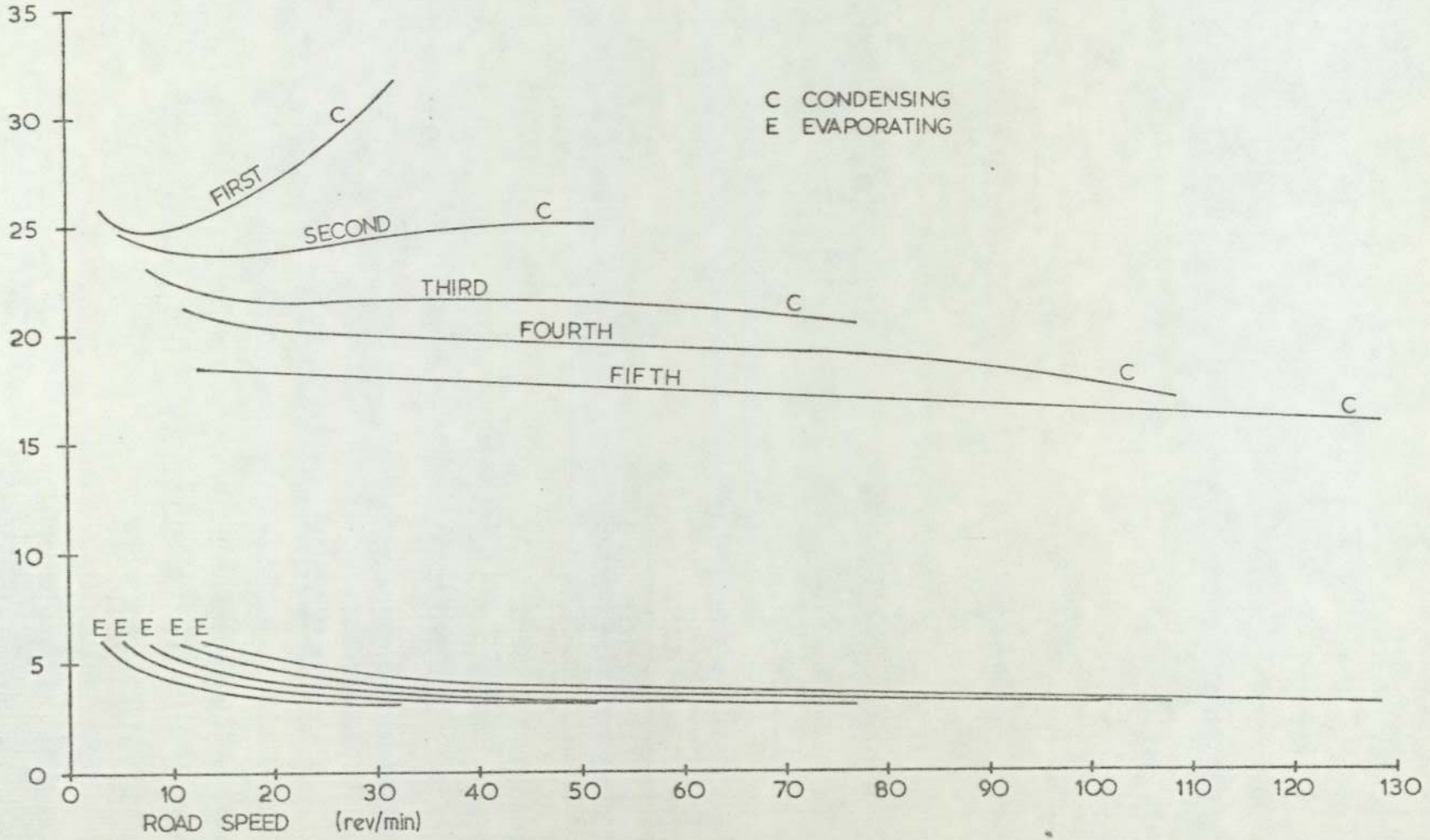

GRAPH 8.6

PLOT OF REFRIGERATION SYSTEM TEMPERATURES AGAINST ROAD SPEED

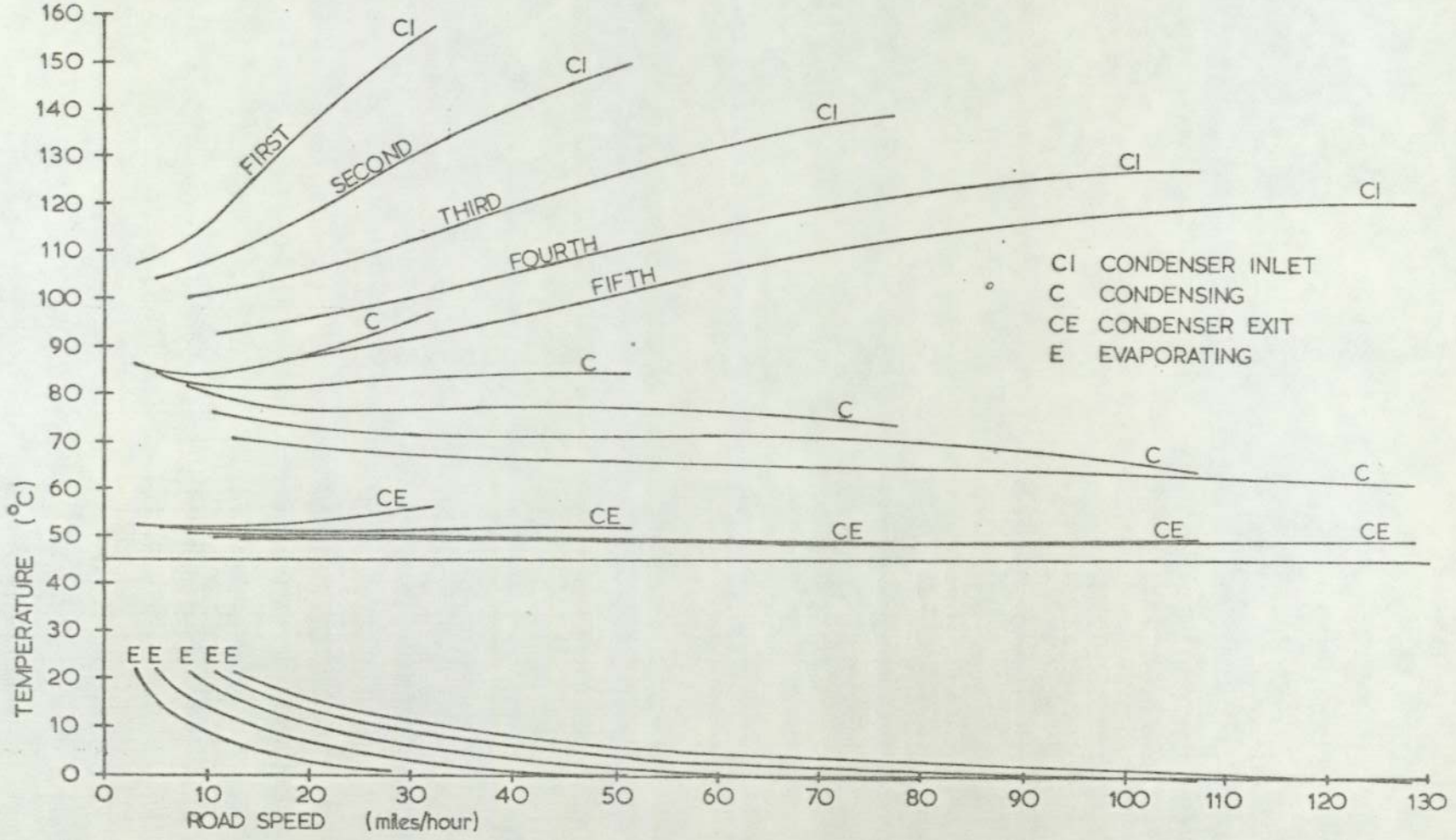

GRAPH 8.7

PLOT OF COMPRESSOR LOAD AS A FRACTION OF MAXIMUM ENGINE BRAKE POWER AGAINST ENGINE SPEED

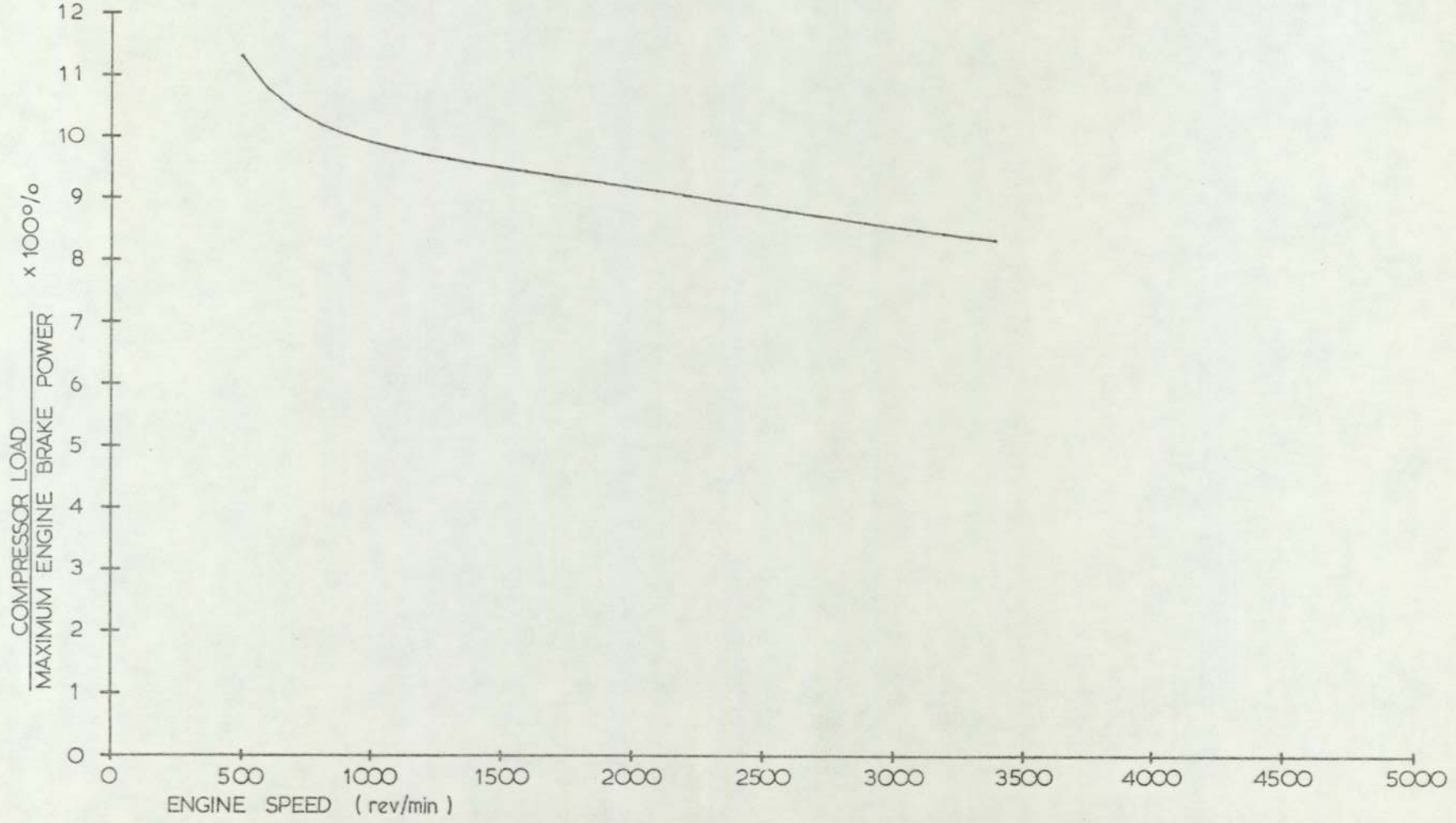

GRAPH 8.8

PLOT OF COMPRESSOR AND EVAPORATOR LOADS AGAINST CONDENSER FIN PITCH

ENGINE IDLING AT 750 rev/min

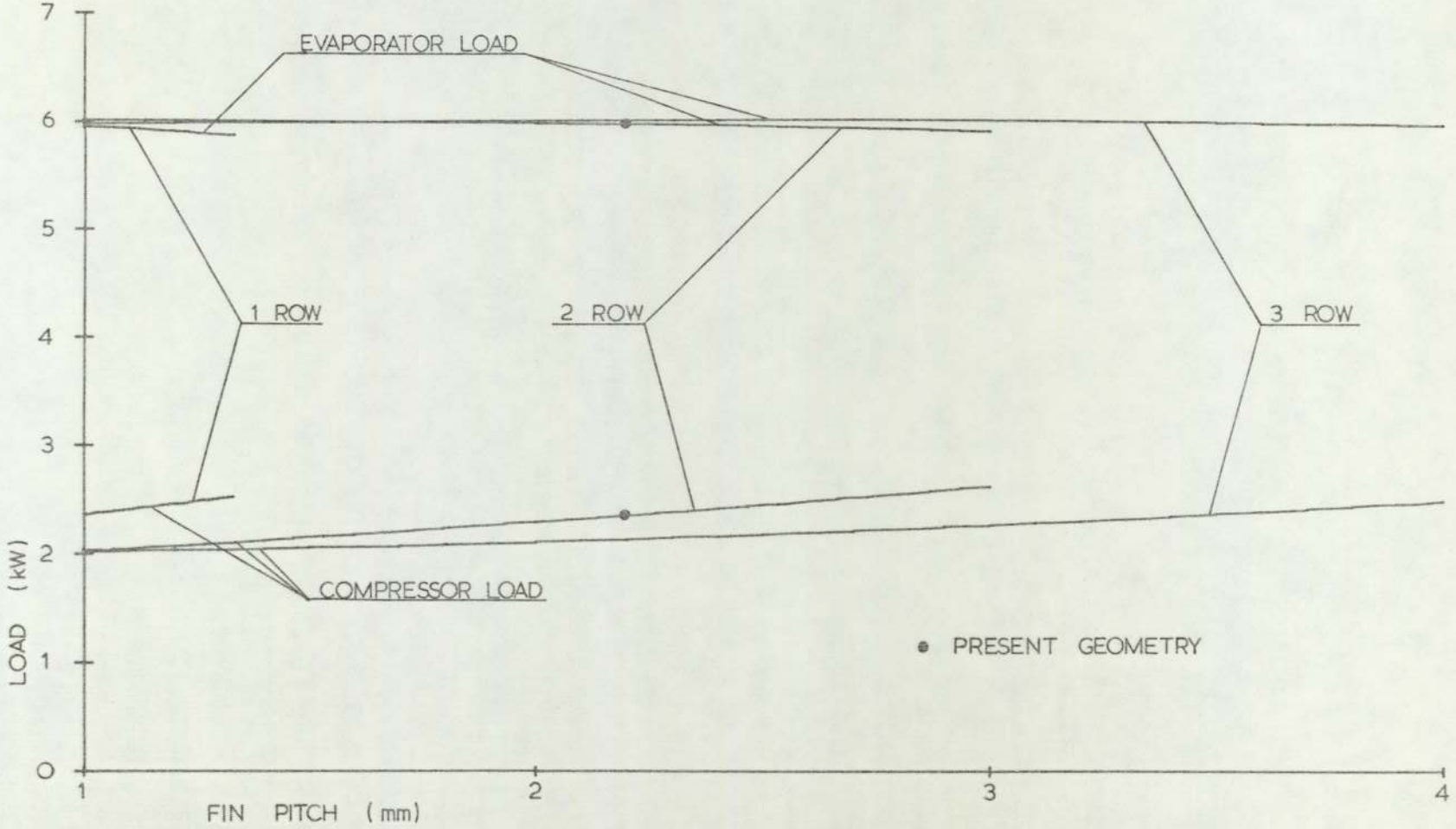

GRAPH 8.9

PLOT OF EVAPORATING AND CONDENSING PRESSURES AGAINST CONDENSER FIN PITCH

ENGINE IDLING AT 750 rev/min

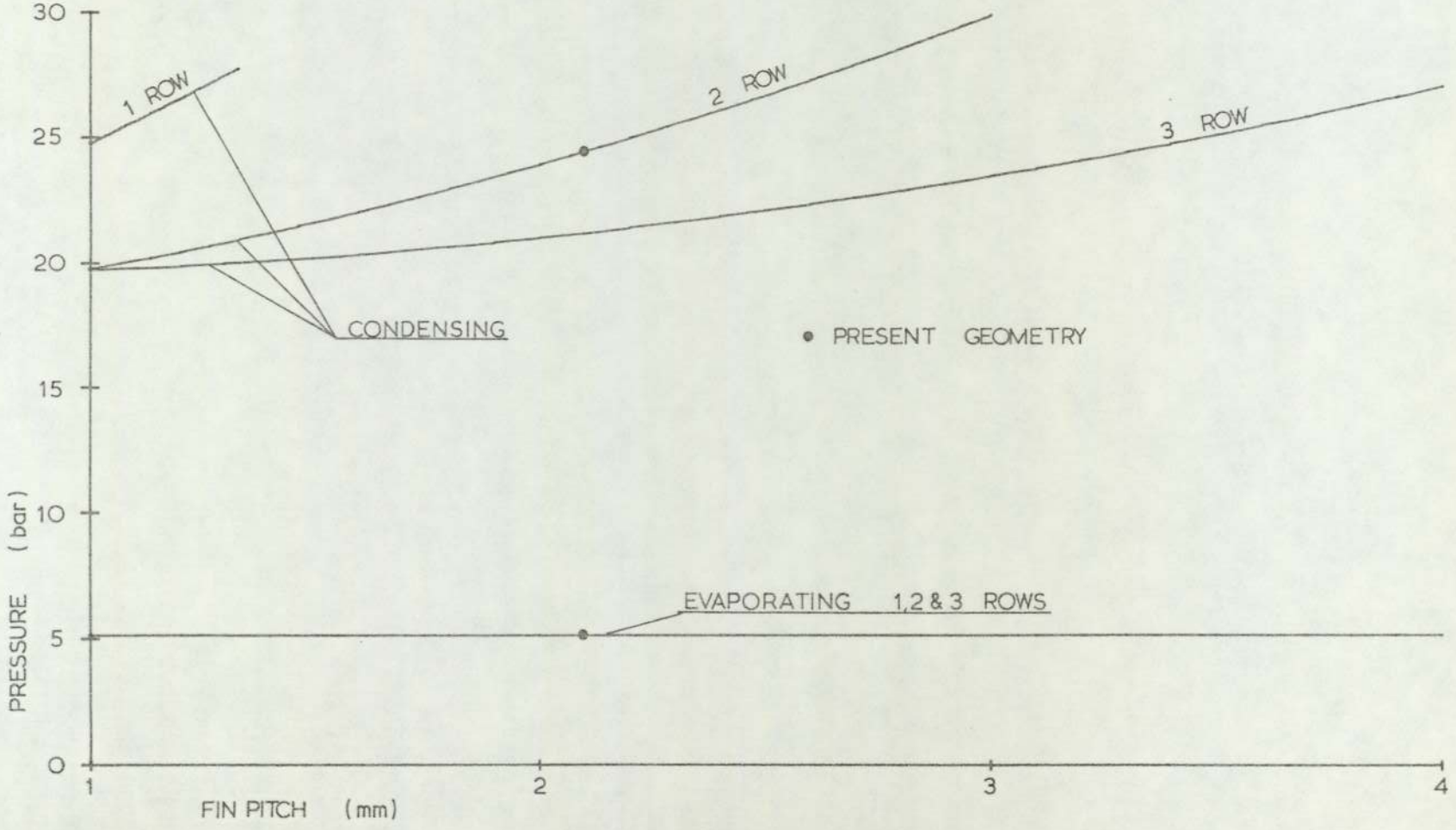

GRAPH 8.10

PLOT OF CONDENSER AIR SIDE REYNOLDS NUMBER AGAINST CONDENSER FIN PITCH

ENGINE IDLING AT 750 rev/min

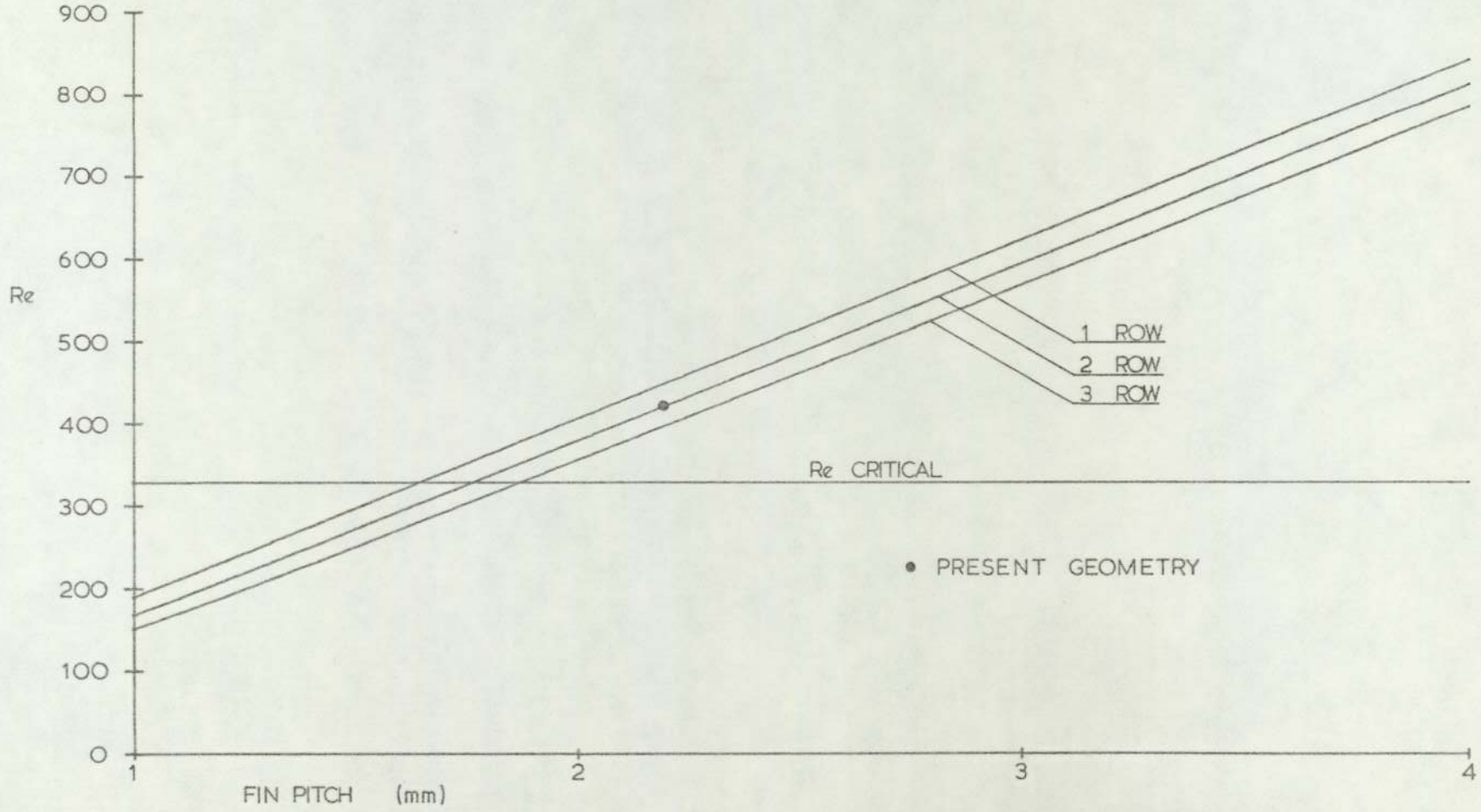

GRAPH 8.11

PLOT OF FRACTION OF TOTAL FUEL FLOW RATE ATTRIBUTABLE TO THE COMPRESSOR LOAD AGAINST ENGINE SPEED

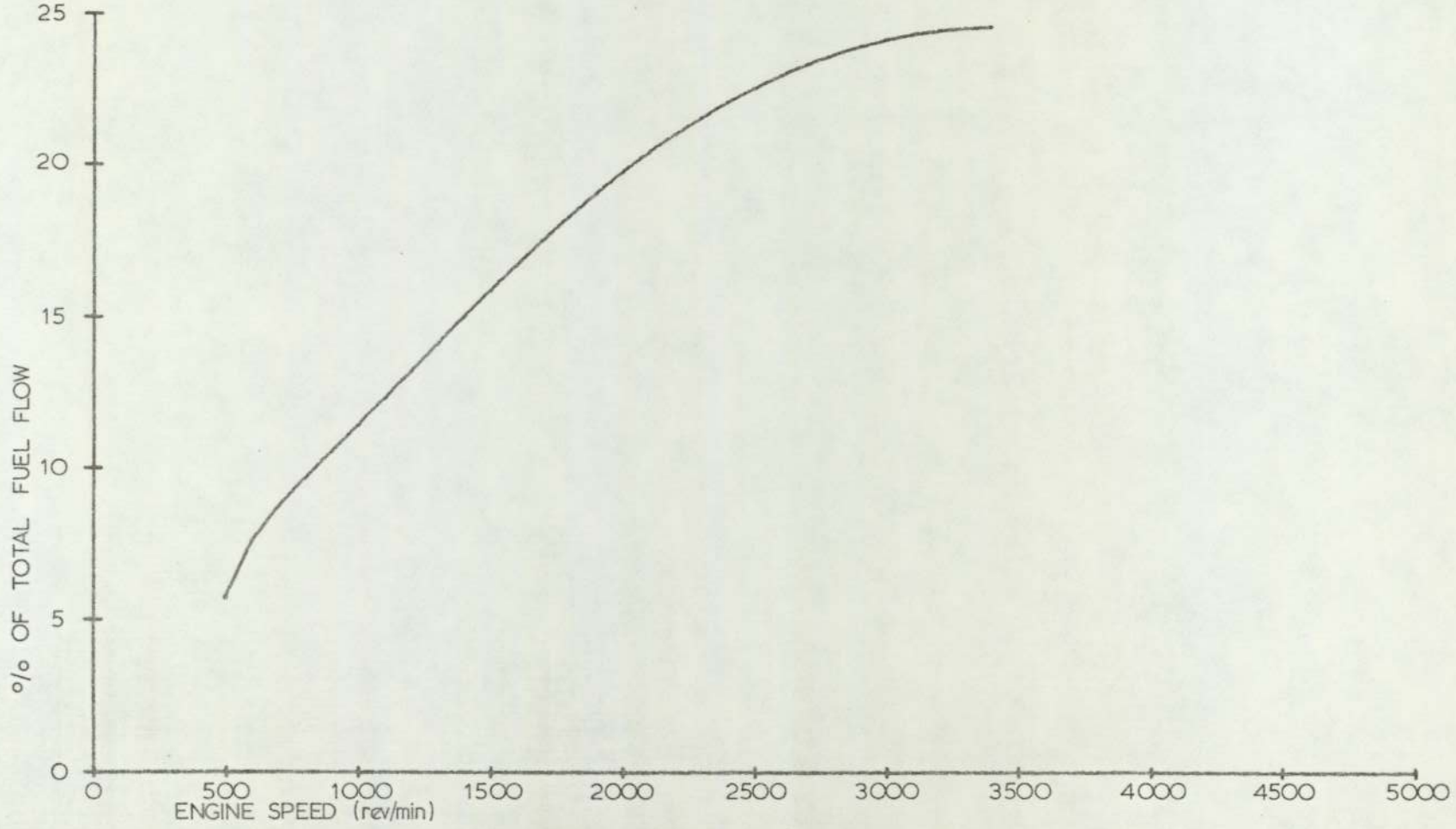

GRAPH 8.12

PLOT OF FRACTION OF TOTAL FUEL FLOW RATE ATTRIBUTABLE TO THE COMPRESSOR LOAD AGAINST ROAD SPEED CAR MID LADEN ON ZERO GRADIENT

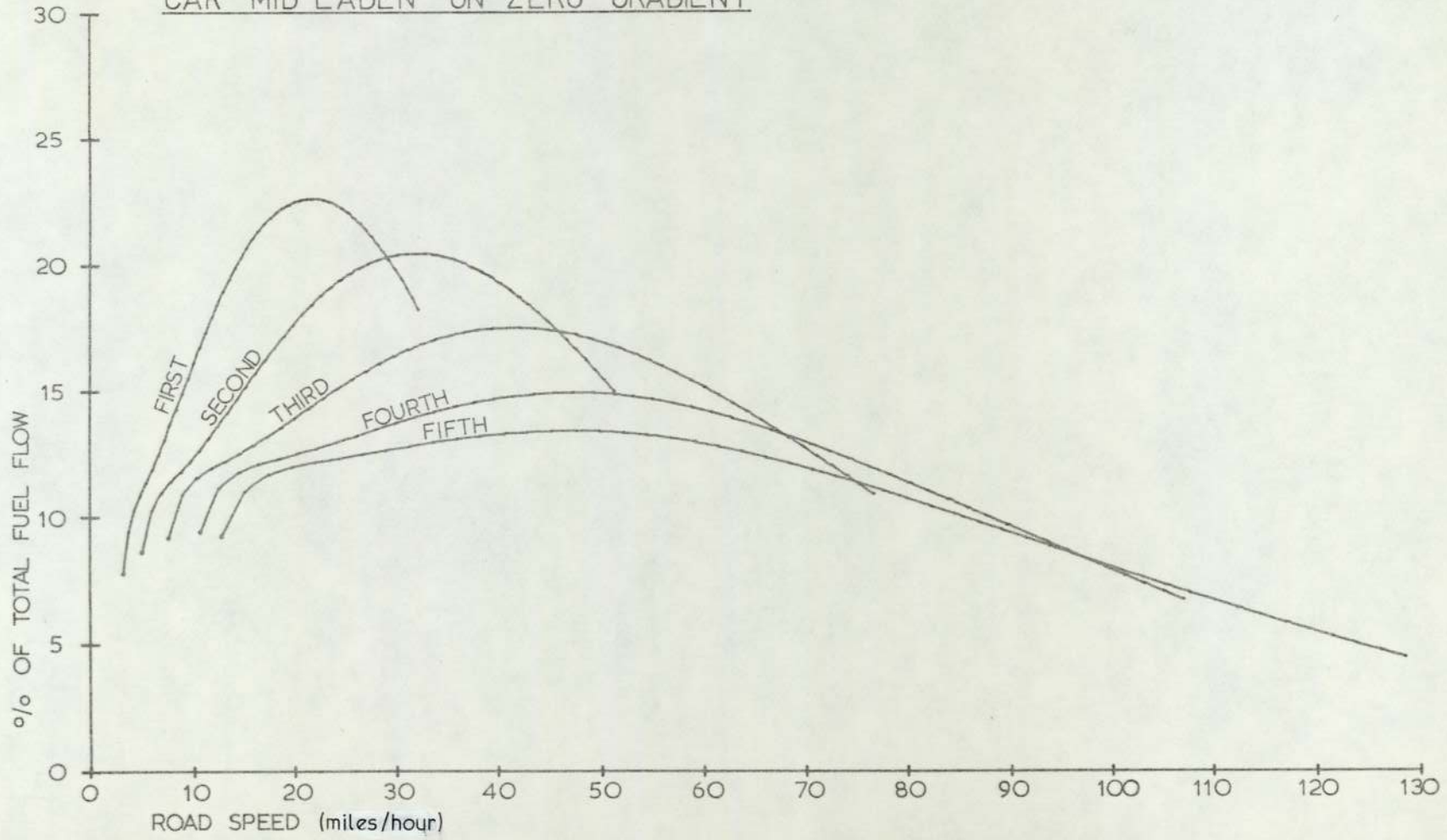

GRAPH 8.13

PLOT OF COMPRESSOR LOAD AGAINST ISENTROPIC EFFICIENCY

ENGINE IDLING AT 750 rev/min

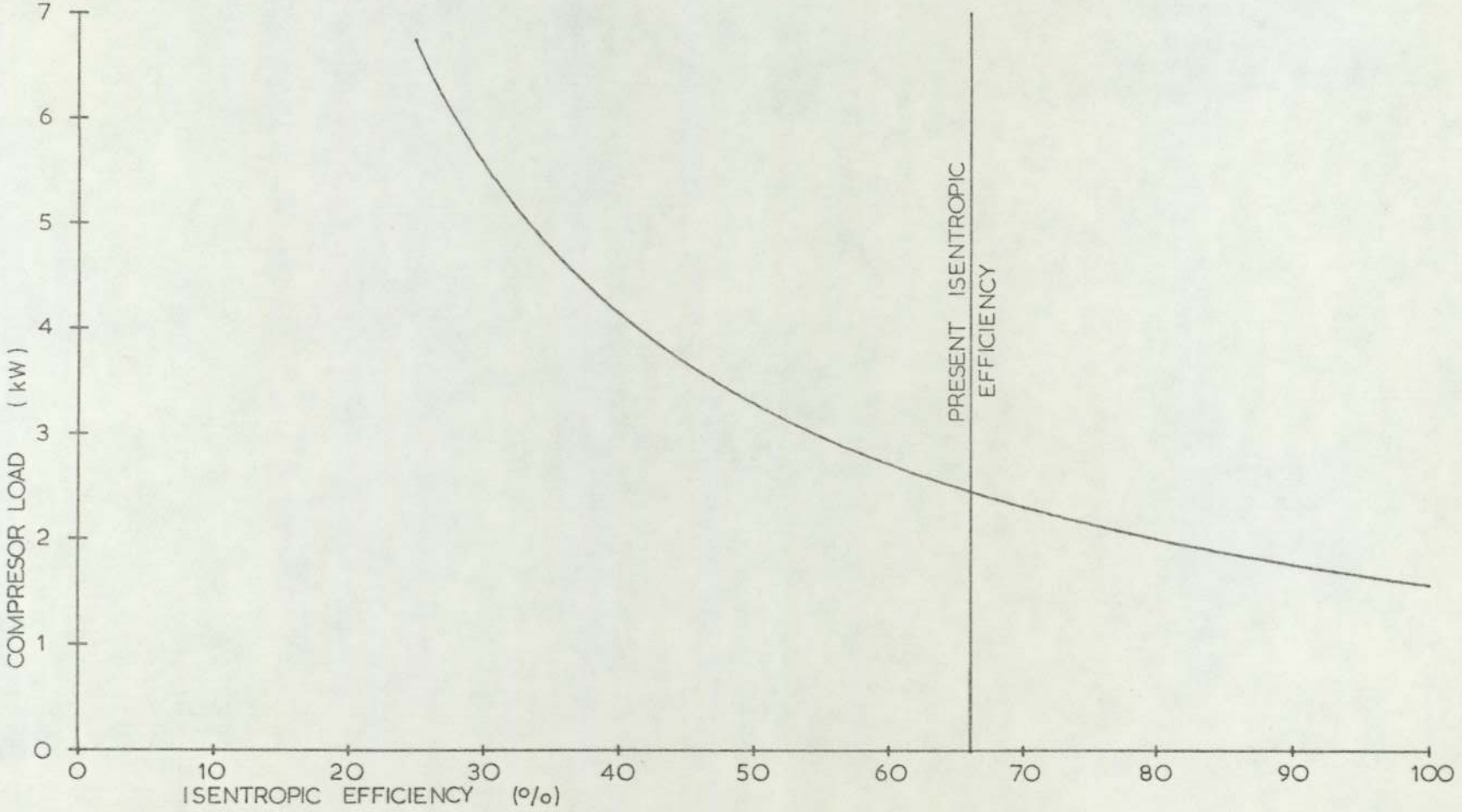

GRAPH 8.14

PLOT OF COOLING SYSTEM TEMPERATURE AGAINST ENGINE SPEED

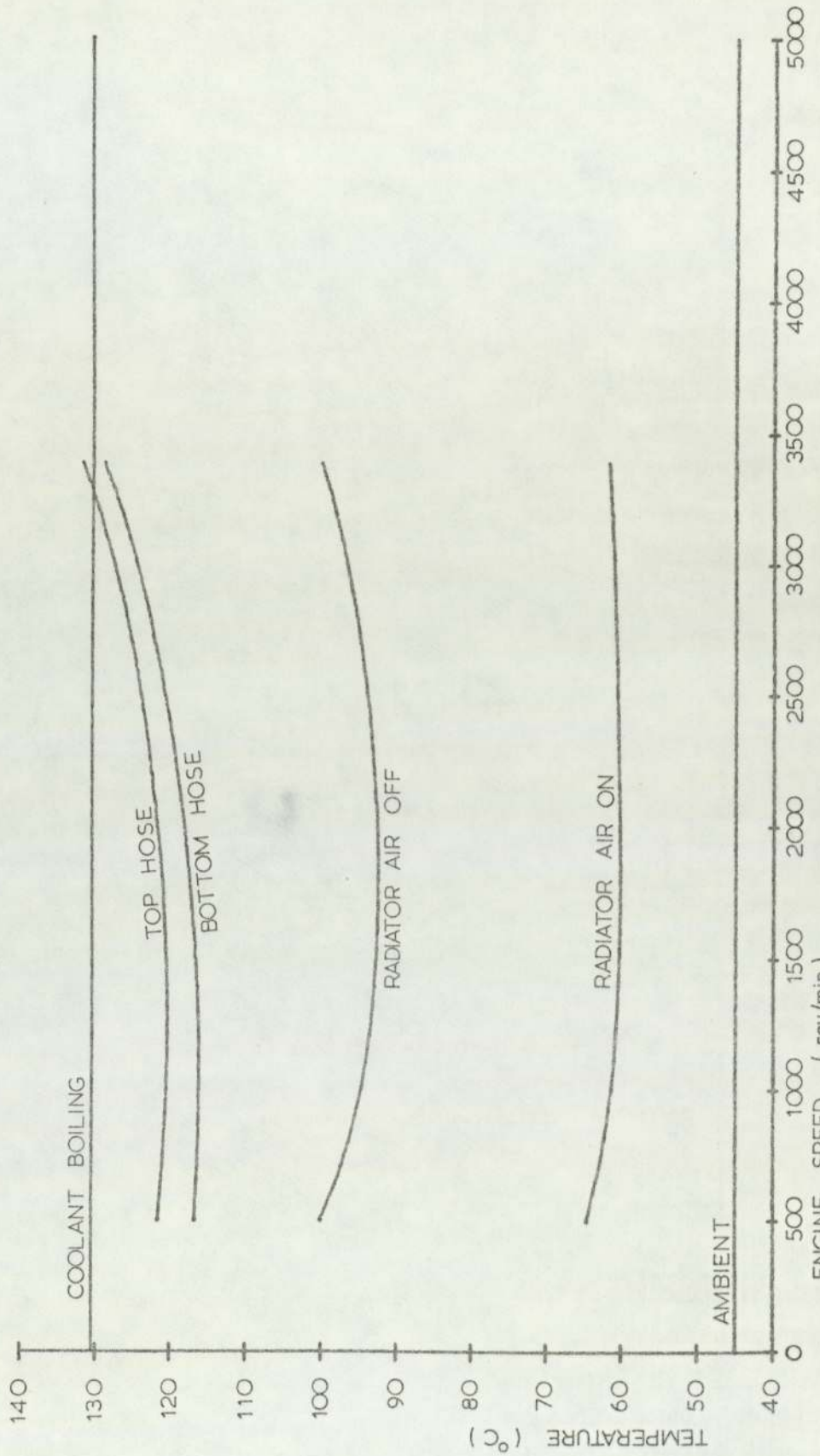

GRAPH 8.15

PLOT OF COOLING SYSTEM TEMPERATURE AGAINST ROAD SPEED

CAR MID LADEN ON ZERO GRADIENT

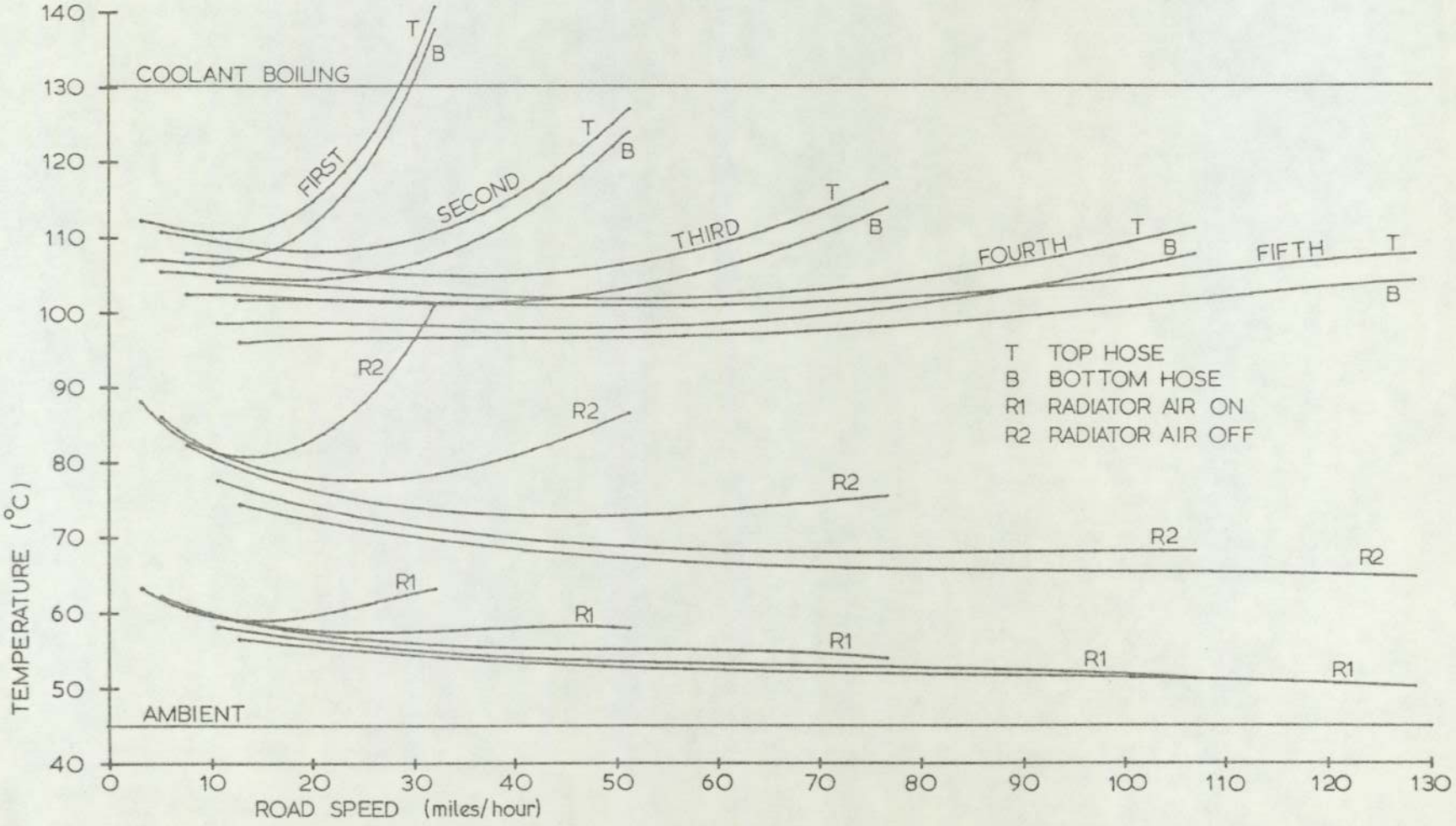

GRAPH 8.16

PLOT OF EVAPORATING AND CONDENSING PRESSURES AGAINST CONDENSER FIN PITCH, FOR VAPOUR COMPRESSION SYSTEM USING REFRIGERANT R 22 AND HAVING A COMPRESSOR PULLEY RATIO REDUCED BY 42 %
ENGINE IDLING AT 750 rev/min

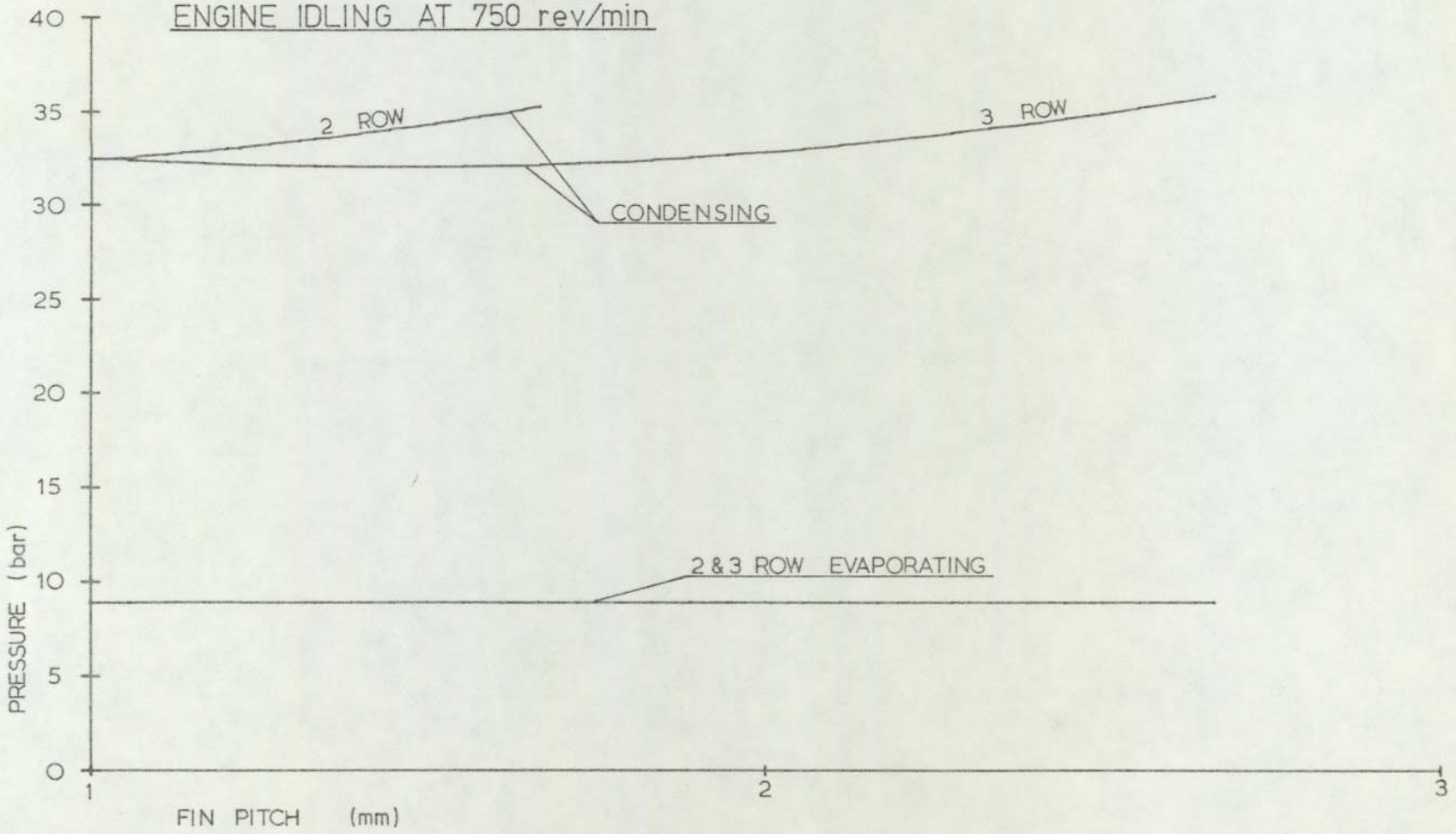

GRAPH 8.17

PLOT OF THE REFRIGERATION LOAD OF AN ABSORPTION SYSTEM AGAINST ENGINE SPEED

TEMPERATURE OF EXHAUST GAS REDUCED TO 177 °C

COP = 0·59

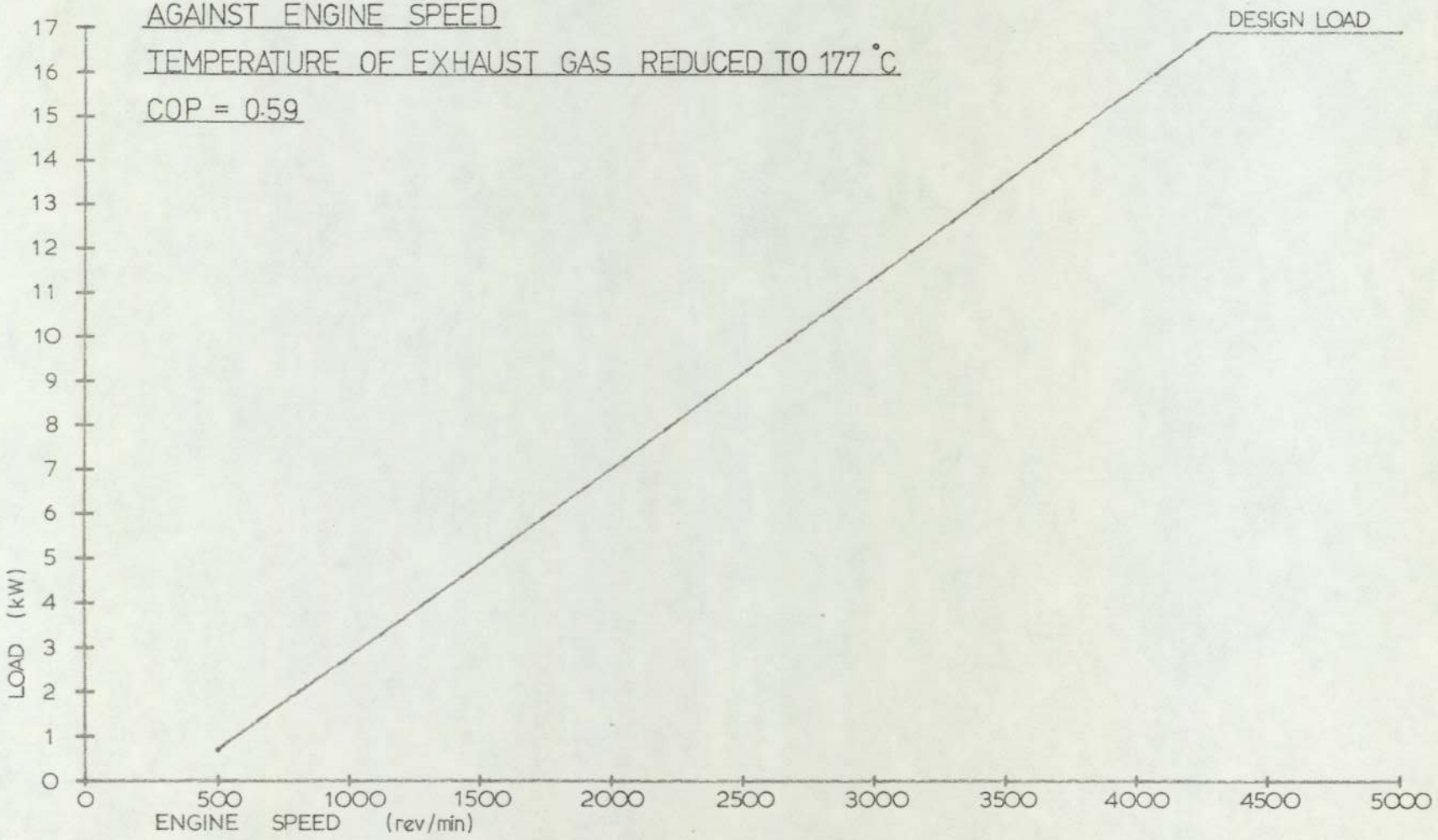

GRAPH 8.18

PLOT OF THE REFRIGERATION LOAD AVAILABLE FROM AN ABSORPTION SYSTEM AGAINST ROAD SPEED

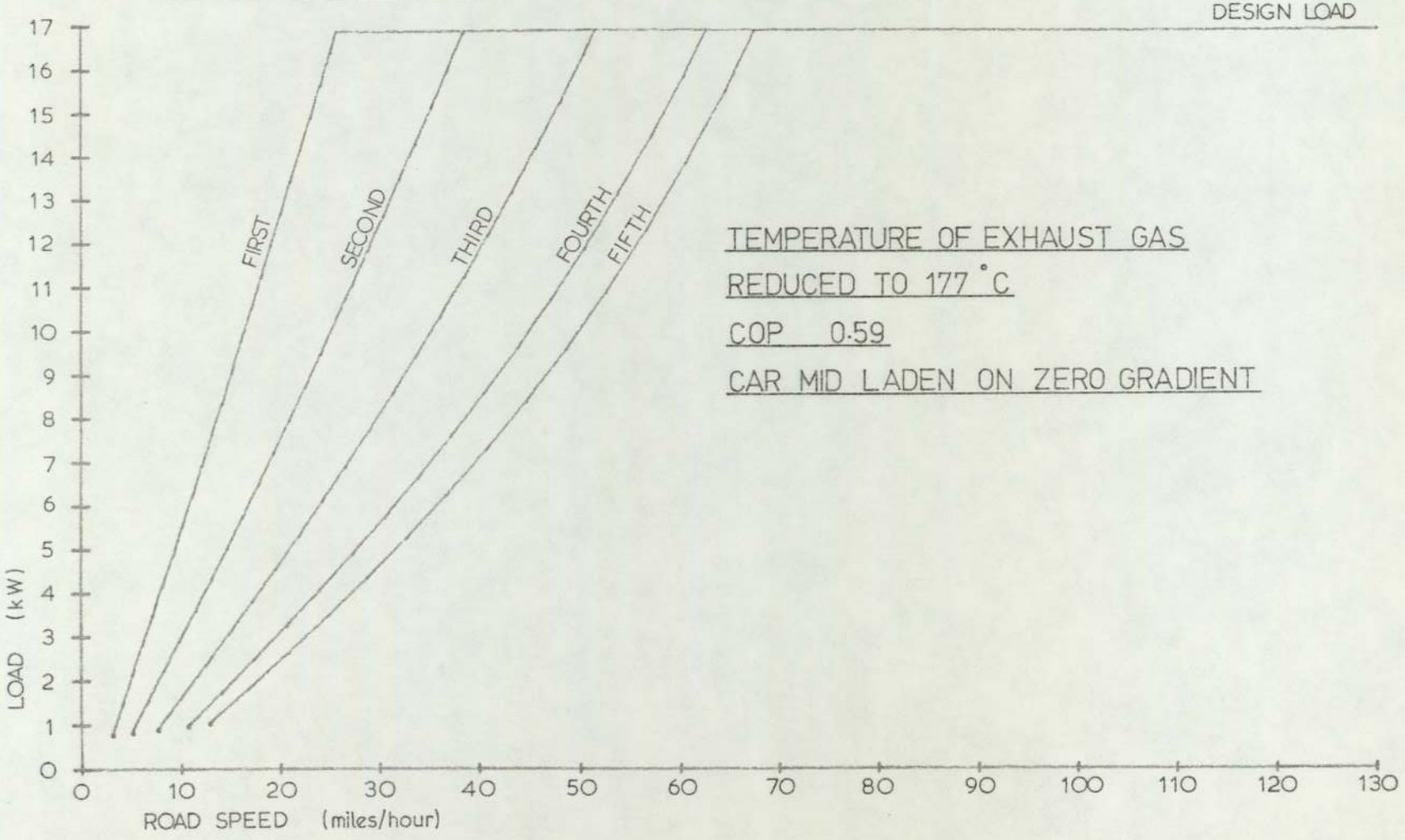

CHAPTER 9

CONCLUSIONS AND RECOMMENDATIONS

The advantage of cooling an engine through the medium of fluidised particles may be that the engine can be run at an optimum temperature, as for an air cooled engine, but with attenuation of noise by the particles.

A fluidised bed, as either an exhaust thermal reactor or catalyst support, would have advantages over conventional systems but for the practical problems of installing such systems in a car. A possibility is to use a bed of particles such that it is fluidised at idle and fixed at higher engine speeds.

Because of the interrelationships between the engine, the engine cooling system and the air-conditioning system a study of any one of these topics necessitates the inclusion of the other two. A mathematical model and the use of a digital computer have been found essential to this end.

The mass and energy transfers to and from the engine may usefully be expressed as functions of engine speed and brake power.

To obtain a model for the purpose of predicting air velocities through the condenser and radiator under any conditions, a hot wire anemometer has been developed and found suitable, and an improved version suggested for studies of velocity distribution.

In studying the condenser and radiator, discontinuities in the relationships between friction factor and air side Reynolds number were observed. These have the characteristics of laminar flow breakdown.

For the calculation of fluid temperatures at the inlets and outlets of the condenser and radiator, the assumption of fluid mixing on the coolant and refrigerant sides simplifies the computation considerably. The condenser may be considered as three separate cross flow heat exchangers responsible for cooling of superheated gas, condensation of vapour,and sub cooling of liquid.

The efficiency and ratios, required for a steplessly variable transmission, to compete with the present manual fixed ratio transmission on the bases of fuel

consumption and acceleration, have been calculated at varying road speed. An overall minimum efficiency of 75% is proposed but higher efficiency at high road speeds is desirable and a lower efficiency at low road speeds acceptable. The use of such a transmission may result in a smaller radiator being sufficient, but a transmission cooling system is necessary.

The engine cooling fan has an influence on fuel consumption, the air-conditioning compressor load (and fuel consumption penalty) and on the cooling system performance and cost. The present fan, although designed as an axial flow fan, acts as a paddle bladed centrifugal fan. The development of a more efficient mixed flow fan would give improvements to the fuel consumption and the refrigeration system, and enable a cost reduction of the engine cooling system to be attained. The viscous coupling used in the power transmission to the cooling fan has a great influence on the power consumption of that fan at high engine speeds, and is more cost effective than would be an electric or hydraulic transmission. A fuel consumption reduction would be obtained by the use of a viscous coupling having a mechanical governor. The effect on coolant temperatures of the non air-conditioned version of the car would be negligible under normal driving conditions.

In comparison with the air-conditioned version of the car, the performance of the cooling system of the non air-conditioned car is greater than necessary and may be reduced to give a cost reduction.

The overall cost of the radiator and coolant pump may be optimised, a larger pump capacity resulting in a higher radiator coolant side heat transfer coefficient to compensate for a reduction in the air side surface area.

The influence of a mixture of water and antifreeze on the performance of the cooling system is to promote higher coolant temperatures than if water is used, owing to the reduced coolant side heat transfer coefficient in the radiator. This is partially compensated for by the higher saturation temperature of the mixture at the same pressure.

The refrigeration load available from the present system is probably limited by the power consumption of the compressor at idle. This may be reduced by an increase in the condenser air velocity or an increase in the isentropic efficiency of the compressor, and potentially either the fuel consumption may be reduced and/or the refrigeration load increased. To this end, the use of a vane compressor having a potentially higher isentropic efficiency is recommended.

An increase in cooling fan speed will result in an increase in the power consumption of the fan but a decrease in the power consumption of the compressor. Optimisation of the fan speed to reduce the total power consumption is possible but is dependent on climatic conditions. A thermostatically controlled fan drive may be advantageous.

The use of refrigerant R22 instead of R12 would provide a cost saving and/or an increase in the refrigeration load and/or a reduction in fuel consumption and is considered safe for use in the present system. An increased condenser air flow rate is necessary for its use but may be provided by modifications, as recommended above, to the engine cooling fan.

For motor car air-conditioning using an absorption cycle, refrigerant R22 and dimethyl ether of tetraethylene glycol as an absorbent have the highest potential of known combinations. The condenser air velocity would need to be increased above that required for R22 in a vapour compression system, owing to the lower coefficient of performance. There is a potential fuel saving but a reduced refrigeration load has to be accepted at idle. An optimum generator temperature may exist, giving the highest refrigeration load at idle, the coefficient of performance theoretically increasing with generator temperature but the heat energy transferable from the exhaust gas decreasing.

RECOMMENDATIONS FOR FURTHER WORK

Experimental test data under steady state conditions of operation should be gathered, pertaining to radiator and condenser air velocities, the engine, the engine cooling system, and the refrigeration system, to examine the authenticity of the results from the models.

The steady state models of the engine cooling system and vapour compression refrigeration system may be improved, given more complete data on the radiator and condenser air side j and f factors, especially at low face velocities. The dependence of j and f factors on non dimensional ratios other than the ratio of mean passage diameter to passage length might be considered. The critical Reynolds numbers should also be examined for a range of condensers and radiators and their dependence on geometrical ratios considered.

The radiator air velocity should be measured to give more complete data on the influence of the relative position of the condenser, radiator, and engine cooling fan.

The influence of thermostat opening on engine coolant flow rate might be studied.

Experimental data relating the compressor isentropic and volumetric efficiencies to compressor speed, pressure ratio and temperature should be gathered with a view to modelling of these parameters, and improving the model of the refrigeration system.

To extend the models to unsteady state, a first step may be to use a driving cycle representative of the use of the vehicle and study the resulting fuel consumption, assuming that the steady state model is applicable. The overall fuel consumption over this cycle may be optimised, and also the required efficiency of a steplessly variable transmission, to compete with the present system on the basis of fuel consumption, calculated. To obtain a true unsteady state model, transient heat transfer data is required on the engine, the radiator, the condenser, the evaporator and the compressor. The most important of these are the engine

and the evaporator.

If the absorption system is considered worthy of further study, in view of the reduced refrigeration load at idle, then the cycle should be modelled and the influence of generator temperature on refrigeration load studied. An optimum generator temperature may exist but may be above the range of temperatures for which stability data is available on the fluids considered. Hence experimental data on the stability may be required.

APPENDIX A1

THE HOT WIRE ANEMOMETER USED FOR THE MEASUREMENT OF THE RADIATOR/CONDENSER AIR VELOCITY (IN SITU)

THE SELECTION OF A SUITABLE METHOD

The device used for the measurement of this air velocity must fulfil the following requirements:

a) It must fit into the very limited space either in front of the condenser or behind the radiator.

b) It must be capable of operating in the environment of a moving car (i.e. it must be insensitive to vibration and changes in level).

c) The pressure drop due to the instrument should be insignificant.

d) The reading should be either the mean effective velocity over the area of flow, or a matrix of point velocities over this area.

A hot wire anemometer was designed and developed in an attempt to fulfil these requirements.

DESIGN AND CONSTRUCTION OF THE HOT WIRE ANEMOMETER

A circuit diagram and pictorial drawing of the anemometer are shown on figures A1.1 and A1.2 and a photograph on plate A1.1.

The active element consists of a 3.386m length of 30 s.w.g. nickel wire, the purity of this wire conforming to Henry Wiggin and Company's specification N200[81]. The wire is silver soldered to 6.3mm diameter copper terminals at each end, and passes through 1mm diameter drilled holes in similar copper studs at the turning points. The result is that 3.328m of the wire is exposed to the air flow. The balancing resistance consists of a 0.818m length of 0.9mm diameter constantan wire manufactured by Tempco Limited. This wire is also silver soldered to 6.3mm diameter copper studs. Both of the wires are tensioned by coil springs acting on the bottom row of studs, the tension being just sufficient to keep the wires taut. The wire lengths were measured against a steel tape and the diameters measured

at 15cm intervals using a travelling microscope. Both the R.M.S. and arithmetic mean diameters were calculated for subsequent use.

The wires complete with studs and connectors were removed from the condenser and mounted into a framework to fit into a temperature calibration bath produced by N. H. Irving and Son to a design of the National Physical Laboratory. Each wire in turn was connected to a wheatstone bridge manufactured by Pye Instruments which was used with an external galvanometer of the same make. The temperature of the silicone oil used in the bath was read from thermometers calibrated by the National Physical Laboratory.

No change in the resistance of the constantan wire was noted over a temperature range of 20 to 180^{o}C.

The resistance of the nickel wire was plotted against temperature and a quadratic found to give an excellent least squares fit. Using this function the resistances at 20^{o}C and 100^{o}C were calculated for subsequent use. Knowing the resistances R_1 and R_2 in fig. A1.2, the resistances R_3 and R_4 were calculated by the relationship:

$$\frac{R_1}{R_2} = \frac{R_3}{R_4} \qquad \text{A 1.1}$$

A precision 10 turn potentiometer provides the resistances R_3 and R_4. The resistance of this potentiometer was chosen to be high (20 kΩ) relative to the nickel and constantan wires, to minimise errors due to the connecting wires but low in relation to the impedance of the digital voltmeter (10 MΩ). The potentiometer has a temperature coefficient of 2 x 10^{-5}/K and was marketed by R.S. Components.

The setting of this potentiometer was achieved using the 'Pye' wheatstone bridge.

The digital voltmeter used with the device was manufactured by the Solartron Electronic group (model number A200). The tolerance of this instrument is stated as $\pm$0.005% on all ranges, except the lowest (10 mV) where this figure is

increased to ±0.01%. The range is 1 μV to 1.2 kV.

The thermocouple, mounted on the condenser for the measurement of air temperature, is of chromel-alumel, with an ice cold junction.

To ensure a pure d.c. power supply, 12 volt lead-acid accumulators were used, the potential being adjusted via a series potentiometer.

ANALYSIS OF ERRORS ARISING FROM NON-UNIFORM VELOCITY DISTRIBUTIONS

Accuracy of the anemometer is reliant on its ability to read a mean effective velocity in a non-uniform velocity distribution. For the purpose of this analysis, the effective mean velocity is taken to be that velocity which produces an identical heat transfer coefficient over a surface for which the heat transfer coefficient varies as velocity to the power of 0.6.

For this analysis the rate of heat transfer from the wire was calculated from an equation, developed by L.V. King[82] which reduces to:

$$q' = \theta [k + (2 \pi \varrho c_v k \, dU)^{\frac{1}{2}}] \qquad \text{A1.2}$$

Noting that $q' = I^2R'$ and using non-dimensional terms:

$$\frac{R'}{R'_m} \frac{\theta_m}{\theta} \quad z = 1 + X\phi^{\frac{1}{2}} \qquad \text{A1.3}$$

where:

$$z = \frac{I^2 R'_m}{k \ \theta_m} \qquad \text{A1.4}$$

$$X = \sqrt{\frac{2 \pi \varrho c_v dU_m}{k}} \qquad \text{A1.5}$$

and $$\phi = \frac{U}{U_m} \qquad \text{A1.6}$$

A linear variation of wire resistance with wire temperature is used, the resistances at 20°C and 100°C (the ambient and mean wire temperatures respectively) being as calculated from the fitted quadratic.

Hence:

$$\frac{R'}{R'_m} = 1 + \beta(\tau - 1) \qquad \text{A1.7}$$

where $$\beta = \alpha_m \theta_m \qquad \text{A1.8}$$

and $$\tau = \theta / \theta_m \qquad \text{A1.9}$$

Combining A1.3 and A1.7:

$$\tau = \frac{z(1-\beta)}{1 - \beta z + X\phi^{\frac{1}{2}}} \qquad \text{A1.10}$$

By definition of mean wire temperature:

$$\int_0^1 \tau \, d\eta = 1 \qquad \text{A1.11}$$

where η is the displacement as a fraction of the semi length.

Hence:

$$\int_0^1 \frac{z(1-\beta)\, d\eta}{1 - \beta z + X\phi^{\frac{1}{2}}} = 1 \qquad \text{A1.12}$$

$\therefore$

$$1 = \frac{2z(1-\beta)}{X} \int_{\phi_0}^{\phi_1} \left[1 - \frac{1-\beta z}{1 - \beta z + X\phi^{\frac{1}{2}}} \right] \left(\frac{d\eta}{d\phi} \right) d\phi^{\frac{1}{2}} \qquad \text{A1.13}$$

Since the actual velocity distribution is not known, a linear distribution is assumed and described as:

$$\phi = \frac{2}{x+2} (x\eta + 1) \qquad \text{A1.14}$$

The factor x describes the non-uniformity of the velocity distribution such that:

$$x = \frac{\text{maximum velocity}}{\text{minimum velocity}} - 1 \qquad \text{A1.15}$$

$\therefore$

$$\frac{\beta X^2 x}{z(1-\beta)(x+2)} = \phi_1^{\frac{1}{2}} - \phi_o^{\frac{1}{2}} - (1-\beta z)\ln\left[\frac{1-\beta z + X\phi_1^{\frac{1}{2}}}{1-\beta z + X\phi_o^{\frac{1}{2}}}\right] \qquad \text{A1.16}$$

where:

$$\phi_o = \frac{2}{x+2} \quad \text{when } \eta = 0 \qquad \text{A1.17}$$

and:

$$\phi_1 = \frac{2(x+1)}{x+2} \quad \text{when } \eta = 1 \qquad \text{A1.18}$$

This equation may be solved numerically to give X as a function of z.

In a uniform velocity distribution $\phi = 1$ and $\tau = 1$ and equation A1.3 reduces to:

$$X = z - 1 \qquad \text{A1.19}$$

which was used to calculate the apparent velocity measured by the device in such a non-uniform velocity distribution and hence to calculate the error defined as:

$$\% \text{ error} = \frac{U \text{ apparent} - U \text{ effective}}{U \text{ effective}} \times 100 \qquad \text{A1.20}$$

A plot of % error against the ratio of maximum to minimum velocity under these conditions is shown on graph A1.1.

Clearly in a non-uniform velocity distribution the wire temperature varies along the wire and there is a danger of the wire oxidising or melting at local hot spots. To study this possibility the temperature distribution along the wire was plotted at varying velocity ratios and varying velocity on graphs A1.2 and A1.3 using equation A1.10. Similarly the maximum wire temperature has been plotted against velocity ratio at various velocities and is shown on graph A1.4. Under the

expected conditions of operation the maximum wire temperature may not be expected to reach damagingly high levels.

CALIBRATION

Calibration of such an anemometer should be under conditions of uniform velocity. The provision of a uniform velocity over an area as large as the condenser is difficult and hence a small anemometer, using wire from the same spool was constructed. This anemometer is illustrated on figure A1.4 and the circuit diagram, basically similar to that of the larger anemometer is shown on figure A1.3. Photographs of the calibration anemometer and equipment are on plates A1.2 and A1.3. Construction and temperature calibration methods were identical to those used for the condenser anemometer.

King's[82] equation, used in the error analysis above, reduces to:

$$Nu = \frac{1}{\pi} + \sqrt{\frac{2\,Re\,Pr}{\pi\gamma}} \qquad A1.21$$

Relationships for the heat transfer by forced convection from a heated cylinder are usually quoted in the form

$$Nu = f(Re, Pr) \qquad A1.22$$

For air, over the temperature range under consideration, the Prandtl number is very nearly constant and the relationship reduces to:

$$Nu = f(Re) \qquad A1.23$$

Both Hilpert[83], and Collis and Williams[84], suggest that the ratio between the absolute temperatures of the wire and free steam forms a further relevent parameter, but this is omitted here since the temperatures may be expected to remain fairly constant.

The effect of upstream turbulence is a further factor which has been discussed in several publications but this is generally in the context of heat transfer to boiler tubes. Kestin[85] suggests that the Nusselt number is a function of

the turbulence defined as the ratio:

$$Tu = \frac{\overline{(U')^2}^{\frac{1}{2}}}{\overline{U_\infty}} \qquad \text{A1.24}$$

i.e. the ratio of the time R.M.S. velocity perpendicular to the direction of flow, to the mean velocity in the direction of flow. He also suggests that some parameter should be included to take into account the scale of the turbulence, this being large in the case of a hot wire anemometer.

As an alternative to a measure of the scale of turbulence the flow may be more fully described by quoting the percentage turbulence as defined above, and also the Strouhal number, defined by Schlichting[86] as:

$$S = \frac{nd}{\overline{U}} \qquad \text{A1.25}$$

where n is the frequency of the turbulence, d is a representative length (in this case the wire diameter) and U is the free stream velocity. This parameter is used in studies of vortex shedding, but in this case it is suggested that n should be the time average frequency of the upstream turbulence.

Heat transfer from the wire may then be more fully described by the relationship:

$$Nu = f(Re, Tu, S) \qquad \text{A1.26}$$

No work has been carried out to substantiate this but the work of Comings[87] illustrates the effect of increasing turbulence on the Nusselt number. In this work the intensity of turbulence was calculated from the apparent change of conductivity of the airstream, after the method used by Schaubaur[88] and described by Dryden[89]. It was shown that at low levels of turbulence the rate of change of Nusselt number was high compared with higher levels of turbulence where the Nusselt number appears to be asymptotic to a finite value. The results from Comings[87] work have been plotted on graph A1.5. Unfortunately the diameter of the body used was large compared with the hot wire anemometer, resulting in a

Reynolds number of 5800. At lower values of Reynolds number (down to 410) Comings'[87] work showed that the influence of turbulence was less.

The location of the hot wire anemometer in the car is such that turbulent flow is produced upstream by the radiator grill. In view of this and the evidence of Comings,[87] calibration of the anemometer was carried out in turbulent flow conditions. The anemometer was placed 25mm inside the open end of a 100mm diameter pipe. Air was blown out of this pipe by two d.c. electric centrifugal fans 3m upstream. The velocity of the airflow was adjusted by varying the voltage applied to the fans, the voltage being infinitely variable over the range of operation. The range of air velocities used was from 0.836 to 20.2 m/s resulting in Reynolds numbers, based on the pipe diameter of 5,500 to 127,000 respectively.

The standard used for measurement of the air velocity in the region of the wire was a pitot-static tube, made to B.S. 1042 (Part 2)[90] by Airflow Developments. The kinetic head from the pitot static tube was measured using a Chattock manometer, manufactured by Cassela, at low velocities and an inclined manometer, manufactured by Airflow Developments, at high velocities. The results noted in the laboratory are shown on table A1.1. The pitot-static tube was also used to measure the distribution across the diameter of the pipe. It was found that the velocity was uniform to within 15mm of the pipe walls.

Calculation of Reynolds and Nusselt numbers for the wire requires values of the properties of air. The effective mean temperature at which these properties should be calculated must lie between the upstream air temperature and the wire temperature. The arithmetic mean temperature was used as did Hilpert,[83] and Collis and Williams.[84]

The heat dissipated from the wire may be calculated from the measured potential across the wire and the known resistance, but this includes heat radiated to the surroundings and conducted to the end connections. Heat transferred by radiation was estimated to constitute less than 1% of the total dissipated, and would be of the same order for both the calibration and large anemometers. Heat

transferred by natural convection would also be of the same order for both anemometers since the angle of inclination for each was the same, and from the work of Collis and Williams[84], would be negligible at Reynolds numbers considered here. The proportion of the heat dissipated by conduction to the end supports is not common to both devices but was taken into account as follows. The assumptions made are:

a) The variation of resistance of the wire with temperature is linear, the coefficient of resistance at the mean temperature of the wire (which is the same for both anemometers) being such that the resistance of the wires is as predicted at 20°C and 100°C.

b) The end connections are at the same temperature as the air stream. This assumption is made on the basis that they are of copper with no internal generation and having a surface area per unit length, and cross section much larger than those of the wire.

c) The convective heat transfer coefficient does not vary with temperature. From the relationships published by Collis and Williams[84] for heat transfer from a wire, the effect of a wire temperature change from 20°C to 120°C results in a change in heat transfer coefficient of less than 2%.

d) The conductivity of the nickel wire does not vary with temperature. The variation is in fact small over the temperature range in question and the value used was at 20°C, i.e. approximately the lowest temperature and hence the temperature at which the temperature gradient is greatest. This data was from Henry Wiggin & Co.[81]

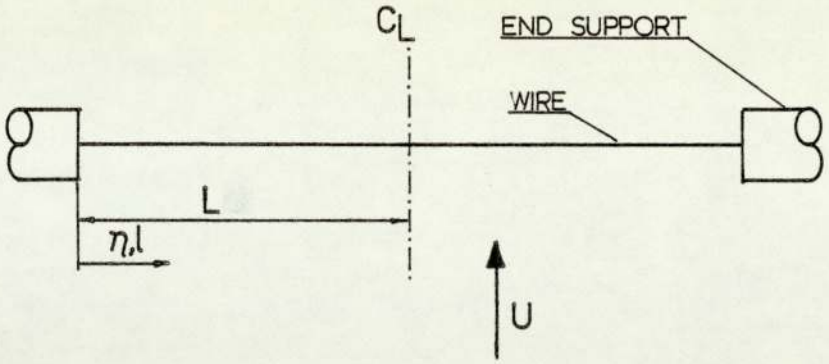

Wire temperature = θ

Mean Wire temperature = θ_m

} relative to ambient

$$q''' = \frac{I^2R'}{\pi r^2} - \frac{2h\theta}{r} \qquad \text{A1.27}$$

$$= \frac{I^2R'_m}{\pi r^2}(1-\alpha\theta_m) - \left[\frac{2h}{r} - \frac{I^2R'_m}{\pi r^2}\right]\theta \qquad \text{A1.28}$$

$$\frac{d^2\theta}{dl^2} + \frac{q'''}{k_w} = 0 \qquad \text{A1.29}$$

$$\therefore \quad \frac{d^2\tau}{d\eta^2} + \frac{q'''L^2}{k_w\theta_m} = 0 \qquad \text{A1.30}$$

$$\therefore \quad \frac{d^2\tau}{d\eta^2} + \frac{I^2R'_mL^2}{\pi r^2 k_w\theta_m}(1-\beta) - \left[\frac{2hL^2}{rk_w} - \frac{I^2R'_m\beta L^2}{\pi r^2 k_w\theta_m}\right]\tau = 0 \qquad \text{A1.31}$$

$$\therefore \quad \frac{d^2\tau}{d\eta^2} - M^2\tau + N = 0 \qquad \text{A1.32}$$

given the boundary conditions when $\eta = 0$, $\tau = 0$ A1.33

and when $\eta = 1$, $\frac{d\tau}{d\eta} = 0$ A1.34

the solution becomes $$\tau = \frac{N}{M^2}\left[1 - \frac{\cosh M(1-\eta)}{M}\right] \qquad \text{A1.35}$$

Integrating the latter equation:

$$\int_0^1 \tau\, d\eta = 1 = \frac{N}{M^2}\int_0^1 \left[1 - \frac{\cosh M(1-\eta)}{\cosh M}\right] d\eta \qquad \text{A1.36}$$

$$\therefore \quad 1 = \frac{N}{M^2}\left[1 - \frac{\tanh M}{M}\right] \qquad \text{A1.37}$$

This equation was solved numerically to give h and hence Nu using the experimental data from the calibration anemometer, and subsequently for the condenser anemometer.

$$M^2 = \frac{L^2}{\pi r^2}\left[2\pi\, Bi - \beta z\right] \qquad \text{A1.38}$$

$$\text{and} \quad N = \frac{L^2}{\pi r^2} z(1-\beta) \qquad \text{A1.39}$$

For an infinitely long wire (i.e. at uniform temperature equal to θ_m)

$$\tau = 1 \qquad \text{A1.40}$$

$$\text{and} \quad M^2 = N \qquad \text{A1.41}$$

$$\text{hence} \quad Bi = \frac{z}{2\pi} \qquad \text{A1.42}$$

Values of Bi are shown on table A1.2 against z for various ratios of length to diameter for a nickel wire as used. This table shows the influence of this aspect ratio on calibration. This is also shown by the graphs of wire distribution for the calibration anemometer and each span of the larger anemometer, plotted from equation A1.35 and shown on graphs A1.6 and A1.7.

Using equation A1.47 values of Nusselt number and Reynolds number for each velocity reading were calculated and unconventionally plotted as Reynolds number against Nusselt number to give the former explicitly as a function of the latter. A cubic was found to give an excellent least squares fit. This plot is

shown on graph A1.8 and tabulated values of Reynolds number, Nusselt number, velocity, and heat transfer coefficient are given on table A1.3.

COMPARISON OF NUSSELT NUMBER REYNOLDS NUMBER DATA WITH PREVIOUSLY PUBLISHED WORK

Plots of Nusselt number against Reynolds number for comparison with the equations given by King[82], McAdams[65], Hilpert[83],, and Collis and Williams[84] are shown on graphs A1.9, A1.10 and A1.11. Comparison on the same graph is made difficult by the different authors' choice of representative temperature for calculation of fluid properties. King[82] used the upstream air temperature, McAdams[65] used the arithmetic mean temperature for all properties except density which is at the upstream air temperature, and Hilpert[83], and Collis and Williams[84] used the arithmetic mean temperature as used here. For the purpose of this comparison Nusselt numbers and Reynolds numbers have been recalculated, and an equation of the form:

$$Nu = A + B\,Re^{n} \qquad \text{A1.43}$$

fitted to the data by the method of least squares.

The resulting values of the constants are given with the results of these other workers, and the deviations of their equations from the fitted equations at either end of the range of Reynolds number on table A1.4.

The major difference between the methods used by these other workers and here is that this anemometer was purposely calibrated in turbulent flow, while the others used equipment designed to produce laminar flow. The result is an increased Nusselt number at a given Reynolds number, as predicted from the work of Comings[87]. It is suggested that the discrepancies between the results of these workers is due to the very low levels of turbulence attained and that at these levels the rate of change of Nusselt number with turbulence is high.

The effect of upstream turbulence on the Nusselt number Reynolds number relationship is not clear, probably because of the difficulty, in experimental work,

of producing and measuring the required levels of turbulence. More data is needed in order to develop a better understanding in this field of heat transfer.

SUGGESTIONS FOR A MORE ACCURATE DEVICE GIVING A MATRIX OF POINT VELOCITIES OVER THE AREA OF FLOW

The device used was designed to give a mean velocity over the area of flow, but a similar device might be used for measurement of velocity distribution, giving a matrix of velocities over the area of flow. A sketch of such a device and a circuit diagram are shown on figures A1.5 and A1.6. This instrument would replace a matrix of separate hot wire anemometers over the area of flow and have the advantage of needing only one power supply and balancing system. The power supply in the diagram is a stabilised unit, the output being controlled by feedback from the wheatstone bridge. By setting the total resistance of the elements in series and measuring the total potential across them the current may be calculated. Measurement of the potential across each individual element enables the resistance of, and power dissipation from, each element to be calculated. By using the equation developed for compensation of end losses by conduction, and a calibration equation relating Nusselt number and Reynolds number the velocity over each element may be computed. An added refinement to enable readings to be made quickly and easily is the use of an automatic scanning switch and data logging device, which outputs the voltage readings onto punched tape for input to a digital computer. Such a system would enable readings to be taken quickly, reducing errors due to time variations in the velocity.

In computing velocity using this device the output could give the velocity distribution over the area and calculate accurately the mean effective heat transfer velocity. A suggested application is for use in developing motor car cooling fans and cowls, and studying the influence of grill design on air flow.

FIGURE A1.1

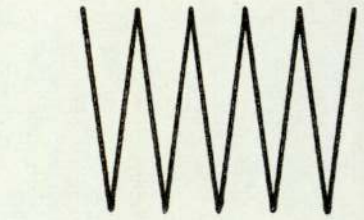

R_1 NICKEL WIRE (ACTIVE)

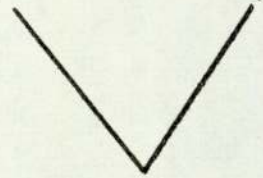

R_2 CONSTANTAN WIRE (BALANCE)

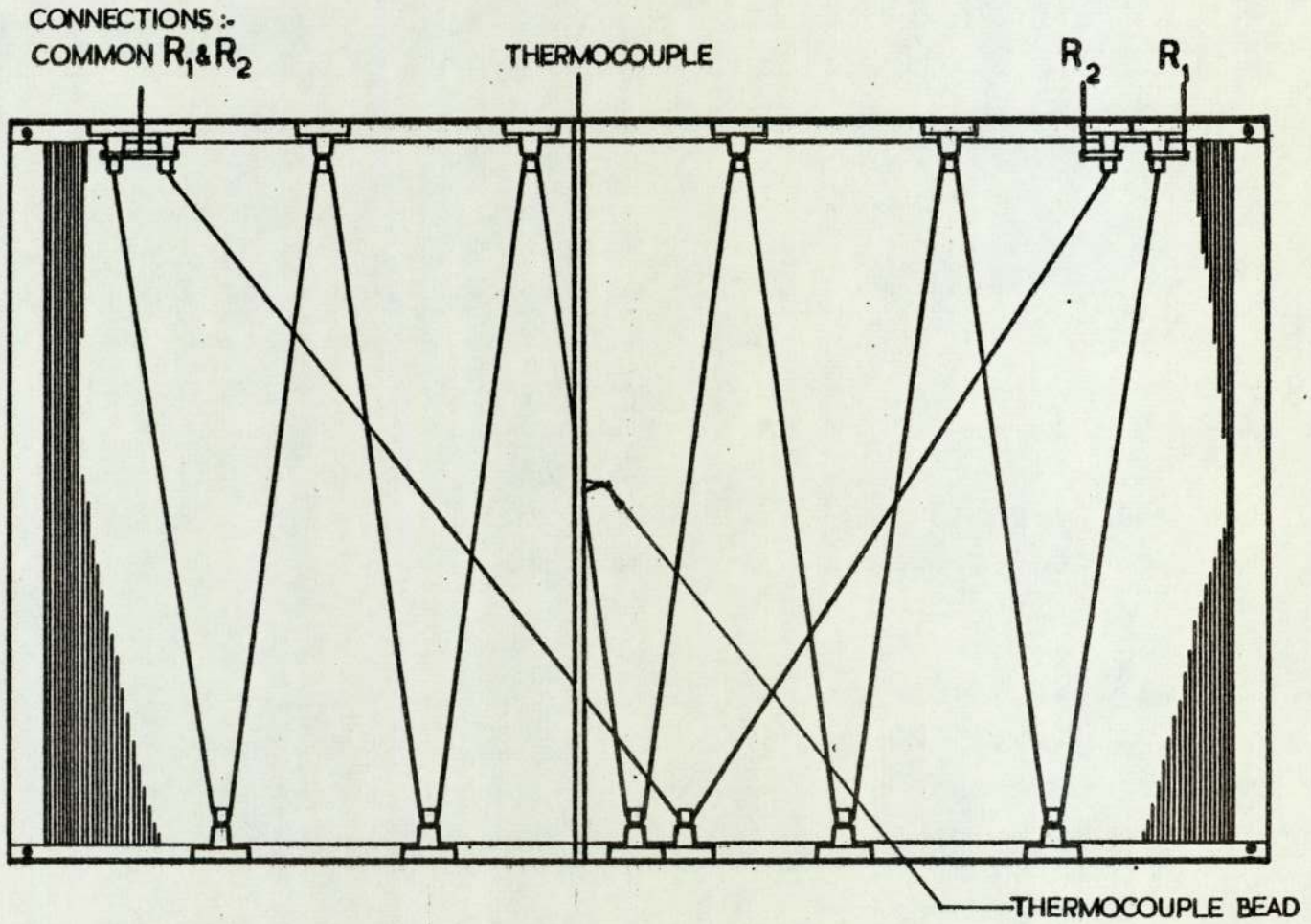

LAYOUT OF THE CONDENSER HOT WIRE ANEMOMETER

FIGURE A1.2

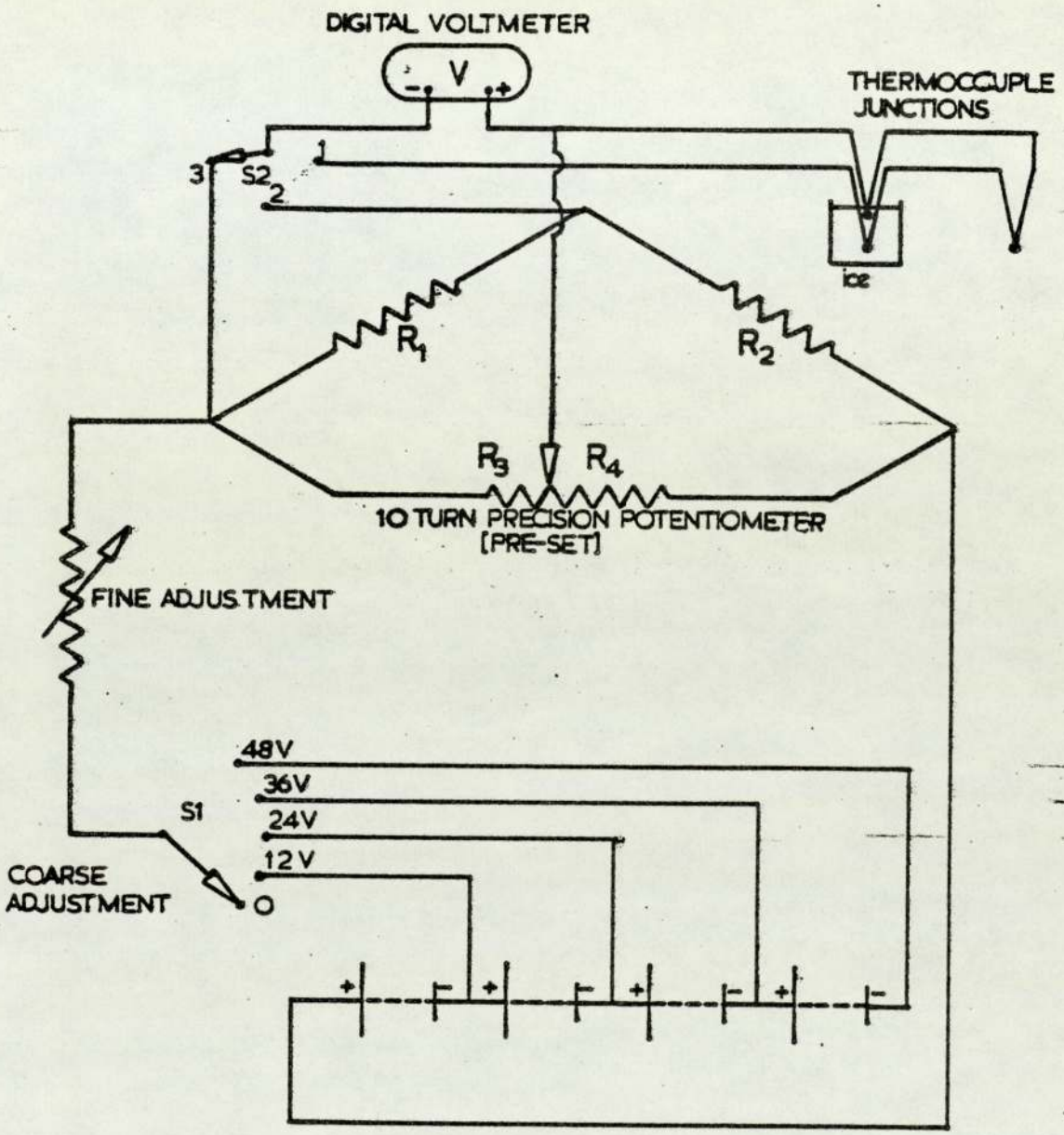

CONDENSER ANEMOMETER

CIRCUIT DIAGRAM

SWITCH POSITIONS S1:

1 temperature reading (air)

2 temperature reading (wire)

3 velocity reading

FIGURE A1.3

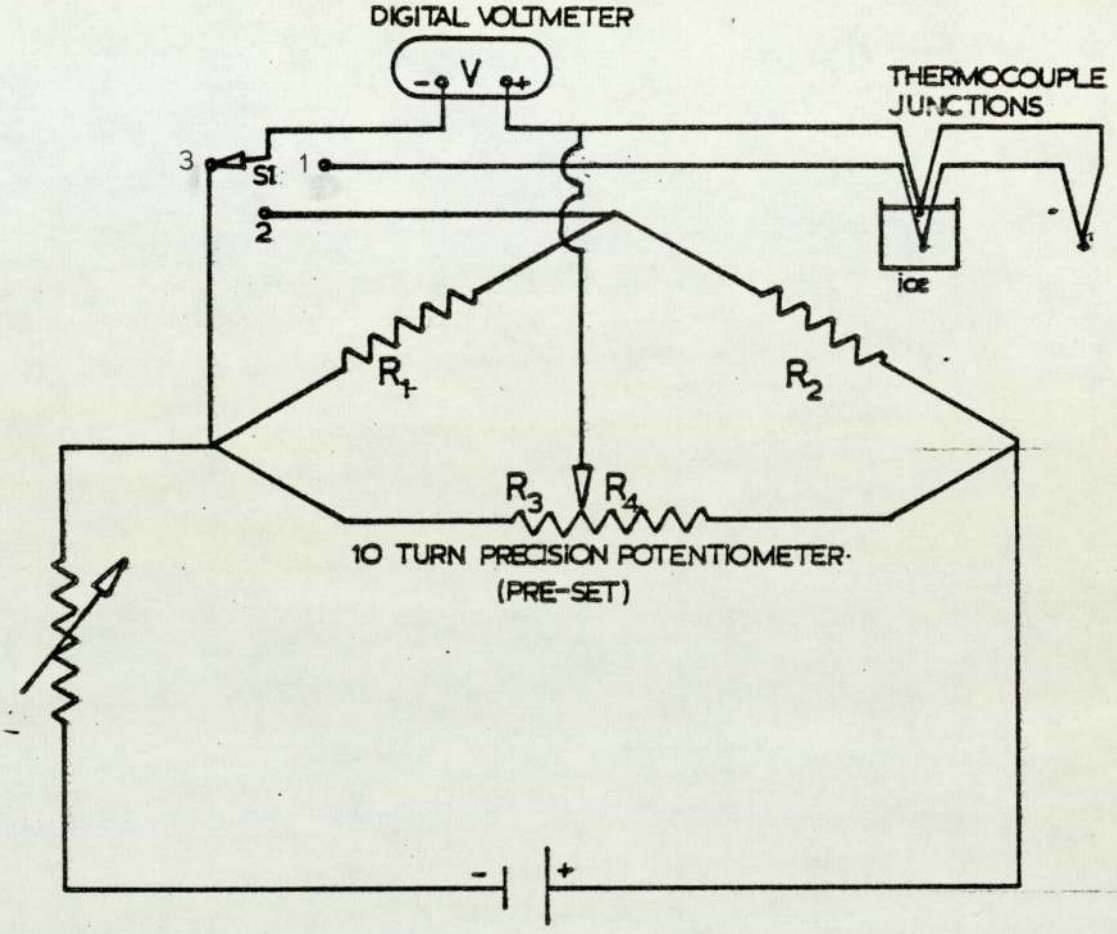

CALIBRATION ANEMOMETER

CIRCUIT DIAGRAM

SWITCH POSITIONS S1: 1 temperature reading (air)
2 temperature reading (wire)
3 velocity reading

FIGURE A1.4

CONSTRUCTION OF THE CALIBRATION ANEMOMETER HEAD

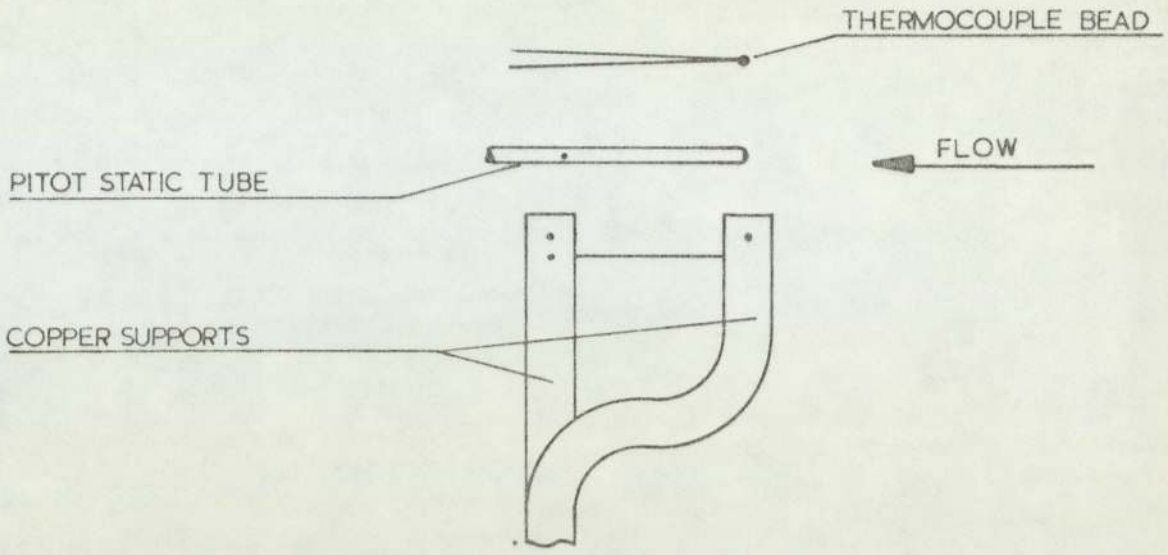

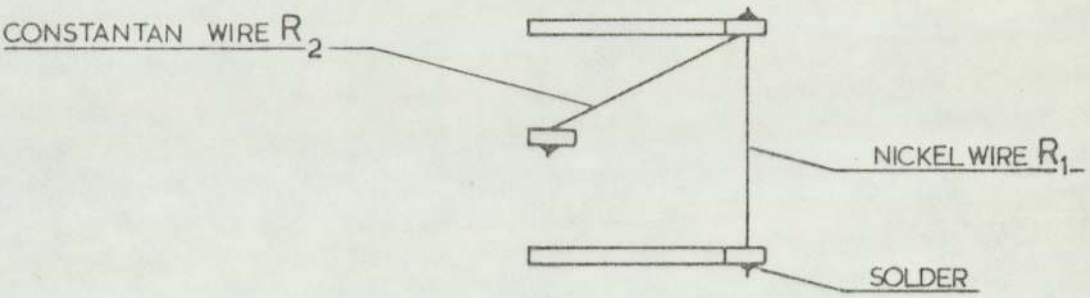

FIGURE A1.5

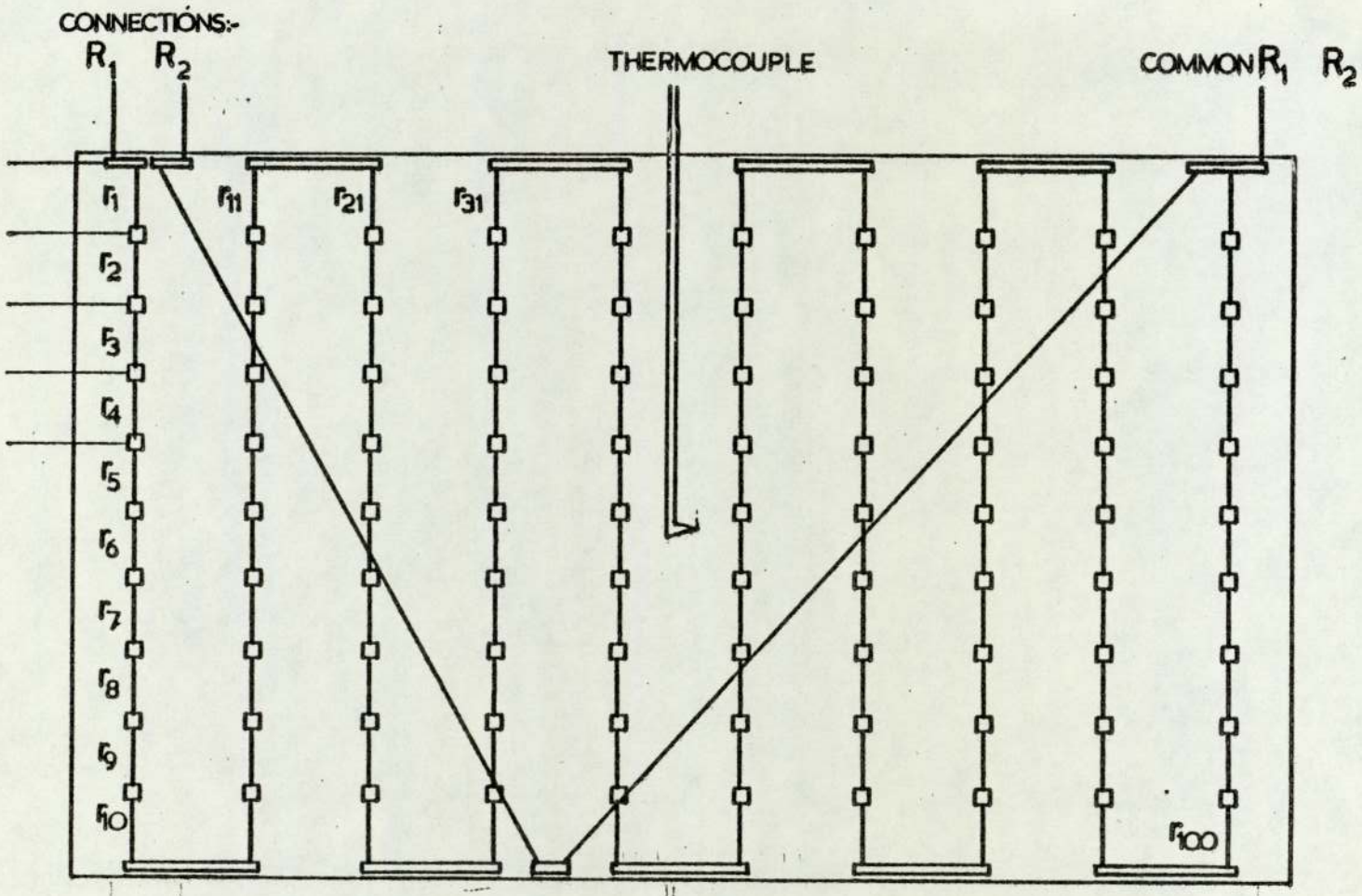

LAYOUT OF A SUGGESTED 100 ELEMENT ANEMOMETER FOR THE MEASUREMENT OF VELOCITY AND VELOCITY DISTRIBUTION.

FIGURE A1.6

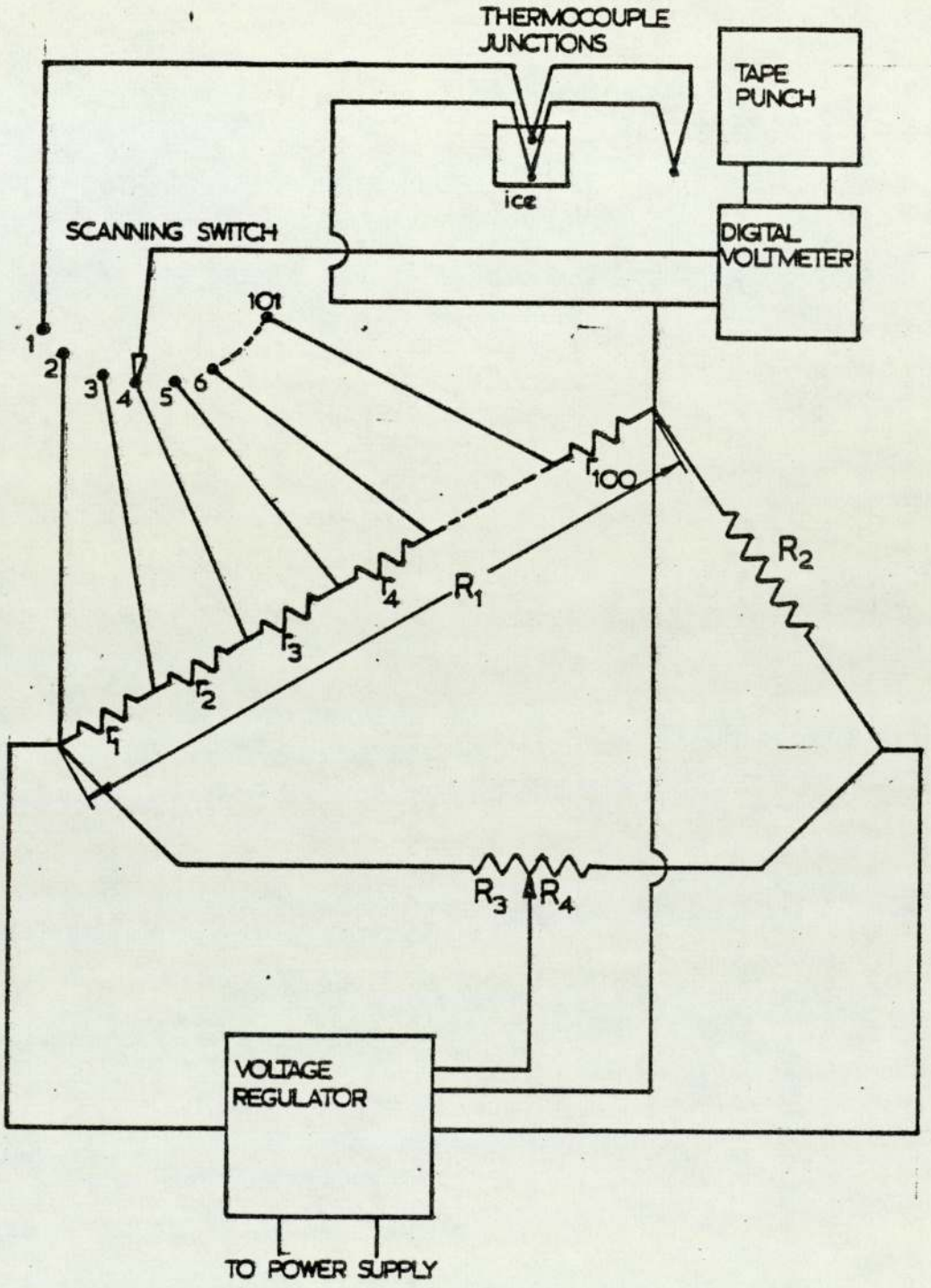

CIRCUIT DIAGRAM OF A SUGGESTED 100 ELEMENT HOT WIRE ANEMOMETER FOR THE MEASUREMENT OF VELOCITY AND VELOCITY DISTRIBUTION

SCANNING SWITCH POSITIONS:

1	temperature reading	
2	R_1	voltage across:—
3	$R_1 - r_1$	
100	$R_1 - [r_1 + r_2 + r_3 + \cdots + r_{99}]$	

PLATE A1.1

THE ANEMOMETER MOUNTED ON THE CONDENSER

IN POSITION IN THE CAR WITH THE BONNET REMOVED


GKV 634N

PLATE A1.2

THE CALIBRATION ANEMOMETER IN POSITION IN THE DUCT

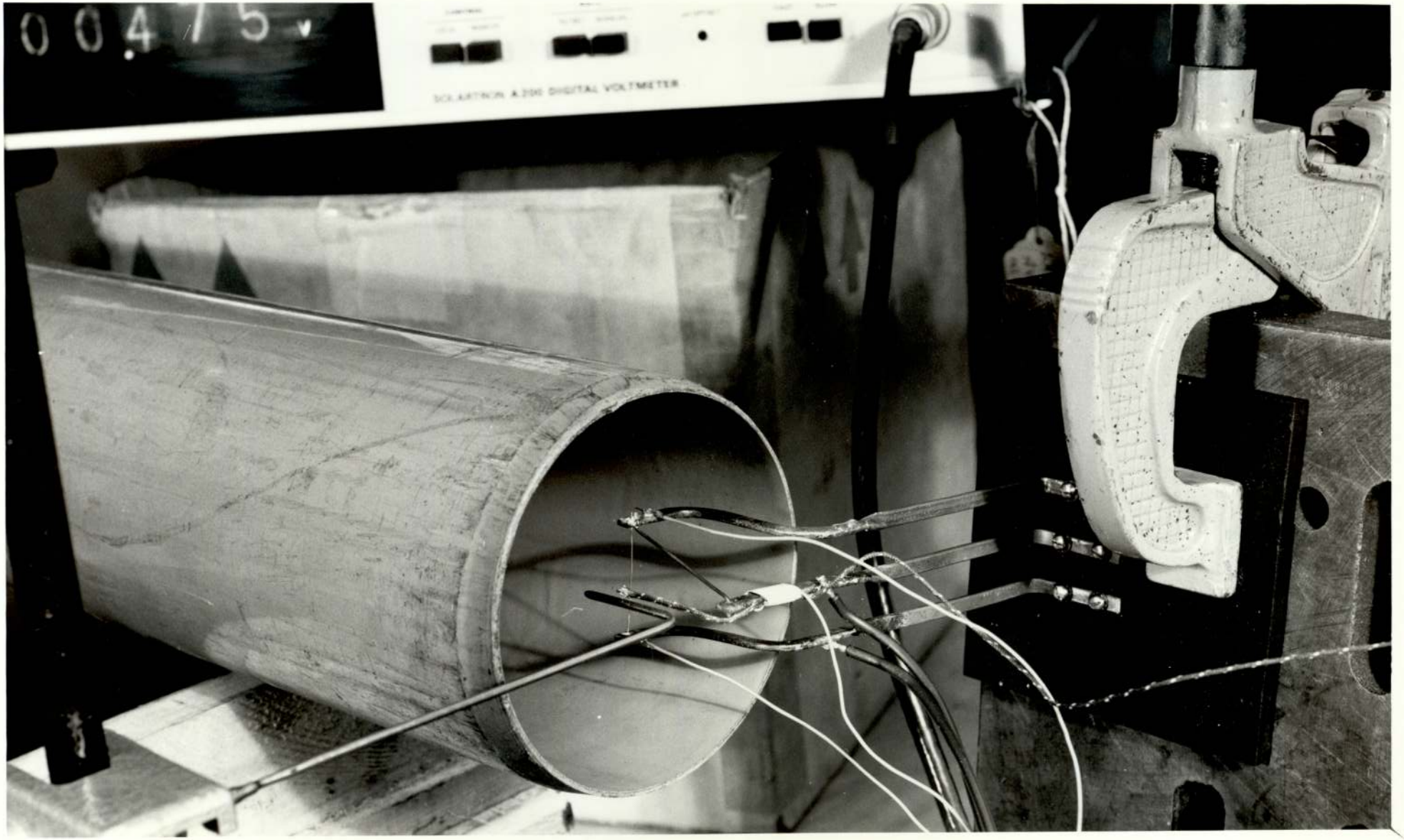
0 0 4 / 5 v
SOLARTRON A 200 DIGITAL VOLTMETER

PLATE A1.3

THE ARRANGEMENT OF THE APPARATUS USED FOR CALIBRATION

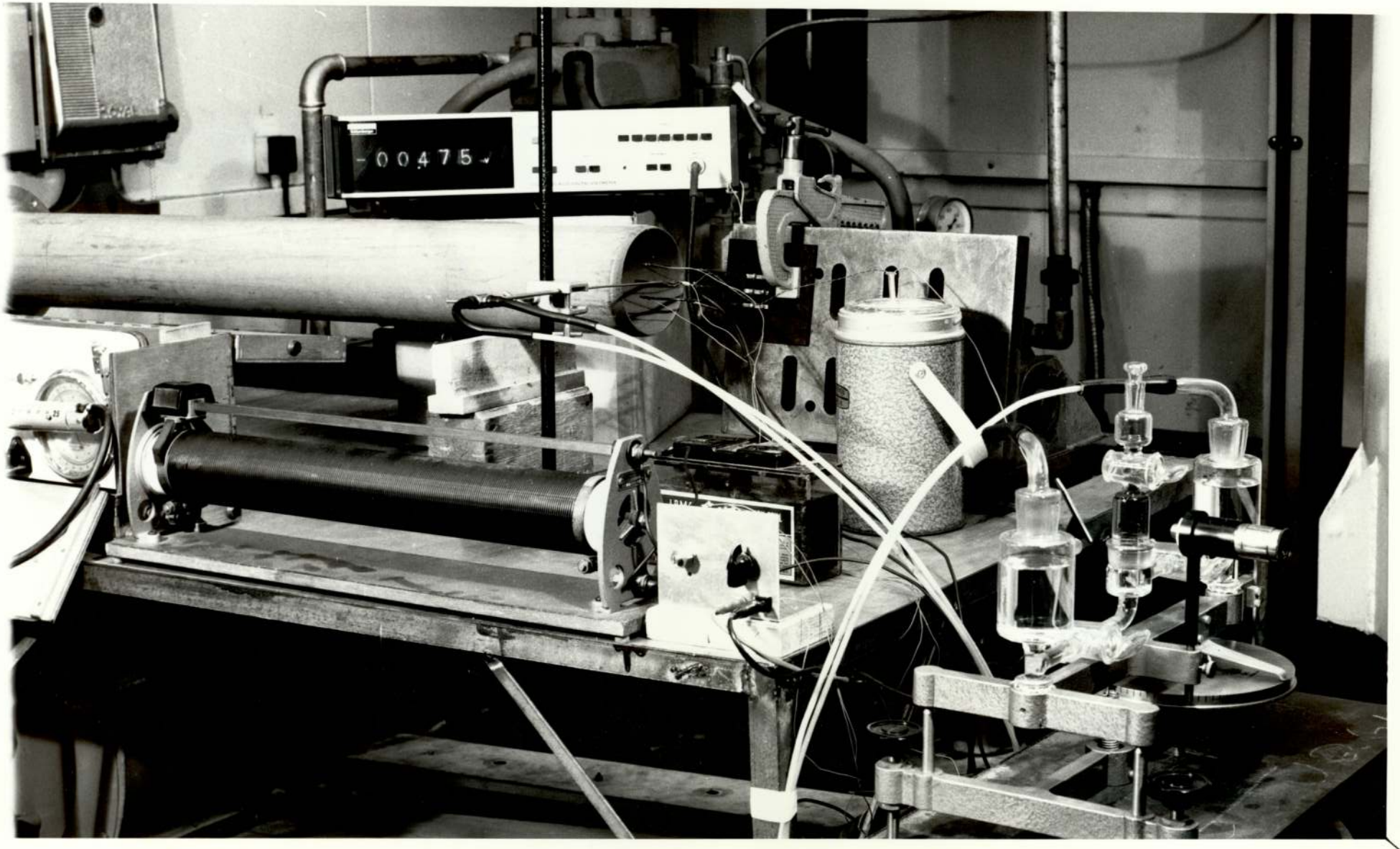
00475

GRAPH A1.1

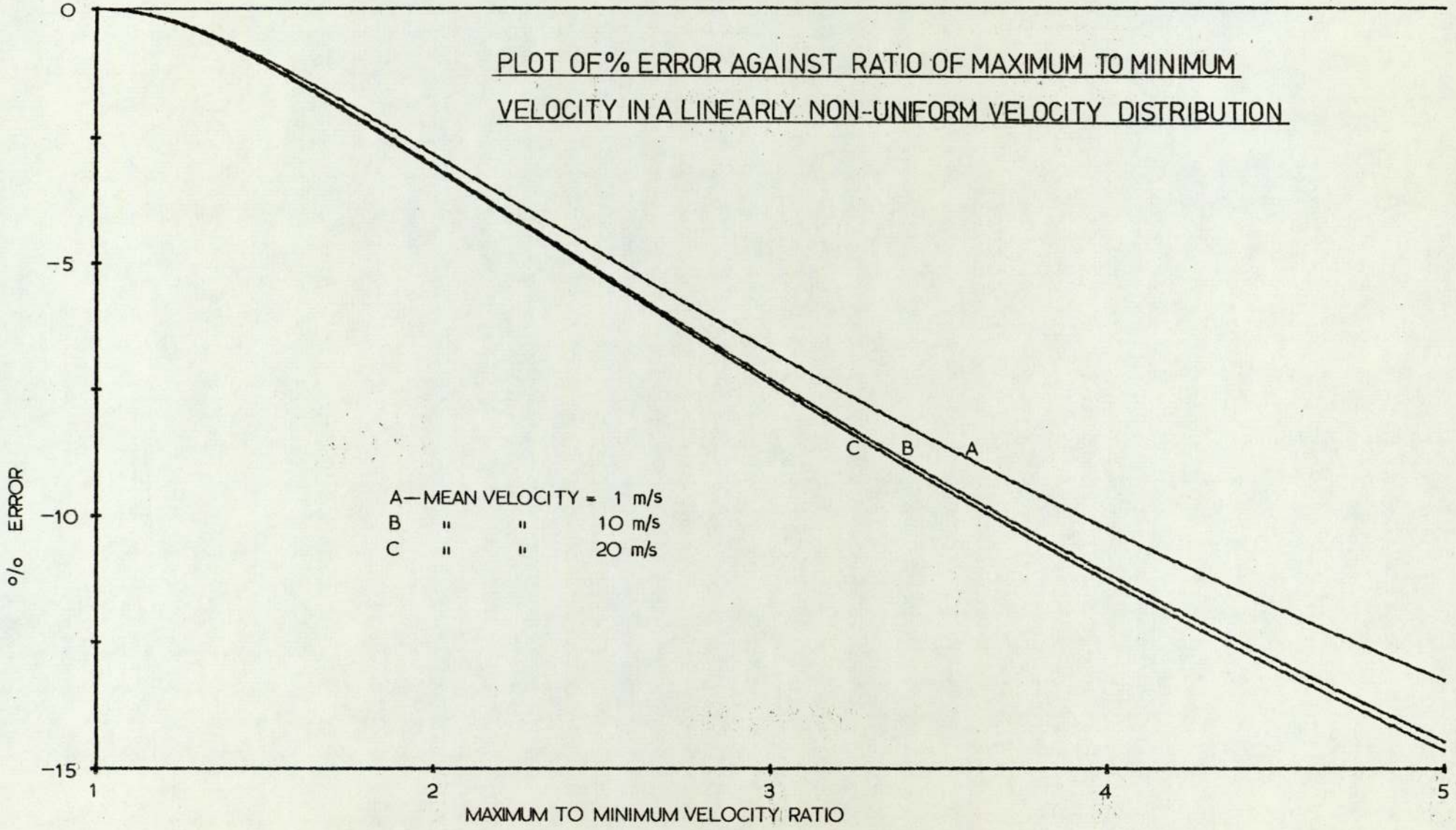
PLOT OF % ERROR AGAINST RATIO OF MAXIMUM TO MINIMUM
VELOCITY IN A LINEARLY NON-UNIFORM VELOCITY DISTRIBUTION
0
-5
-10
-15
% ERROR
1
2
3
4
5
MAXIMUM TO MINIMUM VELOCITY RATIO
A
B
C
A—MEAN VELOCITY = 1 m/s
B " " 10 m/s
C " " 20 m/s

GRAPH A1,2

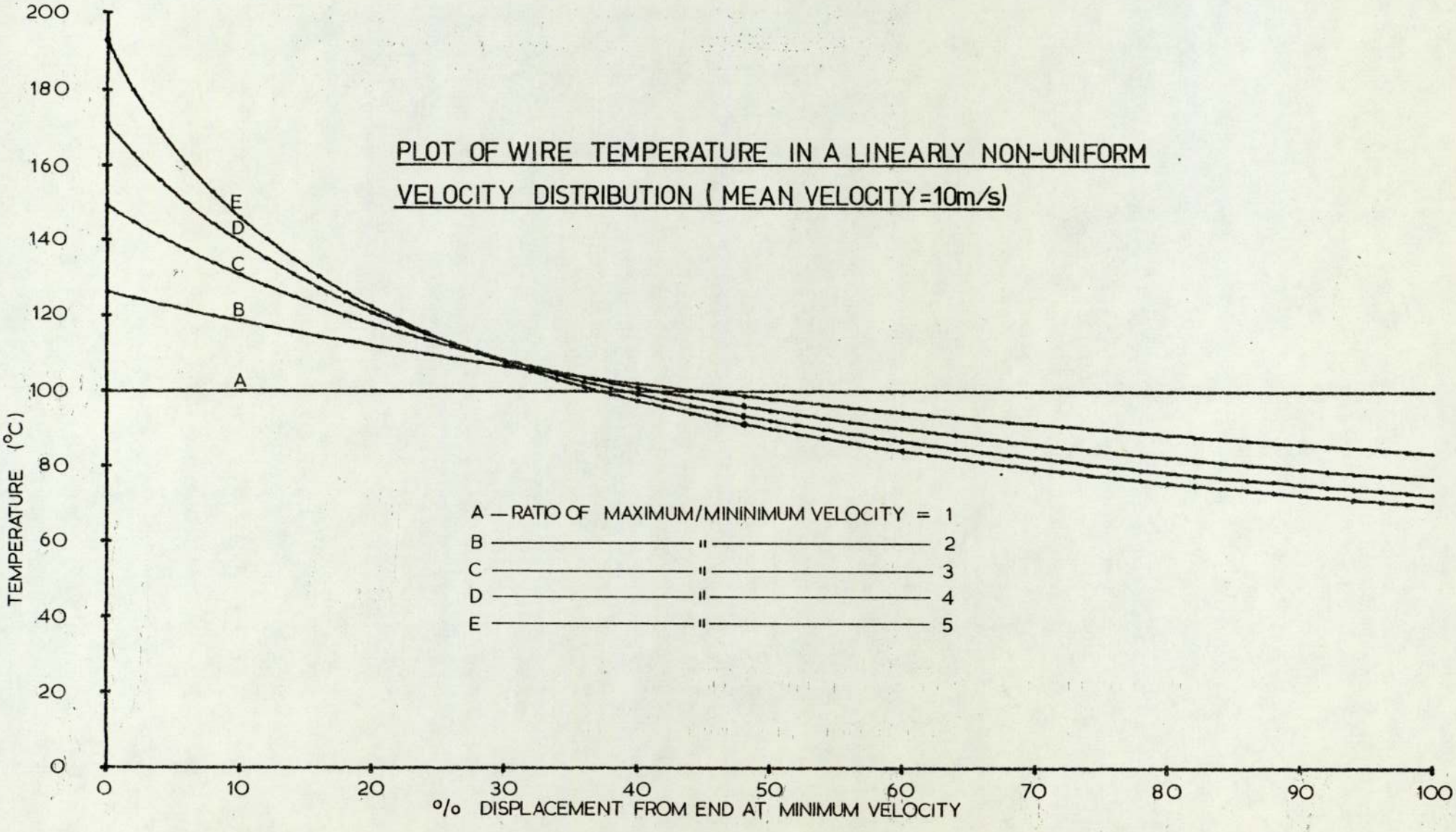
PLOT OF WIRE TEMPERATURE IN A LINEARLY NON-UNIFORM VELOCITY DISTRIBUTION (MEAN VELOCITY=10m/s)
TEMPERATURE (°C)
200
180
160
140
120
100
80
60
40
20
0
E
D
C
B
A
0
10
20
30
40
50
60
70
80
90
100
% DISPLACEMENT FROM END AT MINIMUM VELOCITY
A — RATIO OF MAXIMUM/MININIMUM VELOCITY = 1
B — " — 2
C — " — 3
D — " — 4
E — " — 5

GRAPH A1.3

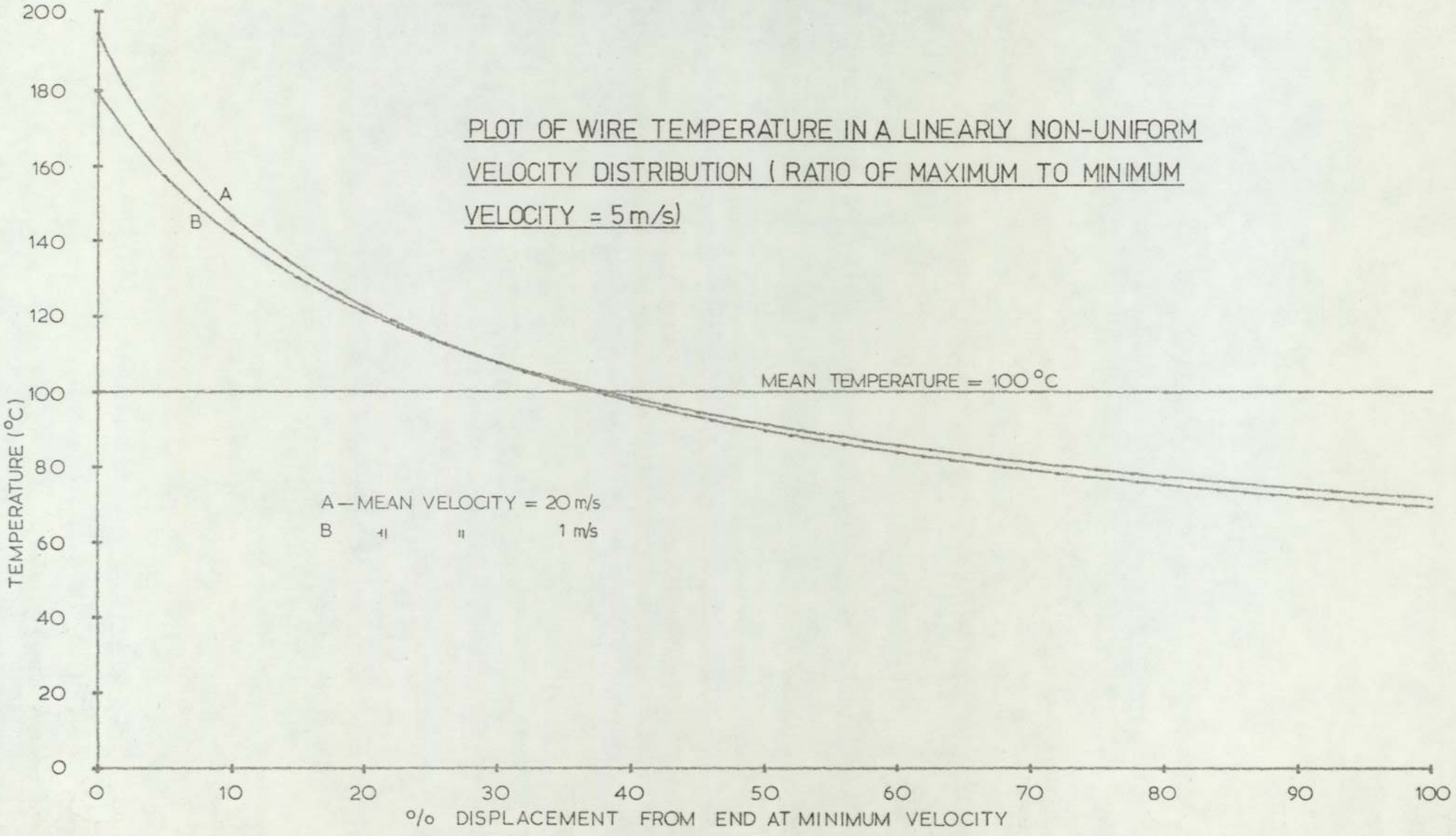
PLOT OF WIRE TEMPERATURE IN A LINEARLY NON-UNIFORM VELOCITY DISTRIBUTION (RATIO OF MAXIMUM TO MINIMUM VELOCITY = 5 m/s)
A
B
MEAN TEMPERATURE = 100 °C
A — MEAN VELOCITY = 20 m/s
B " " 1 m/s
TEMPERATURE (°C)
200
180
160
140
120
100
80
60
40
20
0
0
10
20
30
40
50
60
70
80
90
100
% DISPLACEMENT FROM END AT MINIMUM VELOCITY

GRAPH A1.4

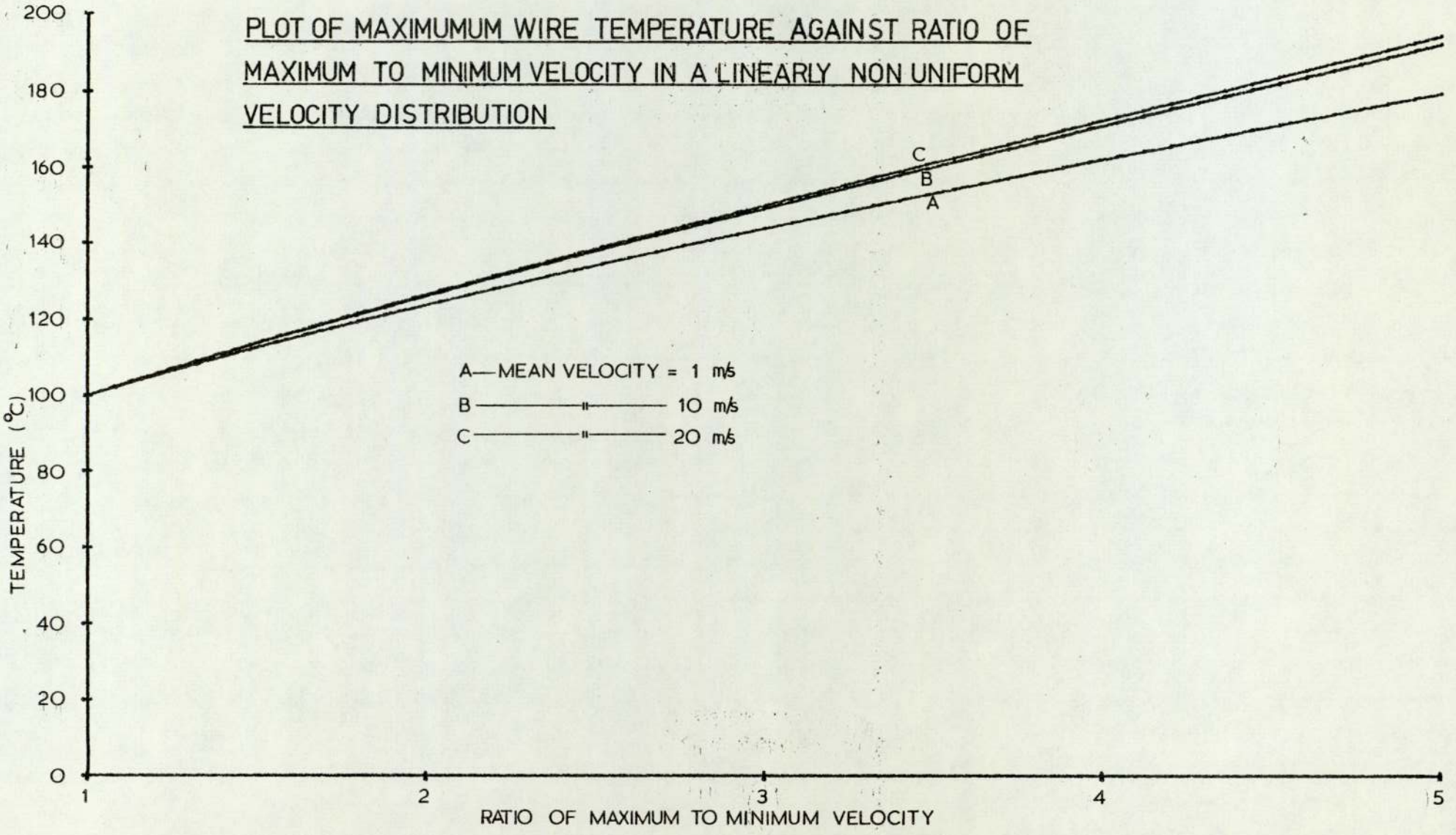
PLOT OF MAXIMUMUM WIRE TEMPERATURE AGAINST RATIO OF MAXIMUM TO MINIMUM VELOCITY IN A LINEARLY NON UNIFORM VELOCITY DISTRIBUTION
TEMPERATURE (°C)
200
180
160
140
120
100
80
60
40
20
0
1
2
3
4
5
RATIO OF MAXIMUM TO MINIMUM VELOCITY
A
B
C
A—MEAN VELOCITY = 1 m/s
B——||——10 m/s
C——||——20 m/s

GRAPH A1.5

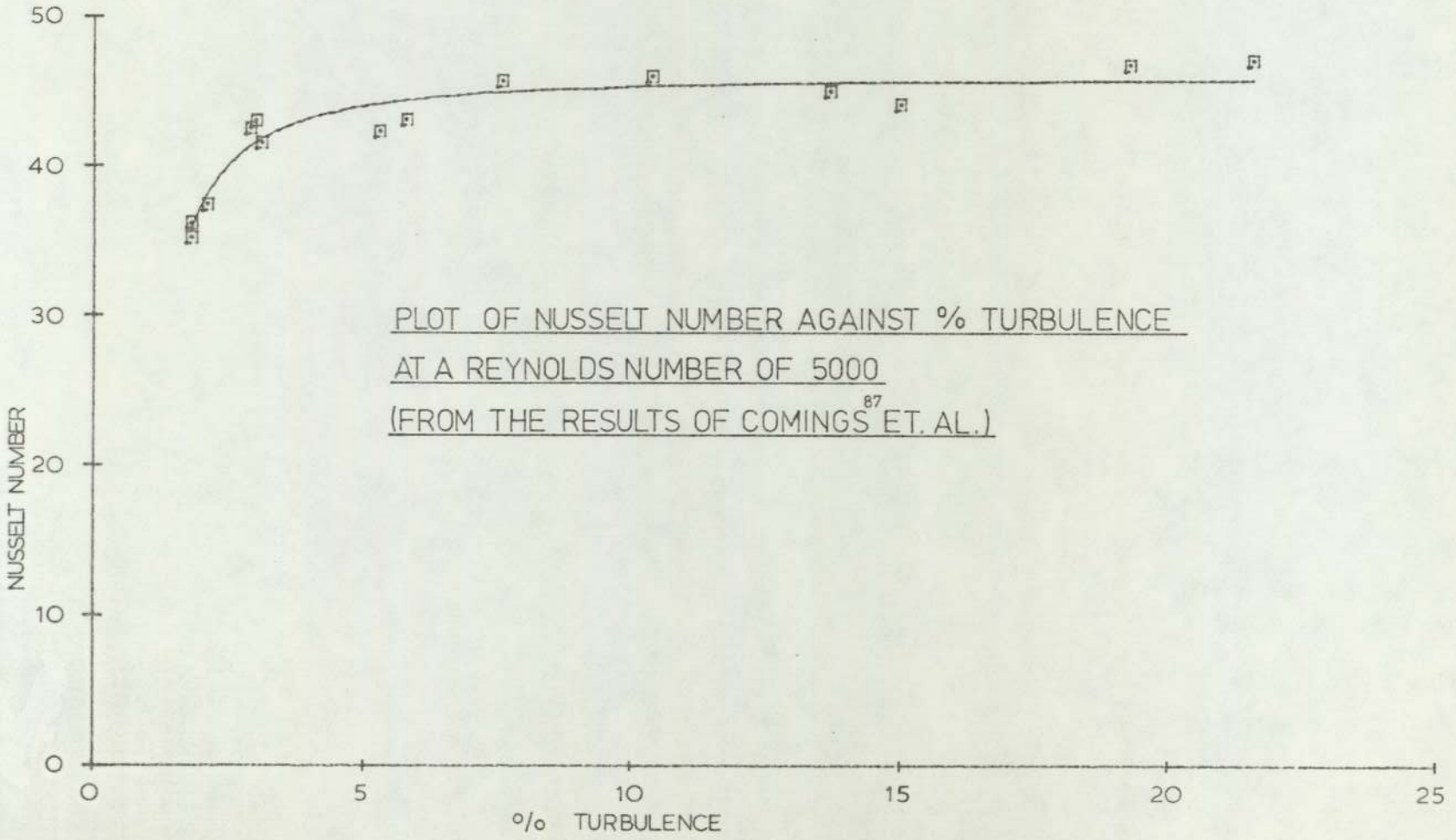

PLOT OF NUSSELT NUMBER AGAINST % TURBULENCE
AT A REYNOLDS NUMBER OF 5000
(FROM THE RESULTS OF COMINGS[87] ET. AL.)

GRAPH A1.6

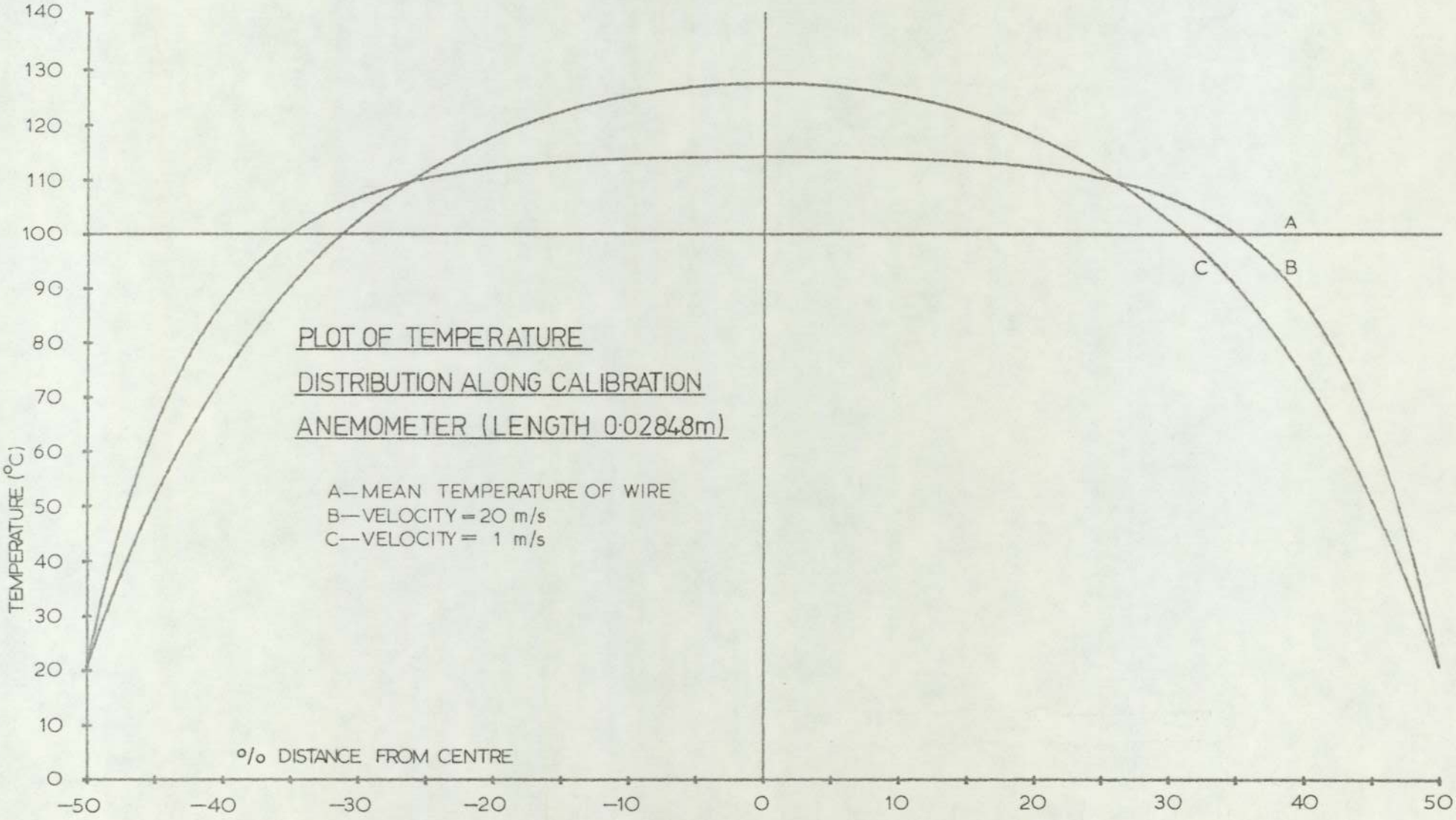
PLOT OF TEMPERATURE
DISTRIBUTION ALONG CALIBRATION
ANEMOMETER (LENGTH 0·02848m)
A—MEAN TEMPERATURE OF WIRE
B—VELOCITY = 20 m/s
C—VELOCITY = 1 m/s
TEMPERATURE (°C)
% DISTANCE FROM CENTRE
A
B
C
140
130
120
110
100
90
80
70
60
50
40
30
20
10
0
−50
−40
−30
−20
−10
0
10
20
30
40
50

GRAPH A1.7

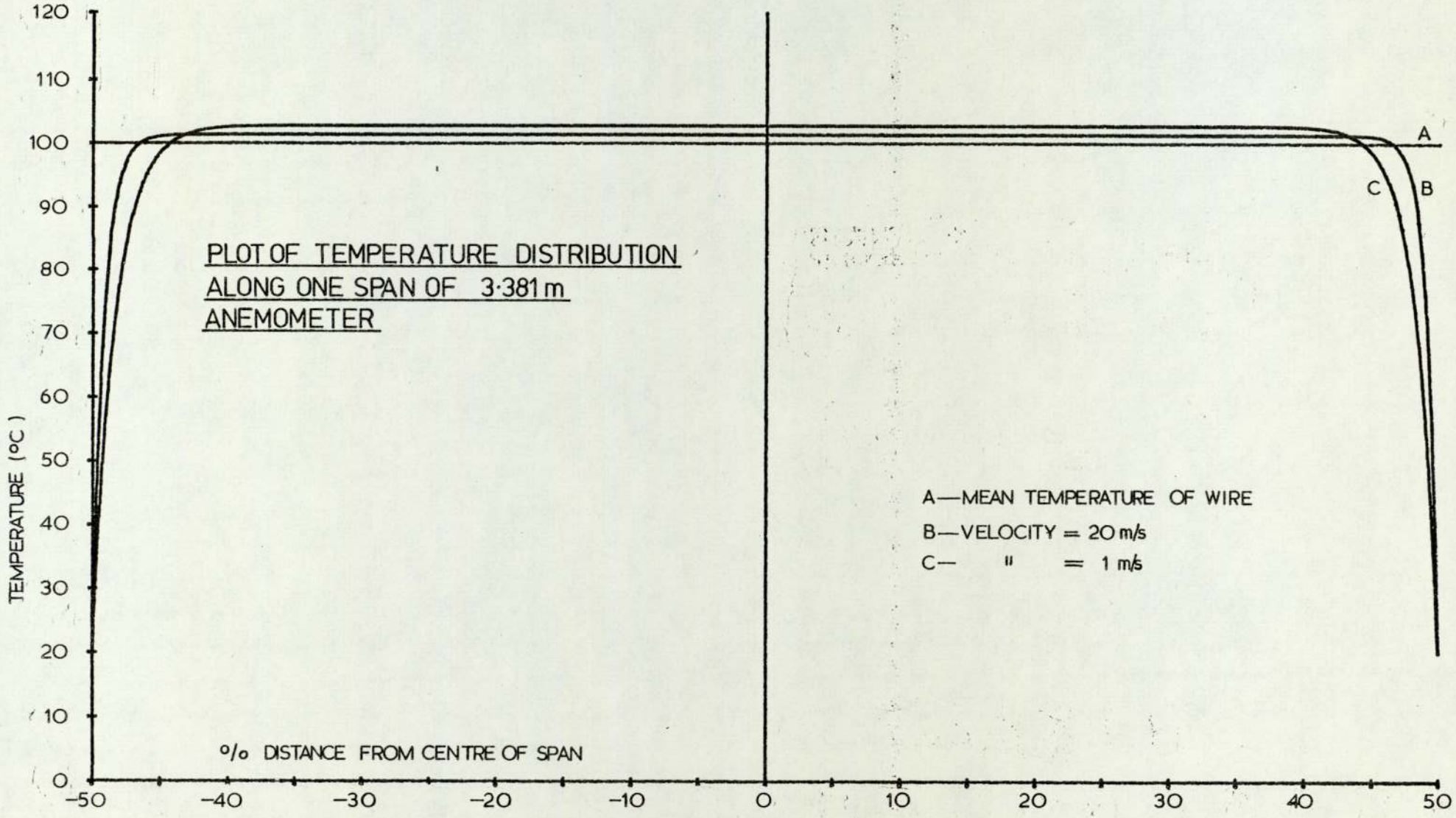
PLOT OF TEMPERATURE DISTRIBUTION
ALONG ONE SPAN OF 3·381 m
ANEMOMETER
TEMPERATURE (°C)
120
110
100
90
80
70
60
50
40
30
20
10
0
-50
-40
-30
-20
-10
0
10
20
30
40
50
% DISTANCE FROM CENTRE OF SPAN
A
B
C
A—MEAN TEMPERATURE OF WIRE
B—VELOCITY = 20 m/s
C— " = 1 m/s

GRAPH A1.8

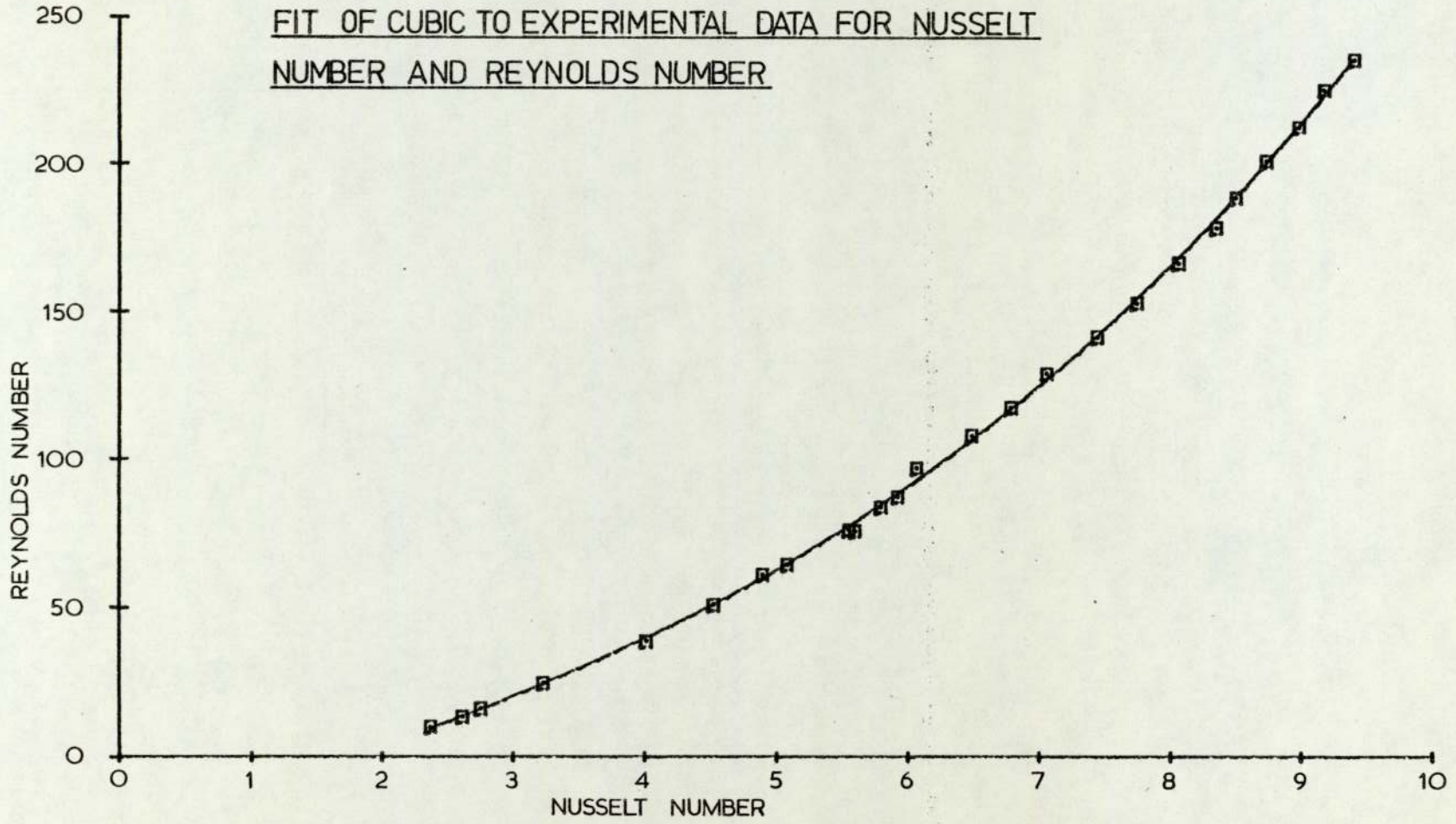
FIT OF CUBIC TO EXPERIMENTAL DATA FOR NUSSELT NUMBER AND REYNOLDS NUMBER
REYNOLDS NUMBER
250
200
150
100
50
0
0
1
2
3
4
5
6
7
8
9
10
NUSSELT NUMBER

GRAPH A1.9

PLOT OF EXPERIMENTAL DATA OF NUSSELT NUMBER AND REYNOLDS NUMBER FOR COMPARISON WITH THE WORK OF KING[82] (1914)

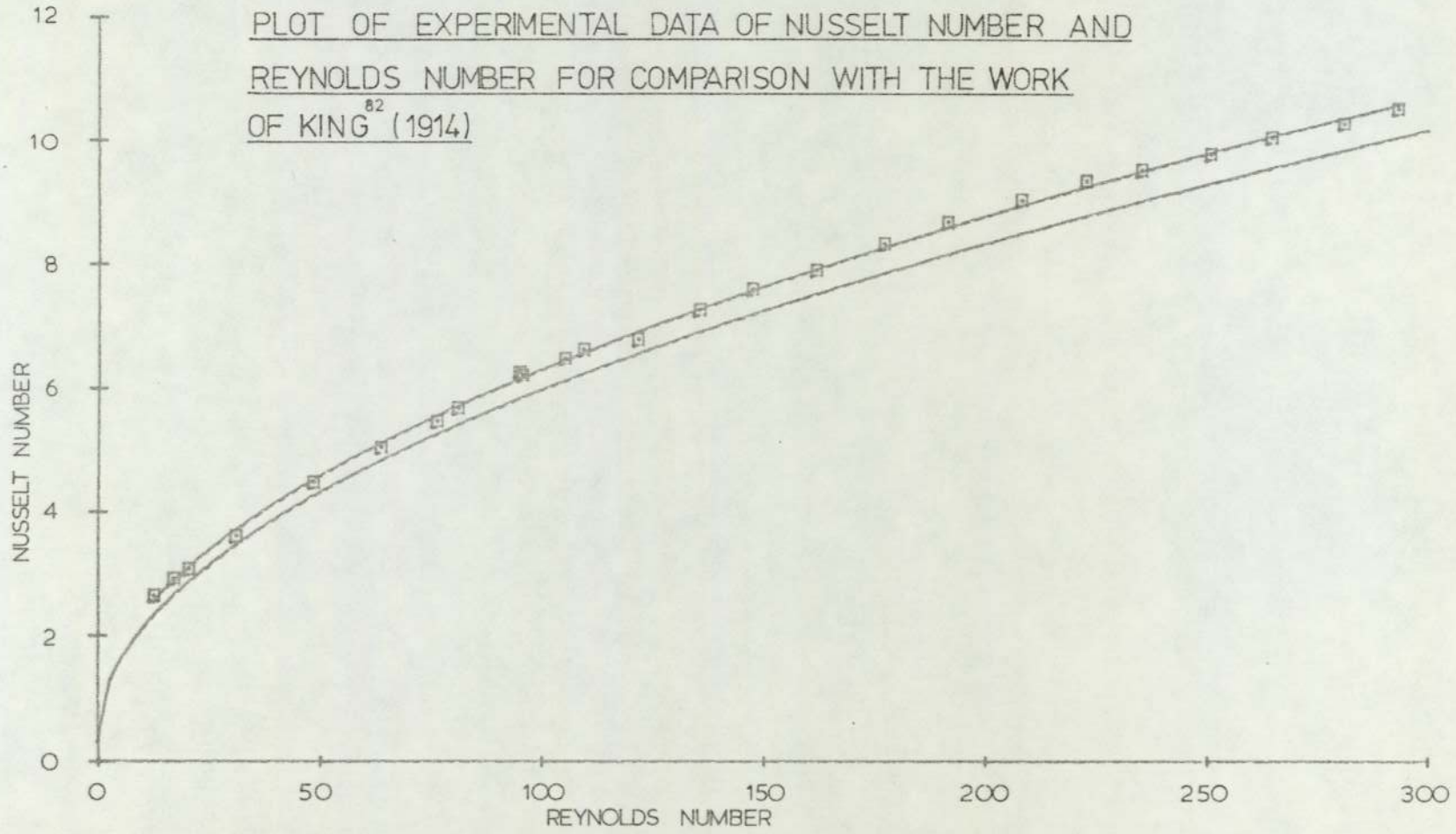

GRAPH A1.10

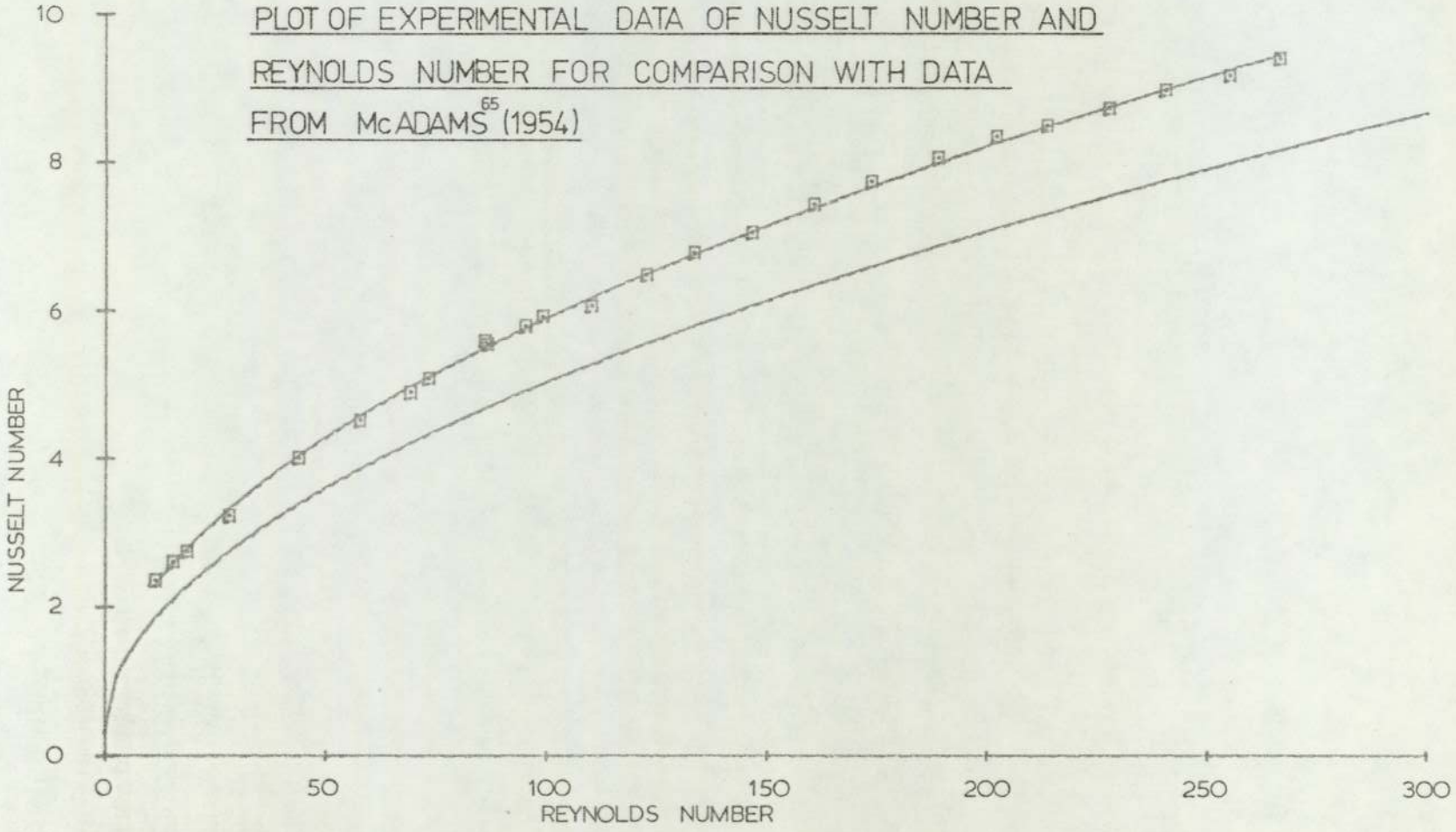
PLOT OF EXPERIMENTAL DATA OF NUSSELT NUMBER AND
REYNOLDS NUMBER FOR COMPARISON WITH DATA
FROM McADAMS[65] (1954)
NUSSELT NUMBER
0
2
4
6
8
10
0
50
100
150
200
250
300
REYNOLDS NUMBER

GRAPH A1.11

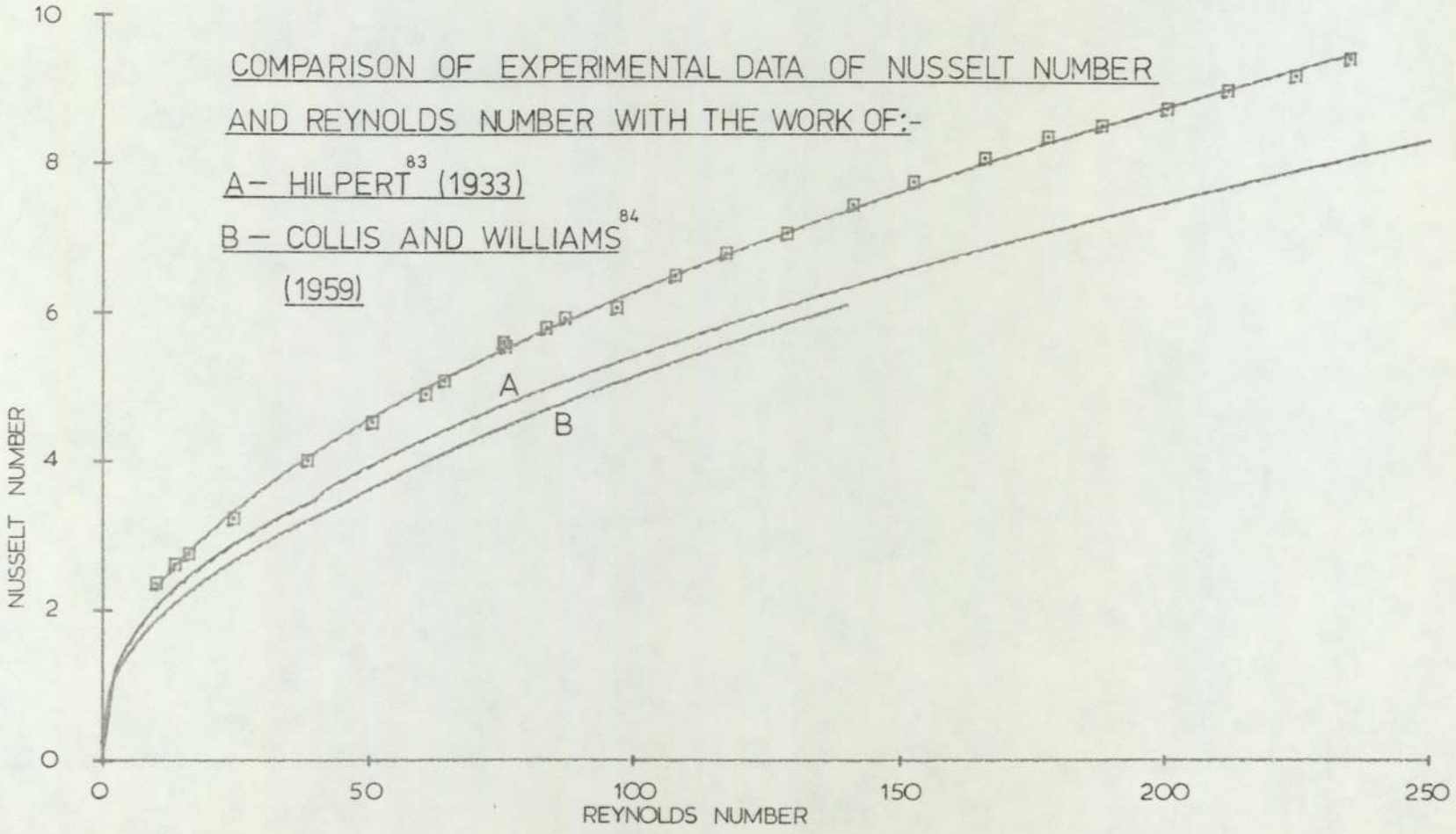
COMPARISON OF EXPERIMENTAL DATA OF NUSSELT NUMBER
AND REYNOLDS NUMBER WITH THE WORK OF:-
A- HILPERT[83] (1933)
B- COLLIS AND WILLIAMS[84]
(1959)
A
B
NUSSELT NUMBER
REYNOLDS NUMBER
0
2
4
6
8
10
0
50
100
150
200
250

EXPERIMENTAL DATA FOR CALIBRATION

PT	TEMP(C)	VOLTAGE(v)	HEAD(mmH2O)	PATTMOS(mmHg)
1	20.8	0.1840	0.0424	750.50
2	20.3	0.1922	0.0787	724.30
3	20.1	0.1967	0.1130	724.30
4	20.6	0.2100	0.2530	750.50
5	20.8	0.2305	0.6220	750.50
6	20.8	0.2430	1.0800	750.50
7	20.8	0.2518	1.5500	750.50
8	19.8	0.2575	1.7970	724.30
9	19.6	0.2682	2.4110	750.50
10	19.8	0.2690	2.4700	724.30
11	19.6	0.2735	2.9190	750.50
12	19.8	0.2760	3.2790	724.30
13	19.8	0.2790	3.9100	750.50
14	19.6	0.2880	5.0190	724.30
15	19.6	0.2940	5.9400	724.30
16	19.6	0.2993	7.1590	724.30
17	19.8	0.3063	8.6000	724.30
18	19.8	0.3120	10.0500	724.30
19	20.1	0.3173	11.9100	724.30
20	20.6	0.3216	13.7000	724.30
21	20.6	0.3243	15.3000	724.30
22	20.6	0.3284	17.3800	724.30
23	21.1	0.3317	19.4500	724.30
24	20.8	0.3356	21.8500	724.30
25	21.3	0.3385	23.9000	724.30

TABLE A1.1

TABULATED VALUES OF BIOT NO. (x1000) AGAINST NON-DIMENSIONAL POWER DISSIPATION (z), FOR VARIOUS RATIOS OF WIRE LENGTH TO DIAMETER

	l/d															
z	100	200	300	400	500	600	700	800	900	1000	1100	1200	1300	1400	1500	INF.
0.0030	0.297	0.403	0.430	0.443	0.450	0.455	0.458	0.461	0.463	0.464	0.465	0.466	0.467	0.468	0.469	0.477
0.0035	0.368	0.478	0.506	0.520	0.528	0.533	0.536	0.539	0.541	0.543	0.544	0.545	0.546	0.547	0.547	0.557
0.0040	0.440	0.553	0.583	0.597	0.605	0.611	0.614	0.617	0.619	0.621	0.623	0.624	0.625	0.626	0.626	0.637
0.0045	0.512	0.628	0.659	0.674	0.683	0.689	0.693	0.696	0.698	0.700	0.701	0.703	0.704	0.705	0.705	0.716
0.0050	0.584	0.703	0.736	0.752	0.761	0.767	0.771	0.774	0.777	0.779	0.780	0.781	0.783	0.784	0.784	0.796
0.0055	0.657	0.779	0.813	0.829	0.839	0.845	0.849	0.853	0.855	0.857	0.859	0.860	0.862	0.863	0.863	0.875
0.0060	0.729	0.854	0.890	0.907	0.917	0.923	0.928	0.931	0.934	0.936	0.938	0.939	0.940	0.942	0.942	0.955
0.0065	0.802	0.930	0.967	0.984	0.995	1.002	1.006	1.010	1.013	1.015	1.017	1.018	1.019	1.021	1.021	1.035
0.0070	0.875	1.006	1.044	1.062	1.073	1.080	1.085	1.089	1.091	1.094	1.096	1.097	1.098	1.100	1.101	1.114
0.0075	0.948	1.082	1.121	1.140	1.151	1.158	1.163	1.167	1.170	1.173	1.175	1.176	1.178	1.179	1.180	1.194
0.0080	1.022	1.159	1.199	1.218	1.229	1.237	1.242	1.246	1.249	1.252	1.254	1.255	1.257	1.258	1.259	1.273
0.0085	1.095	1.235	1.276	1.296	1.308	1.315	1.321	1.325	1.328	1.330	1.332	1.334	1.336	1.337	1.338	1.353
0.0090	1.169	1.311	1.353	1.374	1.386	1.394	1.399	1.404	1.407	1.409	1.411	1.413	1.415	1.416	1.417	1.432
0.0095	1.243	1.388	1.431	1.452	1.464	1.472	1.478	1.482	1.486	1.488	1.490	1.492	1.494	1.495	1.496	1.512
0.0100	1.317	1.464	1.508	1.530	1.542	1.551	1.557	1.561	1.565	1.567	1.570	1.571	1.573	1.574	1.575	1.592
0.0105	1.391	1.541	1.586	1.608	1.621	1.629	1.635	1.640	1.643	1.646	1.649	1.650	1.652	1.653	1.655	1.671
0.0110	1.465	1.618	1.664	1.686	1.699	1.708	1.714	1.719	1.722	1.725	1.728	1.730	1.731	1.733	1.734	1.751
0.0115	1.539	1.694	1.741	1.764	1.778	1.787	1.793	1.798	1.801	1.804	1.807	1.809	1.810	1.812	1.813	1.830
0.0120	1.613	1.771	1.819	1.842	1.856	1.865	1.872	1.877	1.880	1.883	1.886	1.888	1.889	1.891	1.892	1.910
0.0125	1.688	1.848	1.897	1.921	1.935	1.944	1.951	1.955	1.959	1.962	1.965	1.967	1.969	1.970	1.971	1.989
0.0130	1.762	1.925	1.975	1.999	2.013	2.023	2.029	2.034	2.038	2.041	2.044	2.046	2.048	2.049	2.051	2.069
0.0135	1.837	2.002	2.053	2.077	2.092	2.101	2.108	2.113	2.117	2.120	2.123	2.125	2.127	2.129	2.130	2.149
0.0140	1.911	2.079	2.131	2.156	2.170	2.180	2.187	2.192	2.196	2.200	2.202	2.204	2.206	2.208	2.209	2.228
0.0145	1.986	2.156	2.208	2.234	2.249	2.259	2.266	2.271	2.275	2.279	2.281	2.283	2.285	2.287	2.288	2.308
0.0150	2.061	2.233	2.286	2.312	2.327	2.338	2.345	2.350	2.354	2.358	2.360	2.363	2.365	2.366	2.368	2.387

NU BETA=0.2708

TABLE A1.2

CALCULATION OF REYNOLDS NO & NUSSELT NO:-FOR CALIBRATION

PT	REYNOLDS NO	NUSSELT NO	U(m/s)	H(W/m^2K)
1	10.0787	2.3723	0.8367	296.6606
2	13.4949	2.6158	1.1593	326.8948
3	16.1730	2.7560	1.3887	344.3264
4	24.6237	3.2323	2.0431	404.1025
5	38.6027	4.0116	3.2047	501.6565
6	50.8668	4.5192	4.2228	565.1395
7	60.9381	4.8937	5.0589	611.9711
8	64.5106	5.0811	5.5349	634.5822
9	76.0750	5.5478	6.2960	692.6815
10	75.6320	5.5979	6.4891	699.1267
11	83.7068	5.7927	6.9276	723.2620
12	87.1421	5.9243	7.4767	739.8798
13	96.8638	6.0668	8.0207	757.6852
14	107.8291	6.4888	9.2468	810.1693
15	117.3061	6.7879	10.0595	847.5217
16	128.7815	7.0576	11.0436	881.1941
17	141.1258	7.4393	12.1084	929.0923
18	152.5598	7.7429	13.0894	967.0153
19	166.0381	8.0593	14.2569	1006.9203
20	178.0069	8.3470	15.3044	1043.5416
21	188.1145	8.4990	16.1734	1062.5442
22	200.4941	8.7324	17.2377	1091.7201
23	212.0127	8.9762	18.2516	1122.9296
24	224.7670	9.1716	19.3346	1146.9300
25	234.9803	9.3991	20.2393	1176.1406

TABLE A1.3

TABLE A1.4

TABULATED HOT WIRE ANEMOMETER CALIBRATION EQUATIONS FOR COMPARISON

Published Equations			Experimental Data (calculated with properties as published Equations)		% Deviation from Experimental Data	
Author	Range of Re	Equation (at temperatures used in Experimental Data)	Range of Re	Fitted Equation	At Bottom of Range *(1)	At Top of Range *(2)
King[82]	-	$Nu = .318 + .567\ Re^{0.5}$	12.6 - 293	$Nu = .624 + .521\ Re^{.519}$	-9.2	-5.0
McAdams[65]	0.1 - 1000	$Nu = .32 + .43\ Re^{.52}$	11 - 266	$Nu = .573 + .484\ Re^{.521}$	-19.7	-13.6
Hilpert[83]	4 - 40	$Nu = .840\ Re^{.385}$	10 - 235	$Nu = .550 + .527\ Re^{.518}$	-10.9	-15.5
"	40 - 400	$Nu = .633\ Re^{.466}$	"	"	-14.1	-14.8
Collis[84] & Williams	.01 - 44	$Nu = .245 + .572\ Re^{.45}$	"	"	-18.8	-21.2
"	44 - 140	$Nu = .491\ Re^{.51}$	"	"	-21.2	-17.1

* The Reynolds number is in each case at the extremity of the published data or the experimental data whichever is the greater in (1) or the least in (2)

APPENDIX A2

EXPERIMENTAL AND CALCULATED DATA RELATING TO THE HEAT REJECTION SYSTEM

GRAPH A2.1

PLOT OF CALIBRATION OF JAGUAR'S VANE ANEMOMETER AGAINST A PITOT STATIC MEASUREMENT

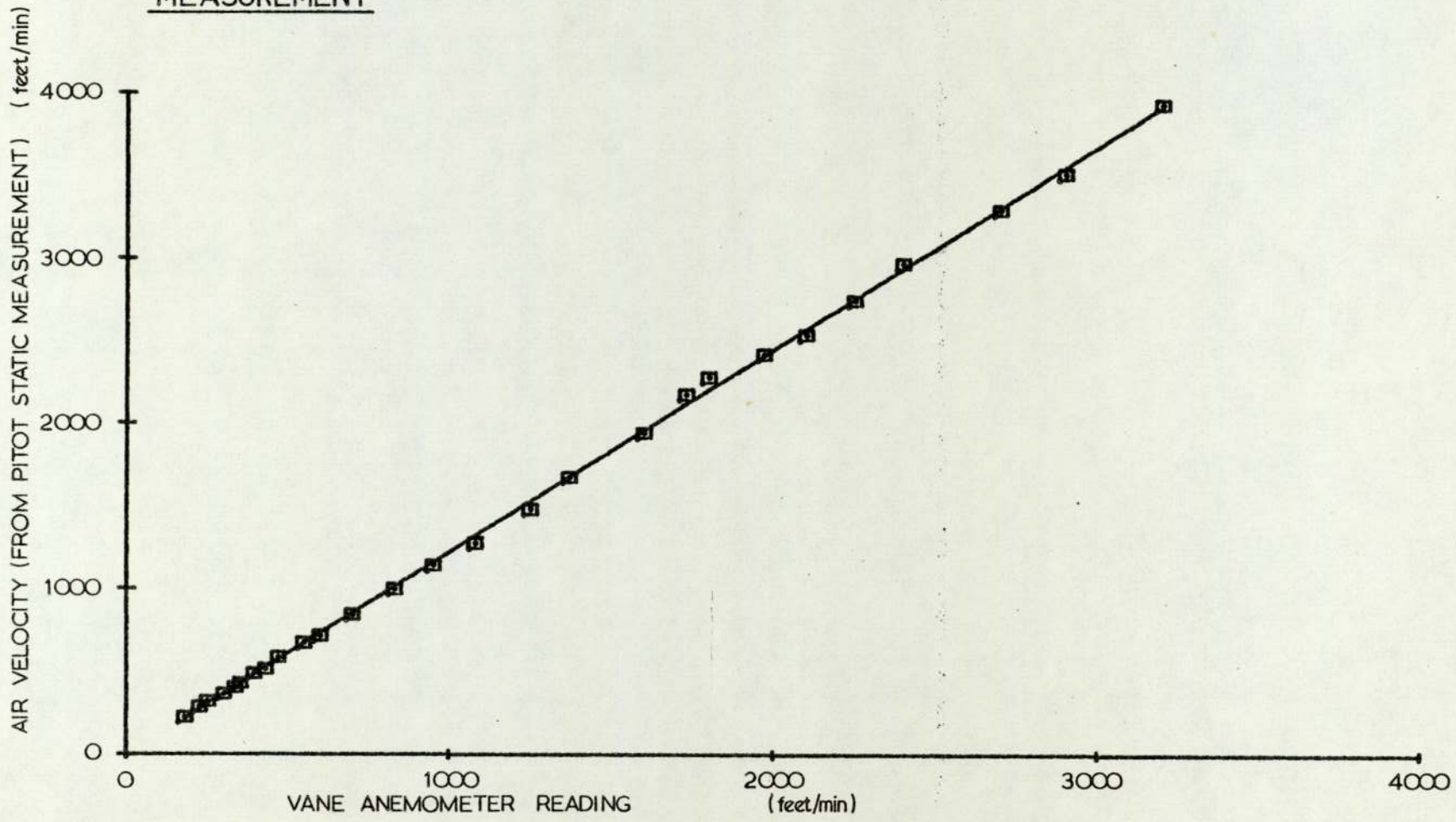

TABLE A2.1

DATA FOR CALCULATION OF VELOCITY

PT	GEAR	VOLTAGE	TEMPERATURE deg.C	IGNITION COUNT	PATTMOS mm(Hg)
1	0	20.67	21.6	286	758.18
2	0	22.26	21.8	377	758.18
3	0	23.85	22.1	514	758.18
4	0	25.14	22.3	636	758.18
5	0	26.18	22.3	741	758.18
6	0	27.24	21.8	876	758.18
7	0	20.67	22.8	303	758.18
8	0	22.14	22.3	390	758.18
9	0	23.80	22.6	518	758.18
10	0	25.13	22.8	690	758.18
11	0	27.08	23.3	871	758.18
12	0	20.82	21.6	310	758.18
13	0	22.40	20.3	407	758.18
14	0	23.48	21.1	502	758.18
15	0	24.97	22.1	633	758.18
16	0	26.16	20.8	750	758.18
17	0	27.12	20.6	879	758.18

N.B. Car Stationary
Viscous Coupling Locked

TABLE A2.2

DATA FOR CALCULATION OF VELOCITY

PT	GEAR	VOLTAGE	TEMPERATURE deg.C	IGNITION COUNT	PATTMOS mm(Hg)
1	3	24.08	9.0	611	754.35
2	2	25.88	8.0	1136	754.35
3	3	26.26	8.2	901	754.35
4	3	27.81	8.7	1073	754.35
5	3	29.44	8.2	1222	754.35
6	3	29.82	9.0	1363	754.35
7	4	30.01	8.7	1095	754.35
8	4	30.72	9.5	1184	754.35
9	4	32.20	8.2	1289	754.35
10	4	32.48	9.0	1408	754.35
11	4	33.10	8.7	1502	754.35
12	4	33.46	8.7	1602	754.35
13	4	33.95	8.7	1728	754.35
14	5	35.07	8.7	1533	754.35
15	5	35.39	8.7	1609	754.35
16	2	25.33	7.7	912	754.35
17	2	26.62	7.7	1120	754.35
18	2	27.30	8.2	1362	754.35
19	2	28.35	7.7	1591	754.35
20	3	28.84	8.2	1202	754.35
21	3	29.72	8.2	1370	754.35
22	3	30.33	0.3	1512	754.35
23	4	31.15	7.7	1206	754.35
24	4	32.16	8.2	1293	754.35
25	4	32.80	8.2	1409	754.35
26	4	32.41	8.0	1512	754.35
27	4	34.47	8.2	1706	754.35
28	4	34.01	8.2	1881	754.35
29	4	35.09	8.5	2200	754.35
30	5	35.55	9.0	1616	754.35
31	2	24.75	8.2	940	754.35
32	2	24.97	7.4	1132	754.35
33	2	26.35	8.0	1377	754.35
34	2	28.05	8.2	1615	754.35
35	2	28.48	8.0	1796	754.35
36	3	29.57	8.0	1360	754.35
37	3	30.12	8.0	1515	754.35
38	3	30.91	7.7	1672	754.35
39	4	31.45	7.7	1294	754.35

N.B. Fan Removed

Cont.

DATA FOR CALCULATION OF VELOCITY (Cont.)

PT	GEAR	VOLTAGE	TEMPERATURE deg.C	IGNITION COUNT	PATTMOS mm(Hg)
40	4	32.30	7.7	1413	754.35
41	4	32.75	8.0	1499	754.35
42	4	33.22	8.0	1651	754.35
43	4	33.75	8.0	1726	754.35
44	4	34.79	8.0	1842	754.35
45	5	35.10	8.2	1604	754.35
46	2	25.04	6.4	962	754.35
47	2	25.57	6.4	1132	754.35
48	2	27.06	6.6	1362	754.35
49	2	27.95	7.1	1590	754.35
50	3	28.49	7.4	1210	754.35
51	3	29.86	7.4	1361	754.35
52	3	30.44	7.4	1522	754.35
53	4	31.53	8.0	1200	754.35
54	4	32.36	8.0	1304	754.35
55	4	32.74	8.0	1399	754.35
56	4	33.34	6.9	1517	754.35
57	4	33.40	7.4	1610	754.35
58	4	34.28	7.7	1806	754.35
59	4	34.53	8.0	1930	754.35
60	5	34.98	8.0	1597	754.35
61	2	25.42	6.9	916	754.35
62	2	26.41	6.9	1125	754.35
63	2	27.33	6.6	1372	754.35
64	2	28.22	7.4	1596	754.35
65	3	29.16	7.1	1230	754.35
66	3	29.51	7.1	1371	754.35
67	3	30.35	7.1	1531	754.35
68	4	31.52	6.6	1210	754.35
69	4	32.10	6.6	1315	754.35
70	4	32.25	6.9	1417	754.35
71	4	32.66	6.9	1538	754.35
72	4	33.16	6.9	1634	754.35
73	4	34.56	6.9	1835	754.35
74	4	35.01	6.9	1835	754.35
75	5	35.24	6.9	1612	754.35

TABLE A2.3

DATA FOR CALCULATION OF VELOCITY

PT	GEAR	VOLTAGE	TEMPERATURE deg.C	IGNITION COUNT	PATTMOS mm(Hg)
1	0	23.26	13.1	368	760.85
2	0	24.44	13.1	485	760.85
3	0	25.81	14.1	675	760.85
4	0	26.14	15.8	774	760.05
5	0	27.08	16.1	1050	760.85
6	0	27.26	18.3	1154	760.85
7	0	27.58	19.8	1372	760.85
8	0	27.21	19.6	1547	760.85
9	0	27.18	20.8	1756	760.85
10	0	27.20	22.1	1953	760.85
11	0	27.03	22.3	2053	760.85
12	0	26.55	22.1	2260	760.85
13	0	22.28	16.1	419	760.85
14	0	23.15	16.1	506	760.05
15	0	24.68	17.3	651	760.05
16	0	25.27	21.1	790	760.85
17	0	26.23	21.8	1003	760.85
18	0	26.93	20.6	1104	760.85
19	0	26.94	23.3	1375	760.85
20	0	26.87	24.6	1564	760.85
21	0	26.70	23.8	1669	760.85
22	0	26.71	24.3	1936	760.85
23	0	26.37	24.6	2060	760.85
24	0	25.97	25.3	2257	760.85
25	0	21.70	14.3	390	760.85
26	0	22.86	15.3	474	760.85
27	0	24.41	19.1	674	760.85
28	0	25.20	20.6	850	760.85
29	0	25.93	22.3	1007	760.85
30	0	26.25	23.1	1113	760.85
31	0	26.59	23.8	1340	760.85
32	0	26.79	24.3	1533	760.85
33	0	26.58	24.6	1694	760.85
34	0	26.68	24.6	1933	760.85
35	0	26.56	24.8	2078	760.85
36	0	26.26	25.3	2206	760.85

N.B. Car Stationary

TABLE A2.4

DATA FOR CALCULATION OF VELOCITY

PT	GEAR	VOLTAGE	TEMPERATURE deg.C	IGNITION COUNT	PATTMOS mm(Hg)
1	1	24.74	6.9	491	739.95
2	1	26.51	6.6	666	739.95
3	1	27.99	7.1	814	739.95
4	1	28.80	6.6	950	739.95
5	1	29.21	6.9	1099	739.95
6	1	29.55	6.6	1290	739.95
7	1	29.77	6.4	1518	739.95
8	1	29.90	6.4	1617	739.95
9	1	30.46	7.4	1867	739.95
10	1	30.54	7.7	2027	739.95
11	1	30.51	7.7	2321	739.95
12	1	30.64	7.7	2041	739.95
13	1	22.86	9.3	370	723.95
14	1	24.17	9.5	505	723.95
15	1	25.91	7.1	675	723.95
16	1	27.28	7.7	900	723.95
17	1	28.52	6.4	1093	723.95
18	1	29.28	6.6	1273	723.95
19	1	29.77	6.6	1484	723.95
20	1	29.94	5.9	1659	723.95

N.B. First Gear

TABLE A2.5

DATA FOR CALCULATION OF VELOCITY

PT	GEAR	VOLTAGE	TEMPERATURE deg.C	IGNITION COUNT	PATTMOS mm(Hg)
1	2	24.73	8.0	461	739.95
2	2	26.63	8.0	666	739.95
3	2	28.10	7.4	787	739.95
4	2	29.28	7.4	1037	739.95
5	2	29.81	7.1	1093	739.95
6	2	30.83	7.4	1292	739.95
7	2	31.20	7.4	1546	739.95
8	2	31.13	7.1	1687	739.95
9	2	31.49	7.1	1952	739.95
10	2	32.37	6.9	2052	739.95
11	2	25.40	6.6	508	739.95
12	2	26.70	6.6	665	739.95
13	2	28.34	6.6	780	739.95
14	2	29.46	6.6	1006	739.95
15	2	29.91	6.6	1131	739.95
16	2	30.50	6.6	1382	739.95
17	2	30.83	6.1	1537	739.95
18	2	31.31	6.1	1695	739.95
19	2	31.52	6.4	1959	739.95
20	2	31.90	6.1	2026	739.95
21	2	32.08	6.4	2212	739.95
22	2	32.07	2.9	1871	723.35
23	2	31.73	3.1	1637	723.35
24	2	30.55	2.6	1343	723.35
25	2	30.28	2.6	1116	723.35
26	2	29.64	2.6	956	723.35

N.B. Second Gear

TABLE A2.6

DATA FOR CALCULATION OF VELOCITY

PT	GEAR	VOLTAGE	TEMPERATURE deg.C	IGNITION COUNT	PATTMOS mm(Hg)
1	3	34.70	4.6	2101	723.35
2	3	34.55	4.6	1986	723.35
3	3	34.50	4.4	1823	723.35
4	3	33.21	4.4	1702	723.35
5	3	32.49	3.1	1536	723.35
6	3	31.92	3.1	1387	723.35
7	3	31.14	3.4	1230	723.35
8	3	30.60	3.1	1078	723.35
9	3	29.58	3.1	923	723.35
10	3	28.28	3.1	761	723.35
11	3	28.24	2.9	648	723.35
12	3	26.76	4.4	487	753.00
13	3	28.99	4.1	647	753.00
14	3	29.40	4.1	776	753.00
15	3	30.48	4.4	1027	753.00
16	3	32.06	4.1	1162	753.00
17	3	32.99	4.1	1279	753.00
18	3	33.74	4.6	1563	753.00
19	3	33.55	5.0	1657	753.00
20	3	33.97	4.6	2028	753.00
21	3	34.72	4.9	2121	753.00
22	3	27.01	4.6	462	753.00
23	3	28.70	4.4	675	753.00
24	3	30.12	4.4	811	753.00
25	3	30.43	4.6	1013	753.00
26	3	31.12	5.1	1112	753.00
27	3	32.95	4.9	1406	753.00
28	3	33.13	4.9	1710	753.00
29	3	33.32	5.1	1671	753.00
30	3	33.78	5.1	2089	753.00
31	3	34.54	4.9	2071	753.00
32	3	25.60	5.1	466	739.95
33	3	28.09	5.4	652	739.95
34	3	28.48	5.6	802	739.95
35	3	30.66	5.6	962	739.95
36	3	31.15	6.1	1128	739.95
37	3	32.00	6.4	1324	739.95

N.B. Third Gear

TABLE A2.7

DATA FOR CALCULATION OF VELOCITY

PT	GEAR	VOLTAGE	TEMPERATURE deg.C	IGNITION COUNT	PATTMOS mm(Hg)
1	4	27.95	4.6	473	753.00
2	4	30.19	4.6	679	753.00
3	4	30.32	5.1	814	753.00
4	4	32.50	4.6	1025	753.00
5	4	32.19	4.6	1163	753.00
6	4	33.69	4.6	1374	753.00
7	4	34.75	4.6	1692	753.00
8	4	35.43	4.6	1679	753.00
9	4	36.46	4.6	2100	753.00
10	4	32.95	2.0	1196	753.00
11	4	35.25	2.9	1709	753.00
12	4	26.87	4.9	461	753.00
13	4	29.17	4.9	634	753.00
14	4	30.91	4.6	800	753.00
15	4	32.38	4.9	961	753.00
16	4	32.75	4.6	1160	753.00
17	4	33.95	4.6	1334	753.00
18	4	34.56	4.1	1537	753.00
19	4	35.02	4.6	1804	753.00
20	4	33.98	4.9	2030	753.00
21	4	36.36	4.6	2110	753.00
22	4	33.43	5.6	1511	723.90
23	4	35.71	6.4	1668	723.90
24	4	36.80	6.4	1911	723.90
25	4	36.32	6.4	2164	723.90
26	4	33.82	5.1	1289	723.35
27	4	34.50	5.1	1497	723.35
28	4	31.36	4.4	886	723.35
29	4	30.56	4.4	668	723.35
30	4	30.27	4.4	773	723.35
31	4	31.36	4.1	992	723.35
32	4	31.88	4.4	1090	723.35
33	4	32.03	4.6	1210	723.35
34	4	34.60	4.6	1435	723.35

N.B. Fourth Gear

TABLE A2.8

DATA FOR CALCULATION OF VELOCITY

PT	GEAR	VOLTAGE	TEMPERATURE deg.C	IGNITION COUNT	PATTMOS mm(Hg)
1	5	34.70	4.9	1268	723.35
2	5	34.33	4.6	1196	723.55
3	5	33.05	4.4	1068	723.55
4	5	32.27	4.4	1005	723.55
5	5	31.40	4.1	927	723.55
6	5	31.06	4.1	824	723.55
7	5	30.46	4.1	732	723.55
8	5	30.28	4.4	644	723.55
9	5	35.50	7.7	1729	723.90
10	5	36.47	6.6	1902	723.90
11	5	28.80	4.6	478	753.00
12	5	29.61	4.9	661	753.00
13	5	31.94	4.4	740	753.00
14	5	32.43	4.6	979	753.00
15	5	33.75	4.6	1127	753.00
16	5	35.01	4.4	1485	753.00
17	5	36.08	4.4	1532	753.00
18	5	27.77	4.6	457	753.00
19	5	30.01	4.9	654	753.00
20	5	31.62	4.9	760	753.00
21	5	33.04	3.9	1026	753.00
22	5	33.70	4.1	1131	753.00

N.B. Fifth Gear

TABLE A2.9

CALCULATION OF AIR VELOCITY

PT	GEAR	CAR SPEED mile/hour	ENGINE SPEED rev/min	AIR VELOCITY m/s
1	0	0	572.00	1.3016
2	0	0	754.00	1.8728
3	0	0	1028.00	2.5568
4	0	0	1272.00	3.2056
5	0	0	1482.00	3.7874
6	0	0	1752.00	4.3969
7	0	0	606.00	1.3527
8	0	0	780.00	1.8537
9	0	0	1036.00	2.5687
10	0	0	1380.00	3.2431
11	0	0	1742.00	4.4647
12	0	0	620.00	1.3507
13	0	0	814.00	1.8467
14	0	0	1004.00	2.3269
15	0	0	1266.00	3.1002
16	0	0	1500.00	3.6312
17	0	0	1758.00	4.1867

N.B. Viscous Coupling Locked

TABLE A2.10

CALCULATION OF AIR VELOCITY

PT	GEAR	CAR SPEED mile/hour	ENGINE SPEED rev/min	AIR VELOCITY m/s
1	3	19	1222.00	1.9177
2	2	23	2272.00	2.5633
3	3	28	1802.00	2.7381
4	3	33	2146.00	3.5114
5	3	37	2444.00	4.3836
6	3	42	2726.00	4.7021
7	4	47	2190.00	4.7937
8	4	51	2368.00	5.3711
9	4	55	2578.00	6.3353
10	4	60	2816.00	6.6872
11	4	64	3004.00	7.1886
12	4	69	3204.00	7.5233
13	4	74	3456.00	8.0003
14	5	79	3066.00	9.1906
15	5	83	3218.00	9.5581
16	2	19	1824.00	2.3228
17	2	23	2240.00	2.8662
18	2	28	2724.00	3.2179
19	2	33	3182.00	3.7162
20	3	37	2404.00	4.0300
21	3	42	2740.00	4.5564
22	3	46	3024.00	4.1909
23	4	52	2412.00	5.4633
24	4	55	2586.00	6.3027
25	4	60	2818.00	6.8418
26	4	65	3024.00	6.4798
27	4	73	3412.00	8.4374
28	4	81	3762.00	7.9687
29	4	94	4400.00	9.1705
30	5	83	3232.00	9.8155
31	2	19	1880.00	2.1251
32	2	23	2264.00	2.1681
33	2	28	2754.00	2.7652
34	2	33	3230.00	3.5972
35	2	37	3592.00	3.8115
36	3	42	2720.00	4.4435
37	3	46	3030.00	4.7912
38	3	51	3344.00	5.2924
39	4	55	2588.00	5.6832

N.B. Fan Removed

Cont.

CALCULATION OF AIR VELOCITY (Cont.)

PT	GEAR	CAR SPEED mile/hour	ENGINE SPEED rev/min	AIR VELOCITY m/s
40	4	60	2826.00	6.3462
41	4	64	2998.00	6.7678
42	4	71	3302.00	7.1839
43	4	74	3452.00	7.6790
44	4	79	3684.00	8.7371
45	5	82	3208.00	9.1182
46	2	20	1924.00	2.1448
47	2	23	2264.00	2.3484
48	2	28	2724.00	2.9946
49	2	33	3180.00	3.4601
50	3	37	2420.00	3.7670
51	3	42	2722.00	4.5638
52	3	47	3044.00	4.9374
53	4	51	2400.00	5.7814
54	4	56	2608.00	6.4383
55	4	60	2798.00	6.7592
56	4	65	3034.00	7.1158
57	4	69	3220.00	7.2503
58	4	77	3612.00	8.1475
59	4	83	3860.00	8.4614
60	5	82	3194.00	8.9436
61	2	19	1832.00	2.3158
62	2	23	2250.00	2.7238
63	2	28	2744.00	3.1204
64	2	33	3192.00	3.6230
65	3	38	2460.00	4.1153
66	3	42	2742.00	4.3208
67	3	47	3062.00	4.8460
68	4	52	2420.00	5.5985
69	4	56	2630.00	6.0363
70	4	61	2834.00	6.1947
71	4	66	3076.00	6.5286
72	4	70	3268.00	6.9562
73	4	79	3670.00	8.2830
74	4	79	3670.00	8.7537
75	5	83	3224.00	9.0032

TABLE A2.11

CALCULATION OF AIR VELOCITY

PT	GEAR	CAR SPEED mile/hour	ENGINE SPEED rev/min	AIR VELOCITY m/s
1	0	0	736.00	1.8003
2	0	0	970.00	2.2435
3	0	0	1350.00	2.8975
4	0	0	1548.00	3.1860
5	0	0	2100.00	3.7073
6	0	0	2308.00	4.0205
7	0	0	2744.00	4.3786
8	0	0	3094.00	4.1227
9	0	0	3512.00	4.2315
10	0	0	3906.00	4.3894
11	0	0	4106.00	4.3008
12	0	0	4520.00	3.9763
13	0	0	838.00	1.5960
14	0	0	1012.00	1.9076
15	0	0	1302.00	2.6007
16	0	0	1580.00	3.1620
17	0	0	2006.00	3.7543
18	0	0	2208.00	4.0538
19	0	0	2750.00	4.3558
20	0	0	3128.00	4.4622
21	0	0	3338.00	4.2557
22	0	0	3872.00	4.3197
23	0	0	4120.00	4.1326
24	0	0	4514.00	3.9567
25	0	0	780.00	1.3329
26	0	0	948.00	1.7613
27	0	0	1348.00	2.5969
28	0	0	1700.00	3.0854
29	0	0	2014.00	3.6285
30	0	0	2226.00	3.8968
31	0	0	2680.00	4.1845
32	0	0	3066.00	4.3727
33	0	0	3388.00	4.2687
34	0	0	3866.00	4.3347
35	0	0	4156.00	4.2787
36	0	0	4412.00	4.1405

N.B. Car Stationary

CALCULATION OF AIR VELOCITY

PT	GEAR	CAR SPEED mile/hour	ENGINE SPEED rev/min	AIR VELOCITY m/s
1	1	6	982.00	2.0979
2	1	9	1332.00	2.8024
3	1	10	1628.00	3.5482
4	1	12	1900.00	3.9447
5	1	14	2198.00	4.2065
6	1	17	2580.00	4.3815
7	1	20	3036.00	4.4967
8	1	21	3234.00	4.5775
9	1	24	3734.00	5.0471
10	1	26	4054.00	5.1353
11	1	30	4642.00	5.1147
12	1	26	4082.00	5.2046
13	1	5	740.00	1.5811
14	1	7	1010.00	2.0566
15	1	9	1350.00	2.6300
16	1	12	1800.00	3.3060
17	1	14	2186.00	3.8572
18	1	16	2546.00	4.3136
19	1	19	2968.00	4.6161
20	1	21	3318.00	4.6538

TABLE A2.12 N.B. First Gear

TABLE A2.13

CALCULATION OF AIR VELOCITY

PT	GEAR	CAR SPEED mile/hour	ENGINE SPEED rev/min	AIR VELOCITY m/s
1	2	9	922.00	2.1487
2	2	14	1332.00	2.9463
3	2	16	1574.00	3.6295
4	2	21	2074.00	4.2944
5	2	22	2186.00	4.5907
6	2	26	2584.00	5.3032
7	2	32	3092.00	5.5695
8	2	35	3374.00	5.4821
9	2	40	3904.00	5.7477
10	2	42	4104.00	6.4134
11	2	10	1016.00	2.3369
12	2	14	1330.00	2.8874
13	2	16	1560.00	3.6932
14	2	21	2012.00	4.3273
15	2	23	2262.00	4.6037
16	2	28	2764.00	4.9865
17	2	32	3074.00	5.1551
18	2	35	3390.00	5.4925
19	2	40	3918.00	5.6826
20	2	42	4052.00	5.9316
21	2	45	4424.00	6.1111
22	2	38	3742.00	5.7923
23	2	34	3274.00	5.5671
24	2	28	2686.00	4.7171
25	2	23	2232.00	4.5491
26	2	20	1912.00	4.1690

N.B. Second Gear

TABLE A2.14

CALCULATION OF AIR VELOCITY

PT	GEAR	CAR SPEED mile/hour	ENGINE SPEED rev/min	AIR VELOCITY m/s
1	3	64	4202.00	8.3492
2	3	61	3972.00	8.1972
3	3	56	3646.00	8.1114
4	3	52	3404.00	6.9113
5	3	47	3072.00	6.1376
6	3	43	2774.00	5.7055
7	3	38	2460.00	5.1870
8	3	33	2156.00	4.7984
9	3	28	1846.00	4.1779
10	3	23	1522.00	3.4756
11	3	20	1296.00	3.4410
12	3	15	974.00	2.7296
13	3	20	1294.00	3.7746
14	3	24	1552.00	3.9976
15	3	31	2054.00	4.6617
16	3	36	2324.00	5.6998
17	3	39	2558.00	6.4164
18	3	48	3126.00	7.1247
19	3	51	3314.00	7.0187
20	3	62	4056.00	7.3310
21	3	65	4242.00	8.0933
22	3	14	924.00	2.8501
23	3	21	1350.00	3.6455
24	3	25	1622.00	4.4408
25	3	31	2026.00	4.6502
26	3	34	2224.00	5.1519
27	3	43	2812.00	6.4950
28	3	52	3420.00	6.6442
29	3	51	3342.00	6.8344
30	3	64	4178.00	7.2387
31	3	63	4142.00	7.9167
32	3	14	932.00	2.3369
33	3	20	1304.00	3.4702
34	3	25	1604.00	3.6880
35	3	29.	1924.00	4.9856
36	3	35	2256.00	5.3781
37	3	41	2648.00	6.0483

N.B. Third Gear

TABLE A2.15

CALCULATION OF AIR VELOCITY

PT	GEAR	CAR SPEED mile/hour	ENGINE SPEED rev/min	AIR VELOCITY m/s
1	4	20	946.00	3.2840
2	4	29	1358.00	4.5022
3	4	35	1628.00	4.6309
4	4	44	2050.00	6.0949
5	4	50	2326.00	5.8580
6	4	59	2748.00	7.0805
7	4	72	3384.00	8.0697
8	4	72	3358.00	8.7655
9	4	90	4200.00	9.9201
10	4	51	2392.00	6.1066
11	4	73	3418.00	8.2636
12	4	20	922.00	2.8071
13	4	27	1268.00	3.9375
14	4	34	1600.00	4.9578
15	4	41	1922.00	6.0411
16	4	50	2320.00	6.2918
17	4	57	2668.00	7.3129
18	4	66	3074.00	7.7984
19	4	77	3608.00	8.3400
20	4	87	4060.00	7.3883
21	4	90	4220.00	9.8024
22	4	65	3022.00	7.2870
23	4	71	3336.00	9.8209
24	4	82	3822.00	11.1949
25	4	93	4328.00	10.5701
26	4	55	2578.00	7.5730
27	4	64	2994.00	8.2370
28	4	38	1772.00	5.4529
29	4	29	1336.00	4.9051
30	4	33	1546.00	4.7176
31	4	42	1984.00	5.4183
32	4	47	2180.00	5.8344
33	4	52	2420.00	5.9739
34	4	61	2870.00	8.2476

N.B. Fourth Gear

TABLE A2.16

CALCULATION OF AIR VELOCITY

PT	GEAR	CAR SPEED mile/hour	ENGINE SPEED rev/min	AIR VELOCITY m/s
1	5	65	2536.00	8.4045
2	5	61	2392.00	7.9763
3	5	55	2136.00	6.7717
4	5	52	2010.00	6.1330
5	5	48	1854.00	5.4452
6	5	42	1648.00	5.2074
7	5	38	1464.00	4.8079
8	5	33	1288.00	4.7227
9	5	89	3458.00	9.8631
10	5	98	3804.00	10.8115
11	5	25	956.00	3.7135
12	5	34	1322.00	4.1858
13	5	38	1480.00	5.6483
14	5	50	1958.00	6.0408
15	5	58	2254.00	7.1335
16	5	76	2970.00	8.2932
17	5	79	3064.00	9.4372
18	5	23	914.00	3.1977
19	5	34	1308.00	4.4216
20	5	39	1520.00	5.4771
21	5	53	2052.00	6.4293
22	5	58	2262.00	7.0130

N.B. Fifth Gear

TABLE A2.17

CAR STATIONARY; EDITTED DATA
DATA TO FUNCTION, DEVIATION CALCULATION

PT	DATA w rev/min	DATA U m/s	FN(w) m/s	ABS DEV. m/s	FRAC DEV
1	1350	2.8975	2.7651	0.1324	0.04569
2	1548	3.1860	3.0663	0.1197	0.03756
3	2100	3.7073	3.7527	-0.0454	-0.01226
4	2308	4.0205	3.9513	0.0692	0.01722
5	2744	4.3786	4.2581	0.1205	0.02752
6	3094	4.1227	4.3953	-0.2726	-0.06613
7	3512	4.2315	4.4293	-0.1979	-0.04676
8	3906	4.3894	4.3299	0.0594	0.01354
9	4106	4.3008	4.2301	0.0707	0.01645
10	4520	3.9763	3.9162	0.0601	0.01511
11	1302	2.6007	2.6878	-0.0871	-0.03348
12	1580	3.1620	3.1123	0.0497	0.01570
13	2006	3.7543	3.6520	0.1023	0.02724
14	2208	4.0538	3.8600	0.1939	0.04782
15	2750	4.3558	4.2613	0.0945	0.02170
16	3128	4.4622	4.4034	0.0589	0.01319
17	3338	4.2557	4.4325	-0.1768	-0.04154
18	3872	4.3197	4.3436	-0.0240	-0.00555
19	4120	4.1326	4.2218	-0.0892	-0.02158
20	4514	3.9567	3.9218	0.0348	0.00880
21	1348	2.5969	2.7619	-0.1651	-0.06356
22	1700	3.0854	3.2781	-0.1927	-0.06244
23	2014	3.6285	3.6609	-0.0324	-0.00892
24	2226	3.8968	3.8770	0.0199	0.00510
25	2680	4.1845	4.2224	-0.0379	-0.00906
26	3066	4.3727	4.3879	-0.0152	-0.00348
27	3388	4.2687	4.4341	-0.1654	-0.03874
28	3866	4.3347	4.3459	-0.0112	-0.00258
29	4156	4.2787	4.1998	0.0789	0.01843
30	4412	4.1405	4.0121	0.1284	0.03100

RMS ABSOLUTE DEVIATION= 0.1167m/s

RMS FRACTIONAL DEVIATION= 0.03177

TABLE A2.18

CAR STATIONARY; COMPLETE DATA
DATA TO FUNCTION, DEVIATION CALCULATION

PT	DATA w rev/min	DATA U m/s	FN(w) m/s	ABS DEV. m/s	FRAC DEV	
1	736	1.8003	1.6542	0.1461	0.08114	*
2	970	2.2435	2.1084	0.1351	0.06022	*
3	1350	2.8975	2.7651	0.1324	0.04569	
4	1548	3.1860	3.0663	0.1197	0.03756	
5	2100	3.7073	3.7527	-0.0454	-0.01226	
6	2308	4.0205	3.9513	0.0692	0.01722	
7	2744	4.3786	4.2581	0.1205	0.02752	
8	3094	4.1227	4.3953	-0.2726	-0.06613	
9	3512	4.2315	4.4293	-0.1979	-0.04676	
10	3906	4.3894	4.3299	0.0594	0.01354	
11	4106	4.3008	4.2301	0.0707	0.01645	
12	4520	3.9763	3.9162	0.0601	0.01511	
13	838	1.5960	1.8567	-0.2608	-0.16339	*
14	1012	1.9076	2.1859	-0.2784	-0.14593	*
15	1302	2.6007	2.6878	-0.0871	-0.03348	
16	1580	3.1620	3.1123	0.0497	0.01570	
17	2006	3.7543	3.6520	0.1023	0.02724	
18	2208	4.0538	3.8600	0.1939	0.04782	
19	2750	4.3558	4.2613	0.0945	0.02170	
20	3128	4.4622	4.4034	0.0589	0.01319	
21	3338	4.2557	4.4325	-0.1768	-0.04154	
22	3872	4.3197	4.3436	-0.0240	-0.00555	
23	4120	4.1326	4.2218	-0.0892	-0.02158	
24	4514	3.9567	3.9218	0.0348	0.00880	
25	780	1.3329	1.7424	-0.4095	-0.30723	*
26	948	1.7613	2.0673	-0.3060	-0.17374	*
27	1348	2.5969	2.7619	-0.1651	-0.06356	
28	1700	3.0854	3.2781	-0.1927	-0.06244	
29	2014	3.6285	3.6609	-0.0324	-0.00892	
30	2226	3.8968	3.8770	0.0199	0.00510	
31	2680	4.1845	4.2224	-0.0379	-0.00906	
32	3066	4.3727	4.3879	-0.0152	-0.00348	
33	3388	4.2687	4.4341	-0.1654	-0.03874	
34	3866	4.3347	4.3459	-0.0112	-0.00258	
35	4156	4.2787	4.1998	0.0789	0.01843	
36	4412	4.1405	4.0121	0.1284	0.03100	

RMS ABSOLUTE DEVIATION= 0.1542m/s

RMS FRACTIONAL DEVIATION= 0.07692

* Points Omitted for Curve Fit

TABLE A2.19

CAR MOVING; FIRST GEAR
DATA TO FUNCTION, DEVIATION CALCULATION

PT	DATA w rev/min	DATA U m/s	FN(w) m/s	ABS DEV. m/s	FRAC DEV
1	982	2.0979	2.2368	-0.1389	-0.06621
2	1332	2.8024	2.8879	-0.0855	-0.03052
3	1628	3.5482	3.3743	0.1739	0.04902
4	1900	3.9447	3.7682	0.1765	0.04474
5	2198	4.2065	4.1410	0.0656	0.01559
6	2580	4.3815	4.5284	-0.1469	-0.03354
7	3036	4.4967	4.8589	-0.3622	-0.08054
8	3234	4.5775	4.9584	-0.3809	-0.08321
9	3734	5.0471	5.0957	-0.0486	-0.00963
10	4054	5.1353	5.1030	0.0323	0.00630
11	4642	5.1147	4.9766	0.1381	0.02700
12	4082	5.2046	5.1008	0.1037	0.01993
13	740	1.5811	1.7397	-0.1585	-0.10026
14	1010	2.0566	2.2919	-0.2352	-0.11439
15	1350	2.6300	2.9192	-0.2892	-0.10995
16	1800	3.3060	3.6293	-0.3233	-0.09779
17	2186	3.8572	4.1272	-0.2700	-0.06999
18	2546	4.3136	4.4981	-0.1845	-0.04277
19	2968	4.6161	4.8186	-0.2026	-0.04388
20	3318	4.6538	4.9927	-0.3389	-0.07282

RMS ABSOLUTE DEVIATION= 0.2187m/s

RMS FRACTIONAL DEVIATION= 0.06498

TABLE A2.20

CAR MOVING; SECOND GEAR
DATA TO FUNCTION, DEVIATION CALCULATION

PT	DATA w rev/min	DATA U m/s	FN(w) m/s	ABS DEV. m/s	FRAC DEV
1	922	2.1487	2.2601	-0.1114	-0.05185
2	1332	2.9463	3.1059	-0.1597	-0.05419
3	1574	3.6295	3.5565	0.0730	0.02012
4	2074	4.2944	4.3720	-0.0776	-0.01808
5	2186	4.5907	4.5335	0.0572	0.01246
6	2584	5.3032	5.0454	0.2578	0.04861
7	3092	5.5695	5.5633	0.0063	0.00112
8	3374	5.4821	5.7891	-0.3070	-0.05601
9	3904	5.7477	6.1078	-0.3601	-0.06265
10	4104	6.4134	6.1969	0.2164	0.03374
11	1016	2.3369	2.4631	-0.1262	-0.05399
12	1330	2.8874	3.1020	-0.2147	-0.07435
13	1560	3.6932	3.5314	0.1618	0.04380
14	2012	4.3273	4.2793	0.0479	0.01107
15	2262	4.6037	4.6387	-0.0350	-0.00760
16	2764	4.9865	5.2458	-0.2594	-0.05201
17	3074	5.1551	5.5474	-0.3924	-0.07611
18	3390	5.4925	5.8007	-0.3082	-0.05611
19	3918	5.6826	6.1145	-0.4319	-0.07601
20	4052	5.9316	6.1752	-0.2436	-0.04106
21	4424	6.1111	6.3116	-0.2005	-0.03281
22	3742	5.7923	6.0239	-0.2316	-0.03998
23	3274	5.5671	5.7138	-0.1467	-0.02636
24	2686	4.7171	5.1613	-0.4442	-0.09417
25	2232	4.5491	4.5976	-0.0485	-0.01066
26	1912	4.1690	4.1248	0.0442	0.01061

RMS ABSOLUTE DEVIATION= 0.2290m/s

RMS FRACTIONAL DEVIATION= 0.04773

TABLE A2.21

CAR MOVING; THIRD GEAR
DATA TO FUNCTION, DEVIATION CALCULATION

PT	DATA w rev/min	DATA U m/s	FN(w) m/s	ABS DEV. m/s	FRAC DEV
1	4202	8.3492	8.0884	0.2608	0.03124
2	3972	8.1972	7.8367	0.3605	0.04398
3	3646	8.1114	7.4572	0.6543	0.08066
4	3404	6.9113	7.1542	-0.2429	-0.03514
5	3072	6.1376	6.7037	-0.5661	-0.09224
6	2774	5.7055	6.2608	-0.5553	-0.09733
7	2460	5.1870	5.7506	-0.5636	-0.10866
8	2156	4.7984	5.2112	-0.4128	-0.08602
9	1846	4.1779	4.6128	-0.4349	-0.10410
10	1522	3.4756	3.9335	-0.4579	-0.13175
11	1296	3.4410	3.4265	0.0145	0.00421
12	974	2.7296	2.6566	0.0730	0.02676
13	1294	3.7746	3.4219	0.3527	0.09344
14	1552	3.9976	3.9988	-0.0012	-0.00031
15	2054	4.6617	5.0198	-0.3581	-0.07681
16	2324	5.6998	5.5149	0.1848	0.03243
17	2558	6.4164	5.9148	0.5016	0.07817
18	3126	7.1247	6.7800	0.3447	0.04838
19	3314	7.0187	7.0363	-0.0176	-0.00250
20	4056	7.3310	7.9299	-0.5989	-0.08170
21	4242	8.0933	8.1311	-0.0377	-0.00466
22	1350	3.6455	3.5501	0.0954	0.02616
23	1622	4.4408	4.1492	0.2916	0.06567
24	2026	4.6502	4.9663	-0.3161	-0.06798
25	2224	5.1519	5.3358	-0.1839	-0.03570
26	2812	6.4950	6.3194	0.1756	0.02703
27	3420	6.6442	7.1749	-0.5307	-0.07988
28	3342	6.8344	7.0733	-0.2389	-0.03496
29	4178	7.2387	8.0626	-0.8240	-0.11383
30	4142	7.9167	8.0238	-0.1071	-0.01353
31	932	2.3369	2.5520	-0.2151	-0.09205
32	1304	3.4702	3.4449	0.0253	0.00729
33	1604	3.6880	4.1107	-0.4228	-0.11464
34	1924	4.9856	4.7681	0.2175	0.04363
35	2256	5.3781	5.3937	-0.0156	-0.00290
36	2648	6.0483	6.0616	-0.0133	-0.00220

RMS ABSOLUTE DEVIATION= 0.3648m/s

RMS FRACTIONAL DEVIATION= 0.06738

TABLE A2.22

CAR MOVING; FOURTH GEAR
DATA TO FUNCTION, DEVIATION CALCULATION

PT	DATA w rev/min	DATA U m/s	FN(w) m/s	ABS DEV. m/s	FRAC DEV
1	1358	4.5022	4.1824	0.3198	0.07103
2	1628	4.6309	4.9154	-0.2845	-0.06145
3	2050	6.0949	5.9973	0.0977	0.01602
4	2326	5.8580	6.6645	-0.8065	-0.13768
5	2748	7.0805	7.6276	-0.5471	-0.07727
6	3384	8.0697	8.9646	-0.8950	-0.11091
7	3358	8.7655	8.9123	-0.1468	-0.01675
8	4200	9.9201	10.5314	-0.6113	-0.06163
9	2392	6.1066	6.8196	-0.7130	-0.11676
10	3418	8.2636	9.0328	-0.7692	-0.09308
11	922	2.8071	2.9291	-0.1220	-0.04345
12	1268	3.9375	3.9307	0.0068	0.00172
13	1600	4.9578	4.8409	0.1168	0.02357
14	1922	6.0411	5.6772	0.3639	0.06024
15	2320	6.2918	6.6503	-0.3586	-0.05699
16	2668	7.3129	7.4500	-0.1372	-0.01876
17	3074	7.7984	8.3285	-0.5302	-0.06798
18	3608	8.3400	9.4083	-1.0683	-0.12810
19	4060	7.3883	10.2710	-2.8827	-0.39017
20	4220	9.8024	10.5684	-0.7660	-0.07815
21	3022	7.2870	8.2190	-0.9320	-0.12791
22	3336	9.8209	8.8679	0.9530	0.09703
23	3822	11.1948	9.8215	1.3733	0.12267
24	4328	10.5700	10.7676	-0.1976	-0.01869
25	2578	7.5730	7.2476	0.3254	0.04297
26	2994	8.2370	8.1597	0.0773	0.00938
27	1772	5.4529	5.2932	0.1597	0.02928
28	1546	4.7176	4.6962	0.0214	0.00453
29	1984	5.4183	5.8331	-0.4148	-0.07656
30	2180	5.8344	6.3154	-0.4810	-0.08244
31	2420	5.9739	6.8848	-0.9109	-0.15248
32	2870	8.2476	7.8940	0.3535	0.04287

RMS ABSOLUTE DEVIATION= 0.7761m/s

RMS FRACTIONAL DEVIATION= 0.10358

TABLE A2.23

CAR MOVING; FIFTH GEAR
DATA TO FUNCTION, DEVIATION CALCULATION

PT	DATA w rev/min	DATA U m/s	FN(w) m/s	ABS DEV. m/s	FRAC DEV
1	2536	8.4045	8.1358	0.2687	0.03197
2	2392	7.9763	7.7386	0.2377	0.02980
3	2136	6.7717	7.0153	-0.2436	-0.03597
4	2010	6.1330	6.6508	-0.5179	-0.08444
5	1854	5.4452	6.1915	-0.7463	-0.13707
6	1648	5.2074	5.5710	-0.3636	-0.06983
7	1464	4.8079	5.0029	-0.1950	-0.04056
8	1288	4.7227	4.4469	0.2757	0.05839
9	3458	9.8631	10.5357	-0.6726	-0.06820
10	3804	10.8114	11.3853	-0.5739	-0.05308
11	1322	4.1858	4.5553	-0.3695	-0.08827
12	1958	6.0408	6.4987	-0.4580	-0.07581
13	2254	7.1335	7.3515	-0.2180	-0.03056
14	2970	8.2932	9.2940	-1.0007	-0.12067
15	3064	9.4372	9.5377	-0.1005	-0.01065
16	914	3.1977	3.2240	-0.0263	-0.00823
17	1308	4.4216	4.5107	-0.0892	-0.02016
18	1520	5.4771	5.1772	0.2999	0.05475
19	2052	6.4293	6.7730	-0.3436	-0.05345
20	2262	7.0130	7.3741	-0.3612	-0.05150

RMS ABSOLUTE DEVIATION= 0.4356m/s

RMS FRACTIONAL DEVIATION= 0.06507

TABLE A2.24

RADIATOR AIR VELOCITY CALCULATED FROM TESTS CARRIED OUT AT JAGUAR USING VANE ANEMOMETER

(ANEMOMETER RESULTS CORRECTED BY CALIBRATION)

PT	ENGINE SPEED	AIR VELOCITY
1	572	1.23466
2	754	1.94718
3	1028	2.76658
4	1272	3.55033
5	1482	4.26286
6	1752	5.06445
7	2030	6.04418
8	2200	6.32918
9	2496	7.2911
10	660	1.48404
11	780	2.12531
12	1036	2.83783
13	1742	5.18915
14	1950	6.11541
15	2212	6.54294
16	2456	7.61172
17	620	1.44841
18	814	2.05406
19	1004	2.6597
20	1266	3.55033
21	1500	4.47662
22	1758	5.15352
23	2014	6.00856
24	2146	6.40043
25	2476	7.64735

N.B. Viscous Coupling Locked
Engine Speed in rev/min
Air Velocity in m/s

TABLE A2.25

JAGUAR XJ6 RADIATOR (MARSTON RADIATOR'S SUPAPACK I)
AIRSIDE PIEZOMETRIC PRESSURE DROP/VELOCITY DATA

fin pitch 3.588mm
fin gauge 0.0584mm
No. of tubes rows 3
test area length 0.360m
test area width 0.336m
core thickness 49.53mm
face area 0.1212m^2
flow area 0.0979m^2
equivalent diameter 3.584mm
L/De ratio 13.82

atmospheric pressure 750.50mm(Hg)
air temperature 24deg.C

volume flow rate m^3/s	delta P mmH2O	face velocity m/s	Re	f
0.0453	0.229	0.374	106	0.3228
0.0510	0.229	0.421	119	0.2550
0.0566	0.254	0.467	133	0.2295
0.0604	0.279	0.498	142	0.2219
0.0665	0.305	0.548	156	0.2001
0.0706	0.330	0.582	165	0.1922
0.0748	0.330	0.617	175	0.1712
0.0959	0.432	0.791	225	0.1361
0.1173	0.584	0.968	275	0.1231
0.1416	0.813	1.168	332	0.1175
0.1661	1.016	1.371	389	0.1067
0.1888	1.270	1.558	442	0.1033
0.2152	1.575	1.776	504	0.0985
0.2360	1.803	1.947	553	0.0939
0.2600	2.210	2.146	609	0.0947
0.2832	2.692	2.337	664	0.0973
0.2997	2.896	2.473	702	0.0934
0.3223	3.200	2.660	755	0.0893
0.3186	3.200	2.629	746	0.0914
0.3356	3.454	2.769	786	0.0889
0.3577	3.861	2.952	838	0.0874
0.3794	4.216	3.131	889	0.0849
0.3997	4.674	3.298	937	0.0848
0.4262	5.182	3.517	999	0.0827
0.4493	5.613	3.707	1053	0.0806
0.4767	6.147	3.933	1117	0.0784
0.5173	7.163	4.268	1212	0.0776
0.5460	7.874	4.506	1279	0.0765
0.5715	8.687	4.716	1339	0.0771
0.6211	9.906	5.125	1455	0.0744
0.6603	11.176	5.448	1547	0.0743
0.7117	12.827	5.873	1668	0.0734
0.7513	13.843	6.200	1760	0.0711
0.7882	15.240	6.503	1847	0.0711
0.7896	15.240	6.515	1850	0.0709
0.7929	15.875	6.542	1858	0.0732
0.8259	16.764	6.815	1935	0.0712
0.8495	17.526	7.010	1991	0.0704
0.8873	19.050	7.321	2079	0.0701
0.9014	19.812	7.438	2112	0.0707
0.9392	21.844	7.750	2201	0.0718
0.9486	21.590	7.828	2223	0.0695
0.9722	22.606	8.022	2278	0.0693
1.0076	24.130	8.314	2361	0.0689
1.0430	25.400	8.606	2444	0.0677

TABLE A2.26

JAGUAR XJ6 CONDENSER(MARSTON RADIATOR'S SHIPLEY FINCOIL)
AIRSIDE PIEZOMETRIC PRESSURE DROP/VELOCITY DATA

fin pitch 2.309mm
fin gauge 0.152mm
No. of tubes rows 2
test area length 0.359m
test area width 0.284m
core thickness 44mm
face area 0.1020m^2
flow area 0.0952m^2
equivalent diameter 4.618mm
L/De ratio 9.53

atmospheric pressure 750.55mm(Hg)
air temperature 23.5deg.C

volume flow rate m^3/s	delta P mmH2O	face velocity m/s	Re	f
0.0748	0.508	0.733	233	0.3611
0.0971	0.686	0.953	302	0.2888
0.1416	1.270	1.389	441	0.2517
0.1911	2.159	1.875	595	0.2347
0.2388	3.277	2.342	743	0.2282
0.2836	4.521	2.782	883	0.2232
0.2869	4.572	2.815	893	0.2206
0.3327	6.172	3.264	1036	0.2215
0.3794	7.696	3.722	1181	0.2123
0.4281	9.652	4.199	1333	0.2092
0.4719	11.430	4.629	1469	0.2038
0.5206	13.843	5.106	1621	0.2029
0.5659	16.510	5.550	1762	0.2048
0.6126	18.745	6.009	1907	0.1984
0.6584	21.844	6.458	2050	0.2002
0.7117	24.892	6.981	2216	0.1952
0.7532	27.432	7.388	2345	0.1921
0.8018	30.988	7.865	2496	0.1915
0.8023	30.480	7.870	2498	0.1881
0.8589	34.036	8.425	2674	0.1833
0.9038	38.100	8.865	2814	0.1853
0.9557	42.418	9.374	2975	0.1845
1.0052	46.482	9.860	3129	0.1827
1.0383	49.022	10.184	3232	0.1806
1.0855	54.102	10.647	3379	0.1824

MARSTON RADIATOR'S SUPAPACK I TEST DATA

TABLE A2.27

test number L768 test date 25/11/69 atmospheric pressure 755mm(Hg)

fin pitch 1.588mm
fin gauge 0.0584mm
no. of tubes 58
no. of tube rows 2
header separation 0.4572m
core width 0.4531m
core thickness 32.26mm

WATER			AIR			
mass flow kg/s	t in deg C	t out deg C	mass flow kg/s	t in deg C	t out deg C	delta P mm H2O
0.43	96.40	75.90	1.29	14.30	47.80	10.312
0.45	91.20	69.25	1.96	12.90	37.00	19.050
0.45	84.90	63.70	2.56	12.00	30.70	28.448
0.45	79.85	59.50	3.08	11.10	26.70	37.846
0.45	77.75	57.75	3.46	11.00	24.80	46.228
0.45	76.40	56.50	3.89	10.90	23.60	55.372

MARSTON RADIATOR'S SUPAPACK I TEST DATA

test number L769 test date 25/11/69 atmospheric pressure 755mm(Hg)

fin pitch 1.588mm
fin gauge 0.0584mm
no. of tubes 58
no. of tube rows 2
header separation 0.4572m
core width 0.4531m
core thickness 32.26mm

WATER			AIR			
mass flow kg/s	t in deg C	t out deg C	mass flow kg/s	t in deg C	t out deg C	delta P mm H2O
0.88	87.35	76.55	1.29	14.60	50.10	10.414
0.90	80.55	68.75	1.98	12.50	38.50	19.304
0.87	76.35	63.85	2.55	12.00	32.90	28.042
0.87	71.80	59.60	3.03	11.60	29.40	37.338
0.87	68.80	56.80	3.50	11.30	26.90	47.142
0.87	67.40	55.35	3.84	11.30	25.70	55.118

MARSTON RADIATOR'S SUPAPACK I TEST DATA

test number L770 test date 22/11/69 atmospheric pressure 751mm(Hg)

fin pitch 1.588mm
fin gauge 0.0584mm
no. of tubes 58
no. of tube rows 2
header separation 0.4572m
core width 0.4531m
core thickness 32.26mm

WATER			AIR			
mass flow kg/s	t in deg C	t out deg C	mass flow kg/s	t in deg C	t out deg C	delta P mm H2O
1.31	90.90	83.00	1.24	17.10	56.80	10.058
1.32	87.40	78.25	2.04	16.20	46.30	19.558
1.28	84.00	74.10	2.51	15.20	40.50	28.448
1.29	81.45	71.25	2.99	15.00	37.10	37.338
1.31	79.40	69.10	3.44	15.00	34.80	46.736
1.30	78.15	67.75	3.79	15.00	32.90	55.626

MARSTON RADIATOR'S SUPAPACK I TEST DATA

test number L771 test date 25/11/69 atmospheric pressure 754mm(Hg)

fin pitch 1.588mm
fin gauge 0.0584mm
no. of tubes 58
no. of tube rows 2
header separation 0.4572m
core width 0.4531m
core thickness 32.26mm

WATER			AIR			
mass flow kg/s	t in deg C	t out deg C	mass flow kg/s	t in deg C	t out deg C	delta P mm H2O
2.54	87.80	83.30	1.25	13.60	55.50	10.262
2.57	83.50	78.20	1.94	13.00	45.50	19.304
2.52	79.40	73.70	2.49	11.60	38.50	28.194
2.53	76.60	70.75	2.99	11.30	35.20	37.846
2.52	74.40	68.40	3.39	11.00	32.70	46.380
2.51	72.10	66.10	3.81	11.00	30.70	55.880

MARSTON RADIATOR'S SUPAPACK I TEST DATA

test number L772 test date 26/11/69 atmospheric pressure 763mm(Hg)

fin pitch 2.117mm
fin gauge 0.0584mm
no. of tubes 87
no. of tube rows 3
header separation 0.4572m
core width 0.4531m
core thickness 49.53mm

WATER			AIR			
mass flow kg/s	t in deg C	t out deg C	mass flow kg/s	t in deg C	t out deg C	delta P mm H2O
0.67	90.50	76.70	1.20	13.90	50.70	8.382
0.67	85.90	70.50	1.75	12.40	41.10	15.240
0.67	80.00	64.60	2.25	11.20	34.50	22.352
0.68	76.40	61.15	2.62	11.10	31.30	28.956
0.68	74.30	59.00	2.97	11.20	29.30	35.814
0.68	73.00	57.20	3.90	12.00	26.10	55.626

MARSTON RADIATOR'S SUPAPACK I TEST DATA

test number L773 test date 26/11/69 atmospheric pressure 762mm(Hg)

fin pitch 2.117mm
fin gauge 0.0584mm
no. of tubes 87
no. of tube rows 3
header separation 0.4572m
core width 0.4531m
core thickness 49.53mm

WATER			AIR			
mass flow kg/s	t in deg C	t out deg C	mass flow kg/s	t in deg C	t out deg C	delta P mm H2O
1.32	95.10	87.35	1.17	19.30	60.90	8.636
1.36	89.70	80.35	1.89	17.10	48.70	18.034
1.31	85.70	75.50	2.49	16.70	42.80	27.686
1.32	82.15	71.15	2.99	16.20	38.90	37.592
1.34	78.40	68.15	3.40	15.90	35.80	47.092
1.35	76.90	66.45	3.81	15.20	34.00	57.150

MARSTON RADIATOR'S SUPAPACK I TEST DATA

test number L774 test date 27/11/69 atmospheric pressure 760mm(Hg)

fin pitch 2.117mm
fin gauge 0.0584mm
no. of tubes 87
no. of tube rows 3
header separation 0.4572m
core width 0.4531m
core thickness 49.53mm

WATER			AIR			
mass flow kg/s	t in deg C	t out deg C	mass flow kg/s	t in deg C	t out deg C	delta P mm H2O
1.96	90.35	84.95	1.19	16.30	57.80	8.738
1.98	86.85	80.25	1.90	15.10	47.70	18.288
2.00	83.30	76.10	2.51	14.70	42.00	27.940
1.97	79.75	72.30	2.99	14.50	38.50	37.846
1.98	77.65	70.10	3.40	14.70	36.20	47.244
1.99	76.00	68.40	3.79	14.50	34.60	56.896

MARSTON RADIATOR'S SUPAPACK 1 TEST DATA

test number L775 test date 27/11/69 atmospheric pressure 759mm(Hg)

fin pitch 2.117mm
fin gauge 0.0584mm
no. of tubes 87
no. of tube rows 3
header separation 0.4572m
core width 0.4531m
core thickness 49.53mm

WATER			AIR			
mass flow kg/s	t in deg C	t out deg C	mass flow kg/s	t in deg C	t out deg C	delta P mm H2O
2.55	96.50	92.00	1.14	16.80	63.30	8.484
2.56	91.10	85.35	1.88	16.20	51.10	18.288
2.55	85.25	79.30	2.49	15.50	44.40	27.940
2.53	80.00	73.95	2.98	15.30	40.00	37.846
2.57	74.00	68.20	3.40	15.00	36.30	47.244
2.57	72.50	66.70	3.81	15.00	34.50	57.658

MARSTON RADIATOR'S SUPAPACK 1 TEST DATA

test number L789 test date 11/12/69 atmospheric pressure 767mm(Hg)

fin pitch 1.588mm
fin gauge 0.0584mm
no. of tubes 116
no. of tube rows 4
header separation 0.4572m
core width 0.4531m
core thickness 66.80mm

WATER			AIR			
mass flow kg/s	t in deg C	t out deg C	mass flow kg/s	t in deg C	t out deg C	delta P mm H2O
1.89	92.10	85.50	1.15	17.20	67.20	12.700
1.98	86.00	77.80	1.94	15.80	54.30	29.210
2.01	80.20	71.60	2.54	15.80	48.10	44.958
1.96	74.75	66.00	3.04	15.00	42.30	61.722
1.96	69.10	60.70	3.44	14.40	37.90	77.724
1.96	67.60	59.20	3.81	15.00	36.60	93.472

MARSTON RADIATOR'S SUPAPACK 1 TEST DATA

test number L790 test date 12/12/69 atmospheric pressure 766mm(Hg)

fin pitch 1.588mm
fin gauge 0.0584mm
no. of tubes 116
no. of tube rows 4
header separation 0.4572m
core width 0.4531m
core thickness 66.80mm

WATER			AIR			
mass flow kg/s	t in deg C	t out deg C	mass flow kg/s	t in deg C	t out deg C	delta P mm H2O
2.64	90.60	85.00	1.41	16.70	64.20	17.526
2.66	81.60	75.25	2.11	15.20	52.40	31.242
2.64	76.75	70.00	2.65	15.00	46.70	49.530
2.64	72.30	65.50	3.14	14.30	42.10	65.278
2.65	68.60	61.80	3.54	14.00	38.70	81.026
2.64	66.40	59.65	3.83	14.10	37.10	92.964

MARSTON RADIATOR'S SUPAPACK I TEST DATA

test number L791 test date 12/12/69 atmospheric pressure 768mm(Hg)

fin pitch 1.588mm
fin gauge 0.0584mm
no. of tubes 87
no. of tube rows 3
header separation 0.4572m
core width 0.4531m
core thickness 49.53mm

WATER			AIR			
mass flow kg/s	t in deg C	t out deg C	mass flow kg/s	t in deg C	t out deg C	delta P mm H2O
2.01	88.35	82.90	1.17	15.70	59.20	10.160
1.97	81.50	74.50	1.94	13.80	47.00	22.860
1.99	74.20	67.10	2.58	13.00	39.70	35.560
1.96	70.00	62.70	3.11	12.80	35.70	48.260
1.96	67.20	59.85	3.49	12.80	33.20	61.214
1.96	65.25	57.80	3.85	12.80	31.60	73.152

MARSTON RADIATOR'S SUPAPACK I TEST DATA

test number L867 test date 7/4/70 atmospheric pressure 756mm(Hg)

fin pitch 1.588mm
fin gauge 0.0584mm
no. of tubes 116
no. of tube rows 4
header separation 0.4572m
core width 0.4572m
core thickness 66.80mm

WATER			AIR			
mass flow kg/s	t in deg C	t out deg C	mass flow kg/s	t in deg C	t out deg C	delta P mm H2O
2.49	91.40	85.60	1.36	19.10	65.20	16.510
2.49	90.10	83.25	1.90	18.60	58.90	29.566
2.53	84.80	77.76	2.34	18.10	52.90	40.894
2.57	79.90	72.75	2.72	17.90	48.10	51.410
2.51	75.80	68.60	3.04	17.50	44.40	63.195
2.54	72.60	65.60	3.27	17.20	41.70	73.152
2.55	69.40	62.40	3.54	17.80	39.50	83.922
2.53	67.90	61.10	3.79	18.00	38.70	92.710

MARSTON RADIATOR'S SUPAPACK I TEST DATA

test number L2393 test date 28/6/76 atmospheric pressure 768mm(Hg)

fin pitch 3.175mm
fin gauge 0.0584mm
no. of tubes 62
no. of tube rows 2
header separation 0.3016m
core width 0.4890m
core thickness 32.26mm

WATER			AIR			
mass flow kg/s	t in deg C	t out deg C	mass flow kg/s	t in deg C	t out deg C	delta P mm H2O
2.62	69.50	68.40	0.84	30.40	43.90	0.559
2.63	70.10	68.80	1.53	31.30	41.00	2.997
2.62	69.20	67.70	1.98	32.10	40.10	5.791
2.61	70.10	68.60	2.34	33.00	40.40	8.433

MARSTON RADIATOR'S SUPAPACK I TEST DATA

test number L2395 test date 29/6/76 atmospheric pressure 768mm(Hg)

fin pitch 2.117mm
fin gauge 0.0584mm
no. of tubes 116
no. of tube rows 4
header separation 0.7071m
core width 0.4572m
core thickness 66.80mm

WATER			AIR			
mass flow kg/s	t in deg C	t out deg C	mass flow kg/s	t in deg C	t out deg C	delta P mm H2O
2.58	69.30	66.30	1.37	29.90	54.80	7.315
2.57	70.40	65.90	2.48	30.10	50.80	19.609
2.57	69.60	64.50	3.17	30.50	48.50	30.582
2.57	69.50	64.10	3.79	31.20	47.40	41.250

MARSTON RADIATOR'S SUPAPACK I TEST DATA

test number L2575 test date 26/2/77 atmospheric pressure 764mm(Hg)

fin pitch 1.969mm
fin gauge 0.0584mm
no. of tubes 116
no. of tube rows 4
header separation 0.6922m
core width 0.4318m
core thickness 66.80mm

WATER			AIR			
mass flow kg/s	t in deg C	t out deg C	mass flow kg/s	t in deg C	t out deg C	delta P mm H2O
2.45	68.10	62.70	1.32	7.70	54.30	8.382
2.53	70.70	63.40	2.27	7.10	46.60	18.796
2.53	70.10	60.70	3.01	6.90	41.60	29.972
2.53	70.60	60.20	3.76	7.80	38.70	43.180
0.76	70.30	55.10	1.54	7.80	44.80	10.058
0.76	69.60	60.00	0.71	9.20	58.60	3.353
0.45	68.90	56.30	0.72	9.90	54.60	3.302
0.45	69.30	49.80	1.50	9.00	40.20	9.500

TABLE A2.28

SUPAPACK I CALCULATED DATA

test number L768 test date 25/11/69

AIR
face area 0.2072m^2
flow area 0.1670m^2
equivalent diameter 2.801mm
primary surface area 0.7748m^2
secondary surface area 7.1065m^2

WATER
flow area 1.5838E-03 m^2
equivalent diameter 3.876mm
surface area 0.747m^2

face velocity m/s	actual velocity m/s	OS overall W/K	hS water W/K	hS air W/K	fin efficiency	h water W/m^2K	h air W/m^2K	Re air	L/De air	j air	f air
5.393	6.689	663	1424	1239	0.829	1906	185.9	1157	11.52	0.0190	0.0851
8.058	9.993	747	1479	1508	0.795	1979	234.8	1792	11.52	0.0158	0.0690
10.369	12.859	748	1479	1511	0.794	1979	235.5	2357	11.52	0.0122	0.0615
12.380	15.353	734	1464	1472	0.799	1959	228.1	2856	11.52	0.0098	0.0569
13.864	17.193	735	1464	1478	0.798	1959	229.2	3217	11.52	0.0088	0.0553
15.555	19.290	740	1464	1495	0.796	1959	232.4	3624	11.52	0.0079	0.0525

SUPAPACK 1 CALCULATED DATA

test number L769 test date 25/11/69

AIR
face area 0.2072m^2
flow area 0.1670m^2
equivalent diameter 2.801mm
primary surface area 0.7748m^2
secondary surface area 7.1065m^2

WATER
flow area 1.5838E-03 m^2
equivalent diameter 3.876mm
surface area 0.747m^2

face velocity m/s	actual velocity m/s	US overall W/K	hS water W/K	hS air W/K	fin efficiency	h water W/m^2K	h air W/m^2K	Re air	L/De air	j air	f air
5.416	6.717	796	2532	1162	0.839	3388	172.5	1154	11.52	0.0176	0.0856
8.148	10.104	887	2566	1355	0.814	3434	206.7	1806	11.52	0.0138	0.0686
10.390	12.885	935	2497	1496	0.796	3341	232.5	2346	11.52	0.0120	0.0606
12.264	15.209	952	2488	1543	0.790	3330	241.4	2802	11.52	0.0105	0.0576
14.067	17.445	971	2497	1590	0.785	3341	250.4	3241	11.52	0.0095	0.0550
15.404	19.102	1000	2506	1664	0.776	3353	264.6	3562	11.52	0.0091	0.0535

SUPAPACK I CALCULATED DATA

test number L770 test date 22/11/69

AIR
face area 0.2072m^2
flow area 0.1670m^2
equivalent diameter 2.801mm
primary surface area 0.7748m^2
secondary surface area 7.1065m^2

WATER
flow area 1.5838E-03 m^2
equivalent diameter 3.876mm
surface area 0.747m^2

face velocity m/s	actual velocity m/s	US overall W/K	hS water W/K	hS air W/K	fin efficiency	h water W/m^2K	h air W/m^2K	Re air	L/De air	j air	f air
5.333	6.613	856	3459	1138	0.842	4629	168.4	1100	11.52	0.0178	0.0871
8.597	10.662	954	3498	1311	0.819	4680	198.7	1833	11.52	0.0128	0.0639
10.447	12.955	1013	3411	1441	0.803	4564	222.3	2272	11.52	0.0117	0.0623
12.394	15.370	1070	3430	1555	0.789	4590	243.8	2724	11.52	0.0107	0.0577
14.179	17.584	1113	3459	1640	0.778	4629	260.1	3138	11.52	0.0100	0.0550
15.570	19.309	1131	3450	1683	0.773	4616	268.5	3465	11.52	0.0094	0.0541

SUPAPACK I CALCULATED DATA

test number L771 test date 25/11/69

AIR
face area 0.2072m^2
flow area 0.1670m^2
equivalent diameter 2.801mm
primary surface area 0.7748m^2
secondary surface area 7.1065m^2

WATER
flow area 1.5838E-03 m^2
equivalent diameter 3.876mm
surface area 0.747m^2

face velocity m/s	actual velocity m/s	US overall W/K	hS water W/K	hS air W/K	fin efficiency	h water W/m^2K	h air W/m^2K	Re air	L/De air	j air	f air
5.309	6.584	950	5897	1132	0.842	7891	167.5	1115	11.52	0.0176	0.0886
8.091	10.034	1099	5944	1349	0.815	7953	205.5	1752	11.52	0.0140	0.0705
10.253	12.715	1156	5855	1440	0.803	7834	222.1	2276	11.52	0.0118	0.0632
12.229	15.165	1205	5873	1516	0.794	7859	236.3	2744	11.52	0.0104	0.0593
13.794	17.106	1248	5846	1587	0.785	7823	249.9	3121	11.52	0.0097	0.0568
15.438	19.145	1273	5832	1629	0.780	7804	257.8	3515	11.52	0.0089	0.0545

SUPAPACK I CALCULATED DATA

test number L772 test date 26/11/69

AIR
face area 0.2072m^2
flow area 0.1686m^2
equivalent diameter 3.584mm
primary surface area 1.1623m^2
secondary surface area 8.2324m^2

WATER
flow area 2.3756E-03 m^2
equivalent diameter 3.876mm
surface area 1.121m^2

face velocity m/s	actual velocity m/s	US overall W/K	hS water W/K	hS air W/K	fin efficiency	h water W/m^2K	h air W/m^2K	Re air	L/De air	j air	f air
4.981	6.120	743	2190	1125	0.866	1954	135.6	1359	13.82	0.0151	0.0684
7.133	8.762	828	2202	1327	0.844	1965	163.6	2010	13.82	0.0125	0.0596
9.088	11.164	853	2202	1391	0.837	1965	172.8	2622	13.82	0.0102	0.0531
10.510	12.912	890	2226	1484	0.827	1986	186.2	3062	13.82	0.0095	0.0512
11.872	14.584	916	2226	1556	0.819	1986	196.8	3479	13.82	0.0088	0.0495
15.524	19.071	960	2226	1687	0.805	1986	216.5	4582	13.82	0.0074	0.0447

SUPAPACK I CALCULATED DATA

test number L773 test date 26/11/69

AIR
face area 0.2072m^2
flow area 0.1686m^2
equivalent diameter 3.584mm
primary surface area 1.1623m^2
secondary surface area 8.2324m^2

WATER
flow area 2.3756E-03 m^2
equivalent diameter 3.876mm
surface area 1.121m^2

face velocity m/s	actual velocity m/s	US overall W/K	hS water W/K	hS air W/K	fin efficiency	h water W/m^2K	h air W/m^2K	Re air	L/De air	j air	f air
4.999	6.141	838	3793	1075	0.872	3384	128.9	1303	13.82	0.0146	0.0719
7.894	9.698	1014	3876	1373	0.839	3457	170.2	2144	13.82	0.0120	0.0588
10.305	12.660	1075	3751	1507	0.824	3346	189.6	2850	13.82	0.0101	0.0525
12.276	15.081	1231	3793	1823	0.791	3384	237.5	3439	13.82	0.0106	0.0498
13.871	17.041	1185	3824	1717	0.802	3411	221.1	3925	13.82	0.0087	0.0486
15.471	19.006	1219	3845	1785	0.795	3430	231.7	4411	13.82	0.0081	0.0472

SUPAPACK 1 CALCULATED DATA

test number L774 test date 27/11/69

AIR
face area 0.2072m^2
flow area 0.1686m^2
equivalent diameter 3.584mm
primary surface area 1.1623m^2
secondary surface area 8.2324m^2

WATER
flow area 2.3756E-03 m^2
equivalent diameter 3.876mm
surface area 1.121m^2

face velocity m/s	actual velocity m/s	US overall W/K	hS water W/K	hS air W/K	fin efficiency	h water W/m^2K	h air W/m^2K	Re air	L/De air	j air	f air
5.060	6.216	880	5198	1059	0.874	4637	126.7	1338	13.82	0.0141	0.0705
7.933	9.746	1037	5237	1293	0.848	4671	158.9	2167	13.82	0.0111	0.0589
10.340	12.703	1160	5285	1487	0.827	4714	186.6	2876	13.82	0.0099	0.0525
12.265	15.068	1215	5218	1585	0.816	4654	201.1	3449	13.82	0.0089	0.0502
13.889	17.063	1266	5237	1670	0.807	4671	213.9	3929	13.82	0.0084	0.0487
15.417	18.939	1291	5246	1712	0.803	4680	220.4	4385	13.82	0.0078	0.0475

SUPAPACK I CALCULATED DATA

test number L775 test date 27/11/69

AIR
face area 0.2072m^2
flow area 0.1686m^2
equivalent diameter 3.584mm
primary surface area 1.1623m^2
secondary surface area 8.2324m^2

WATER
flow area 2.3756E-03 m^2
equivalent diameter 3.876mm
surface area 1.121m^2

face velocity m/s	actual velocity m/s	US overall W/K	hS water W/K	hS air W/K	fin efficiency	h water W/m^2K	h air W/m^2K	Re air	L/De air	j air	f air
4.901	6.021	898	6413	1044	0.875	5721	124.8	1273	13.82	0.0145	0.0738
7.907	9.714	1143	6432	1390	0.837	5737	172.7	2130	13.82	0.0122	0.0598
10.352	12.718	1196	6404	1471	0.828	5713	184.3	2849	13.82	0.0098	0.0527
12.291	15.100	1272	6359	1591	0.815	5672	202.0	3428	13.82	0.0090	0.0502
13.917	17.097	1344	6450	1698	0.804	5753	218.3	3927	13.82	0.0085	0.0486
15.540	19.091	1356	6450	1717	0.802	5753	221.1	4409	13.82	0.0077	0.0474

SUPAPACK I CALCULATED DATA

test number L789 test date 11/12/69

AIR
face area 0.2072m^2
flow area 0.1670m^2
equivalent diameter 2.801mm
primary surface area 1.5497m^2
secondary surface area 14.7153m^2

WATER
flow area 3.1675E-03 m^2
equivalent diameter 3.876mm
surface area 1.495m^2

face velocity m/s	actual velocity m/s	US overall W/K	hS water W/K	hS air W/K	fin efficiency	h water W/m^2K	h air W/m^2K	Re air	L/De air	j air	f air
4.903	6.080	1159	5343	1481	0.898	3575	100.3	1003	23.84	0.0115	0.0625
8.106	10.053	1465	5547	1991	0.865	3711	139.5	1727	23.84	0.0095	0.0514
10.500	13.021	1628	5608	2295	0.845	3752	164.1	2277	23.84	0.0085	0.0467
12.426	15.410	1691	5506	2441	0.836	3684	176.3	2747	23.84	0.0076	0.0453
13.942	17.290	1739	5506	2542	0.830	3684	184.8	3128	23.84	0.0071	0.0449
15.432	19.137	1783	5506	2638	0.824	3684	193.0	3470	23.84	0.0067	0.0440

SUPAPACK I CALCULATED DATA

test number L790 test date 12/12/69

AIR
face area 0.2072m^2
flow area 0.1670m^2
equivalent diameter 2.801mm
primary surface area 1.5497m^2
secondary surface area 14.7153m^2

WATER
flow area 3.1675E-03 m^2
equivalent diameter 3.876mm
surface area 1.495m^2

face velocity m/s	actual velocity m/s	US overall W/K	hS water W/K	hS air W/K	fin efficiency	h water W/m^2K	h air W/m^2K	Re air	L/De air	j air	f air
6.021	7.466	1350	6976	1674	0.885	4667	114.8	1242	23.84	0.0107	0.0570
8.783	10.892	1591	7024	2058	0.860	4699	144.8	1882	23.84	0.0090	0.0467
10.943	13.571	1737	6976	2314	0.844	4667	165.7	2385	23.84	0.0082	0.0473
12.850	15.936	1804	6976	2433	0.836	4667	175.6	2845	23.84	0.0074	0.0448
14.375	17.826	1902	7005	2610	0.825	4686	190.6	3217	23.84	0.0071	0.0441
15.534	19.264	1941	6985	2687	0.820	4674	197.3	3492	23.84	0.0068	0.0433

SUPAPACK 1 CALCULATED DATA

test number L791 test date 12/12/69

AIR
face area 0.2072m^2
flow area 0.1670m^2
equivalent diameter 2.801mm
primary surface area 1.1623m^2
secondary surface area 10.9109m^2

WATER
flow area 2.3756E-03 m^2
equivalent diameter 3.876mm
surface area 1.121m^2

face velocity m/s	actual velocity m/s	US overall W/K	nS water W/K	hS air W/K	fin efficiency	h water W/m^2K	h air W/m^2K	Re air	L/De air	j air	f air
4.937	6.123	958	5294	1170	0.892	4723	107.4	1039	17.68	0.0120	0.0654
7.973	9.888	1208	5218	1572	0.856	4654	149.6	1747	17.68	0.0102	0.0552
10.440	12.948	1302	5246	1731	0.843	4680	167.2	2343	17.68	0.0086	0.0494
12.503	15.505	1382	5189	1883	0.830	4629	184.4	2841	17.68	0.0078	0.0464
13.995	17.356	1453	5198	2016	0.819	4637	199.7	3204	17.68	0.0076	0.0468
15.407	19.107	1517	5198	2142	0.808	4637	214.6	3544	17.68	0.0074	0.0460

SUPAPACK I CALCULATED DATA

test number L867 test date 7/4/70

AIR
face area 0.2090m^2
flow area 0.1689m^2
equivalent diameter 2.801mm
primary surface area 1.5497m^2
secondary surface area 14.7153m^2

WATER
flow area 3.1675E-03 m^2
equivalent diameter 3.876mm
surface area 1.495m^2

face velocity m/s	actual velocity m/s	US overall W/K	hS water W/K	hS air W/K	fin efficiency	h water W/m^2K	h air W/m^2K	Re air	L/De air	j air	f air
5.845	7.232	1395	6667	1763	0.879	4461	121.7	1177	23.84	0.0119	0.0583
8.094	10.016	1528	6667	1982	0.865	4461	138.8	1661	23.84	0.0097	0.0538
9.821	12.154	1638	6735	2164	0.853	4506	153.4	2053	23.84	0.0087	0.0500
11.350	14.045	1797	6832	2438	0.836	4571	176.0	2406	23.84	0.0086	0.0467
12.589	15.578	1838	6696	2534	0.830	4480	184.1	2701	23.84	0.0081	0.0464
13.499	16.705	1881	6764	2605	0.826	4525	190.1	2922	23.84	0.0077	0.0465
14.545	17.999	2042	6793	2921	0.806	4545	217.8	3163	23.84	0.0082	0.0458
15.555	19.249	1986	6745	2814	0.813	4513	208.3	3388	23.84	0.0073	0.0442

SUPAPACK I CALCULATED DATA

test number L2393 test date 28/6/76

AIR
face area 0.1475m^2
flow area 0.1214m^2
equivalent diameter 4.953mm
primary surface area 0.5464m^2
secondary surface area 2.5577m^2

WATER
flow area 1.6930E-03 m^2
equivalent diameter 3.876mm
surface area 0.527m^2

face velocity m/s	actual velocity m/s	US overall W/K	hS water W/K	hS air W/K	fin efficiency	h water W/m^2K	h air W/m^2K	Re air	L/De air	j air	f air
4.975	6.043	390	4038	431	0.843	7661	159.5	1816	6.51	0.0181	0.0100
9.012	10.947	429	4049	480	0.827	7683	180.2	3309	6.51	0.0112	0.0163
11.623	14.118	511	4032	586	0.792	7651	227.6	4268	6.51	0.0110	0.0190
13.756	16.709	499	4021	569	0.798	7630	220.2	5034	6.51	0.0090	0.0198

SUPAPACK 1 CALCULATED DATA

test number L2395 test date 29/6/76

AIR
face area 0.3233m^2
flow area 0.2637m^2
equivalent diameter 3.584mm
primary surface area 2.3967m^2
secondary surface area 17.1715m^2

WATER
flow area 3.1675E-03 m^2
equivalent diameter 3.876mm
surface area 2.312m^2

face velocity m/s	actual velocity m/s	US overall W/K	hS water W/K	hS air W/K	fin efficiency	h water W/m^2K	h air W/m^2K	Re air	L/De air	j air	f air
3.747	4.594	1327	10581	1517	0.912	4577	84.0	970	18.64	0.0127	0.0806
6.734	8.256	1779	10566	2139	0.877	4571	122.5	1762	18.64	0.0103	0.0665
8.607	10.552	2026	10566	2507	0.858	4571	146.4	2264	18.64	0.0096	0.0633
10.260	12.579	2130	10566	2667	0.849	4571	157.1	2702	18.64	0.0086	0.0601

SUPAPACK 1 CALCULATED DATA

test number L2575 test date 26/2/77

AIR
face area 0.2989m^2
flow area 0.2400m^2
equivalent diameter 3.372mm
primary surface area 2.3462m^2
secondary surface area 18.0373m^2

WATER
flow area 3.1675E-03 m^2
equivalent diameter 3.876mm
surface area 2.263m^2

face velocity m/s	actual velocity m/s	US overall W/K	hS water W/K	hS air W/K	fin efficiency	h water W/m^2K	h air W/m^2K	Re air	L/De air	j air	f air
3.772	4.697	1702	9947	2054	0.887	4396	112.0	990	19.81	0.0161	0.0806
6.414	7.987	1893	10197	2324	0.873	4506	128.5	1726	19.81	0.0107	0.0617
8.431	10.499	2494	10197	3301	0.823	4506	192.0	2304	19.81	0.0121	0.0564
10.519	13.100	2657	10197	3594	0.809	4506	212.2	2891	19.81	0.0107	0.0520
4.353	5.421	1302	3890	1956	0.892	1719	106.1	1175	19.81	0.0130	0.0715
2.068	2.575	1030	3890	1402	0.922	1719	73.9	534	19.81	0.0196	0.1083
2.063	2.569	718	2581	995	0.944	1141	51.4	538	19.81	0.0136	0.1066
4.201	5.232	1017	2581	1678	0.907	1141	89.7	1146	19.81	0.0114	0.0721

APPENDIX A3

EXPERIMENTAL AND CALCULATED DATA

RELATING TO THE ENGINE TESTS

P.BAROM	751.50	751.50	751.50	751.50	751.50	751.50	751.50	751.50	mm Hg
SPEED	500	500	500	500	500	500	500	500	rev/min
BRAKE LOAD	0.0	13.0	15.7	19.0	22.5	26.5	32.5	39.5	lbs
THROTTLE	6.2	5.6	6.8	7.3	7.7	7.9	8.3	8.7	degrees
WATER FLOW	0.95	1.10	1.25	1.35	1.50	1.55	2.10	2.70	cms
T WATER IN	1.725	1.673	1.598	1.603	1.596	1.576	1.700	1.858	mV
T WATER OUT	3.296	3.300	3.253	3.258	3.256	3.258	3.270	3.313	mV
AIR P1	3.90	4.45	4.70	4.90	5.20	5.50	5.85	6.63	cms
SLOPE P1	L	L	L	L	L	L	L	L	
AIR P2	4.05	4.55	4.82	5.10	5.40	5.70	6.10	6.90	cms
SLOPE P2	L	L	L	L	L	L	L	L	
AIR TEMP	20.5	15.5	20.0	19.5	19.5	19.0	17.0	17.0	deg. C
FUEL VOL.	100	100	100	100	100	100	100	100	cm^3
FUEL TIME	203.5	162.5	154.4	149.5	140.6	133.0	121.0	105.0	s
FUEL TEMP F	0.898	0.740	0.853	0.853	0.808	0.775	0.760	0.744	mV
FUEL TEMP R	0.940	0.717	0.842	0.830	0.791	0.756	0.717	0.714	mV
EX. CO %	1.1	1.7	2.3	2.7	2.3	1.7	2.8	3.2	
EX. CO2 %	9.5	12.0	12.1	13.0	13.2	12.7	12.5	11.1	
EX. TEMP 1	18.95	18.60	18.00	17.92	18.11	18.03	18.11	18.13	mV
EX. TEMP 2	17.17	18.30	17.55	17.60	17.70	17.87	17.98	18.05	mV
EX. TEMP 3	17.25	16.60	15.85	16.00	16.52	16.97	17.30	17.87	mV
EX. TEMP 4	19.35	18.50	18.00	18.10	18.40	18.70	18.87	18.95	mV
EX. TEMP 5	15.00	17.60	17.30	17.57	17.94	18.33	18.42	18.50	mV
EX. TEMP 6	18.50	18.30	18.20	18.62	19.10	19.00	18.97	18.71	mV

TABLE A3.1 ENGINE TEST EXPERIMENTAL DATA

P.BAROM	744.75	744.75	744.75	744.75	744.75	744.75	744.75	744.75	mm Hg
SPEED	1003	1003	997	1002	1003	993	993	1001	rev/min
BRAKE LOAD	0.0	8.6	18.8	33.5	53.0	62.0	79.0	87.0	lbs
THROTTLE	11.3	11.0	11.8	12.8	14.5	15.6	20.0	87.5	degrees
WATER FLOW	2.05	2.40	3.70	4.60	6.10	6.95	7.15	6.90	cms
T WATER IN	1.086	1.012	1.166	1.220	1.361	1.435	1.364	1.353	mV
T WATER OUT	3.255	3.190	3.212	3.248	3.275	3.285	3.283	3.295	mV
AIR P1	7.40	9.60	11.90	14.80	19.10	20.75	24.10	24.60	cms
SLOPE P1	L	L	L	L	L	L	L	L	
AIR P2	7.70	10.10	12.60	16.00	20.90	22.95	26.90	27.90	cms
SLOPE P2	L	L	L	L	L	L	L	L	
AIR TEMP	21.0	25.0	26.0	27.5	28.0	29.5	30.5	27.5	deg. C
FUEL VOL.	100	100	100	200	200	300	400	200	cm^3
FUEL TIME	97.0	87.0	84.5	119.5	92.8	127.0	140.0	119.0	s
FUEL TEMP F	0.811	1.075	1.106	1.133	1.152	1.142	1.080	0.954	mV
FUEL TEMP R	0.785	1.088	1.111	1.132	1.150	1.133	1.075	0.968	mV
EX. CO %	3.5	3.3	1.3	1.3	1.2	1.5	2.2	3.8	
EX. CO2 %	10.0	9.0	9.9	9.2	9.7	9.8	9.2	8.7	
EX. TEMP 1	24.30	23.60	24.60	24.90	24.96	24.90	23.75	25.00	mV
EX. TEMP 2	23.17	22.80	24.55	25.23	25.31	25.10	25.52	24.00	mV
EX. TEMP 3	24.08	23.55	24.30	25.00	25.82	25.75	25.30	24.68	mV
EX. TEMP 4	24.61	23.37	25.60	25.60	26.00	25.85	25.10	24.95	mV
EX. TEMP 5	24.57	23.88	25.10	25.00	25.30	25.20	25.25	23.40	mV
EX. TEMP 6	24.75	24.10	24.80	24.70	24.27	24.05	23.01	25.13	mV

P.BAROM	744.75	744.75	744.75	744.75	744.75	744.75	744.75	744.75	744.75	751.50	mm Hg
SPEED	1550	1493	1507	1493	1499	1490	1500	1495	1500	1500	rev/min
BRAKE LOAD	0.0	10.8	19.0	32.5	44.6	59.0	74.0	86.3	99.0	107.0	lbs
THROTTLE	12.1	12.0	12.5	13.7	14.7	15.8	18.3	21.2	27.2	87.0	degrees
WATER FLOW	4.60	4.80	5.20	5.90	6.80	7.80	8.75	9.60	11.40	13.60	cms
T WATER IN	1.330	1.140	1.162	1.190	1.246	1.330	1.395	1.473	1.538	1.900	mV
T WATER OUT	3.260	3.230	3.232	3.248	3.263	3.260	3.283	3.284	3.275	3.326	mV
AIR P1	10.10	13.80	15.65	19.00	22.00	25.60	30.65	35.30	38.65	40.10	cms
SLOPE P1	L	L	L	L	L	L	L	L	L	L	
AIR P2	10.75	14.80	16.80	20.80	24.60	29.15	35.40	41.50	46.70	22.90	cms
SLOPE P2	L	L	L	L	L	L	L	L	L	M	
AIR TEMP	24.5	26.3	25.5	26.0	28.0	28.0	24.8	25.5	25.5	28.0	deg. C
FUEL VOL.	100	100	100	200	200	200	200	200	400	400	cm^3
FUEL TIME	58.0	65.8	57.0	92.8	78.5	64.0	47.5	40.0	97.4	67.5	s
FUEL TEMP F	0.872	1.144	1.103	1.087	1.080	1.043	1.005	0.981	0.980	0.831	mV
FUEL TEMP R	0.846	1.106	1.076	1.053	1.032	1.060	0.972	0.946	0.946	0.832	mV
EX. CO %	1.9	1.2	1.0	1.0	1.0	1.9	3.9	5+	5+	5+	
EX. CO2 %	10.8	10.0	10.2	9.9	9.2	9.2	8.3	8.0	7.2	10.0	
EX. TEMP 1	27.48	26.35	26.26	26.20	26.80	26.65	25.70	25.11	26.86	26.27	mV
EX. TEMP 2	27.07	26.60	26.47	26.70	27.18	26.67	27.00	26.60	26.80	25.08	mV
EX. TEMP 3	26.40	25.80	26.23	26.81	27.20	26.32	25.48	25.06	25.52	24.03	mV
EX. TEMP 4	27.13	26.95	27.91	27.50	27.45	26.65	25.53	25.10	24.23	24.60	mV
EX. TEMP 5	26.48	26.40	26.45	26.41	26.52	26.43	26.40	26.00	25.31	25.00	mV
EX. TEMP 6	26.80	26.50	26.45	26.41	26.33	25.50	24.80	24.40	25.27	26.26	mV

P.BAROM	744.75	744.75	744.75	744.75	744.75	744.75	752.75	752.75	751.50	mm Hg
SPEED	2047	2019	2004	2001	2000	1997	2002	1995	2000	rev/min
BRAKE LOAD	0.0	11.4	21.5	35.4	47.5	73.0	90.5	106.0	109.0	lbs
THROTTLE	13.2	13.1	14.3	15.3	16.7	20.5	24.8	34.5	87.0	degrees
WATER FLOW	7.90	9.60	9.10	9.40	10.30	12.90	13.10	14.80	16.50	cms
T WATER IN	1.570	1.800	1.580	1.510	1.560	1.732	1.575	1.727	1.970	mV
T WATER OUT	3.291	3.207	3.254	3.266	3.292	3.316	3.304	3.320	3.310	mV
AIR P1	13.40	16.90	20.20	24.90	29.40	18.70	21.00	23.80	25.65	cms
SLOPE P1	L	L	L	L	L	M	M	M	M	
AIR P2	14.50	18.40	22.35	28.15	33.80	22.60	26.40	30.50	33.00	cms
SLOPE P2	L	L	L	L	L	M	M	M	M	
AIR TEMP	26.2	22.0	23.7	24.7	25.0	27.3	23.0	25.8	32.0	deg. C
FUEL VOL.	200	100	100	200	200	400	200	400	400	cm^3
FUEL TIME	121.5	51.6	42.0	66.2	51.8	70.0	29.2	52.5	46.0	s
FUEL TEMP F	0.928	0.887	0.909	0.950	0.941	0.918	0.687	0.771	0.938	mV
FUEL TEMP R	0.883	0.874	0.891	0.926	0.928	0.906	0.683	0.760	0.936	mV
EX. CO %	1.1	1.1	1.3	2.5	4.7	5+	5+	5+	5+	
EX. CO2 %	11.0	9.2	11.5	10.5	9.0	8.2	9.2	10.4	8.8	
EX. TEMP 1	31.00	28.52	28.52	27.95	27.11	25.45	26.79	28.10	26.90	mV
EX. TEMP 2	29.35	28.40	28.50	28.13	26.75	26.48	27.01	28.05	25.47	mV
EX. TEMP 3	28.45	28.40	28.89	27.70	26.15	24.90	24.70	26.10	23.66	mV
EX. TEMP 4	29.17	29.45	29.30	27.83	26.11	24.85	24.00	24.18	23.91	mV
EX. TEMP 5	29.25	28.90	28.50	27.68	26.90	26.50	26.15	26.00	23.04	mV
EX. TEMP 6	28.63	28.16	28.20	27.30	26.05	25.27	26.44	24.60	24.38	mV

P.BAROM	744.75	752.75	752.75	752.75	752.75	752.75	752.75	752.75	752.75	751.50	mm Hg
SPEED	2558	2509	2500	2502	2504	2499	2507	2504	2503	2500	rev/min
BRAKE LOAD	0.0	12.5	20.5	31.5	41.3	55.0	73.0	87.5	104.0	104.0	lbs
THROTTLE	14.1	14.3	15.0	31.5	17.7	19.5	23.0	27.7	43.8	87.0	degrees
WATER FLOW	11.05	13.80	14.90	13.80	13.40	13.80	16.00	18.10	18.70	19.30	cms
T WATER IN	1.755	2.011	2.022	1.886	1.810	1.823	1.873	1.875	1.883	2.125	mV
T WATER OUT	3.317	3.325	3.300	3.306	3.303	3.322	3.328	3.322	3.350	3.330	mV
AIR P1	17.00	9.75	10.25	13.35	15.60	18.75	23.20	27.05	31.20	34.10	cms
SLOPE P1	L	M	M	M	M	M	M	M	M	M	
AIR P2	18.70	10.90	12.80	15.40	18.50	22.80	29.30	35.00	41.60	45.40	cms
SLOPE P2	L	M	M	M	M	M	M	M	M	M	
AIR TEMP	30.0	26.0	26.2	26.0	27.0	25.0	28.5	31.5	32.5	42.0	deg. C
FUEL VOL.	200	200	200	200	400	400	400	400	400	400	cm^3
FUEL TIME	97.2	76.2	68.4	54.6	86.8	68.8	55.0	50.0	41.0	35.8	s
FUEL TEMP F	1.000	0.984	0.985	0.971	0.966	0.885	0.879	0.926	0.928	1.000	mV
FUEL TEMP R	0.947	0.933	0.945	0.931	0.927	0.858	0.855	0.890	0.902	0.975	mV
EX. CO %	1.3	1.5	2.2	4.1	5+	5+	5+	5+	5+	5+	
EX. CO2 %	11.5	12.0	11.5	10.5	9.2	8.7	10.0	11.0	9.5	7.8	
EX. TEMP 1	32.10	30.82	30.00	28.60	27.60	27.70	27.78	29.90	29.61	26.67	mV
EX. TEMP 2	30.66	30.40	30.00	28.70	27.70	28.80	29.50	30.62	30.02	25.55	mV
EX. TEMP 3	30.80	29.82	29.42	28.00	26.40	26.50	26.62	28.02	26.48	24.82	mV
EX. TEMP 4	31.19	30.14	29.15	27.60	26.27	25.90	25.85	25.45	24.15	23.62	mV
EX. TEMP 5	31.17	29.55	29.29	28.06	27.50	27.61	27.30	27.02	27.30	24.10	mV
EX. TEMP 6	30.60	29.20	28.77	27.40	26.50	26.48	26.60	27.15	25.50	25.70	mV

P.BAROM	744.75	752.75	752.75	752.75	752.75	752.75	752.75	752.75	751.50	mm Hg
SPEED	3063	3007	3004	3003	3004	2989	3003	2997	3000	rev/min
BRAKE LOAD	0.0	14.0	23.8	36.5	46.3	63.5	78.5	92.0	102.0	lbs
THROTTLE	15.0	15.5	16.8	18.7	20.0	23.2	27.5	35.3	87.0	degrees
WATER FLOW	13.55	14.00	15.80	16.80	18.30	18.90	21.30	22.40	23.70	cms
T WATER IN	1.888	1.840	1.952	1.977	1.980	1.938	1.990	1.990	2.211	mV
T WATER OUT	3.334	3.315	3.333	3.345	3.336	3.360	3.368	3.372	3.351	mV
AIR P1	20.22	12.30	14.50	17.90	20.70	25.50	30.60	34.95	23.30	cms
SLOPE P1	L	M	M	M	M	M	M	M	H	
AIR P2	22.55	14.10	16.90	21.55	25.40	32.60	40.50	47.70	33.20	cms
SLOPE P2	L	M	M	M	M	M	M	M	H	
AIR TEMP	28.0	27.0	27.0	26.5	27.0	28.3	30.5	31.7	45.0	deg. C
FUEL VOL.	200	200	400	400	400	400	400	400	400	cm^3
FUEL TIME	79.0	62.6	99.2	78.8	76.0	52.4	43.8	38.5	29.5	s
FUEL TEMP F	1.048	1.078	1.030	1.020	0.950	0.923	0.939	0.952	1.050	mV
FUEL TEMP R	1.017	1.036	0.993	0.976	0.914	0.896	0.905	0.924	1.037	mV
EX. CO %	1.8	2.2	4.3	5+	5+	5+	5+	5+	5+	
EX. CO2 %	11.0	10.8	10.0	9.9	8.4	10.0	10.2	10.0	8.0	
EX. TEMP 1	32.05	31.45	30.18	29.77	29.05	29.45	30.70	30.69	27.99	mV
EX. TEMP 2	31.80	32.04	30.27	30.55	30.36	30.57	31.44	31.60	26.23	mV
EX. TEMP 3	31.05	30.26	29.25	28.53	28.45	28.57	29.02	28.68	26.86	mV
EX. TEMP 4	31.48	29.68	28.29	27.12	26.71	26.97	26.66	26.07	24.22	mV
EX. TEMP 5	31.70	30.11	28.19	28.66	28.39	28.05	28.35	28.80	24.92	mV
EX. TEMP 6	30.80	29.40	28.21	27.46	27.31	27.43	28.47	27.80	27.27	mV

P.BAROM	744.75	752.75	752.75	752.75	752.75	752.75	752.75	752.75	745.55	745.55	mm Hg
SPEED	3567	3507	3505	3498	3501	3497	3489	3506	3500	3500	rev/min
BRAKE LOAD	0.0	11.5	22.0	27.5	32.5	42.0	53.5	65.0	82.0	95.0	lbs
THROTTLE	16.0	16.3	18.5	18.8	20.0	21.3	23.2	26.2	33.7	87.0	degrees
WATER FLOW	16.45	17.10	16.80	17.10	18.40	19.40	21.00	23.10	24.00	20.80	cms
T WATER IN	1.972	1.970	1.978	1.896	1.956	1.964	1.983	2.013	2.200	1.884	mV
T WATER OUT	3.349	3.338	3.364	3.337	3.341	3.352	3.368	3.370	3.290	3.316	mV
AIR P1	23.40	11.40	16.80	18.35	20.20	23.10	27.00	32.00	25.40	24.20	cms
SLOPE P1	L	M	M	M	M	M	M	M	H	H	
AIR P2	26.80	15.60	20.00	22.30	24.70	28.90	34.80	42.30	28.10	34.20	cms
SLOPE P2	L	M	M	M	M	M	M	M	H	H	
AIR TEMP	26.0	26.0	27.3	27.5	29.0	28.5	30.0	34.0	33.0	31.5	deg. C
FUEL VOL.	200	200	400	300	400	400	400	400	400	400	cm^3
FUEL TIME	69.0	55.0	82.5	55.4	66.2	57.2	49.4	43.2	37.0	25.8	s
FUEL TEMP F	0.927	0.987	0.962	0.974	0.968	0.978	1.013	1.022	1.100	0.912	mV
FUEL TEMP R	0.910	0.944	0.930	0.936	0.940	0.948	0.983	0.993	1.002	0.898	mV
EX. CO %	1.6	5+	5+	5+	5+	5+	5+	5+	5+	5+	
EX. CO2 %	11.5	10.8	9.2	9.8	8.2	8.0	9.5	10.0	10.5	8.0	
EX. TEMP 1	33.30	31.14	30.30	29.93	29.42	29.40	29.93	30.96	32.60	30.77	mV
EX. TEMP 2	34.12	31.79	30.38	30.50	30.78	30.80	31.20	31.82	37.30	28.77	mV
EX. TEMP 3	32.30	30.61	29.05	28.96	28.23	28.64	28.60	28.80	29.15	28.23	mV
EX. TEMP 4	32.18	29.79	28.42	27.96	27.20	27.16	27.15	27.23	27.15	29.00	mV
EX. TEMP 5	33.11	30.99	29.96	29.83	29.46	29.02	28.62	28.67	29.14	27.65	mV
EX. TEMP 6	31.80	30.12	29.10	28.65	28.30	28.04	28.09	28.78	28.80	27.80	mV

P.BAROM	744.75	752.75	752.75	752.75	752.75	752.75	752.75	752.75	mm Hg
SPEED	4076	4013	4030	4010	4010	4000	4000	4000	rev/min
BRAKE LOAD	0.0	11.5	16.0	25.3	35.3	44.8	55.0	63.8	lbs
THROTTLE	17.0	18.0	15.4	20.0	21.7	23.3	25.2	28.1	degrees
WATER FLOW	20.05	20.10	21.30	21.30	22.50	23.45	24.70	25.70	cms
T WATER IN	2.096	2.024	2.213	2.200	2.195	2.204	2.203	2.203	mV
T WATER OUT	3.367	3.365	3.380	3.380	3.383	3.389	3.389	3.388	mV
AIR P1	27.80	16.80	17.00	20.00	23.80	27.30	31.60	35.70	cms
SLOPE P1	L	M	M	M	M	M	M	M	
AIR P2	38.20	19.80	20.50	24.70	30.30	35.50	42.30	49.20	cms
SLOPE P2	L	M	M	M	M	M	M	M	
AIR TEMP	32.0	31.5	22.0	23.0	26.0	26.5	30.0	32.5	deg. C
FUEL VOL.	300	400	400	400	400	400	400	400	cm^3
FUEL TIME	88.0	87.7	79.4	65.0	53.6	47.0	41.2	36.6	s
FUEL TEMP F	1.040	1.083	0.837	0.930	0.970	0.970	0.984	1.025	mV
FUEL TEMP R	0.982	1.036	0.803	0.889	0.938	0.942	0.970	1.012	mV
EX. CO %	2.8	4.5	5+	5+	5+	5+	5+	5+	
EX. CO2 %	10.5	9.5	12.5	11.5	11.2	11.0	11.2	11.2	
EX. TEMP 1	33.00	31.40	30.60	29.79	29.77	30.06	30.60	31.16	mV
EX. TEMP 2	34.00	31.47	31.40	30.40	30.11	30.15	30.70	31.20	mV
EX. TEMP 3	32.50	30.39	29.90	29.30	29.15	28.80	28.80	28.70	mV
EX. TEMP 4	30.76	29.50	29.30	28.80	28.20	27.90	27.80	27.80	mV
EX. TEMP 5	31.58	30.96	31.50	30.90	29.96	29.50	29.50	29.60	mV
EX. TEMP 6	30.88	29.95	30.40	29.90	29.26	29.20	29.70	30.17	mV

P.BARO	744.75	752.75	751.50	751.50	751.50	mm Hg
SPEED	4512	4500	4500	4500	4500	rev/min
BRAKE LOAD	0.0	16.5	30.5	42.2	58.0	lbs
THROTTLE	18.5	17.8	23.3	25.6	30.6	degrees
WATER FLOW	22.70	26.80	22.80	25.00	27.00	cms
T WATER IN	2.142	2.288	2.155	2.136	2.131	mV
T WATER OUT	3.399	3.406	3.406	3.415	3.426	mV
AIR P1	33.00	21.10	15.00	17.80	22.60	cms
SLOPE P1	L	M	H	H	H	
AIR P2	37.70	26.00	19.40	23.80	31.60	cms
SLOPE P2	L	M	H	H	H	
AIR TEMP	35.0	28.5	36.0	39.0	42.5	deg. C
FUEL VOL.	300	400	400	400	400	cm^3
FUEL TIME	70.5	63.6	47.6	41.2	33.7	s
FUEL TEMP F	1.110	1.091	1.042	1.086	1.069	mV
FUEL TEMP R	1.037	1.000	1.035	1.072	1.049	mV
EX. CO %	4.5	5+	5+	5+	5+	
EX. CO2 %	9.0	11.7	10.5	10.5	10.5	
EX. TEMP 1	31.90	30.32	30.57	31.38	33.42	mV
EX. TEMP 2	32.04	30.57	31.70	32.32	34.37	mV
EX. TEMP 3	31.77	29.84	29.30	29.43	29.93	mV
EX. TEMP 4	30.05	29.50	28.68	28.35	28.36	mV
EX. TEMP 5	30.79	31.10	30.17	30.15	30.10	mV
EX. TEMP 6	29.95	30.20	29.53	29.55	30.97	mV

SPEED	500	500	500	500	500	500	500	500	rev/min
POWER	0.000	1.731	2.091	2.530	2.996	3.529	4.328	5.260	kW
WATER FLOW	3.01	3.10	3.20	3.26	3.35	3.39	3.73	4.12	g/s
T WATER IN	42.77	41.50	39.67	39.80	39.62	39.14	42.16	46.01	deg. C
T WATER OUT	80.73	80.83	79.69	79.82	79.77	79.82	80.10	81.14	deg.C
AIR FLOW	4.79	5.63	5.79	6.05	6.42	6.81	7.33	8.31	g/s
AIR TEMP	20.50	15.50	20.00	19.50	19.50	19.00	17.00	17.00	deg.C
FUEL FLOW	0.366	0.458	0.482	0.498	0.529	0.559	0.615	0.709	g/s
FUEL TEMP	22.47	18.56	21.36	21.36	20.24	19.43	19.05	18.66	deg.C
A/F RATIO	13.09	12.30	12.01	12.16	12.13	12.17	11.92	11.73	
% CO	1.10	1.70	2.30	2.70	2.30	1.70	2.80	3.20	
% CO2	9.50	12.00	12.10	13.00	13.20	12.70	12.50	11.10	
EX. FLOW	5.15	6.09	6.27	6.55	6.95	7.37	7.95	9.02	g/s
EX. TEMP	450.1	452.1	444.5	447.6	455.3	459.3	460.3	462.5	deg.C

TABLE A3.2 ENGINE TEST INTERMEDIATE CALCULATED DATA

SPEED	1003	1003	997	1002	1003	993	993	1001	rev/min
POWER	0.000	2.297	4.992	8.939	14.157	16.396	20.891	23.192	kW
WATER FLOW	3.70	3.93	4.78	5.38	6.42	7.03	7.17	6.99	g/s
T WATER IN	27.12	25.29	29.09	30.42	33.88	35.69	33.95	33.68	deg. C
T WATER OUT	79.74	78.18	78.71	79.57	80.22	80.47	80.42	80.71	deg.C
AIR FLOW	8.97	11.36	13.99	17.24	22.17	23.86	27.54	28.61	g/s
AIR TEMP	21.00	24.95	26.00	27.50	28.00	29.50	30.50	27.50	deg.C
FUEL FLOW	0.767	0.855	0.880	1.245	1.603	1.757	2.126	1.250	g/s
FUEL TEMP	20.32	26.85	27.61	28.28	28.74	28.50	26.97	23.86	deg.C
A/F RATIO	11.69	13.28	15.89	13.84	13.82	13.58	12.96	22.88	
% CO	3.50	3.30	1.30	1.30	1.20	1.50	2.20	3.80	
% CO2	10.00	9.00	9.90	9.20	9.70	9.80	9.20	8.70	
EX. FLOW	9.74	12.22	14.87	18.48	23.77	25.62	29.67	29.86	g/s
EX. TEMP	604.3	591.7	622.7	629.9	635.3	633.5	623.0	617.1	deg.C

SPEED	1550	1493	1507	1493	1499	1490	1500	1495	1500	1500	rev/min
POWER	0.000	4.294	7.625	12.922	17.804	23.411	29.560	34.359	39.547	42.742	kW
WATER FLOW	5.38	5.52	5.80	6.28	6.92	7.65	8.35	8.99	10.39	12.18	g/s
T WATER IN	33.12	28.45	28.99	29.68	31.05	33.12	34.71	36.62	38.21	47.03	deg. C
T WATER OUT	79.86	79.14	79.19	79.57	79.94	79.86	80.42	80.44	80.22	81.45	deg.C
AIR FLOW	11.98	16.19	18.44	22.31	25.52	29.68	36.18	41.46	45.36	46.78	g/s
AIR TEMP	24.50	26.30	25.50	26.00	28.00	28.00	24.80	25.50	25.50	28.00	deg.C
FUEL FLOW	1.283	1.131	1.305	1.603	1.896	2.325	3.133	3.720	3.055	4.409	g/s
FUEL TEMP	21.83	28.55	27.54	27.14	26.97	26.06	25.12	24.53	24.50	20.81	deg.C
A/F RATIO	9.34	14.32	14.13	13.91	13.46	12.76	11.55	11.14	14.85	10.61	
% CO	1.90	1.20	1.00	1.00	1.00	1.90	3.90	5+	5+	5+	
% CO2	10.80	10.00	10.20	9.90	9.20	9.20	8.30	8.00	7.20	10.00	
EX. FLOW	13.27	17.32	19.75	23.92	27.41	32.00	39.31	45.18	48.42	51.19	g/s
EX. TEMP	670.2	661.0	664.8	666.3	674.0	661.1	645.0	635.3	642.1	633.6	deg.C

SPEED	2047	2019	2004	2001	2000	1997	2002	1995	2000	rev/min
POWER	0.000	6.129	11.474	18.864	25.299	38.823	48.250	56.316	58.055	kW
WATER FLOW	7.72	8.99	8.61	8.84	9.53	11.60	11.77	13.19	14.65	g/s
T WATER IN	38.99	44.60	39.23	37.52	38.75	42.94	39.11	42.82	48.73	deg. C
T WATER OUT	80.61	78.59	79.72	80.01	80.63	81.21	80.92	81.31	81.07	deg.C
AIR FLOW	15.73	20.33	24.04	29.44	34.67	46.75	54.38	60.53	62.76	g/s
AIR TEMP	26.20	22.00	23.70	24.70	25.00	27.30	23.00	25.80	32.00	deg.C
FUEL FLOW	1.225	1.442	1.771	2.248	2.873	4.251	5.096	5.669	6.470	g/s
FUEL TEMP	23.22	22.20	22.75	23.76	23.54	22.97	17.24	19.33	23.46	deg.C
A/F RATIO	12.84	14.10	13.57	13.10	12.07	11.00	10.67	10.68	9.70	
% CO	1.10	1.10	1.30	2.50	4.70	5+	5+	5+	5+	
% CO2	11.00	9.20	11.50	10.50	9.00	8.20	9.20	10.40	8.80	
EX. FLOW	16.96	21.77	25.81	31.68	37.54	51.00	59.47	66.20	69.23	g/s
EX. TEMP	729.4	709.3	711.2	691.1	661.6	641.7	644.0	654.4	622.2	deg.C

SPEED	2558	2509	2500	2502	2504	2499	2507	2504	2503	2500	rev/min
POWER	0.000	8.352	13.648	20.989	27.540	36.603	48.737	58.348	69.323	69.240	kW
WATER FLOW	10.12	12.35	13.27	12.35	12.01	12.35	14.22	16.08	16.62	17.18	g/s
T WATER IN	43.50	49.72	49.99	46.69	44.84	45.16	46.37	46.42	46.61	52.49	deg. C
T WATER OUT	81.24	81.43	80.83	80.97	80.90	81.36	81.50	81.36	82.03	81.55	deg.C
AIR FLOW	19.51	24.91	26.14	34.06	39.54	48.02	58.10	66.45	76.06	78.55	g/s
AIR TEMP	30.00	26.00	26.20	26.00	27.00	25.00	28.50	31.50	32.50	42.00	deg.C
FUEL FLOW	1.531	1.953	2.175	2.725	3.429	4.326	5.411	5.952	7.259	8.313	g/s
FUEL TEMP	25.00	24.60	24.63	24.28	24.16	22.15	22.00	23.17	23.22	25.00	deg.C
A/F RATIO	12.74	12.76	12.02	12.50	11.53	11.10	10.74	11.17	10.48	9.45	
% CO	1.30	1.50	2.20	4.10	5+	5+	5+	5+	5+	5+	
% CO2	11.50	12.00	11.50	10.50	9.20	8.70	10.00	11.00	9.50	7.80	
EX. FLOW	21.04	26.86	28.32	36.79	42.96	52.35	63.51	72.41	83.32	86.86	g/s
EX. TEMP	776.0	745.6	732.5	699.4	675.0	677.1	683.1	704.0	684.8	644.1	deg.C

SPEED	3063	3007	3004	3003	3004	2989	3003	2997	3000	rev/min
POWER	0.000	11.211	19.040	29.190	37.039	50.546	62.778	73.427	81.490	kW
WATER FLOW	12.14	12.51	14.04	14.92	16.26	16.81	19.06	20.12	21.40	g/s
T WATER IN	46.74	45.57	48.29	48.90	48.97	47.95	49.21	49.21	54.57	deg. C
T WATER OUT	81.64	81.19	81.62	81.91	81.69	82.27	82.46	82.56	82.05	deg.C
AIR FLOW	23.46	31.21	36.76	45.46	52.36	63.87	75.49	85.45	100.56	g/s
AIR TEMP	28.00	27.00	27.00	26.50	27.00	28.30	30.50	31.70	45.00	deg.C
FUEL FLOW	1.884	2.377	3.000	3.777	3.916	5.679	6.795	7.730	10.088	g/s
FUEL TEMP	26.18	26.92	25.74	25.49	23.76	23.09	23.49	23.81	26.23	deg.C
A/F RATIO	12.46	13.13	12.25	12.04	13.37	11.25	11.11	11.05	9.97	
% CO	1.80	2.20	4.30	5+	5+	5+	5+	5+	5+	
% CO2	11.00	10.80	10.00	9.90	8.40	10.00	10.20	10.00	8.00	
EX. FLOW	25.34	33.59	39.76	49.23	56.27	69.55	82.29	93.18	110.65	g/s
EX. TEMP	783.6	758.7	724.4	714.8	708.0	712.3	728.9	726.1	674.8	deg.C

SPEED	3567	3507	3505	3498	3501	3497	3489	3506	3500	3500	rev/min
POWER	0.000	10.740	20.535	25.617	30.301	39.114	49.709	60.689	76.430	88.547	kW
WATER FLOW	14.61	15.18	14.92	15.18	16.35	17.27	18.77	20.80	21.70	18.58	g/s
T WATER IN	48.78	48.73	48.92	46.93	48.39	48.58	49.04	49.77	54.30	46.64	deg. C
T WATER OUT	82.01	81.74	82.37	81.72	81.81	82.08	82.46	82.51	80.59	81.21	deg.C
AIR FLOW	27.46	29.09	42.48	46.32	50.50	57.85	66.92	77.32	116.69	111.76	g/s
AIR TEMP	26.00	26.00	27.30	27.50	29.00	28.50	30.00	34.00	33.00	31.50	deg.C
FUEL FLOW	2.157	2.705	3.607	4.029	4.495	5.203	6.024	6.889	8.043	11.535	g/s
FUEL TEMP	23.19	24.67	24.06	24.35	24.21	24.45	25.32	25.54	27.46	22.82	deg.C
A/F RATIO	12.73	10.75	11.78	11.50	11.23	11.12	11.11	11.22	14.51	9.69	
% CO	1.60	5+	5+	5+	5+	5+	5+	5+	5+	5+	
% CO2	11.50	10.80	9.20	9.80	8.20	8.00	9.50	10.00	10.50	8.00	
EX. FLOW	29.61	31.79	46.09	50.35	55.00	63.06	72.94	84.21	124.73	123.29	g/s
EX. TEMP	813.9	763.7	735.9	730.6	722.4	720.6	724.2	738.8	770.2	720.1	deg.C

SPEED	4076	4013	4030	4010	4010	4000	4000	4000	rev/min
POWER	0.000	12.290	17.172	27.018	37.697	47.722	58.588	67.962	kW
WATER FLOW	17.87	17.92	19.06	19.06	20.22	21.15	22.40	23.43	g/s
T WATER IN	51.78	50.04	54.62	54.30	54.18	54.40	54.37	54.37	deg. C
T WATER OUT	82.44	82.39	82.75	82.75	82.82	82.97	82.97	82.94	deg.C
AIR FLOW	31.45	41.46	44.36	51.81	60.47	69.05	78.15	86.84	g/s
AIR TEMP	32.00	31.50	22.00	23.00	26.00	26.50	30.00	32.50	deg.C
FUEL FLOW	2.536	3.393	3.748	4.578	5.552	6.332	7.223	8.131	g/s
FUEL TEMP	25.98	27.04	20.96	23.27	24.25	24.25	24.60	25.61	deg.C
A/F RATIO	12.40	12.22	11.83	11.32	10.89	10.90	10.82	10.68	
% CO	2.80	4.50	5+	5+	5+	5+	5+	5+	
% CO2	10.50	9.50	12.50	11.50	11.20	11.00	11.20	11.20	
EX. FLOW	33.98	44.85	48.11	56.39	66.02	75.38	85.37	94.97	g/s
EX. TEMP	803.2	766.0	754.4	739.3	731.6	728.8	738.2	746.8	deg.C

SPEED	4512	4500	4500	4500	4500	rev/min
POWER	0.000	19.773	36.551	50.572	69.506	kW
WATER FLOW	20.41	24.57	20.51	22.71	24.78	g/s
T WATER IN	52.90	56.43	53.21	52.75	52.63	deg. C
T WATER OUT	83.21	83.38	83.38	83.60	83.86	deg.C
AIR FLOW	36.69	52.89	68.62	79.86	98.99	g/s
AIR TEMP	35.00	28.50	36.00	39.00	42.50	deg.C
FUEL FLOW	3.166	4.679	6.252	7.223	8.831	g/s
FUEL TEMP	27.71	27.24	26.03	27.12	26.70	deg.C
A/F RATIO	11.59	11.30	10.98	11.06	11.21	
% CO	4.50	5+	5+	5+	5+	
% CO2	9.00	11.70	10.50	10.50	10.50	
EX. FLOW	39.86	57.57	74.87	87.08	107.82	g/s
EX. TEMP	780.9	754.4	755.5	763.5	791.3	deg.C

SPEED	500	500	500	500	500	500	500	500	rev/min
POWER	0.000	1.731	2.091	2.530	2.996	3.529	4.328	5.260	kW
HEAT TO WATER	7.974	8.516	8.929	9.103	9.395	9.610	9.887	10.103	kW
EX. ENTHALPY	1.209	1.450	1.438	1.525	1.684	1.821	1.977	2.270	kW (datum at 250 deg. C)
EX. m*Cp/t	5.898	7.010	7.232	7.546	8.011	8.493	9.177	10.430	W/K (at 250 deg. C)
FUEL FLOW	0.366	0.458	0.482	0.498	0.529	0.559	0.615	0.709	g/s

TABLE A3.3 ENGINE TEST FINAL CALCULATED DATA

SPEED	1003	1003	997	1002	1003	993	993	1001	rev/min
POWER	0.000	2.297	4.992	8.939	14.157	16.396	20.891	23.192	kW
HEAT TO WATER	13.596	14.492	16.544	18.468	20.774	21.961	23.258	22.946	kW
EX. ENTHALPY	4.153	4.972	6.553	8.380	10.936	11.746	13.253	12.719	kW (datum AT 250 deg. C)
EX. m*Cp/t	11.264	13.965	16.750	21.055	27.080	29.235	33.992	32.826	W/K (at 250 deg. C)
FUEL FLOW	0.767	0.855	0.880	1.245	1.603	1.757	2.126	1.250	g/s

SPEED	1550	1493	1507	1493	1499	1490	1500	1495	1500	1500	rev/min
POWER	0.000	4.294	7.625	12.922	17.804	23.411	29.560	34.359	39.547	42.742	kW
HEAT TO WATER	17.562	19.528	20.300	21.874	23.607	24.942	26.633	27.500	30.473	29.253	kW
EX. ENTHALPY	6.878	8.508	9.804	11.929	13.968	15.841	18.794	21.101	22.588	23.892	kW (datum at 250 deg. C)
EX. m*Cp/t	15.717	19.674	22.456	27.231	31.305	36.717	45.534	52.518	54.832	59.808	W/K (at 250 deg. C)
FUEL FLOW	1.283	1.131	1.305	1.603	1.896	2.325	3.133	3.720	3.055	4.409	g/s

SPEED	2047	2019	2004	2001	2000	1997	2002	1995	2000	rev/min
POWER	0.000	6.129	11.474	18.864	25.299	38.823	48.250	56.316	58.055	kW
HEAT TO WATER	22.419	21.331	24.333	26.209	27.859	30.982	34.326	35.412	33.066	kW
EX. ENTHALPY	9.860	12.032	14.362	16.856	18.678	24.254	28.528	32.628	31.545	kW (datum at 250 deg. C)
EX. m*Cp/t	19.443	24.764	29.456	36.270	43.299	59.364	69.442	77.296	81.678	W/K (at 250 deg. C)
FUEL FLOW	1.225	1.442	1.771	2.248	2.873	4.251	5.096	5.669	6.470	g/s

SPEED	2558	2509	2500	2502	2504	2499	2507	2504	2503	2500	rev/min
POWER	0.000	8.352	13.648	20.989	27.540	36.603	48.737	58.348	69.323	69.240	kW
HEAT TO WATER	26.639	27.311	28.555	29.531	30.226	31.182	34.848	39.194	41.080	34.828	kW
EX. ENTHALPY	13.500	16.185	16.654	20.021	22.176	27.239	33.616	40.152	44.365	42.085	kW (datum at 250 deg. C)
EX. m*Cp/t	24.140	30.824	32.675	42.293	49.774	60.877	74.108	84.154	97.475	102.777	W/K (at 250 deg. C)
FUEL FLOW	1.531	1.953	2.175	2.725	3.429	4.326	5.411	5.952	7.259	8.313	g/s

SPEED	3063	3007	3004	3003	3004	2989	3003	2997	3000	rev/min
POWER	0.000	11.211	19.040	29.190	37.039	50.546	62.778	73.427	81.490	kW
HEAT TO WATER	29.564	31.095	32.660	34.362	37.125	40.247	44.210	46.810	41.040	kW
EX. ENTHALPY	16.537	20.765	22.940	27.831	31.105	39.286	48.276	54.351	57.719	kW (datum at 250 deg. C)
EX. m*Cp/t	29.145	38.440	45.798	56.801	64.295	80.775	95.684	108.402	130.142	W/K (at 250 deg. C)
FUEL FLOW	1.884	2.377	3.000	3.777	3.916	5.679	6.795	7.730	10.088	g/s

SPEED	3567	3507	3505	3498	3501	3497	3489	3506	3500	3500	rev/min
POWER	0.000	10.740	20.535	25.617	30.301	39.114	49.709	60.689	76.430	88.547	kW
HEAT TO WATER	33.875	34.975	34.812	36.853	38.134	40.358	43.768	47.527	39.794	44.819	kW
EX. ENTHALPY	20.458	20.132	27.346	29.577	31.779	36.315	42.349	50.446	78.482	71.689	kW (datum at 250 deg. C)
EX. m*Cp/t	33.985	37.093	53.285	58.343	63.883	73.317	84.819	97.824	141.529	145.476	W/K (at 250 deg. C)
FUEL FLOW	2.157	2.705	3.607	4.029	4.495	5.203	6.024	6.889	8.043	11.535	g/s

SPEED	4076	4013	4030	4010	4010	4000	4000	4000	rev/min
POWER	0.000	12.290	17.172	27.018	37.697	47.722	58.588	67.962	kW
HEAT TO WATER	38.229	40.452	37.409	37.827	40.402	42.163	44.699	46.698	kW
EX. ENTHALPY	23.045	28.281	29.678	33.794	39.021	44.272	51.205	58.079	kW (datum at 250 deg. C)
EX. $\dot{m}*C_p/t$	39.094	51.669	55.590	65.450	76.925	87.822	99.540	110.882	W/K (at 250 deg. C)
FUEL FLOW	2.536	3.393	3.748	4.578	5.552	6.332	7.223	8.131	g/s

SPEED	4512	4500	4500	4500	4500	rev/min
POWER	0.000	19.773	36.551	50.572	69.506	kW
HEAT TO WATER	43.170	46.193	43.168	48.870	53.989	kW
EX. ENTHALPY	25.993	35.631	46.541	55.003	71.937	kW (datum at 250 deg. C)
EX. m*Cp/t	46.151	66.826	87.170	101.310	125.261	W/K (at 250 deg. C)
FUEL FLOW	3.166	4.679	6.252	7.223	8.831	g/s

APPENDIX A4

REFRIGERATION SYSTEM COMPONENTS

MANUFACTURERS' DATA

GRAPH A4.1

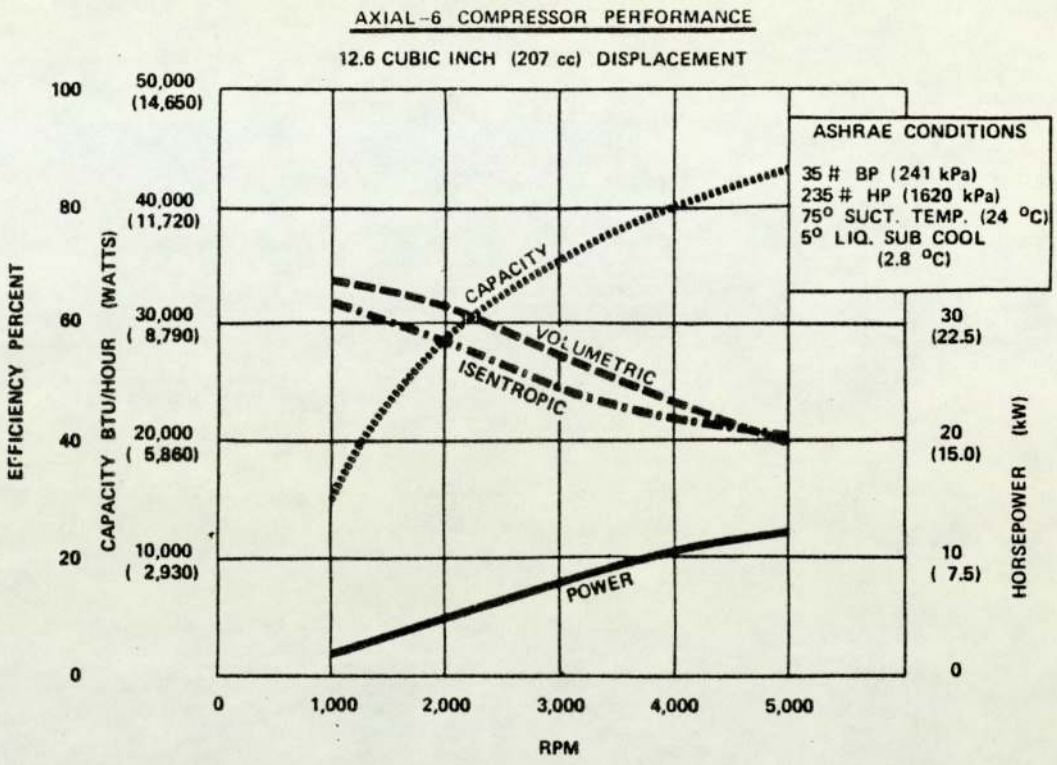

THE DATA OF THE COMPRESSOR MANUFACTURER

RELATING TO COMPRESSOR EFFICIENCIES

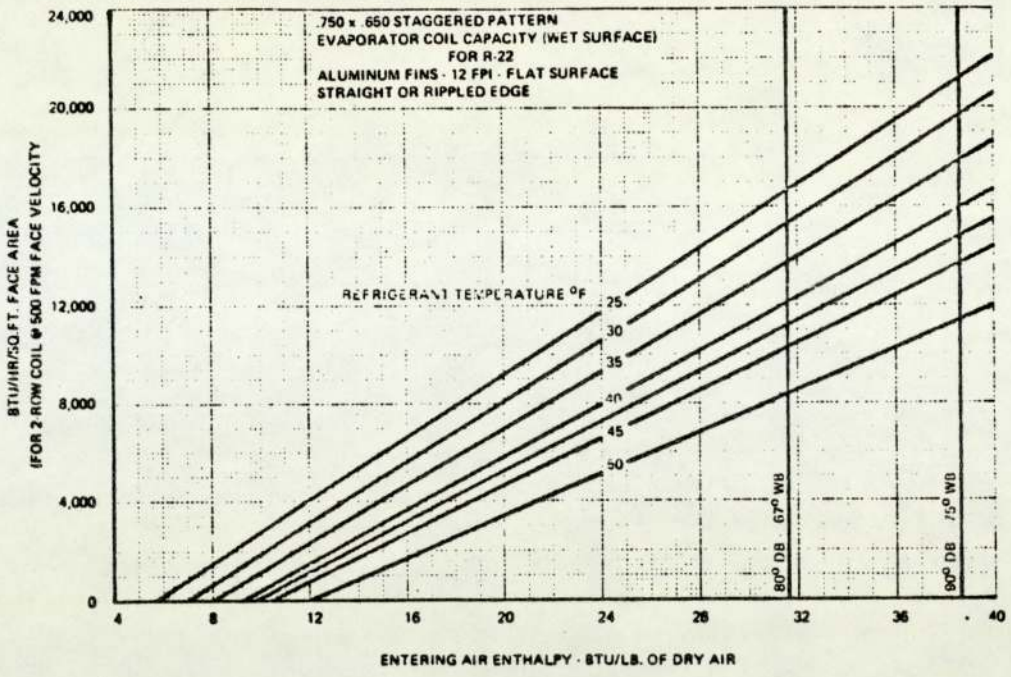

GRAPH A4.2

THE DATA OF THE EVAPORATOR MANUFACTURER

RELATING TO THE EVAPORATOR CONDUCTANCE

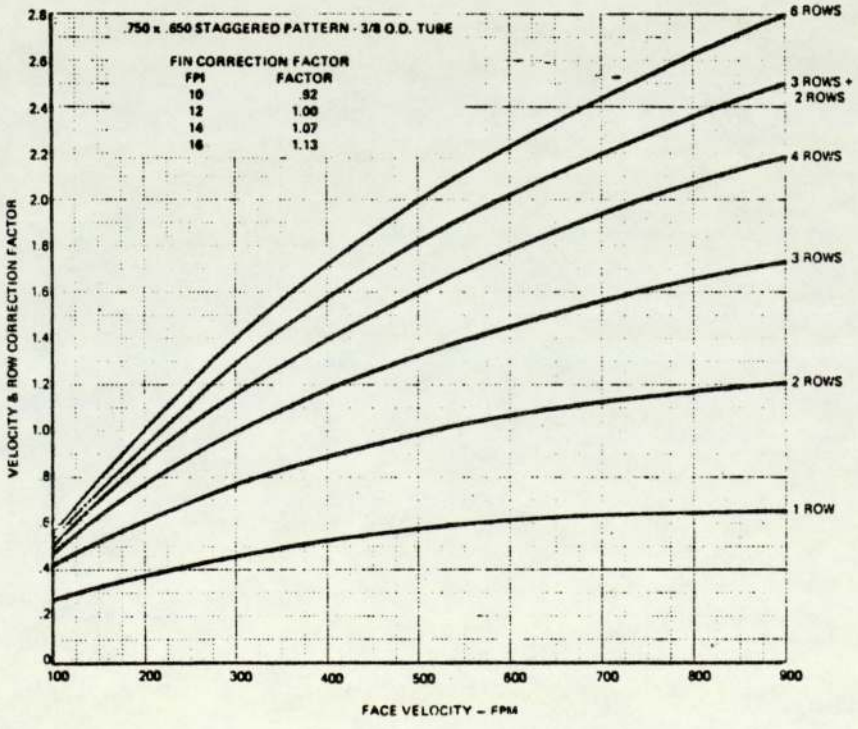

APPENDIX A5

THE COMPUTER PROGRAM OF THE MATHEMATICAL MODEL OF THE REFRIGERATION SYSTEM, THE ENGINE, THE ENGINE COOLING SYSTEM, AND THE ROAD AND AUXILIARY BRAKE LOADS

The program is listed as for the present vehicle at 750 rev/min engine speed in third gear. Refrigerant R12 is used and a 45/55 water antifreeze mixture as the engine coolant.

The language used is Basic as adapted by Hewlett-Packard for use on their 9830 calculator. Although listed here as one program, the capacity of the above machine is insufficient, having only 8k words of storage capacity, and the program must be split into two or more sections.

```
2 GOSUB 3600
4 GOSUB 5000
6 REM O9= CONTROLLED EVAPORATOR TEMPERATURE
8 O9=3
10 REM O0= AMBIENT RELATIVE HUMIDITY
12 O0=0.5
14 REM D0= COMPRESSOR DISPLACEMENT/RADIAN
16 D0=3.286E-05
18 REM M8= EVAPORATOR DRY AIR MASS FLOW RATE
20 M8=0.15102
22 REM B0= VISCOUS COUPLING CONSTANT
24 B0=4.5254E-04
26 REM M9= VEHICLE MASS
28 M9=1902.5
30 REM R0= COOLANT DENSITY
32 R0=1.0736
34 REM G1= FAN & COOLANT PUMP PULLEY RATIO
36 G1=1.25
38 REM G3= COMPRESSOR PULLEY RATIO
40 G3=1.05
42 REM F=RADIATOR FIN PITCH
44 F=2.117E-03
46 REM L1= RADIATOR HEADER DISTANCE
48 L1=0.651
50 REM L2= RADIATOR CORE DEPTH
52 L2=0.451
54 REM R= NUMBER OF RADIATOR TUBE ROWS
56 R=3
58 REM Z9= NUMBER OF RADIATOR TUBES
60 Z9=87
62 REM L3=RADIATOR CORE THICKNESS
64 L3=0.0495
```

```
66 REM F1=CONDENSER FIN PITCH
68 F1=2.31E-03
70 REM L4= CONDENSER CORE LENGTH
72 L4=0.584
74 REM L5= CONDENSER CORE DEPTH
76 L5=0.381
78 REM L6= CONDENSER CORE THICKNESS
80 L6=0.044
82 REM Z8= NUMBER OF CONDENSER TUBES
84 Z8=30
86 REM R1= NUMBER OF CONDENSER TUBE ROWS
88 R1=2
90 REM T0= AMBIENT TEMPERATURE
92 T0=45
94 REM W= ENGINE SPEED IN RADIANS/SECOND
96 W=78.54
98 REM G2= TRANSMISSION GEAR RATIO IN METRES/RADIAN
100 REM THIRD GEAR
102 G2=6.5443E-02
104 REM E0= 1/TRANSMISSION EFFICIENCY
106 E0=1.1439
108 GOSUB 3700
110 GOSUB 3800
112 GOSUB 3900
114 GOSUB 2600
116 IF M7=1E+50 THEN 174
118 GOSUB 8800
120 GOSUB 3000
122 GOSUB 3100
124 GOSUB 4500
126 GOSUB 3200
128 GOSUB 3300
130 GOSUB 3400
```

```
132 PRINT "HEAT REJECTED TO COOLANT="Q
134 PRINT "TOP HOSE TEMPERATURE="T3
136 PRINT "BOTTOM HOSE TEMPERATURE="T4
138 PRINT "COOLANT MASS FLOW RATE="M1
140 PRINT "RADIATOR AIR VELOCITY="U2
142 PRINT "EVAPORATOR LOAD="M8*H0
144 PRINT "EVAPORATOR TEMPERATURE="O1
146 PRINT "EVAPORATOR PRESSURE="C1
148 PRINT "COMPRESSOR LOAD="M7*(H3-H2)
150 PRINT "REFRIGERANT TEMPERATURE AT COMPRESSOR EXIT="O3
152 PRINT "CONDENSING TEMPERATURE="O5
154 PRINT "CONDENSING PRESSURE="C2
156 PRINT "FRACTION OF CONDENSER USED FOR GAS COOLING="A6/L4/L5
158 PRINT "FRACTION OF CONDENSER USED FOR CONDENSATION="A5/L4/L5
160 PRINT "FRACTION OF TIME COMPRESSOR RUNNING="M7/M0
162 PRINT "RADIATOR AIR ON TEMPERATURE="T1
164 PRINT "RADIATOR AIR OFF TEMPERATURE="T2
166 PRINT "FUEL MASS FLOW RATE="G
168 PRINT "EXHAUST ENTHALPY AT 250 deg. C="E1,"(DATUM 0 deg. C)"
170 PRINT "EXHAUST GAS MASS CAPACITY="E2,"(AT 250 deg. C)"
172 GOTO 178
174 PRINT "CONDENSING PRESSURE>0.762*CRITICAL PRESSURE"
176 STOP
178 END
```

```
2600 REM*****SUBROUTINE:- CALC. REF. CYCLE PROPERTIES AND MASS FLOW RATES*****
2602 H6=FNIT0
2604 Z2=Z3=0
2606 O=1
2608 T=O9
2610 GOSUB 6700
2612 H0=H
2614 O=O0
2616 T=T2=T0
2618 GOSUB 6700
2620 H0=H-H0
2622 Q0=H
2624 GOSUB 8100
2626 T=(O1+273.15)/T9
2628 GOSUB 5100
2630 C1=P*P9
2632 T=T+2.5/T9
2634 O2=T*T9-273.15
2636 GOSUB 5600
2638 V0=V*V9
2640 GOSUB 5800
2642 H2=H*P9*V9
2644 M7=D0*G3*W/V0*FNL(W*G3)
2646 M0=M7
2648 H7=H2-H0*M8/M7
2650 IF Z2#2 THEN 2656
2652 IF ABS(ABS(M7*(H2-H6)/(M8*H0))-1)<1E-02 THEN 2666
2654 GOTO 2658
2656 IF M7*(H2-H6)>M8*H0 THEN 2670
2658 H0=M7*(H2-(H6+H7)/2)/M8
2660 H=Q0
2662 Z2=2
2664 GOTO 2624
```

```
2666 H7=H6
2668 IF T0#T2 THEN 2680
2670 O5=FNY(H7/P9/V9)*T9-273.15
2672 T4=(H2-H7)*M7/(L4*L5*1.71562*U^0.5697*R1/F1)
2674 IF O5-T0>T4 THEN 2680
2676 O5=T4+T0
2678 Z2=1
2680 T=(O5+273.15)/T9
2682 GOSUB 5100
2684 IF T0#T2 THEN 2710
2686 IF P<0.762 THEN 2710
2688 P=0.762
2690 GOSUB 5500
2692 O5=T*T9-273.15
2694 GOSUB 5600
2696 GOSUB 5800
2698 C2=P*P9
2700 H5=H*P9*V9
2702 GOSUB 5300
2704 GOSUB 5400
2706 H7=H5-H*P9*V9
2708 M7=H0*M8/(H2-H7)
2710 C2=P*P9
2712 V=V0/V9
2714 T=(O2+273.15)/T9
2716 GOSUB 5700
2718 S2=S*P9*V9/T9
2720 IF T2#T0 THEN 2736
2722 GOSUB 2864
2724 IF Z2=1 THEN 2728
2726 IF L4*L5>A5+A6 OR M0>M7 THEN 2820
2728 H6=H5-Q3/M7*(L4*L5-A6)/A5
2730 B3=B3*(H5-H7)/(H5-H6)
```

```
2732 O5=EXP((T1-T0)/B3)
2734 O5=(T0-T1*O5)/(1-O5)
2736 T=(O5+273.15)/T9
2738 IF T>0.96 THEN 2870
2740 GOSUB 5100
2742 C2=P*P9
2744 GOSUB 2862
2746 IF (L4*L5)<(A5+A6) THEN 2728
2748 GOSUB 8500
2750 B[1,1]=O5
2752 B[2,1]=H6
2754 FOR I2=2 TO 3
2756 B3=B3*(H5-H7)/(H5-H6)
2758 O5=EXP((T1-T0)/B3)
2760 O5=(T0-T1*O5)/(1-O5)
2762 T=(O5+273.15)/T9
2764 IF T>0.96 THEN 2870
2766 GOSUB 5100
2768 C2=P*P9
2770 GOSUB 2862
2772 GOSUB 8500
2774 B[1,I2]=O5
2776 B[2,I2]=H6
2778 NEXT I2
2780 B[1,5]=(B[2,2]-B[2,1])/(B[1,2]-B[1,1])
2782 B[2,5]=(B[2,3]-B[2,2])/(B[1,3]-B[1,2])
2784 B[1,4]=(B[1,5]+B[2,5])/2
2786 B[2,4]=(B[2,5]-B[1,5])/((B[1,3]-B[1,1])/2)
2788 O5=(B[1,3]+2*B[1,2]+B[1,1])/4-B[1,4]/B[2,4]
2790 T=(O5+273.15)/T9
2792 IF T>0.96 THEN 2870
2794 GOSUB 5100
2796 C2=P*P9
```

```
2798 GOSUB 2862
2800 GOSUB 8500
2802 IF ABS(H6-H7)<5E+02 THEN 2860
2804 IF Z3=1 THEN 2808
2806 IF H6>H7 OR T2#T0 THEN 2814
2808 M7=M8*H0/(H2-H6)
2810 Z3=1
2812 GOTO 2736
2814 T2=O6
2816 GOTO 2652
2818 B3=B3*A5/(L4*L5-A6)
2820 O5=EXP((T1-T0)/B3)
2822 O5=(T0-T1*O5)/(1-O5)
2824 T=(O5+273.15)/T9
2826 IF T>0.96 THEN 2870
2828 GOSUB 5100
2830 C2=P*P9
2832 GOSUB 5600
2834 GOSUB 5800
2836 H5=H*P9*V9
2838 GOSUB 5300
2840 GOSUB 5400
2842 H7=H5-H*P9*V9
2844 M7=M8*H0/(H2-H7)
2846 Q3=H*P9*V9*M7
2848 GOSUB 8400
2850 GOSUB 8200
2852 GOSUB 8315
2854 IF ABS(L4*L5-A5-A6)>L4*L5*1E-03 THEN 2818
2856 H6=H8=H7
2858 O6=O5
2860 RETURN
2862 GOSUB 8400
```

```
2864 GOSUB 8200
2866 GOSUB 8300
2868 RETURN
2870 M7=H0=O1=O3=O5=O6=H2=H3=H5=H6=H8=A5=A6=C1=C2=T1=1E+50
2872 RETURN
```

```
3000 REM*****ENGINE BRAKE POWER*****
3002 B=5.36722E-01*(W*G2)^3
3004 B=B+M9*9.806*W*G2*(1.27679E-02+1.74933E-05*W*G2+4.61979E-18*(W*G2)^8.817)
3006 B=B*E0+8.95862E-05*(W*G1)^3*(1-B0*(W*G1)^1.138)^2
3008 RETURN


3100 REM******ENGINE HEAT TO COOLANT*****
3102 Q=B/(1.15915E-02*W+8.48805E-01)
3104 Q=Q*(-3.6E-06*B+1)
3106 Q=Q+((3.82599E-04*W-3.11021E-01)*W+1.52298E+02)*W
3108 RETURN


3200 REM******FUEL MASS FLOW RATE*****
3202 G=1+2.5714E+03/W^3.61571*B
3204 G=G*B*((-4.27896E-13*W+3.98877E-10)*W-1.53203E-08)
3206 G=G+((3.86223E-11*W-2.36786E-08)*W+9.30922E-06)*W
3208 RETURN


3300 REM*****EXHAUST ENTHALPY (AT 250 deg. C)*****
3302 E1=B*(6.3E-06*B+1)*(3.1308E-04*W+2.52686E-01)
3304 E1=E1+5.97131E+01*W-2.37932E+03
3306 RETURN
```

```
3400 REM*****EXHAUST GAS CAPACITY RATE (AT 250 deg. C)*****
3402 E2=B*(4E-06*B+1)*8.64E-04
3404 E2=E2+((3.43872E-07*W-2.17024E-04)*W+1.23398E-01)*W
3406 RETURN



3500 REM*****MAXIMUM ENGINE BRAKE POWER*****
3502 DEF FNZ(W)=(((-3.65824E-06*W+2.08688E-03)*W-2.02364E-01)*W+2.99158E+02)*W
```

```
3600 REM*****SUBROUTINE:- INITIALISE FAN EQN. CONSTANTS*****
3602 DIM M[11,5]
3604 MAT READ M
3606 DATA -5602.491295,2060.836004,-414.1952242,149.6,0
3608 DATA -5602.491295,-798.1153039,-199.4064331,111.2,0.1701
3610 DATA 26366.28239,-1554.451629,-305.271945,100.1,0.2151
3612 DATA -15396.54169,2653.607041,-246.7968771,83.43,0.2683
3614 DATA 12986.71704,-1221.702501,-126.6600862,72.31,0.3522
3616 DATA -4782.443675,188.6549695,-164.0564069,66.74,0.3884
3618 DATA 2025.673709,-739.6173479,-199.7036728,55.62,0.4531
3620 DATA -10180.82252,-319.0874859,-272.9660473,38.93,0.5223
3622 DATA 20276.21973,-1455.267279,-338.9720445,27.81,0.5595
3624 DATA 20276.21973,722.3987193,-365.208739,14.74,0.5953
3626 DATA 0,0,0,0,0.6526
3628 RETURN
```

```
3700 REM*****FAN AIR VELOCITY CONSTANT & RADIATOR DIMENSIONS*****
3702 W1=SQR(F*F+1.59997201E-04)
3704 D=F*1.2649E-02*2/(F+W1)
3706 A1=(L2-Z9/R*2.54E-03-(Z9/R+1)*W1*5.842E-05/F)/L2
3708 S1=Z9*L1*2.922E-02
3710 S2=2*L3*(Z9/R+1)*L1/F*W1
3712 N1=9.34013E-02*L3^0.67/D^1.07/A1^1.6
3714 N2=8.28499E-03*R1/F1
3716 U=0.5/(L1*L2)
3718 P1=N1*U^1.6+N2*U^1.737+195.387194*U*L1*L2-147.3
3720 P2=N1*1.6*U^0.6+N2*1.737*U^0.737+195.387194*L1*L2
3722 U=U-P1/P2
3724 IF ABS(P1/P2)>1E-02 THEN 3718
3726 Q=L1*L2*U/1.155209596
3728 FOR I=1 TO 11
3730 IF Q>M[I,5] AND Q<M[I+1,5] THEN 3734
3732 NEXT I
3734 P1=N1*U^1.6+N2*U^1.737
3736 Q1=Q-M[I,5]
3738 P1=P1-0.98431*(((M[I,1]*Q1+M[I,2])*Q1+M[I,3])*Q1+M[I,4])
3740 P2=1.6*N1*U^0.6+1.737*U^0.737
3742 P2=P2-0.98431*((3*M[I,1]*Q1+2*M[I,2])*Q1+M[I,3])*L1*L2/1.155209569
3744 U=U-P1/P2
3746 Q=L1*L2*U/1.15520956
3748 IF Q<M[I,5] OR Q>M[I+1,5] THEN 3728
3750 IF ABS(P1/P2)>1E-04 THEN 3734
3752 A=U/104.71976
3754 RETURN
```

```
3800 REM*****RAM AIR CONSTANT*****
3802 C=0.25
3804 IF W*G2=0 THEN 3820
3806 K1=1+10.43677*(W*G2)^(-0.263)+12.67973*(W*G2)^(-0.4)
3808 P1=N1/(C*G2*W)^0.4+N2/(C*G2*W)^0.263
3810 P3=C*C/5.79211E-02-K1/(P1+1)
3812 P2=0.4*N1/(G2*W)^0.4/C^1.4+0.263*N2/(G2*W)^0.263/C^1.263
3814 P2=C/2.89606E-02+K1/((P1+1)*(P1+1))*P2
3816 C=C-P3/P2
3818 IF ABS(P3/P2/C)>1E-04 THEN 3808
3820 RETURN


3900 REM*****AIR VELOCITIES AND RADIATOR AIR MASS FLOW RATE*****
3902 U=SQR((A*W*G1*(1-B0*(W*G1)^1.138))^2+(C*G2*W)^2)
3904 U2=U/1.155209569
3906 M2=U2*FNPT0*L1*L2
3908 RETURN
```

```
4000 REM*****COOLANT MASS FLOW RATE (WITHOUT THERMOSTAT)*****
4002 M1=W*G1*(7.51253E-03-1.1644E-01*L1/Z9)*R0
4004 RETURN


4100 REM*****COOLANT MASS FLOW RATE (WITH THERMOSTAT)*****
4102 T3=8*M1/(R0*W*G1*(7.51253E-03-1.1644E-01*L1/Z9))+82
4104 RETURN


4200 REM*****RADIATOR AIR OFF TEMPERATURE*****
4202 T2=T1+Q/(1004*M2)
4204 P1=(FNGT2-FNGT1)*M2-Q
4206 P2=FNAT2*M2
4208 T2=T2-P1/P2
4210 IF ABS(P1/P2)>1E-04 THEN 4204
4212 RETURN


4300 REM*****BOTTOM HOSE TEMPERATURE*****
4302 T4=T3-Q/(4.2E+03*M1)
4304 P1=(FNHT3-FNHT4)*M1-Q
4306 P2=-FNW(T4)*M1
4308 T4=T4-P1/P2
4310 IF ABS(P1/P2)>1E-04 THEN 4304
4312 RETURN
```

```
4400 REM*****RADIATOR HEAT TRANSFER & BOTTOM HOSE TEMPERATURE*****
4402 B1=(T3+T4)/2
4404 B2=(T1+T2)/2
4406 T5=1.478032/(FNPB2*U2/A1*D/FNVB2)^0.476
4408 T5=T5/(L3/D)^0.47*FNAB2*M2/(L1*L2*A1)
4410 T5=T5/(FNAB2*FNVB2/FNKB2)^(2/3)
4412 X9=W1*SQR(T5/4.6736E-02)
4414 E=EXP(-2*X9)
4416 E=(1-E)/(1+E)/X9
4418 T5=T5*(S1+S2*E)
4420 T5=1/(1/T5+1/FNT(M1))
4422 T5=1-EXP(-T5/(M2*FNAB2))
4424 N3=(1-EXP(-M2*FNAB2/(M1*FNWB1)*T5))
4426 T5=T1+(T3-T4)/N3
4428 RETURN
```

```
4500 REM*****ENGINE COOLANT TEMPERATURES & MASS FLOW RATE*****
4502 GOSUB 4200
4504 T3=100
4506 GOSUB 4000
4508 M3=M1
4510 GOSUB 4300
4512 GOSUB 4400
4514 IF T5<100 THEN 4522
4516 IF ABS(T5-T3)<1E-06 THEN 4536
4518 T3=T5
4520 GOTO 4510
4522 M1=(T1-82+SQR((82-T1)^2+4*(18/M3)*(Q/4.2E+03/N3)))/(36/M3)
4524 GOSUB 4100
4526 GOSUB 4300
4528 GOSUB 4400
4530 IF ABS(T3-T5)<1E-02 THEN 4536
4532 M1=M1-(T3-T5)/(18/M3+Q/(M1*M1*4.2E+03*N3))
4534 GOTO 4524
4536 RETURN


4600 REM*****COOLANT SIDE CONDUCTIVITY*****
4602 REM WATER/ANTI-FREEZE
4604 DEF FNT(M1)=4.7807E+02*Z9*L1*(M1/Z9)^0.8
```

```
5000 REM*****R12 SUBROUTINE:- INITIALISE CONSTANTS*****
5002 DIM C[3],D[3],E[3],F[5],G[5],H[6],P[3],T[4],U[5],V[5],W[5],X[2],Y[4],Z[4]
5004 MAT READ T
5006 DATA 3.862336922,-11.41020509,-12.46463173,7.547868173
5008 MAT READ U
5010 DATA 0,-6.934977529,4.267936535,-1.354488423,0
5012 MAT READ V
5014 DATA 3.590772057,2.24780781,-0.9232594576,0,0.2068197136
5016 MAT READ W
5018 DATA 0,-115.1596917,92.90090309,0,-2.187472214
5020 MAT READ X
5022 DATA 0.2267871,-5.475
5024 MAT READ Y
5026 DATA 1.772181,50.42774,-25.36853,4.898847
5028 MAT READ Z
5030 DATA 0.536468,0.630984,1.53101,-0.090434
5032 P9=41.15*1E+05
5034 V9=0.00179
5036 T9=385.15
5038 RETURN


5100 REM*****R12 SUBROUTINE:- PSAT=F(T)*****
5102 P=EXP(T[1]+T[2]/T+T[3]*LOGT+T[4]*T)
5104 RETURN
```

```
5200 REM*****R12 SUBROUTINE:- P=F(V,T)*****
5202 V8=V-X[1]
5204 V7=V8
5206 P=V[1]*T/V8
5208 FOR I=2 TO 5
5210 V7=V7*V8
5212 P=P+(U[I]+V[I]*T+W[I]*EXP(X[2]*T))/V7
5214 NEXT I
5216 RETURN


5300 REM*****R12 SUBROUTINE:- VF=F(T)*****
5302 V5=1-T
5304 V5=1+Z[1]*V5+Z[2]*SQR(V5)+Z[3]*V5^(1/3)+Z[4]*V5*V5
5306 V5=1/V5
5308 RETURN


5400 REM*****R12 SUBROUTINE:- HFG=F(TSAT,P,VG,VF)*****
5402 H=P*((-T[2]/T+T[3])/T+T[4])
5404 H=T*(V-V5)*H
5406 RETURN
```

```
5500 REM*****R12 SUBROUTINE:- TSAT=F(P)*****
5502 T=1
5504 P8=P
5506 GOSUB 5100
5508 IF ABS(1-P/P8)<5E-06 THEN 5516
5510 P7=P*((-T[2]/T+T[3])/T+T[4])
5512 T=T-(P-P8)/P7
5514 GOTO 5506
5516 P=P8
5518 RETURN
```

```
5600 REM*****R12 SUBROUTINE:- V=F(P,T)*****
5602 E9=EXP(X[2]*T)
5604 FOR I=1 TO 5
5606 F[I]=U[I]+V[I]*T+W[I]*E9
5608 G[I]=I*F[I]
5610 NEXT I
5612 IF ABS(T-0.999)>0.001 THEN 5620
5614 IF P<0.9875 THEN 5620
5616 V=1+2.832*SQR(1-T)+36.72*(1-T)
5618 RETURN
5620 X=P/F[1]
5622 X=(P-(F[2]+(F[3]+(F[4]+F[5]*X)*X)*X)*X*X)/F[1]
5624 V2=X[1]+1/X
5626 Y=-P
5628 D9=0
5630 H[1]=1
5632 FOR I=2 TO 6
5634 H[I]=H[I-1]*X
5636 NEXT I
5638 FOR I=1 TO 5
5640 Y=Y+F[I]*H[I+1]
5642 D9=D9+G[I]*H[I]
5644 NEXT I
5646 X=X-Y/D9
5648 V=X[1]+1/X
5650 IF ABS(1-V2/V)<5E-06 THEN 5618
5652 GOTO 5624
```

```
5700 REM*****R12 SUBROUTINE:- S=F(V,T)*****
5702 S9=-4.78453976
5704 F9=X[2]*EXP(X[2]*T)
5706 V8=V-X[1]
5708 V7=1
5710 F8=V[1]*LOG(V8)
5712 FOR I=2 TO 5
5714 V7=V7*V8
5716 F8=F8-(V[I]+W[I]*F9)/((I-1)*V7)
5718 NEXT I
5720 S=Y[1]*LOGT+(Y[2]+(Y[3]*0.5+Y[4]/3*T)*T)*T
5722 S=S9+S+F8
5724 RETURN


5800 REM*****R12 SUBROUTINE:- H=F(V,T)*****
5802 H9=12.474812015
5804 K9=X[2]*T
5806 F9=(K9-1)*EXPK9
5808 V8=V-X[1]
5810 V7=1
5812 F7=0
5814 FOR I=2 TO 5
5816 V7=V7*V8
5818 F7=F7+(U[I]-W[I]*F9)/((I-1)*V7)
5820 NEXT I
5822 H=(Y[1]+(Y[2]*0.5+(Y[3]/3+Y[4]*0.25*T)*T)*T)*T
5824 GOSUB 5200
5826 H=H9+H+F7+P*V
5828 RETURN
```

```
6100 REM*****R12 SUBROUTINE:- V,T=F(P,S)*****
6102 P6=P
6104 S7=S
6106 P=P6
6108 GOSUB 5500
6110 P=P6
6112 F6=1.1
6114 GOSUB 5600
6116 GOSUB 5700
6118 IF ABS(1-S/S7)<5E-04 THEN 6144
6120 IF F6>1 THEN 6124
6122 F6=1/F6
6124 IF S7>S THEN 6128
6126 F6=1/F6
6128 T7=T
6130 T=F6*T
6132 GOSUB 5600
6134 S8=S
6136 GOSUB 5700
6138 F6=EXP(LOGF6*(S7-S8)/(S-S8))
6140 T=F6*T7
6142 GOTO 6114
6144 S=S7
6146 P=P6
6148 RETURN
```

```
6700 REM*****PSYCHROMETRY SUBROUTINE, H=F(T,REL.HUM.)*****
6702 P8=O*((((7.57183E-09*T+8.30986E-10)*T+1.97711E-05)*T+4.0718E-04)*T)
6704 P8=P8+O*6.14896E-03
6706 H=P8/(1.01325-P8)*0.6216
6708 P8=LOGP8
6710 P8=((0.074540453*P8+2.472135755)*P8+44.91656376)*P8+2675.325095
6712 H=H*(((4E-07*T+9E-05)*T+1.859)*T+P8)
6714 H=(H+((9.51517E-08*T+1.9625E-05)*T+1.003696108)*T)*1E+03
6716 RETURN


6800 REM*****PROPERTIES OF AIR (-100 TO 120deg.C, 760mm(Hg))*****
6802 REM SPECIFIC HEAT CAPACITY
6804 DEF FNA(T)=(2.85455E-04*T+3.92499E-02)*T+1.0037E+03
6806 REM ENTHALPY
6808 DEF FNG(T)=((9.51517E-05*T+1.9625E-02)*T+1.0037E+03)*T
6810 REM VISCOSITY
6812 DEF FNV(T)=((5.65657E-14*T-4.37079E-11)*T+4.955E-08)*T+1.71626E-05
6814 REM CONDUCTIVITY
6816 DEF FNK(T)=(-3.7697E-08*T+7.97849E-05)*T+2.41282E-02
6818 REM DENSITY
6820 DEF FNP(T)=3.52984E+02/(273.15+T)


7000 REM*****PROPERTIES OF WATER ANTI-FREEZE MIXTURE (55/45)*****
7002 REM SPECIFIC HEAT CAPACITY
7004 DEF FNW(T)=(7.89835E-04*T+4.54032)*T+3.06598E+03
7006 REM ENTHALPY
7008 DEF FNH(T)=((2.63278E-04*T+2.27016)*T+3.06598E+03)*T
```

```
7200 REM*****TSAT=F(HF)******
7202 REM R12
7204 DEF FNY(H)
7206 T=(((-8.5015055E-08*H-4.66526785E-06)*H-4.3270119E-05)*H+2.1502148E-02)
7208 T=T*H+6.057516E-01
7210 RETURN T
```

```
8000 REM*****COMPRESSOR EFFICIENCIES*****
8002 REM VOLUMETRIC
8004 DEF FNL(W)=0.7536-6.78E-04*W
8006 REM ISENTROPIC
8008 DEF FNM(W)=(6.64377E-07*W-9.7512E-04)*W+0.7338


8100 REM*****REFRIGERANT EVAPORATING TEMPERATURE*****
8102 P4=8.0487*M8^0.73
8104 O1=-5
8106 IF O1<0 THEN 8114
8108 P3=593.17
8110 GOTO 8116
8112 O1=O1-P1/P2
8114 P3=1038.4
8116 P2=(M8*H0/(P4*0.06125*1.0784*0.9)+P3*O1)/H
8118 P1=((-374.29*P2+751.68)*P2-538.18)*P2+142.5-O1
8120 P2=((-1122.87*P2+1503.36)*P2-538.18)*(P3/H)-1
8122 O1=O1-P1/P2
8124 IF ABS(P1/P2/O1)>1E-03 THEN 8106
8126 RETURN
```

```
8200 REM*****SUBROUTINE:- CALC GAS COOLING AREA*****
8202 A6=0.1*L4*L5
8204 Q2=(H3-H5)*M7
8206 A6=0.1*L4*L5
8208 B1=(O3+O5)/2
8210 U7=1.71562*U^0.5697*R1/F1
8212 M6=U*A6*FNPT0
8214 T1=T0+Q2/(1004*M6)
8216 B2=(T1+T0)/2
8218 A7=Q2/U7/(B1-B2)
8220 IF ABS(A6-A7)<1E-02 THEN 8226
8222 A6=A7
8224 GOTO 8212
8226 A6=-2*M7*C3/FNAB2*LOG(1-(O3-O5)/(O3-T0))/U/FNPT0
8228 M6=U*A6*FNPT0
8230 P1=(FNGT1-FNGT0)*M6-Q2
8232 P2=FNAT1*M6
8234 T1=T1-P1/P2
8236 IF ABS(P1/P2)>1E-02 THEN 8230
8238 B2=(T1+T0)/2
8240 B1=(O3+O5)/2
8242 U3=-FNAB2*M6*LOG(C3*M7/(FNAB2*M6)*LOG(1-(O3-O5)/(O3-T0))+1)
8244 U4=A6*U7
8246 U5=A6/(L4*L5)*Z8*L4*9.525E-03*PI
8248 U5=U5*0.023*FNEB1/9.525E-03*(M0/R1*1.4034E+04/FNCB1)^0.8
8250 U5=U5*(FNCB1*C3/FNEB1)^0.4*M7/M0
8252 U5=1/(1/U4+1/U5)
8254 A6=U3/U5*A6-M7*C3/FNAB2*LOG(1-(O3-O5)/(O3-T0))/U/FNPT0*(1-U3/U5)
8256 IF ABS(U3/U5-1)>1E-02 THEN 8228
8258 RETURN
```

```
8300 REM*****AREA FOR CONDENSATION*****
8302 P=C2/P9
8304 T=(O5+273.15)/T9
8306 GOSUB 5300
8308 GOSUB 5600
8310 GOSUB 5400
8312 Q3=H*P9*V9*M7
8314 A5=2*Q3/((O5-T0)*FNAT0*FNPT0*U)
8316 M5=A5*U*FNPT0
8318 T1=T0+Q3/(1004*M5)
8320 P1=(FNGT1-FNGT0)*M5-Q3
8322 P2=FNAT1*M5
8324 T1=T1-P1/P2
8326 IF ABS(P1/P2)>1E-02 THEN 8320
8328 B3=(T1-T0)/LOG((O5-T0)/(O5-T1))
8330 P1=Q3/(B3*1.71562*U^0.5697*R1/F1)
8332 IF ABS((P1-A5)/P1)>1E-03 THEN 8338
8334 A5=P1
8336 RETURN
8338 A5=P1+Q3/((O5-T0)*FNA(T0+B3/2)*FNPT0*U)*(1-P1/A5)
8340 GOTO 8316
```

```
8400 REM*****PROPERTIES AT COMPRESSOR EXIT*****
8402 P=C2/P9
8404 GOSUB 6100
8406 O4=T*T9-273.15
8408 GOSUB 5800
8410 H4=H*P9*V9
8412 H3=H2+(H4-H2)/FNM(W*G3)
8414 T=(O5+273.15)/T9
8416 GOSUB 5600
8418 GOSUB 5800
8420 H5=H*P9*V9
8422 C3=(H4-H5)/(O4-O5)
8424 O3=O5+(H3-H5)/C3
8426 RETURN
```

```
8500 REM*****ENTHALPY & TEMPERATURE AFTER LIQUID SUBCOOLING*****
8502 A4=L4*L5-A5-A6
8504 H8=H5-Q3/M7
8506 M4=A4*U*FNPT0
8508 B1=O5
8510 B2=T0
8512 Z1=0
8514 U3=A4/(L4*L5)*Z8*L4*9.525E-03*PI
8516 U5=U3*0.023*FNDB1/9.525E-03*(M0/R1*1.403E+04/FNBB1)^0.8
8518 U5=U5*(FNBB1/FNDB1)^0.4*M7/M0
8520 U5=1/(1/U5+1/(A4*1.71562*U^0.5697*R1/F1))
8522 U6=1-EXP(-(1-EXP(-U5/(M4*FNAB2)))*M4*FNAB2/(M7*FNFB1))
8524 O6=O5-U6*(O5-T0)
8526 B1=(O5+O6)/2
8528 H6=FNIO6
8530 IF ABS((Z1-H6)/H6)>1E-03 THEN 8534
8532 GOTO 8552
8534 Z1=H6
8536 Q4=(H8-H6)*M7
8538 B2=T0+Q4/(1004*M4)
8540 P1=(FNGB2-FNGT0)*M4-Q4
8542 P2=FNAB2*M4
8544 B2=B2-P1/P2
8546 IF ABS(P1/P2)>1E-03 THEN 8540
8548 B2=(T0+B2)/2
8550 GOTO 8516
8552 H6=FNIO6
8554 RETURN
```

```
9900 REM*****R12 PHYSICAL PROPERTIES*****
9902 REM LIQUID VISCOSITY
9904 DEF FNB(T)
9906 T=T*1.8+32
9908 X=((-6.90794E-16*T+2.65948E-13)*T-4.97267E-11)*T
9910 X=((X+8.6513E-09)*T-1.76604E-06)*T+3.14111E-04
9912 T=(T-32)/1.8
9914 RETURN X
9916 REM GAS VISCOSITY
9918 DEF FNC(T)
9920 T=T*1.8+32
9922 X=(-5.65726E-12*T+2.27365E-08)*T+1.06565E-05
9924 T=(T-32)/1.8
9926 RETURN X
9928 REM LIQUID CONDUCTIVITY
9930 DEF FND(T)
9932 T=T*1.8+32
9934 X=((-5.47909E-14*T+4.56436E-12)*T+1.61078E-09)*T
9936 X=((X-7.7626E-08)*T-2.1303E-04)*T+8.50211E-02
9938 T=(T-32)/1.8
9940 RETURN X
9942 REM GAS CONDUCTIVITY
9944 DEF FNE(T)
9946 T=T*1.8+32
9948 X=(5.0849E-09*T+2.78889E-05)*T+7.4484E-03
9950 T=(T-32)/1.8
9952 RETURN X
9954 REM CP LIQUID
9956 DEF FNF(T)
9960 X=(((1.88648E-05*T-2.57398E-03)*T+1.53532E-01)*T-1.22257)*T+9.3682E+02
9964 RETURN X
```

```
9966 REM*****H LIQUID REFRIGERANT*****
9968 DEF FNI(T)
9970 T=(273.15+T)/T9
9972 GOSUB 5100
9974 GOSUB 5600
9976 GOSUB 5800
9978 H1=H*P9*V9
9980 GOSUB 5300
9982 GOSUB 5400
9984 H=H1-H*P9*V9
9986 T=T*T9-273.15
9988 RETURN H
```

The following functions are alternatives to represent water as the engine coolant.

```
4600 REM*****COOLANT SIDE CONDUCTIVITY*****
4602 REM WATER
4604 REM DEF FNT(M1)=2.709E+03*Z9*L1*(M1/Z9)^0.8
```

```
6900 REM*****PROPERTIES OF WATER (0 TO 200deg.C)*****
6902 REM SPECIFIC HEAT CAPACITY
6904 DEF FNW(T)=(1.41424E-02*T-1.34713)*T+4.20133E+03
6906 REM ENTHALPY
6908 DEF FNH(T)=((4.71413E-03*T-6.73565E-01)*T+4.20133E+03)*T
```

The following subroutines and functions are alternatives for a vapour compression system using refrigerant R22.

In addition, the reducing factor of 0.9 in line 8112 relating to the evaporator conductance should be omitted for R22.

```
5000 REM*****INITIALISING SUBROUTINE:- R22*****
5002 DIM C[3],D[3],E[3],F[6],G[6],H[6],T[6],U[6],V[6],W[6],X[3],Y[4],Z[4]
5004 MAT READ T
5006 DATA 7.030569532,-10.33053763,-7.85605432
5008 DATA 3.349627065,0.4458604956,1.032506622
5010 MAT READ U
5012 DATA 0,-6.401590102,-1.010345093,3.835663598,-1.993351592,1.888547241E+05
5014 MAT READ V
5016 DATA 3.742165661,2.378064754,2.468598352,-3.822806065,1.860077265
5018 DATA -1.537861679E+05
5020 MAT READ W
5022 DATA 0,-66.42566806,72.25908413,0,-9.643264456,0
5024 MAT READ X
5026 DATA 0.06552,-4.2,16.733822
5028 MAT READ Y
5030 DATA 0.09495332,4.583511,24.42053,-4.683452
5032 MAT READ Z
5034 DATA 1.6677,1.121739,-0.6804608,0.6249227
5036 P9=4.97866E+06
5038 V9=0.0019054
5040 T9=369.167
5042 RETURN


5100 REM*****R22 SUBROUTINE:- PSAT=F(T)*****
5102 P=T[1]+T[2]/T+T[3]*LOGT+T[4]*T
5104 IF T>T[6] THEN 5108
5106 P=P+T[5]*(T[6]/T-1)*LOG(T[6]-T)
5108 P=EXPP
5110 RETURN
```

```
5200 REM*****R22 SUBROUTINE:- P=F(V,T)*****
5202 E8=EXP(X[2]*T)
5204 V8=V-X[1]
5206 V7=V8
5208 P=V[1]*T/V8
5210 IF V>13.6 THEN 5214
5212 P=P+(U[6]+V[6]*T)*EXP(-X[3]*V)
5214 FOR I=2 TO 5
5216 V7=V7*V8
5218 P=P+(U[I]+V[I]*T+W[I]*E8)/V7
5220 NEXT I
5222 RETURN


5300 REM*****R22 SUBROUTINE:- VF=F(T)*****
5302 V5=1-T
5304 F5=V5^(1/3)
5306 V5=1+Z[1]*F5+Z[2]*F5*F5+Z[3]*V5+Z[4]*V5*F5
5308 V5=1/V5
5310 RETURN


5400 REM*****R22 SUBROUTINE:- HFG=F(TSAT,P,VG,VF)*****
5402 H=P*((-T[2]/T+T[3])/T+T[4]-T[5]*(1+T[6]*LOG(T[6]-T)))
5404 H=T*(V-V5)*H
5406 RETURN
```

```
5500 REM*****R22 SUBROUTINE:- TSAT=F(P)*****
5502 T=1
5504 P8=P
5506 GOSUB 5100
5508 IF ABS(1-P/P8)>5E-07 THEN 5514
5510 P=P8
5512 RETURN
5514 P7=(-T[2]/T+T[3])/T+T[4]
5516 IF T>T[6] THEN 5520
5518 P7=P7-T[5]*(1+T[6]*LOG(T[6]-T)/T)/T
5520 P7=P*P7
5522 T=T-(P-P8)/P7
5524 GOTO 5506
```

```
5600 REM*****R22 SUBROUTINE:- V=F(P,T)*****
5602 P5=P
5604 GOSUB 5100
5606 IF P5<(P-1E-06) THEN 5618
5608 IF ABS(T-0.99973)>0.00027+1E-08 THEN 5618
5610 X=ABS(1-T)
5612 V=1+6.9160182*SQRX+9.7333861*X
5614 P=P5
5616 RETURN
5618 P=P5
5620 E7=0
5622 E9=EXP(X[2]*T)
5624 FOR I=1 TO 5
5626 F[I]=U[I]+V[I]*T+W[I]*E9
5628 G[I]=I*F[I]
5630 NEXT I
5632 F[6]=U[6]+V[6]*T
5634 F5=F[1]*F[1]+4*F[2]*P
5636 IF F5>1E-08 THEN 5642
5638 X=P/F[1]
5640 GOTO 5644
5642 X=0.5*(SQRF5-F[1])/F[2]
5644 V2=X[1]+1/X
5646 H[1]=1
5648 FOR I=2 TO 6
5650 H[I]=H[I-1]*X
5652 NEXT I
5654 IF V2>13.6 THEN 5658
5656 E7=EXP(-X[3]*V2)
5658 Y=F[6]*E7-P
5660 D9=F[6]*X[3]*E7/H[3]
5662 FOR I=1 TO 5
5664 Y=Y+F[I]*H[I+1]
5666 D9=D9+G[I]*H[I]
5668 NEXT I
5670 X=X-Y/D9
5672 V=X[1]+1/X
5674 IF ABS(1-V2/V)>5E-06 THEN 5644
5676 RETURN
```

```
5700 REM*****R22 SUBROUTINE:- S=F(V,T)*****
5702 S9=9.347625337
5704 F9=X[2]*EXP(X[2]*T)
5706 V8=V-X[1]
5708 V7=1
5710 F8=V[1]*LOGV8
5712 IF V>13.6 THEN 5716
5714 F8=V[1]*LOGV8-V[6]*EXP(-X[3]*V)/X[3]
5716 FOR I=2 TO 5
5718 V7=V7*V8
5720 F8=F8-(V[I]+W[I]*F9)/((I-1)*V7)
5722 NEXT I
5724 S=-Y[1]*0.5/(T*T)+Y[2]*LOGT+(Y[3]+Y[4]*0.5*T)*T
5726 S=S9+S+F8
5728 RETURN


5800 REM*****R22 SUBROUTINE:- H=F(V,T)*****
5802 F7=0
5804 H9=15.303597099
5806 K9=X[2]*T
5808 F9=(K9-1)*EXPK9
5810 V8=V-X[1]
5812 V7=1
5814 IF V>13.6 THEN 5818
5816 F7=U[6]*EXP(-X[3]*V)/X[3]
5818 FOR I=2 TO 5
5820 V7=V7*V8
5822 F7=F7+(U[I]-W[I]*F9)/((I-1)*V7)
5824 NEXT I
5826 H=-Y[1]/T+(Y[2]+(Y[3]*0.5+Y[4]/3*T)*T)*T
5828 GOSUB 5200
5830 H=H9+H+F7+P*V
5832 RETURN
```

```
6100 REM*****R22 SUBROUTINE:- V,T=F(P,S)*****
6102 P6=P
6104 S7=S
6106 GOSUB 5500
6108 T5=T
6110 GOSUB 5600
6112 GOSUB 5700
6114 S8=S
6116 F6=1.1
6118 T=F6*T
6120 IF T>(T5-5E-07) THEN 6124
6122 T=T5
6124 GOSUB 5600
6126 GOSUB 5700
6128 IF ABS(1-S/S7)>5E-06 THEN 6136
6130 P=P6
6132 S=S7
6134 RETURN
6136 F6=EXP(-LOGF6*(S7-S)/(S8-S))
6138 S8=S
6140 GOTO 6118
```

```
9900 REM*****R22 PHYSICAL PROPERTIES*****
9902 REM LIQUID VISCOSITY
9904 DEF FNB(T)
9906 T=1.8*T+32
9908 X=(((-3.68441E-14*T-1.94523E-11)*T+6.953E-09)*T-1.24131E-06)*T+2.64535E-04
9910 T=(T-32)/1.8
9912 RETURN X
9914 REM GAS VISCOSITY
9916 DEF FNC(T)
9918 T=1.8*T+32
9920 X=(-3.72138E-12*T+2.37179E-08)*T+1.09558E-05
9922 T=(T-32)/1.8
9924 RETURN X
9926 REM LIQUID CONDUCTIVITY
9928 DEF FND(T)
9930 T=1.8*T+32
9932 X=((-2.45782E-09*T+1.41039E-07)*T-2.51535E-04)*T+1.08611E-01
9934 T=(T-32)/1.8
9936 RETURN X
9938 REM GAS CONDUCTIVITY
9940 DEF FNE(T)
9942 T=1.8*T+32
9944 X=(-1.08214E-10*T+3.34157E-05)*T+8.32567E-03
9946 T=(T-32)/1.8
9948 RETURN X
9950 REM CP LIQUID
9952 DEF FNF(T)
9954 X=(((1.1438E-04*T-1.5783E-02)*T+7.67293E-01)*T-1.11954)*T+1.21952E+03
9960 RETURN X
```

APPENDIX A6

REFERENCES

1. CAWLEY, R.J., 'Automotive Cooling of Passenger Cars and Small Commercial Vehicles', Coolaire Corpn., U.S.A.
2. RANDLE, J.N., Vehicle Research, Jaguar Cars (B.L.U.K.) Ltd., Personal Communications 1974-77.
3. WENTWORTH, J.T., S.A.E. Preprint No. 710587,1971.
4. MACKERLE, J., 'Air Cooled Motor Engines', Clever-Hulme Press 1961.
5. HOWARD, J.R., The University of Aston in Birmingham, Personal Communication 1977.
6. BOTTERILL, J.S.M., AND WILLIAMS, J.R., Trans. Inst. Chem. Engrs. Vol. 41, 1963, p217.
7. AL-ALI, B.M.A., PhD Thesis, The University of Aston in Birmingham, 1976.
8. STEINHAGEN, W.K., ET AL, S.A.E., pt. 12, p146, 1963-66).
9. BROWNSON, D.A., AND STEBAR, R.F., S.A.E. pt. 12, p103, 1963-66.
10. WARREN, J.A., ET AL, S.A.E. Preprint 680123, 1968.
11. ENVIRONMENTAL PROTECTION AGENCY, 'Automobile Emission Control, The State of the Art as of December 1972', National Technical Information Service, U.S. Dept. of Commerce.
12. SCHWING, R.C., S.A.E. pt. 14, p368, 1967-70.
13. LEVENSPIEL, O., 'Chemical Reactor Engineering', John Wiley and Sons 1968.
14. BLENK, M.H., AND FRANKS, R.G.E., S.A.E. Preprint 710607, 1971.
15. PATTERSON, D.J., 'Kinetics of Oxidation and Quenching of Combustibles in Exhaust Systems of Gasoline Engines', Second Annual Progress Report on Project Cape-8-68, submitted to C.R.C. 1971.
16. DAVIDSON, J.F., AND HARISON, D., 'Fluidisation', Academic Press, 1971.
17. KUNI, D., AND LEVENSPIEL, O., 'Fluidisation Engineering', John Wiley and Sons, 1969.
18. SHRIKHANDE, K.V., Jnl. of Sci. and Ind. Res. 14b, 457, 1955.

19. LEWIS, W.K., GILLIAND, E.R., GIROUARD, H., Chem. Eng. Prog. Vol. 58, p87, 1962.

20. ZABRODSKY, S.S., 'Hydrodynamics and Heat Transfer in Fluidised Beds', M.I.T. Press, 1966.

21. BROUGHTON, J., PhD Thesis, University of Newcastle, 1972.

22. DAVIDSON, J.F., Trans., I. Chem. E., 39, 230, 1961.

23. ELLIOTT, D.E., AND VIRR M.J., 'Third International Conference on Fluidised Bed Combustion', Hueston Woods, Ohio, U.S.A., 1972.

24. JARRY, R.L., ANASTASIA, L.J., CARLS, E.L., JONKE, A.A., VOGEL, G.J., 'Second International Conference on Fluidised Bed Combustion', Hueston Woods, Ohio, U.S.A. 1970.

25. COLE, W.E., ESSENHIGH, R.H., 'Third International Conference on Fluidised Bed Combustion', 1972.

26. METCALFE, C.I., The University of Aston in Birmingham. Unpublished work.

27. HUNTER, J.E., General Motors Research Publication GMR-1061, 1971.

28. BERNSTEIN, L.S. ET AL, S.A.E. Preprint 710014, 1971.

29. BOSNJAKOVIC, 'Technische Thermodynamik', Zweiter Teil.

30. THRELKELD, J.L., 'Thermal Environmental Engineering', Prentice-Hall International, 1970.

31. BRITISH STANDARDS INSTITUTION, BS4580, 1970.

32. KUPRIANOFF, J., PLANK, R., STEINLE, H., 'Handbuch Der Kalktetechnik', Springer, Berlin, 1956.

33. AMERICAN SOCIETY OF HEATING, REFRIGERATING, AND AIR-CONDITIONING ENGINEERS, 'Handbook of Fundamentals 1972'.

34. BRITISH STANDARDS INSTITUTION, BS4434, Pt. 1, 1969.

35. AMERICAN NATIONAL STANDARDS INSTITUTION, ANSI-B9.1, 1958.

36. UNDERWRITERS' LABORATORIES, 'Underwriters' Laboratories Classification of Comparative Hazard to Life of Gases and Vapours'.

37. ANDERSON, S.A., 'Automatic Refrigeration', MacLaren and Sons Ltd., 1959.

38. ELLINGTON, R.T., KUNST, G., PECK, R.E., REED, J.F., Inst. Gas Tech. Res. Bul. 14, 1957.

39. ARCHIE, J.L., A.S.H.R.A.E. Jnl., Sept. 1971.

40. MACRIS, R.A., EAKIN, B.E., ELLINGTON R.T., HUEBLER, J., Inst. Gas Tech. Res. Bul. 34, 1964.

41. HALA, E., PICK, J., FRIED, V., VILIM, O., 'Vapour Liquid Equilibrium', Pergamon Press, 1958.

42. BUFFINGTON, R.M., Ref. Eng. April 1949.

43. JACOB, X., ALBRIGHT, L.F., TUCKER, W.H., A.S.H.R.A.E. Trans. Vol. 75, Pt. 1, p103, 1969.

44. HAINSWORTH, W.R., Ref. Eng., Aug. 1944.

45. HAINSWORTH, W.R., Ref. Eng., Sept. 1944.

46. ZELLHOEFER, G.F., Heating Piping and Air-Con., April 1937.

47. ZELLHOEFER, G.F., Jnl. A.S.R.E., May 1937.

48. ZELLHOEFER, G.F., Ind. and Eng. Chem. Vol 29, p548, 1937.

49. ZELLHOEFER, G.F., COPLEY, M.J., MARVEL, C.S., Jnl. of Am. Chem. Soc., Vol. 60, p 1337, 1938.

50. ALBRIGHT, L.F., DOODEY, T.C., BUCLEZ, P.C., PLUCH, C.R., A.S.H.R.A.E. Trans. Vol. 66, p423, 1960.

51. ALBRIGHT, L.F., THIEME, A., A.S.H.R.A.E. Trans, Vol. 67, p431, 1961.

52. ALBRIGHT, L.F., HESSELBERTH, J.F., A.S.H.R.A.E. Trans., Vol. 71, p27, 1965.

53. MASTRANGELO, S.V.R., A.S.H.R.A.E. Jnl., Oct. 1959.

54. MASTRANGELO, S.V.R., Jnl. of Phys. Chem., Vol. 63, p608, 1959.

55. EISEMAN, B.J., A.S.H.R.A.E. Jnl, Dec. 1959.

56. HALE, D.V., THOENES,J., LIU, C.K., Lockheed Missiles and Space Company, March 1971, N.A.S.A. Contract No. NAS8-25986.

57. SIMS, W.H., O'NEILL, M.J., REID, H.C., BISENIUS, P.M., Lockheed Missiles and Space Company, Nov. 1972, N.A.S.A. Contract No. NAS8-25986.

58. DUNN, P., REAY, D.A., 'Heat Pipes', Pergamon 1976.

59. WOODS OF COLCHESTER LTD., 'Woods Practical Guide to Fan Engineering', 1972.

60. ROWLAND, B.K., Marston Radiators Ltd., Personal Communication.

61. RICKERS, D.A., Smiths Industries, Witney, Rept. on Test 185/72, June 1972, (communicated to Jaguar Cars (B.L.U.K.) Ltd.).

62. BRITISH STANDARDS INSTITUTION, BS1042, Pt. 1, 1964.

63. STEVENS, R.A., M.S. Thesis, Southern Methodist University, U.S.A., 1955.

64. ROHSENOW, W.M., HARTNETT, J.P., 'Handbook of Heat Transfer', McGraw-Hill, 1973.

65. McADAMS, W.H., 'Heat Transmission', McGraw-Hill, 1954.

66. MAYHEW, Y.R., ROGERS, G.F.C., 'Thermodynamic and Transport Properties of Fluids, S.I. Units', Oxford, Basil Blackwell, 1969.

67. VENN, B.R., Vehicle Instrumentation Division, Smiths Industries Ltd., Personal Communication.

68. FAN MANUFACTURERS ASSOCIATION LTD., F.M.A., Code 3, 1952.

69. BRITISH LEYLAND (B.L.U.K.) LTD., Pub. No. E188/1.

70. BRITISH LEYLAND (B.L.U.K.) LTD., Part No. RTC 9097B, August 1975.

71. BUCK, G., Engine Experimental Dept., Jaguar Cars (B.L.U.K.) Ltd., Personal Communication, 1975.

72. BRITISH STANDARDS INSTITUTION, BS 4937, Pt. 4, 1973.

73. SPIERS, H.M., 'Technical Data on Fuel', The British National Committee, World Power Conference, 1961.

74. HAMBLIN, F.D., 'Abridged Thermodynamic and Thermochemical Tables, S.I. Units', Pergamon Press, 1971.

75. JAGUAR CARS (B.L.U.K.) LTD., 'Heat to Water Test', July 1966.

76. LINGS, G.P., Stress Analysis, Jaguar Cars (B.L.U.K.) Ltd., Personal Communication, 1976.

77. BUSH, I.F., Engine Experimental Dept., Jaguar Cars (B.L.U.K.) Ltd., Internal Report ED2206/IFB, Dec. 1976.

78. OLIVER, M.G., Vehicle Development, Jaguar Cars (B.L.U.K.) Ltd., Internal Report EXP 3995, Dec. 1976.

79. OLIVER, M.G., Vehicle Development, Jaguar Cars (B.L.U.K.) Ltd., Personal Communication.

80. "FREON" PRODUCTS DIVISION, E.I. Du Pont De Nemours and Co. (Inc.), Delaware, U.S.A.

81. HENRY WIGGIN AND CO. LTD., 'Wiggin Electrical Resistance Alloys', 1975.

82. KING, L.V., Phil. Trans. Roy. Soc., Vol. A214, p373, 1914.

83. HILPERT, R., Forsch. Gebiete Ingenieurw, Vol. 4, p215, 1933.

84. COLLIS, D.C., WILLIAMS, M.J., Jnl. Fluid Mechs., Vol. 6, p357, 1959.

85. KESTIN, J., Advances in Heat Trans., Vol. 3, p1, 1966.

86. SCHLICHTING, H., 'Boundary Layer Theory', McGraw-Hill, 1960.

87. COMINGS, E.W., CLAP, J.T., TAYLOR, J.F., Ind. and Eng. Chem., Vol. 40, No. 6, p1076, 1948.

88. SCHAUBAUR, G.B., Natl. Advisory Comm. Aeronaut., Tech. Rept. 524, 1935.

89. DRYDEN, H.L., Ind. & Eng. Chem., Vol. 31, p416, 1939.

90. BRITISH STANDARDS INSTITUTION, BS1042, part 2, 1943.